İSTANBUL TECHNICAL UNIVERSITY ★ INSTITUTE OF SCIENCE AND TECHNOLOGY

THE GRAVITY AND SEISMIC ANALYSIS AND DESIGN OF BEAM-COLUMN JOINTS

126638

T.C. YÜKSEKÖĞRETİM KURULU
DOKÜMANTASYON MERKEZİ

Ph.D. Thesis by

Pelin GÜNDEŞ BAKIR, DIC, M.Sc.

(501952027)

Date of submission : 1 October 2001

Date of defence examination: 19 April 2002

Supervisor (Chairman): Prof. Dr. Hasan BODUROĞLU

Members of the Examining Committee Prof.Dr. Zekai CELEP (İTÜ.)

Prof.Dr. Tuncer ÇELİK (İÜ.)

Prof.Dr. Zeki HASGÜR (İTÜ.)

Prof.Dr. Faruk YÜKSELER (YÜ.)

MAY 2002

Doktora tezi tarafından
Kontrol edilmiştir.
Arş. Gör. Recep Kadir Polatgözoz :

PREFACE

The completion of a text not only brings an appreciated respite from many years of demanding effort, but it also provides a welcome opportunity to acknowledge in writing the many kind souls who supported you along the way. The first among them is naturally Professor Boduroğlu, who has provided immeasurable encouragement and support throughout these years. His help was willingly and expertly given, often at times of great pressure and need. This work is dedicated to Professor Boduroğlu, who enlightens others with his accomplishments and excellence and helps others with his superior commitment and devotion. Thanks are also due to Faruk Yükseler, Professor Zekai Celep, Professor Zeki Hasgür and Professor Tuncer Çelik for revising the thesis and for their helpful suggestions.

I am also greateful to my beloved husband, heart surgeon Dr. İhsan Bakır for his patience love and understanding over the many years it took to make this thesis a reality. Without the happy, confident family life he has given me, the completion of this text would not be possible. Preparing a doctoral thesis is a lonely business that inevitably excludes others for long periods of time. To my beloved husband İhsan, and terrific kid Murat, my apologies for my protracted and repeated absences.

Particularly deserving of my thanks are my mother and father, Maral and Erhan Gündeş; my mother and father in law, Ümran H. And Abdullah Bakır. Without their encouragement and logistic support, this work would not be possible.

Finally, but no less deeply felt, my special thanks to department secretary Gülcihan Güley for her warm friendship and support.

April, 2002

Pelin GÜNDEŞ BAKIR

CONTENTS

TABLE CAPTIONS x

FIGURE CAPTIONS xii

SYMBOLS xvi

ÖZET xix

SUMMARY xxiv

1. INTRODUCTION 1

1.1. The Objective of the Thesis 2

2. DESIGN OF REINFORCED CONCRETE STRUCTURES USING STRUT AND TIE MODELS 3

2.1. Introduction 3

2.2. Division of the Structures into B and D Regions 3

2.3. Theoretical Background for Strut and Tie Modeling 7

2.4. Modeling of D Regions 8

2.5. Basic Compression Fields 11

2.6. Designing by Strut and Tie Models 11

2.7. Dimensioning 17

2.7.1. Dimensioning the ties 17
2.7.2. Dimensioning the concrete struts or compression stress fields 17
2.7.3. Nodes 19

2.8. Failure of Reinforced Concrete Structures 21

2.8.1. Biaxial and triaxial compression 21
2.8.2. Transverse tension 21

2.8.3. Cracks which are not parallel to compressive stresses 21

2.9. Design Stresses for Concrete 22

2.10. The Advantages and Disadvantages of Strut and Tie Modeling 24

2.10.1. The Advantages 24
2.10.2. The Disadvantages 24

3. CYCLICALLY LOADED BEAM-COLUMN JOINTS **26**

3.1. Introduction 26

3.2. Comparison Between Interior and Exterior Reinforced Concrete Beam Column Joint Behavior 26

3.3. The Design Philosophy of Weak Beams Strong Columns 32

3.4. Difference in Various Codes in the Design of Reinforced Concrete Beam- Column Joints 33

3.4.1. Comments on the Work of Bonacci and Pantazopulou 37

3.5. The Models Demonstrating the Shear Resistance of a Joint 37

3.5.1. The Shear Resisting Mechanisms Proposed by Ichinose 37
3.5.1.1. Comments on the model of Ichinose 37
3.5.2. The Shear Resistance of a Joint with Poor Bond 38
3.5.2.1. Comments on the Model of Kamimura 38
3.5.3. Paulay's Equilibrium Models 40
3.5.3.1. Comments on Paulay's model 42

3.6. Review of Cyclic Tests on Interior Beam-Column Joints 44

3.6.1. Effect of bond along beam longitudinal reinforcement within a joint on the joint shear strength 44
3.6.2. The influence of concrete compressive strength, lateral reinforcement, column axial load and hooked bar development on the joint shear strength 48
3.6.3. Effect of slab on the flexural behaviour of a beam 48

3.7. Cyclic Tests on Exterior Reinforced Concrete Joints 49

3.7.1.1. The behavior of exterior beam column joints of

reinforced concrete frames with low axial load 49
3.7.1.2. Comments on Megget's conclusions by the author 49
3.7.2. Anchorage behavior of bent bar in exterior beam-column joints under seismic loading 50
3.7.2.1. Commentary on the works of Marquez and Jirsa and that of Nishimura and Minami 51

4. DESIGN AND ANALYSIS OF MONOTONICALLY LOADED EXTERIOR BEAM-COLUMN CONNECTIONS 52

4.1. Introduction 52

4.2. The Review of Tests on Monotonically Loaded Exterior Beam Column Connections 53
4.2.1. Calculation of joint shear strength 53
4.2.2. Scott's tests 55
4.2.2.1. The Effect of detailing 55
4.2.2.2. Analysis of Scott's tests 59
4.2.2.3. Parametric studies on Scott's tests 59
4.2.3. The Experimental work of Ortiz 65
4.2.3.1. Reinforcement properties 65
4.2.3.2. Test results 68
4.2.3.2.1. Influence of column axial load 69
4.2.3.2.2. Influence of column bar ratio 70
4.2.3.2.3. Influence of the radius of bend 70
4.2.3.2.4. Influence of the vertical anchorage length 71
4.2.3.2.5. Influence of joint stirrups 71
4.2.3.2.6. Inspection of the effect of the concrete cylinder strength on the joint shear strength of exterior beam-column joints 72
4.2.3.3. Conclusions from the experiments of ortiz 73
4.2.4. Scott and Hamill specimens 75
4.2.4.1. The analysis of Scott and Hamill tests 75
4.2.5. The tests of Parker and Bullmann 79
4.2.5.1. Analysis of Parker and Bullmann specimens 79
4.2.5.1.1. The influence of column axial load 79
4.2.5.1.2. Increase in column bar ratio 82
4.2.5.1.3. The influence of joint stirrups 82
4.2.5.1.4. The influence of beam bend radius 84
4.2.5.2. Summary 84
4.2.5.3. The Possible reasons for the low normalized joint shear strengths of Parker and Bullmann 86
4.2.5.4. Objections of the author for the low joint shear strength of Parker and Bullmann 87
4.2.6. Kordina 87

4.2.6.1. The Tests of Kordina 87
4.2.6.2. The Analysis of the specimens by the author 88
4.2.6.3. Summary 95
4.2.7. Taylor 98
4.2.7.1. Internal forces in the joint zone 98
4.2.7.2. Cracking analysis 98
4.2.7.3. The Ultimate limit state design approach 101
4.2.7.4. Inspection of the specimens of Taylor in more detail 106
4.2.7.4.1. The loading 106
4.2.7.4..2. Test results 109
4.2.7.5. Commentary on Taylor's tests 109

4.3. The Parameters Affecting the Shear Strength of Monotonically Loaded Specimens 112

4.3.1. Concrete Cylinder Strength 113
4.3.1.1. Analysis of Tables 4.26 and 4.27 113
4.3.2. The Effect of the Ratio of the Beam Height to Column Height 114
4.3.3. Influence of Column Axial Load 117
4.3.4. Comparison of the Tests of Ortiz, Parker and Bullmann 117
4.3.4.1. Comparison of Parker and Bullmann specimens 4a, 4d and Ortiz specimen BCJ1 118
4.3.4.2. Comparison of the tests of Scott and Parker & Bullman 119
4.3.4.3. Comparison of the specimens of Scott and Scott & Hamill 120
4.3.5. Development of design equations for monotonically loaded exterior beam column connections 121
4.3.5.1. Effect of concrete cylinder strength 121
4.3.5.2. Column bar ratio 122
4.3.5.3. Beam bar ratio 126
4.3.5.4. Column axial stress 126
4.3.5.5. Joint aspect ratio 130
4.3.5.6. Effect of joint stirrups 130
4.3.5.6.1. Determining the contribution of joint stirrups 131
4.3.5.7. Stirrup index vs the normalised joint shear strength 131
4.3.5.8. Formulation of the contribution of joint stirrups 138
4.3.5.9. Results 135

4.4.Designing the joints 138

4.4.1. The strut and tie models 138
4.4.1.1. The strut and tie model of Ortiz 138
4.4.1.1.1. The model 139
4.4.1.1.2. Horizontal shear in the joint 139
4.4.1.1.3. Cracking analysis 142

4.4.1.1.4. Vertical shear 142
4.4.1.1.5. Equilibrium and the angle of inclination 143
4.4.1.1.6. The width of the direct strut 143
4.4.1.1.7. The axial force in the diagonal strut 143
4.4.1.1.8. The width of the indirect strut 145
4.4.1.1.9. The joint failure load 145
4.4.1.1.10. Design method 145
4.4.1.1.11. The micro-model of Ortiz 146
4.4.1.1.12. The procedure followed in micro model 146
4.4.1.1.13. Application of the model on experiments 146
4.4.1.1.14. Comments on Ortiz model by the author 146
4.4.1.1.15. The parametric studies on Ortiz model 151
4.4.1.1.15.1. Analysis of tests 151
4.4.1.1.15.2. Joints without stirrups 153
4.4.1.1.15.3. Concrete cylinder strength 153
4.4.1.1.15.4. Column axial stress 153
4.4.1.1. 15.5. Joint aspect ratio 156
4.4.1.1.15.6. Column bar ratio 156
4.4.1.1.15.7. Joints with stirrups 156
4.4.1.1.15.7.1. The effect of concrete cylinder strength 156
4.4.1.1.15.7.2. The effect of column axial stress 159
4.4.1.1.15.7.3. The effect of joint aspect ratio 159
4.4.1.1.15.7.4. The effect of column bar ratio 159
4.4.1.1.15.8. Results 159
4.4.1.2. The strut and tie model of Vollum 162
4.4.1.2.1. Introduction 162

4.5. Overview of the design equations suggested for exterior beam column connections 165

4.5.1. The empirical equation of Sarsam and Phillips 165
4.5.1.1. Comments on Sarsam and Phillips design equation by the author of this thesis. 167
4.5.2. The design equation of Vollum 168
4.5.2.1.The commentary on the design equation of Vollum by the author 168
4.5.3. The design equation of the author of this thesis 169

5. THE STRUT AND TIE MODELING OF JOINTS 177

5.1. Introduction 177

5.1.1. Vertical Joint Shear 179
5.1.2. Horizontal Joint Shear 179
5.1.3. The Upper and lower column moments 179

5.1.3. Beam Moments 180
5.1.4. Section analysis 180
5.1.5. Assumptions made when modeling the joint 181
5.1.6. The depth of the beam and columns compressive rectangular stress blocks 182
5.1.7. The Angle of inclination of the direct and indirect struts 183
5.1.8. The Cracked Concrete Strength Adapted 183

5.2. Model without stirrups 183

5.2.1. The Width of the direct strut in the top node 184
5.2.2. The Axial Force in the Direct Strut 185
5.2.3. Failure 185
5.2.4. The Final procedure adapted for the joints without stirrups 185

5.3. Model with stirrups 186

5.3.1.Modeling of the joint 187

5.4. Results 190

5.5. The Parametric Studies on Author's model 191

5.5.1. Concrete Cylinder Strength 191
5.5.2. Column Bar Ratio 191
5.5.3. Joint aspect ratio 194
5.5.4. Column axial load 194
5.5.5. Concrete Cylinder Strength (Joints with stirrups) 194
5.5.6. Joint aspect ratio (with stirrups) 194
5.5.7. Column bar ratio 194
5.5.8. Column axial stress 197

5.6. A Simple Methodology for Predicting the Failure Modes 197

5.6.1. Results 203

6. CONCLUSIONS **209**

6.1. Overview of the thesis 209

6.2. The Proposed Design Equation 209

6.3. The proposed strut and tie model 210

6.4. The Proposed Methodology for Failure Modes 213

6.5. Joint Mechanics 215

6.6. Recommendations for future research 217

6.7. Final words 218

REFERENCES 219

APPENDIX A 223

APPENDIX B 235

RESUME 238

TABLE LIST

		Page Number
Table 2.1.	Analysis leading to stresses or strut and tie forces.....	12
Table 2.2.	Structural analysis of statically indeterminate structures.....	12
Table 4.1.	The specimen details of Scott tests.....	57
Table 4.2.	The experimental beam moments as percentages of theoretical values at ultimate.....	58
Table 4.3.	Failure modes and shear stresses.....	58
Table 4.4.	Yield strength of the reinforcement in Scott's tests.....	59
Table 4.5.	Analysis of Scott's tests.....	60
Table 4.6.	Beam reinforcement of Ortiz specimens.....	65
Table 4.7.	Column reinforcement of Ortiz specimens.....	68
Table 4.8.	Concrete splitting and crushing strengths.....	68
Table 4.9.	Shear reinforcement.....	68
Table 4.10.	The radius of bend of beam bars and corresponding failure modes of Ortiz specimens.....	69
Table 4.11.	Normalized joint shear strengths of Ortiz specimens and corresponding vertical anchorage lengths.....	69
Table 4.12.	Anchorage lengths and normalized joint shear strengths of Ortiz specimens.....	70
Table 4.13.	Stirrup forces reported by Ortiz.....	72
Table 4.14.	The details of Scott and Hamill tests adapted from Vollum.....	74
Table 4.15.	The analysis of Scott and Hamill tests.....	75
Table 4.16.	The details of the tests of Parker and Bullman.....	81
Table 4.17.	The material properties of the tests of Parker and Bullman.....	81
Table 4.18.	Normalized joint shear strengths and failure loads of Parker and Bullmans specimens.....	82
Table 4.19.	Details of Kordina's specimens.....	90
Table 4.20.	Failure loads of Kordina's specimens.....	90
Table 4.21.	Analysis of Kordina specimens.....	92
Table 4.22.	The details of the test specimens of Taylor.....	107
Table 4.23.	The test results of Taylor specimens.....	108
Table 4.24.	The analysis of Taylor's results.....	109
Table 4.25.	Analysis of Ortiz specimens.....	112
Table 4.26.	Analysis of Parker and Bullman specimens.....	112
Table 4.27.	The results of the analysis carried out by the author of this thesis on the specimens of Kordina and Scott.....	114
Table 4.28.	The normalized joint shear strength of the test specimens of Ortiz and Parker and Bullman with different joint aspect ratios	118
Table 4.29.	The analysis of the specimens of Parker and Bullman.....	119

Page number

Table 4.30.	The comparison of the tests of Scott and Parker and Bullman.....	120
Table 4.31.	The yield capacity of stirrups and the normalized joint shear strengths of the test specimens of Ortiz and Parker and Bullman..	138
Table 4.32.	The predicted failure loads of Ortiz's tests.....	147
Table 4.33.	The predicted failure loads of Parker and Bullman tests.....	147
Table 4.34.	The predicted failure loads of Scott and Hamill tests.....	148
Table 4.35.	The design equation of the author applied on the experimental database.....	176
Table 5.1.	Results of the parametric study of the author on the relative contributions of truss and strut mechanisms to shear.....	186
Table 5.2.	Predicted failure loads of Ortiz specimens.....	186
Table 5.3.	The predicted failure loads and modes of the specimens of Parker and Bullman.....	188
Table 5.4.	The predicted failure loads and modes of the specimens of Kordina.....	188
Table 5.5.	Predicted failure loads and modes of specimens tested by Scott...	189
Table 5.6.	Predicted failure loads and modes of specimens tested by Scott and Hamill.....	191
Table 5.7.	Predicted failure loads of Taylor using author's model.....	197
Table 5.8.	The application of the model on the experimental database.....	204
Table B-1.	The results of the analysis of Scott and Hamill tests carried out by the author of this thesis.....	234
Table B-2.	The results of the analysis of carried out by the author on Taylor's tests.....	234
Table B-3.	The results of the analysis of the normalized joint shear strengths of the tests of Scott and Hamill and Kordina.....	235
Table B-4.	The results of the analysis of the tests of Scott and Scott and Hamill specimens regarding the joint aspect ratio.....	235
Table B-5.	The normalized joint shear strengths of the test specimens of Ortiz and Parker and Bullman with column bar ratios.....	236

FIGURE LIST

		Page Number
Figure 2.1 :	The identification of B and D regions.....	5
Figure 2.2 :	The principle of Saint Venant.....	6
Figure 2.3 :	D regions in structures with different geometries.....	6
Figure 2.4 :	Load path method.....	9
Figure 2.5 :	The combination of two models.....	9
Figure 2.6 :	Two alternative models.....	10
Figure 2.7 :	The stress fields in a D region: a.fan mechanism, b.bottle shaped stress field, c. prismatic stress field.....	10
Figure 2.8 :	The load paths and the corresponding strut and tie model.	14
Figure 2.9 :	A typical D region with the elastic stress trajectories and the elastic stresses.....	14
Figure 2.10:	The two most frequent and most useful strut tie models....	16
Figure 2.11:	Four examples of strut and tie models.....	16
Figure 2.12:	Some typical examples of strut and tie models.....	18
Figure 2.13:	Some typical examples of stress fields, nodes and corresponding reinforcement.....	18
Figure 3.1 :	The specimen configuration and loading equipment.....	27
Figure 3.2 :	The details of the joint reinforcement.....	27
Figure 3.3 :	Typical crack patterns in the exterior and interior beam column connections.....	28
Figure 3.4 :	The comparison of the test results for exterior and interior joints.....	28
Figure 3.5 :	Degradation model of shear rigidity.....	29
Figure 3.6 :	The envelopes of cyclic joint shear stress vs shear strain curves.....	30
Figure 3.7 :	The shear transfer mechanisms of joint reinforcement.....	31
Figure 3.8 :	The fan shaped mechanism.....	31
Figure 3.9 :	The actions of interior beam column connections.....	38
Figure 3.10:	Shear resisting mechanisms.....	39
Figure 3.11:	The mechanisms of shear transfer in beam column joints..	39
Figure 3.12:	Mechanisms of joint shear resistance.....	43
Figure 4.1 :	Layout of the test specimens of Scott.....	54
Figure 4.2 :	Stress strain relationships for Scott specimens.....	55
Figure 4.3 :	Earthquake representation of Scott tests.....	55
Figure 4.4 :	The failure loads of specimen C4, C4A and C4AL.....	62
Figure 4.5 :	The relative joint shear strength of C4, C4A and C4AL....	63
Figure 4.6 :	The details of the cross sections of Ortiz specimens.....	64
Figure 4.7 :	The details of the beam column joints 1 and 2 respectively	64
Figure 4.8 :	The details of the beam column joints 3, 4 and 6.....	66
Figure 4.9 :	The properties of the test specimens 5 and 7.....	67

Page number

Figure 4.10 : The failure loads of two identical specimens of Scott and Scott and Hamill which fail by different failure modes..... 76
Figure 4.11 : The normalized joint shear strengths of two identical monotonically loaded exterior beam column connections which exhibit different failure modes..... 77
Figure 4.12 : The layout of the specimens of Parker and Bullman..... 80
Figure 4.13 : The interactions between the column bar ratio and the column axial load..... 83
Figure 4.14 : The details of Kordina specimens..... 89
Figure 4.15 : The internal forces in the joint zone in Taylor's tests..... 96
Figure 4.16 : The layout of the test specimens of Taylor..... 97
Figure 4.17 : The reinforcement details of the test specimens of Taylor 99
Figure 4.18 : The boundary forces acting outside the joint..... 100
Figure 4.19 : The notation used in preparation of the design formula.... 100
Figure 4.20 : The relation between shear on a short beam and in a joint zone..... 102
Figure 4.21 : Plot of ultimate joint shear compared with nominal joint shear compared with nominal shear stress in CP110..... 103
Figure 4.22 : Plot of shear test results with concentrated loads..... 105
Figure 4.23 : The test instrumentation of Taylor specimens..... 110
Figure 4.24 : Stress strain curves for the steel..... 111
Figure 4.25a: The normalized joint shear strength of exterior beam column connections with high and normal concrete strength..... 115
Figure 4.25b: The percentage of increase in the normalized joint shear strength with column bar ratio vs the column axial load... 116
Figure 4.26a: The influence of the concrete cylinder strength on the joint shear strength..... 122
Figure 4.26b: The influence of the column longitudinal reinforcement ratio on the joint shear strength..... 122
Figure 4.26c : The influence of the beam longitudinal reinforcement ratio on the joint shear strength..... 123
Figure 4.26d: The influence of the joint aspect ratio on the joint shear strength..... 123
Figure 4.27 : Increase in the normalized joint shear strengths with increase in beam bar ratio..... 125
Figure 4.28 : The increase in normalized joint shear strength with column axial load..... 127
Figure 4.29 : The effect of column axial load on the normalized joint shear strength of monotonically loaded exterior beam column connections..... 128
Figure 4.30 : Stirrup index vs the normalized joint shear strength..... 133
Figure 4.31 : Stirrup index vs the normalized joint shear strength..... 134
Figure 4.32 : The relationship between the stirrup index and the $(V_j-A_sf_y)/b_eh_c\sqrt{f_c}$..... 137
Figure 4.33 : The normalized joint shear strength of identical specimens with different beam bar detailing..... 140

Page Number

Figure 4.34 :	Micromodel of Ortiz.....	141
Figure 4.35 :	Simplified macromodel of Ortiz.....	141
Figure 4.36 :	The concrete and steel stress strain diagrams.....	144
Figure 4.37 :	The diagonal strut definition.....	144
Figure 4.38 :	The effect of concrete cylinder strength on the predicted normalized shear strength of Ortiz model without stirrups	152
Figure 4.39 :	The effect of column axial stress on the normalized joint shear strength predicted by Ortiz model for joints without stirrups.....	154
Figure 4.40 :	The effect of the joint aspect ratio on the normalized joint shear strength of joints without stirrups predicted by Ortiz model.....	155
Figure 4.41 :	The effect of the column bar ratio on the normalized joint shear strength predicted by Ortiz model.....	157
Figure 4.42 :	The influence of column bar ratio on the normalized joint shear strength.....	158
Figure 4.43 :	The effect of concrete cylinder strength on the normalized joint shear strength of joints with stirrups predicted by Ortiz model.....	160
Figure 4.44 :	The effect of column axial stress on the normalized joint shear strength of exterior beam column connections predicted by Ortiz model.....	161
Figure 4.45 :	The effect of the joint aspect ratio on the normalized joint shear strength of joints with stirrups predicted by Ortiz model.....	163
Figure 4.46 :	The effect of column bar ratio on the normalized joint shear strength of joints with stirrups predicted by Ortiz model.....	164
Figure 4.47 :	The model of Vollum.....	166
Figure 4.48 :	Joint geometry.....	175
Figure 4.49 :	The stress equilibrium	175
Figure 5.1 :	The author's strut and tie model.....	178
Figure 5.2 :	The influence of concrete cylinder strength on the predicted normalized joint shear strength of the author's model without stirrups.....	192
Figure 5.3 :	The effect of column bar ratio on the normalized joint shear strength of exterior beam column connections predicted by the author's model without stirrups.....	193
Figure 5.4 :	The effect of the joint aspect ratio on the normalized joint shear strength of joints predicted by the author's model.....	195
Figure 5.5 :	The effect of column axial load on the normalized joint shear strength of joints without stirrups.....	196
Figure 5.6 :	The effect of concrete cylinder strength on the normalized joint shear strength predicted by the author's model with stirrups.....	198

Page Number

Figure 5.7 : The effect of joint aspect ratio on the normalized joint shear strength of joints with stirrups predicted by the author's model..... 199

Figure 5.8 : The effect of column bar ratio on the normalized joint shear strength of joints with stirrups predicted by the author's model..... 201

Figure 5.9 : The effect of the column axial stress on the normalized joint shear strength of joints with stirrups predicted by the author's model..... 202

Figure 5.10: The simple methodology for predicting the failure modes of monotonically loaded exterior beam column connections with low amount of stirrups..... 207

Figure 5.11: The simple methodology for predicting the failure modes of monotonically loaded exterior beam column connections with medium and high amount of stirrups..... 208

Figure 6.1 : The proposed simplified strut and tie model..... 212

SYMBOLS

A_{sb} : Beam bar area

A_{scol} : Column bar area.

A_{sje} : The cross-sectional area of the joint stirrups within the top five-eights of the beam depth below the main beam reinforcement

b_b : The breadth of the beam

b_c : The breadth of the column

b_e : The effective joint width

C_{ctop} : The force in the compressive rectangular stress block of the top column

C_{stop} : The compressive force in the compressive bars of the top column.

d' : The cover

d : The depth of the beam

d_b^1 : The depth of the centroid of the tensile reinforcement in the beam measured from its top surface.

D : The total force in the diagonal strut.

f_{2max} : The maximum concrete stress in the equation of Mitchell and Collins.

f_c : The concrete cylinder strength

f_{ck} : The characteristic cylinder strength

f_{cd} : The design compressive strength

f_y : The yield stress of the longitudinal reinforcement

f_{ct} : The tensile strength of the concrete

F_v : The vertical shear in the joint,

h_b : The height of the beam

h_c : The height of the column

H : The distance between the horizontal restraints

L : The distance from the applied loading to the face of the column

$\tan\theta$: The ratio given by height of the beam to the height of the column

M_b : The moment in the beam induced due to the applied loading

M_{col} : The moment induced in the column due to the applied loading

P : The beam load.

T : The tensile force in the beam reinforcement which is calculated from conventional section analysis.

T_{sbot} : The tensile force in the tensile bars of the bottom column.

β : Capacity reduction factor

$V_{colupper}$: The shear force in the upper column

V_j : The joint shear force.

V_c : The joint shear strength without stirrups which is given by equation

V_y : The joint shear force corresponding to yielding of beam reinforcement.

y_R : The depth of the compressive stress block in the beam that balances the shear force in the lower column.

θ : The angle of inclination of direct strut.

σ_b : The stress in the beam.

ϕ : The angle of inclination of the strut coming from the upper column which is dependent on bond conditions for the beam bars and the strains in the ties of the lower and upper columns.

ρ_s : The stirrup ratio.

σ_x : Average normal stress in the concrete in the x direction

f_s : Average stress in the beam reinforcement,

f_w : Average stress in the transverse reinforcement

σ_y : Average normal concrete stress in the *y* direction

ϵ_1 : Principal tensile strain

ϵ_2 : Principal compressive strain

ϵ_x : Strain in x direction

ϵ_y : Strain in y direction

f_{scol} : The average stress in the column reinforcement

τ_{av} : The average joint shear stress in the joint

σ_1 : The principal tensile stress

σ_2 : The principal compressive stress

DIŞ KENARLARDAKİ KOLON KİRİŞ BİRLEŞİMLERİNİN DÜŞEY VE DEPREM YÜKLERİ ALTINDA ANALİZ VE TASARIMI

ÖZET

1. Tezin genel değerlendirilmesi

Bu tezde kolon-kiriş birleşimleri için üç orijinal yöntem önerilmiştir. Bunlardan birincisi kolon-kiriş birleşimlerinin kesme dayanımlarını belirleyen bir tasarım denklemidir. İkincisi kolon-kiriş birleşimlerinin göçme biçimlerini belirleyen yeni bir metodolojidir. Üçüncüsü ise kolon-kiriş birleşimleri için yeni bir basınç çubuğu-gergi yöntemidir.

2. Önerilen tasarım denklemi

Kolon-kiriş birleşimleri üzerine pek çok parametrik çalışma yapılmış ve birleşim kesme dayanımının kiriş çekme donatısı oranı, beton silindir dayanımı, etriye oranı arttırıldıkça artacağı, h_b/h_c oranı arttıkça azalacağı, kolon eksenel yükü ve kolon donatı oranından ise bağımsız olduğu görülmüştür. Kolon-kiriş birleşimleri için önerilen denklem aşağıdaki gösterilmiştir:

$$V_j = \frac{0.71\ \beta\ \gamma (100\ * \frac{A_{sb}}{b_b d_b})^{0.4289}\ (\frac{b_c + b_b}{2})\ h_c \sqrt{f_c}}{(\frac{h_b}{h_c})^{0.61}} + \alpha\ A_{sye} f_y \qquad (1)$$

$\alpha = 0.664$ düşük etriyeli birleşimler
$\alpha = 0.600$ orta miktarlı etriyeli birleşimler
$\alpha = 0.370$ yüksek miktarlı etriyeli birleşimler
b_c = Kolonun gövde genişliği (mm)
b_b = Kirişin gövde genişliği (mm)
A_{sb}=Kiriş çekme donatı alanı (mm^2)
d = Kirişin faydalı yüksekliği (mm)
f_c = Beton silindir dayanımı (MPa)

Önerilen denklem, ilgili kaynaklarda verilen diğer denklemlere göre daha fazla ayrıntılı olarak geliştirilmiştir. Zira:

1. Etriyelerin birleşim kesme dayanımına katkısını gerçekçi bir biçimde modellemektedir.
2. Kiriş boyuna donatı oranı, h_b/h_c ve beton silindir dayanımının, birleşim kesme dayanımı üzerindeki etkisini gerçekçi bir biçimde dikkate alır.
3. Önerilen denklem basittir ve birleşimlerin kesme dayanımlarını çok iyi yakınsaklıkla ve standard sapma küçük çıkacak şekilde belirlemektedir.

3. Önerilen basınç çubuğu-gergi modeli

Yazar tarafından önerilen basınç çubuğu gergi modeli Şekil 1'de görülmektedir. Önerilen model göçme yüklerini 99% gerçeklikle belirlemektedir.

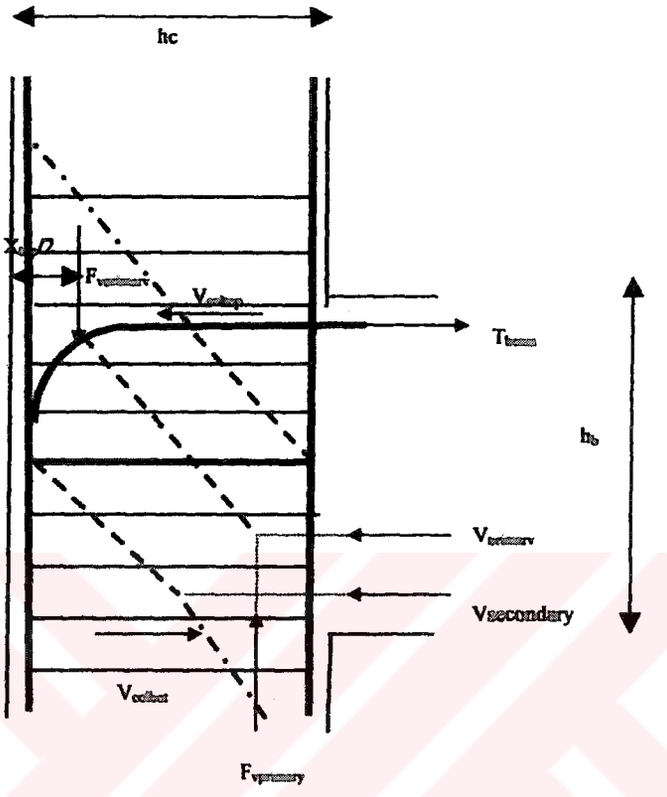

Şekil 1: Önerilen basınç çubuğu-gergi modeli

Model üzerinde yapılan parametrik çalışmaların hepsi, deney sonuçlarıyla uyumludur.

1. Etriyesiz birleşimlerde yapılan parametrik çalışmada model tarafından bulunan, $V/b_e\ h_c\ f_c$ (normalize edilmiş kesme dayanımı) artan beton silindir dayanımı karşısında hafifçe azalmaktadır. Bu bulgu test sonuçları ile uyumludur. Çünkü gerçekte birleşim kesme dayanımı beton silindir dayanımının kendisi ile değil karekköküyle orantılıdır.
2. Etriyeli birleşimlerde yapılan parametrik çalışmada model tarafından bulunan, $V/b_e\ h_c\ f_c$ (normalize edilmiş kesme dayanımı) artan beton silindir dayanımı karşısında hafifçe azalmaktadır. Bu bulgu test sonuçları ile uyumludur. Çünkü gerçekte birleşim kesme dayanımı, beton silindir dayanımının kendisi ile değil karekköküyle orantılıdır.
3. Etriyesiz birleşimlerde model, birleşim kesme dayanımının, kolon eksenel gerilmesinden bağımsız olduğunu öngörmektedir. Bu sonuç, Şekil 4.29'da görülen test sonuçları ile uyumludur.
4. Etriyeli birleşimlerde model, birleşim kesme dayanımının, kolon eksenel gerilmesinden bağımsız olduğunu öngörmektedir. Bu sonuç, Şekil 4.29'da görülen test sonuçları ile uyumludur.

5. Etriyesiz birleşimlerde model, birleşim kesme dayanımının, kolon boyuna donatı oranından bağımsız olduğunu öngörmektedir. Bu sonuç, Şekil 4.26b'de görülen test sonuçları ile uyumludur.
6. Etriyeli birleşimlerde model, birleşim kesme dayanımının, kolon boyuna donatı oranından bağımsız olduğunu öngörmektedir. Bu sonuç, Şekil 4.26b'de görülen test sonuçları ile uyumludur.
7. Etriyesiz birleşimlerde model, h_b/h_c oranı arttıkça birleşim kesme dayanımının azalacağını öngörmektedir. Bu bulgular, Şekil 4.26d'deki deney sonuçları ile uyumludur.
8. Etriyeli birleşimlerde model, h_b/h_c oranı arttıkça birleşim kesme dayanımının azalacağını öngörmektedir. Bu bulgular, Şekil 4.26d'deki deney sonuçları ile uyumludur.

Yukarıda da anlatıldığı gibi model deney sonuçları ile tam uyumludur.

4. Göçme biçimlerini belirleyen yeni bir model

Tezin bu kısmında göçme biçimlerini belirleyen yeni bir model önerilmiştir. Bu modelde kiriş boyuna donatı oranı etriyesiz birleşimlerde aşağıdaki denklemle sınırlandırılmıştır.

$$\rho_{b\,lim} = 0.15\, h_c^{\,2}\,(b_c + b_b)\,\frac{f_c\,(1 - \frac{f_c}{250})}{h_b\; b_b d\; f_y} \qquad (2)$$

Orta miktarlı etriyeli birleşimlerde bu oran % 18 kadar arttırılır.

$$\rho_{b\,lim\,II} = 0.18 h_c^{\,2}(b_c + b_b)\frac{f_c(1 - \frac{f_c}{250})}{h_b b_b d\; f_y} \qquad (3)$$

Yüksek miktarlı etriyeli birleşimlerde bu oran, %22 kadar arttırılır.

$$\rho_{b\,lim\,II} = 0.22 h_c^{\,2}(b_c + b_b)\frac{f_c(1 - \frac{f_c}{250})}{h_b b_b d\; f_y} \qquad (4)$$

Yukarıdaki denklemlerde;
b_c = Kolonun birleşime bitişik kenar genişliği (mm)
b_b = Kirişin kenar genişliği (mm)
d = Kirişin faydalı yüksekliği (mm)
f_c = Beton silindir dayanımı (MPa)
h_b = Kiriş yüksekliği (mm)
h_c = Birleşimi oluşturan kolon kenar uzunluğu (mm)
f_y kiriş çekme donatıları akma dayanımı (MPa)

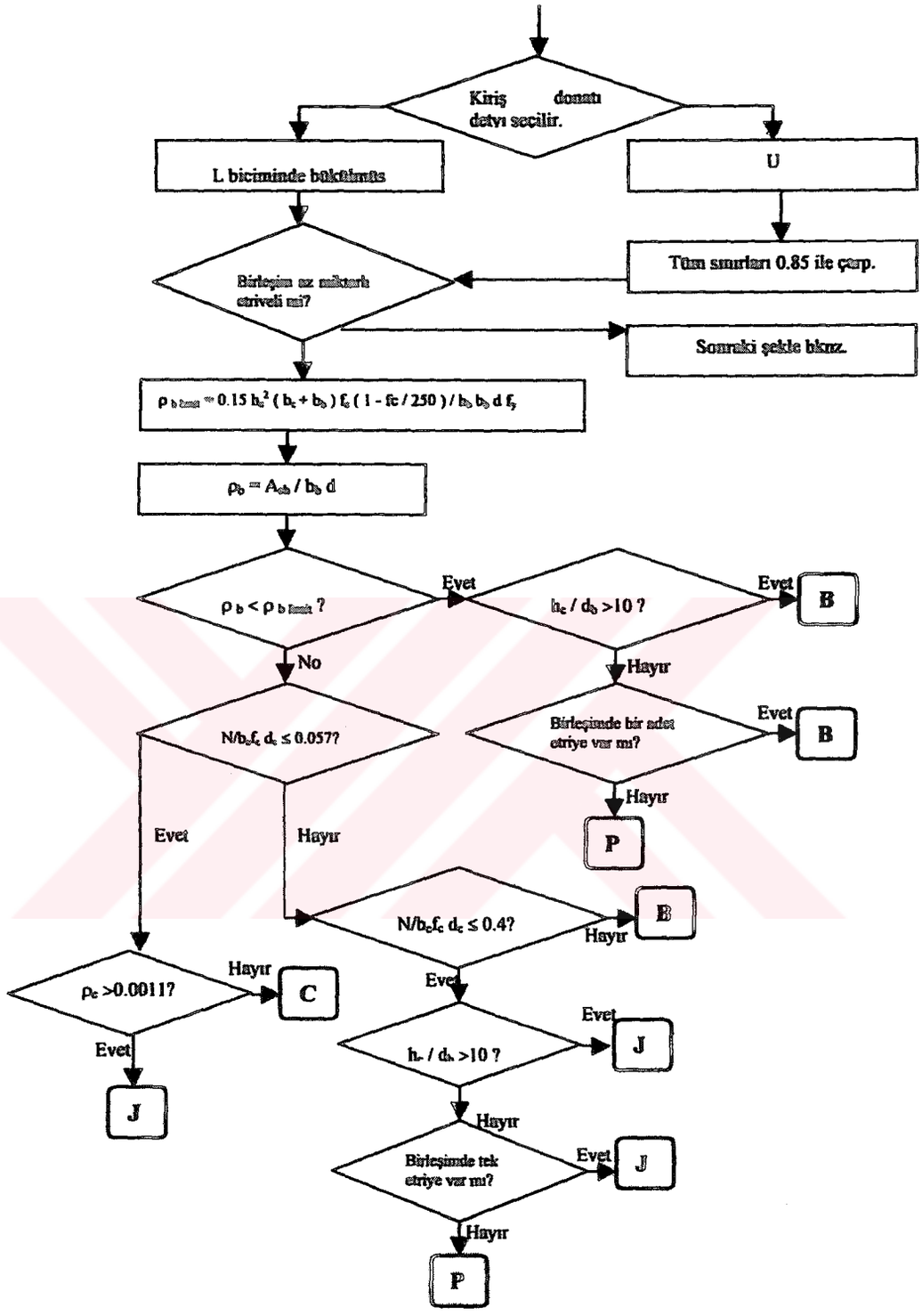

Şekil 2: Etriyesiz birleşimlerin göçme biçimlerini belirleyen model

Not: P ankraj göçmesi
C kolonda göçme
B kirişte göçme
JS birleşimde kesme göçmesi

T.C. YÜKSEKÖĞRETİM KURULU
DOKÜMANTASYON MERKEZİ

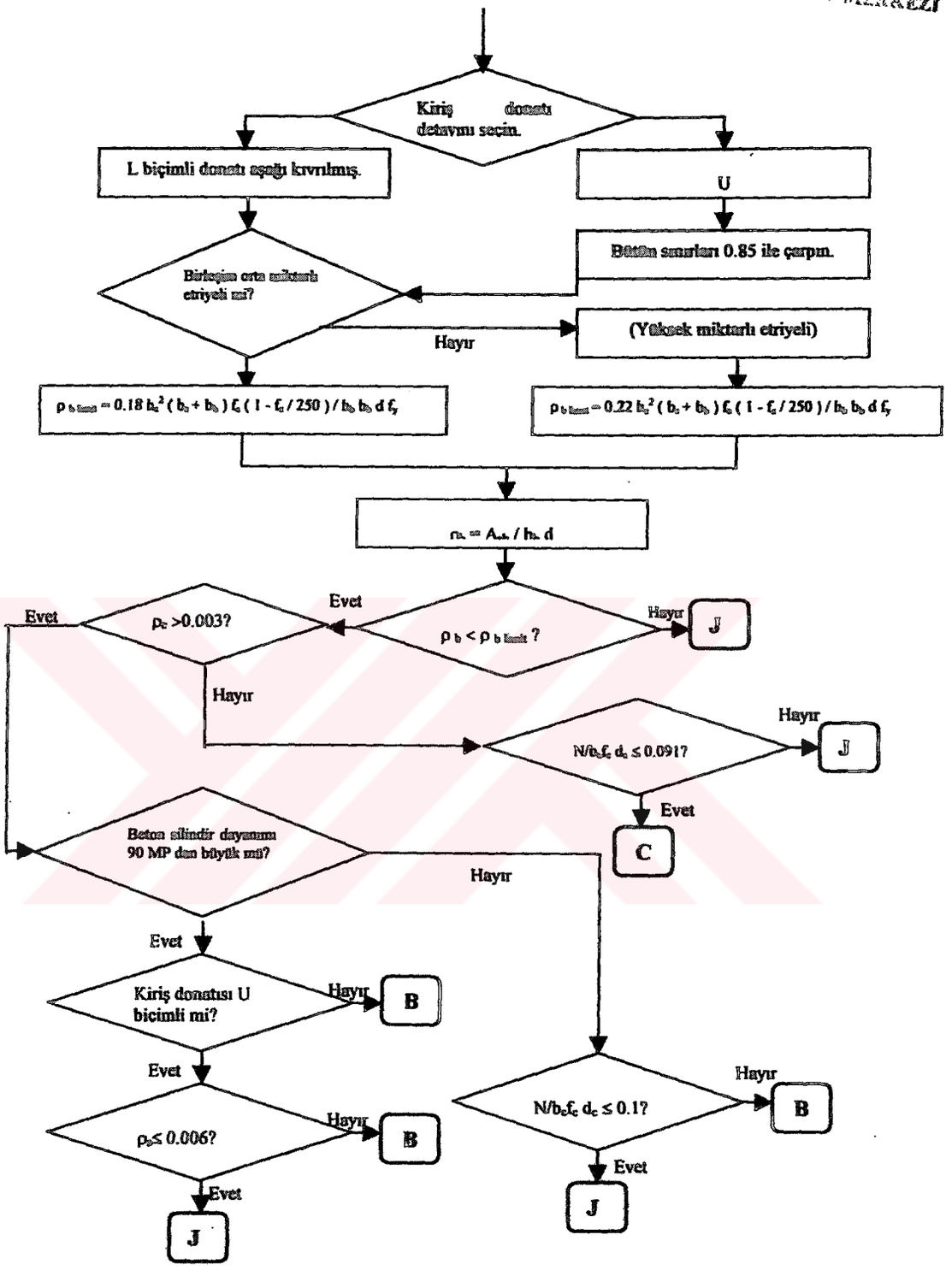

Şekil 3: Etriyeli birleşimlerin göçme biçimlerini belirleyen model

Not: P ankraj göçmesi
C kolonda göçme
B kirişte göçme
JS birleşimde kesme göçmesi

THE GRAVITY AND SEISMIC ANALYSIS AND DESIGN OF EXTERIOR BEAM-COLUMN JOINTS

SUMMARY

1. Overview of the thesis

This thesis has three original contributions. The first is the proposal for a new design equation for predicting the joint shear strength. The second is the proposal for a new methodology for predicting the failure modes of joints and the third is the proposal for a new strut and tie model for joints.

2. The Proposed Design Equation

Several parametric studies are carried out on an experimental database. The results have shown that the joint shear strength increases as the concrete cylinder strength, the beam longitudinal reinforcement ratio and the stirrup ratio increases. The joint shear strength decreases when the joint aspect ratio increases and the shear strength is independent of the column axial stress and the column longitudinal reinforcement ratio. The author has proposed Eq. (1) for predicting the shear strength of monotonically loaded exterior beam-column joints.

$$V_j = \frac{0.71\ \beta\ \gamma(100\ * \frac{A_{sb}}{b_b d_b})^{0.4289}\ (\frac{b_c + b_b}{2})\ h_c \sqrt{f_c}}{(\frac{h_b}{h_c})^{0.61}} + \alpha\ A_{sjc} f_y \qquad (1)$$

where $\alpha = 0.664$ for joints with low amount of stirrups
$\alpha = 0.6$ for joints with medium amount of stirrups
$\alpha = 0.37$ for joints with high amount of stirrups
b_c = Width of the column (mm)
b_b = Width of the beam (mm)
A_{sb}=Cross-sectional area of the beam tensile reinforcement (mm^2)
d = Effective depth of the beam (mm)
f_c = Concrete cylinder strength (MPa)

The equation is an improvement to other equations because:

1. It realistically models the contribution of stirrups in the joint.
2. It takes the influences of beam longitudinal reinforcement ratio into account.
3. It realistically models the influence of the joint aspect ratio.
4. It realistically models the influence of concrete cylinder strength.
5. The equation is simple and accurately predicts the joint shear strength.

3. The proposed strut and tie model

The author's simplified strut and tie model is shown in Figure 1. The model gives accurate predictions of the failure loads.

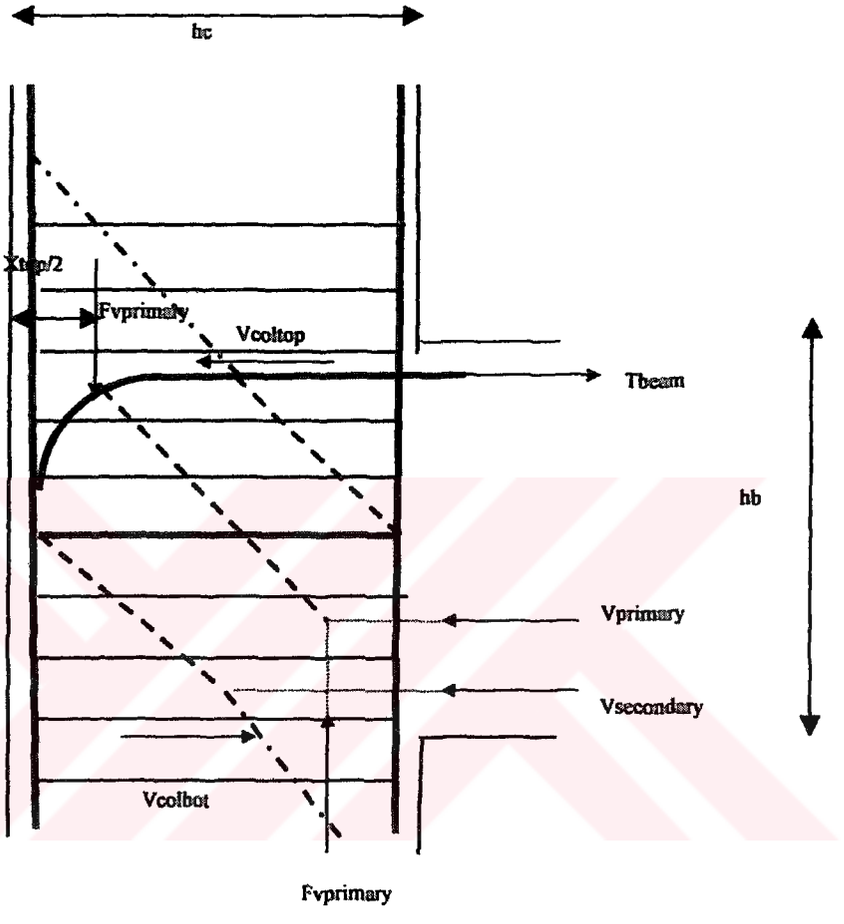

Figure 1: The proposed simple model of the author.

Parametric studies are carried out to investigate the influence of the concrete cylinder strength, column longitudinal reinforcement ratio, column axial stress and the joint aspect ratio in joints with and without stirrups.

1. The model predicted that the joint shear strength normalized by the concrete cylinder strength, $V/b_e\ h_c\ f_c$, slightly decreased due to increasing concrete cylinder strength in joints without stirrups. This prediction is in agreement with the test data because the joint shear strength, in reality, is proportional to the square root of the concrete cylinder strength.
2. The model predicted that the joint shear strength, normalized by the concrete cylinder strength: $V/b_e\ h_c\ f_c$, slightly decreased due to increasing concrete cylinder strength in joints with stirrups. This prediction is in agreement with the

test data because the joint shear strength, in reality, is proportional to the square root of the concrete cylinder strength, $\sqrt{f_c}$ not to f_c.

3. In joints without stirrups, the model predicted that the joint shear strength is independent of the column axial stress as the test data suggests.
4. In joints with stirrups, the model predicted that the joint shear strength is independent of the column axial stress as the test data suggests.
5. In joints without stirrups, the model predicted that the joint shear strength is independent of the column longitudinal reinforcement ratio as the test data suggests.
6. In joints with stirrups, the model predicted that the joint shear strength is independent of the column longitudinal reinforcement ratio as the test data suggests.
7. In joints without stirrups, the model predicted that the joint shear strength decreased with increasing joint aspect ratio. This is in agreement with the test data.
8. In joints with stirrups, the model predicted that the joint shear strength decreased with increasing joint aspect ratio. This is in agreement with the test data.

As apparent from the parametric studies, the model is in good agreement with the test data.

4. The Proposed Methodology for Failure Modes

In this part of the thesis, a new methodology for predicting the failure modes of joints is presented as shown in Figs. 2 and 3. The proposed methodology is different for joints without significant amount of stirrups and for joints with medium or high amount of stirrups. For joints without stirrups, the following limit equation is proposed for the beam longitudinal reinforcement ratio:

$$\rho_{b\,\lim} = 0.15\, h_c^{\,2}\,(b_c + b_b)\,\frac{f_c\,(1 - \frac{f_c}{250})}{h_b\, b_b d\, f_y} \qquad (2)$$

For joints with medium stirrups, this limit is increased by 18 %.

$$\rho_{b\,\lim it} = 0.18 h_c^{\,2}(b_c + b_b)\frac{f_c(1 - \frac{f_c}{250})}{h_b b_b d\, f_y} \qquad (3)$$

For joints with high amount of stirrups, this limit is increased by 30%.

$$\rho_{b\,\lim it} = 0.22 h_c^{\,2}(b_c + b_b)\frac{f_c(1 - \frac{f_c}{250})}{h_b b_b d\, f_y} \qquad (4)$$

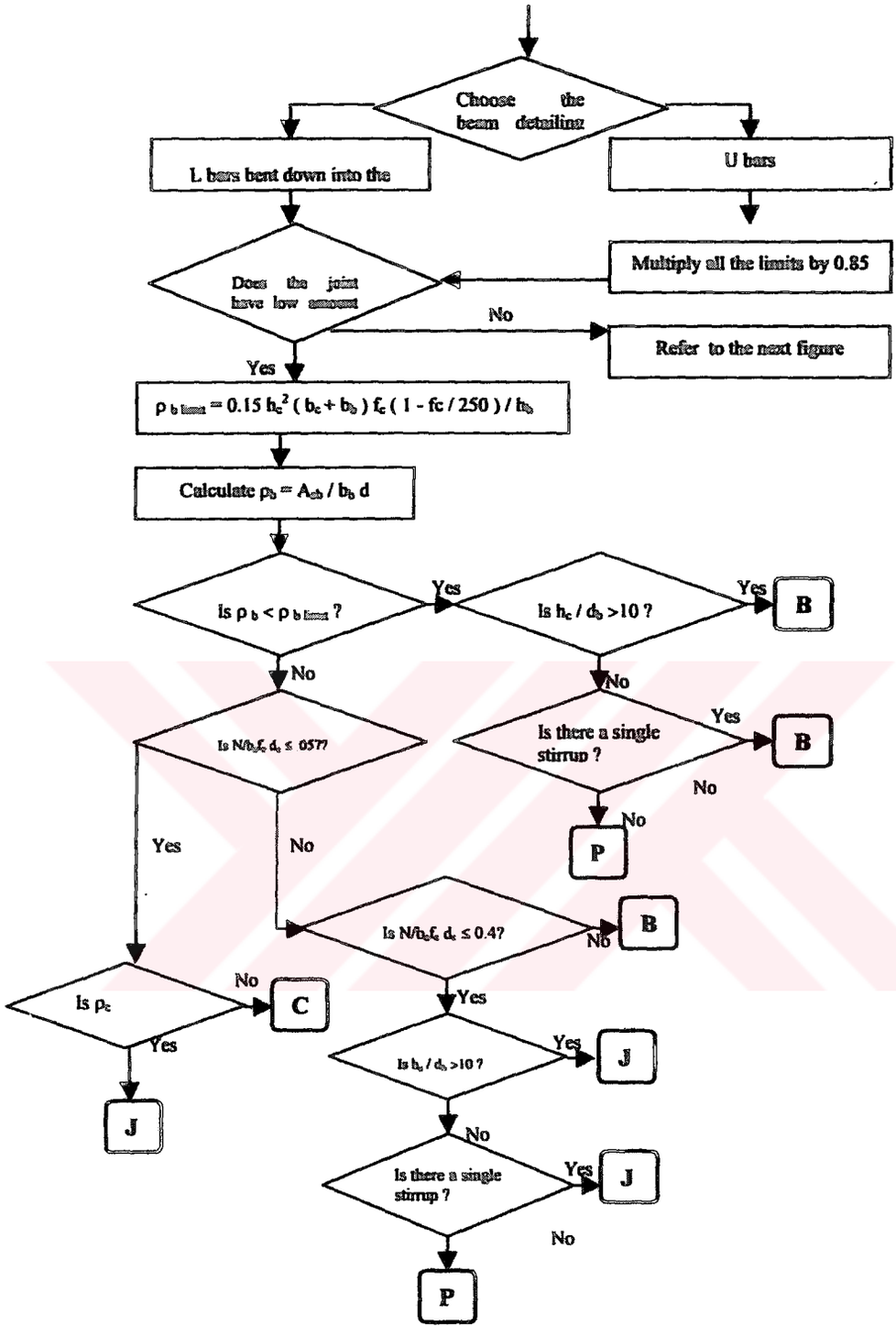

Figure 2 : The methodology for joints with low amount of stirrups

Note: P represents the connection zone reinforcement pullout
C represents the column failure
B represents the beam failure
JS represents the joint shear failure

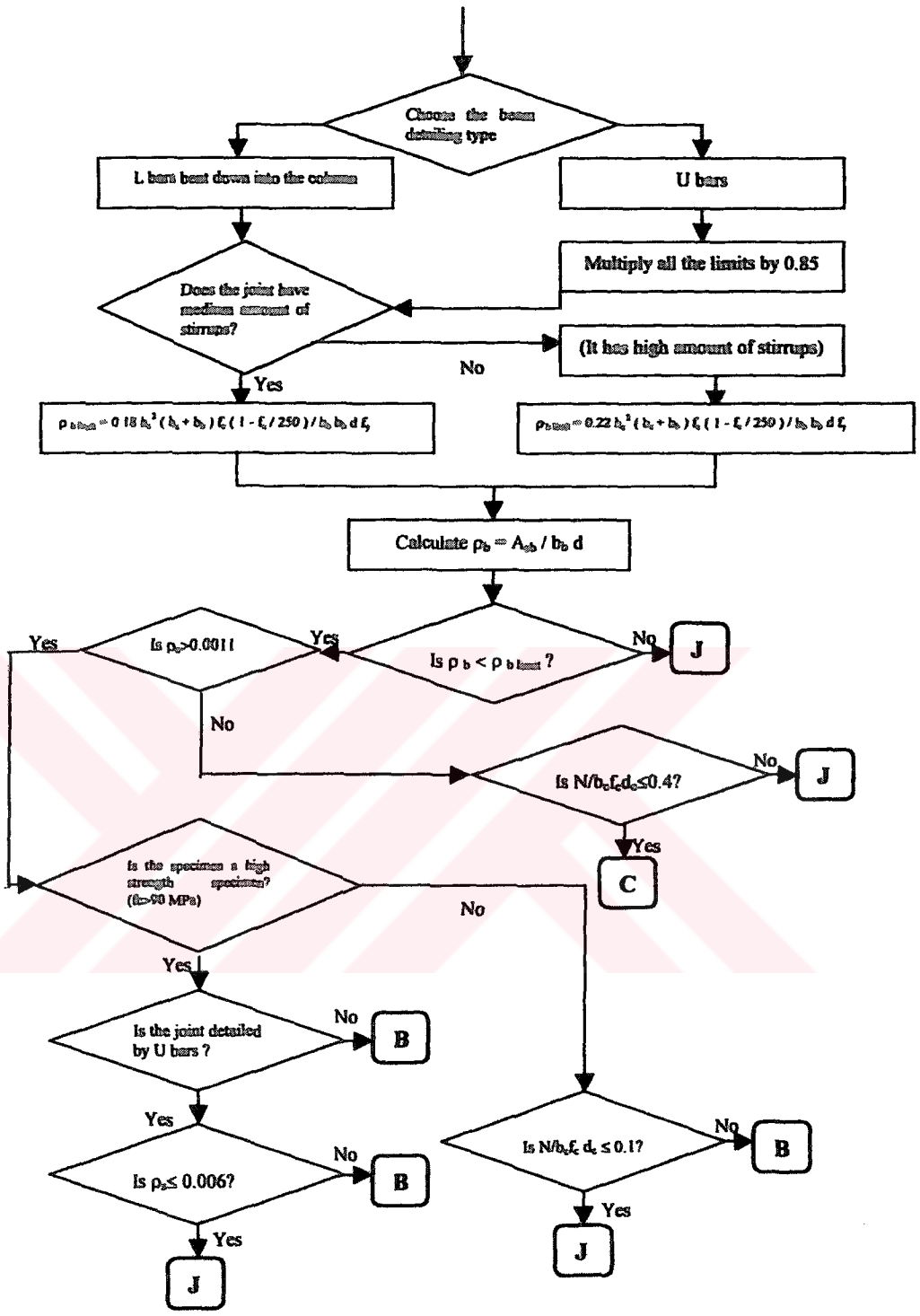

Figure 3: The methodology for joints with medium and high amount of stirrups

1. INTRODUCTION

The aim of this thesis is to propose alternative simple methods and design equations for predicting the failure modes and failure loads of exterior beam-column joints. The author carried out an extensive literature review on the tests of exterior beam column joints. The details of this survey with a commentary of the author at the back are given in Chapter 3 and Chapter 4. The survey also highlighted an important problem. The codes all over the world conflicted with each other. The American Code relied on the concrete resistance to joint shear while the New Zealand Code relied on the transverse reinforcement. It seemed that the Turkish Code was similar to the American code in this respect. Greater part of the author's time has been spent on methodologies for predicting the shear resisting mechanisms of exterior beam column joints. The codes all over the world generally were dependent on the empirical results, lower bound particularly, of various tests that are piled. The author of this thesis on the other hand, believed that the use of rational was so much imperative in structural engineering. This implied that simple hand analysis techniques could produce member forces of adequate accuracy with relative speed and may result in a more accurate representation of the effects, which involved the use of appropriate models to reflect the true nature of reinforced concrete. For this reason, the author aimed at developing a simple model for the exterior beam-column joints. The beam-column joints were designed with the simple strut and tie model developed. The model predicted both the failure load and the failure mode. The results of the parametric studies on the predictions of the failure loads of the existing tests on exterior beam column connections were quite accurate. Following this, a simple design equation is developed for predicting the joint shear strength. The equation developed and the background of the equation are given in Chapter 4. The author's literature survey showed that there was no model in literature, except for the model of Taylor, for predicting the failure modes of monotonically loaded beam-column joints. The author's model for predicting the failure modes is given in

Chapter 5. As far as the author's knowledge is concerned, this is the most comprehensive model in literature for predicting the failure modes.

1.1 The objective of the thesis

The objective of this thesis is to analyze exterior beam column connections and develop design methods. In this respect, the exterior joints are investigated both as monotonically loaded joints and cyclically loaded joints. The outline of the thesis is given below:

Chapter 1. Summary of the objectives of the thesis

Chapter 2. General literature review on strut and tie modeling

Chapter 3. Design and analysis of the cyclically loaded beam column joints

Chapter 4. Design and analysis of the monotonically loaded exterior beam-column joints and the development of a design equation for predicting the shear strength of joints.

Chapter 5. Development of a strut and tie model and the development of a simple methodology for predicting the failure modes.

Chapter 6. Conclusions

Appendix A: The algorithms of the computer programs written by the author.

Appendix B: The results of the parametric studies of the author.

In the rest of the thesis the author of this thesis will be referred to as the author.

2. DESIGN OF REINFORCED CONCRETE STRUCTURES USING STRUT AND TIE MODELS

2.1 Introduction

The history of strut and tie modeling dates back to the beginning of the last century when **Ritter (1899)** and **Mörsch (1912)** introduced the truss analogy. This method was later improved by **Leonhardt (1965), Rüsch (1964)** and **Kupfer (1964)** and based on rational principles by **Marti (1985)** and **Mueler (1978). Collins and Mitchell (1980)** further expanded the model taking the deformations into account and applied the model on shear and torsion design of non-prestressed and concrete beams. In this chapter, the strut and tie modelling technique will be described in detail using the work of **Schlaich and Schafer (1987, 1991).**

2.2 Division of The Structures into B and D Regions

The regions of a structure, in which the Bernoulli hypothesis of plane sections remain plane is valid are called B regions. **Hsu (1996)** calls these regions the main regions. **Hsu (1996)** states that a main region is one where the stresses and strains are distributed so regularly that they can easily be expressed mathematically. This means the stresses and the strains in the main regions are governed by simple equilibrium and compatibility equations. If this region is un-cracked, then the bending theory for linear elastic materials apply. For cracked B regions on the other hand, applying the code of practice rules will be adequate. **Hsu (1996)** explains the equations to be used for different parts of a frame as follows:

" For columns that are under M and N , the equilibrium equations come from the parallel force equilibrium condition; while the compatibility equations are governed by Bernoulli's hypothesis of plane sections remain plane. In the case of beams

subjected to V and T, the stresses and strains should satisfy the two dimensional equilibrium and Mohr's circular compatibility conditions. Thus the main regions of a structure are designed directly using the sectional values of M, N, V and T according to the four action diagrams derived from structural analysis. In contrast, a local region is one where the stresses and strains are so disturbed and irregular that they are not amenable to mathematical solution. In particular, compatibility conditions are difficult to apply. Local regions include the connections between a beam and a column, the ends of a column or a beam, the corbels and the region adjacent to a concentrated load. In the design of local regions, the stresses are usually determined by equilibrium conditions alone, while the strain compatibility conditions are neglected. A local region is treated as an isolated free body subjected to external boundary forces. Boundary forces are calculated from the four action diagrams at the boundary regions."

The above mentioned methods for the design of main regions or the B regions can not be used however, when the strain distribution in the structure is non-linear. Corners, bends, openings, the regions around the concentrated loads are all typical examples to these D or the above mentioned local regions. Here D is the abbreviated form of discontinuity or the disturbance regions. Figure 2.1. demonstrates the identification of D and B regions. In determining the division line between the D and B regions, increased effort for accuracy is certainly unnecessary. This is due to the Saint-Venant principle which says that:

"If the forces that are acting on an elastic structure are interchanged with a system of forces that are statically equivalent to the previous system, the new redistribution of this loading will change the stresses around a small region in the vicinity of this loading. However at a greater distance with respect to the dimensions of the structure that the replacement is made, the effect of the new loading on the stresses can be neglected."

Figure 2.2. explains the principle of Saint Venant. According to the above considerations, the B regions can be assumed to lie at a distance h from the geometrical discontinuity or the concentrated load where h is equal to the depth of

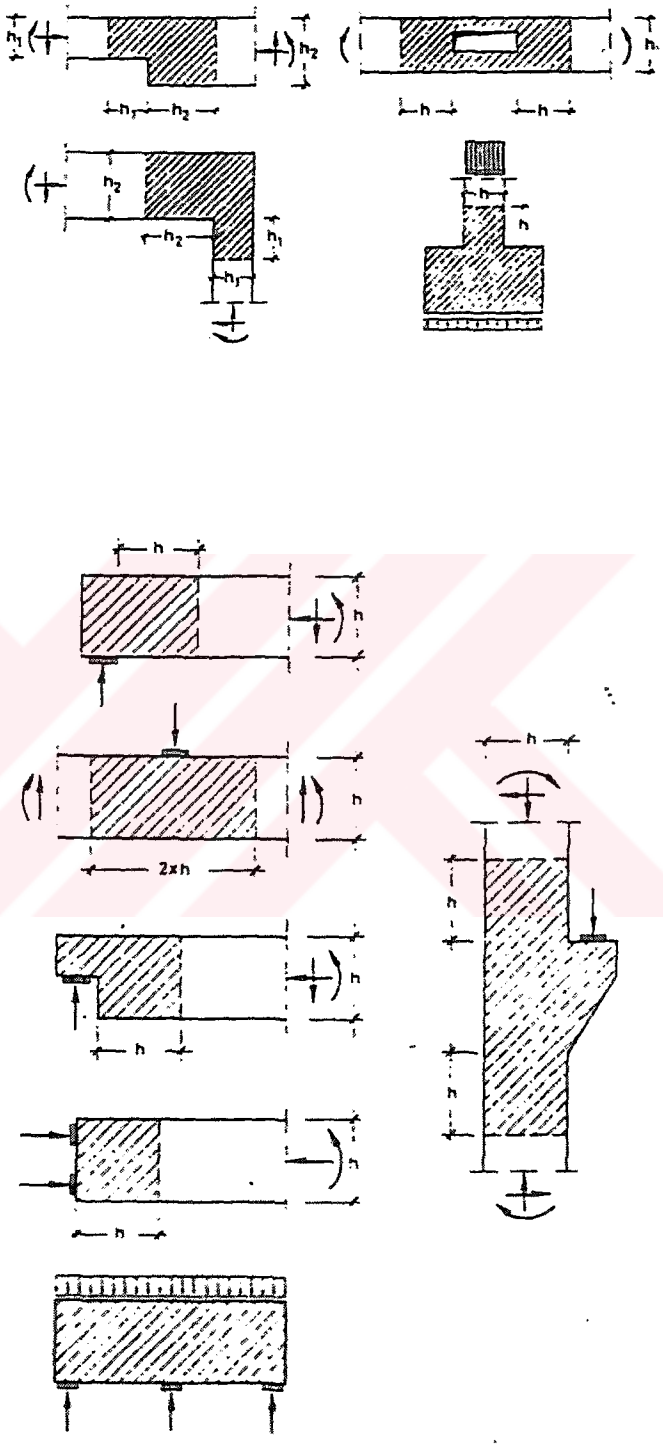

Figure 2.1 : The identification of B and D regions.

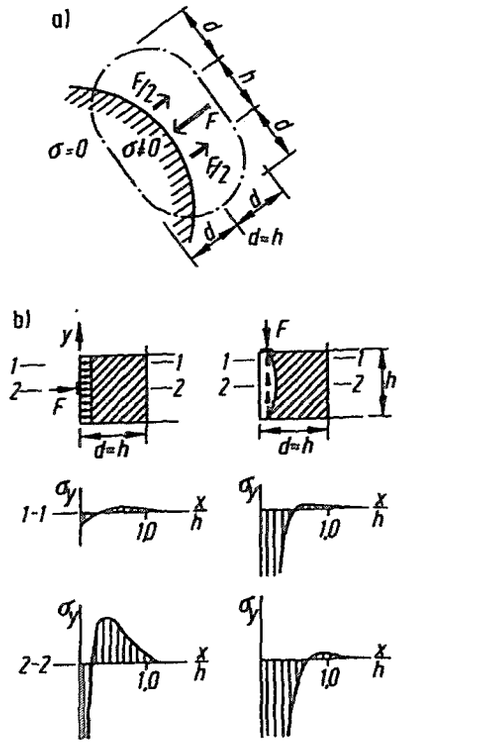

Figure 2.2 : The principal of Saint Venant.

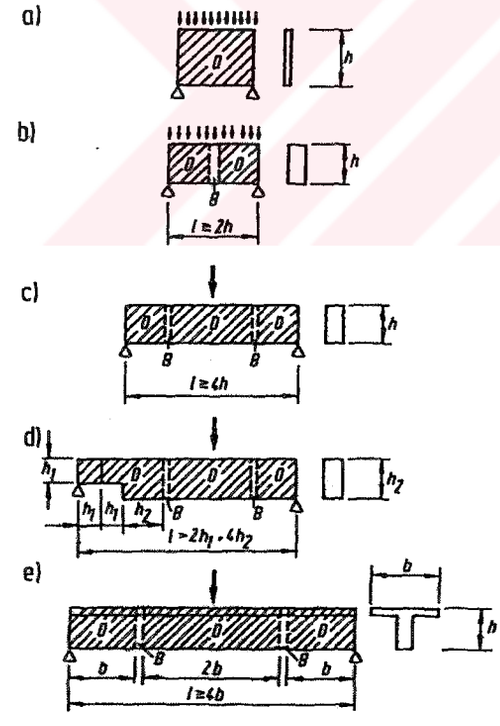

Figure 2.3 : D regions in structures with different geometries.

the adjacent B region. Figure 2.3 is adapted from the paper of **Schlaich and Schafer (1991)** and depicts the D regions in structures with different geometries.

2.3 Theoretical background for strut and tie modelling

In a strut and tie model, struts will represent the compressive stress fields, whereas the ties are used to account for one or several layers of tensile reinforcement. However model ties can also be used to represent the concrete tensile stress fields. In short, concrete ties can be assumed at places where no reinforcement is provided. **Hsu (1996)** formulates this as follows:

"A rational design of reinforced concrete structures must be based on the mechanical properties of the materials. Concrete has high strength in compression but very low strength in tension. When concrete is used in a structure to carry loads, the tensile regions are expected to crack and therefore, must be reinforced by materials of high tensile strength, such as steel. This concept of utilising concrete struts to resist compression, and reinforcing ties to carry tension, gave rise to the term "strut and tie model." In this model, the concrete compression struts and the steel tension ties form a truss that is capable of resisting the applied loads. As such, this concept has been used, intuitively, by engineers to design reinforced concrete structures since the late 19^{th} century."

Hsu (1996) states that when the concept of strut and tie truss is applied in the main regions where the angles of the struts are regular, the model is defined as "truss model" whereas when it is applied on the local regions where the angles of the struts are irregular, the model should be defined as "strut and tie model". The above considerations imply that the structures are designed according to the lower bound theorem of plasticity which says that:

"A load system that is based on a statically admissible stress field which nowhere violates the yield condition is a lower bound to the collapse load. In other words, in plastic design if a stress field that is in equilibrium with the applied loads and satisfies the static boundary conditions, the structure will be safe provided that the yield criteria is nowhere violated. This can be ensured by proportioning the cross

sectional dimensions of struts and ties such that their strength is greater than or equal to the corresponding internal actions."

Structural materials, especially concrete allows only limited plastic deformations, the strut and tie model has to be developed such that the deformations are nowhere greater than the deformation capacity before the assumed state of stress is reached in the rest of the structure.

In highly stressed regions, the ductility requirement is satisfied by adjusting the struts and ties of the model to the direction and size of the internal forces determined from the theory of elasticity. In normally or lightly stressed regions, however, the direction of the struts and ties in the model may depart significantly from the elastic pattern without violating the structure's ductility. The ties can be arranged according to the practical considerations. The structure will adapt itself to the assumed internal structural system.

If the theory of plasticity is applied instead of the theory of elasticity, some more ultimate load capacity can be utilised. The serviceability requirement should be checked, however, in this case.

2.4 Modelling of D regions

All the forces acting on the boundaries of the D regions have to be determined before the D regions are designed using the strut and tie models. This implies that if the D sections are bounded by B regions, the forces and stresses have to be taken from B regions designed according to the conventional section analysis . New models can be developed by tracing the flow of forces through the structure, using the load path method (Figure 2.4).

The load paths of the strut and tie model should not cross each other. Developing a strut and tie model will be much more simplified if the elastic stresses and the principle stress directions are known beforehand from an elastic FEM analysis. This would lead the designer to place the struts in the main direction of principle

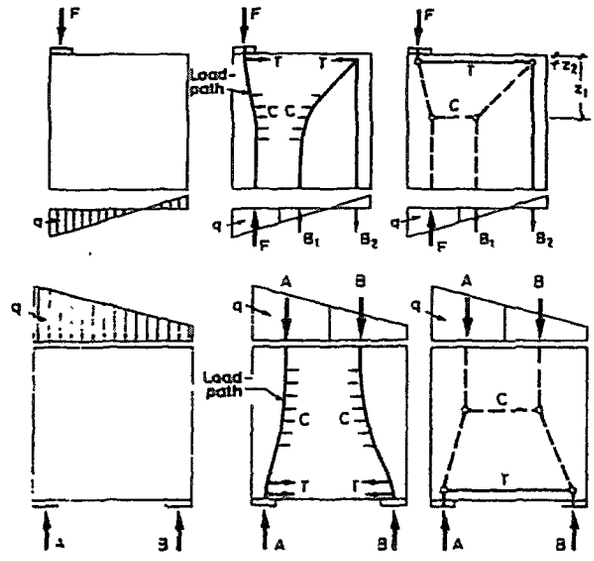

Figure 2.4 : Load path method

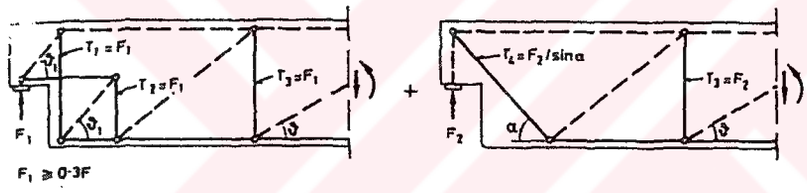

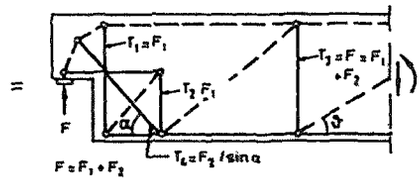

Figure 2.5 : The combination of two models

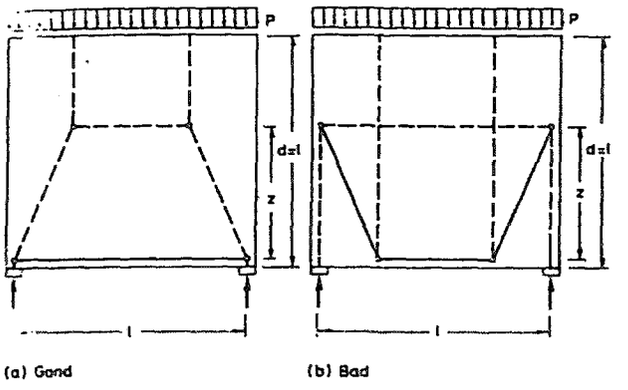

Figure 2.6 : Two alternative models

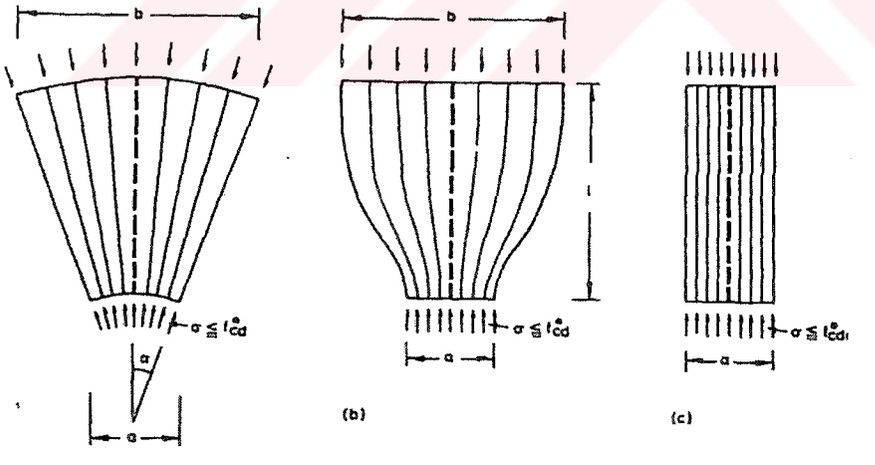

a. Fan mechanism b. Bottle shaped stress field c. Prismatic stress field

Figure 2.7 : The stress fields in a D region

compressive stresses and ties in the mean direction of the tensile stresses. The angles between the struts and ties should be chosen larger than 45^0 (better 60^0). The above would mean that the strut and tie model proposed is confined only to a particular loading condition and can not be applied to another loading pattern without appropriate modifications. Two models can be superimposed only if the angles between the struts and ties satisfy the above rule for the angles. Figure 2.5 demonstrates the combination of two models. Figure 2.6. shows two alternative models, one good model with short ties and one bad model with longer ties.

2.5 Basic Compression Fields

There are three basic compression fields to be considered for strut and tie modelling. These stress fields are clearly explained in the paper of **Schlaich and Schafer (1987, 1991).**

a. The fan shaped stress field (Figure 2.7.a) is an idealisation of a stress field with negligible curvature. No transverse stresses are developed in this type stress field.

b. The bottle shaped stress field (Figure 2.7.b), there are significant transverse stresses: compression in the bottle neck and tension further away. The transverse tension can cause early failure. This can be incorporated into design via two methods: The first is reinforcing the tensile stress field by transverse ties or if this is not possible, second, to consider the transverse tension when determining the failure load of the strut.

c. The prismatic or parallel stress field (Figure 2.7.c) is a frequent special case of the preceding two stress fields.

2.6 Designing by Strut and Tie Models

Schlaich and Schafer (1987,1991) established the principles of the design of structures using strut and tie models in their papers. They recommended that before starting the analysis, it is necessary to divide the structure into B and D regions. The

B regions can be analysed by the help of standard methods using codes of practice and the bending moments (M), normal forces (N), shear forces (V) and torsional moments (M_T) are determined. These internal forces or moments of the B regions constitute the boundary forces for the D regions. Structures such as slabs and shells are consisted of mainly by B regions while structures consisting of deep beams are typical D regions. Table 2.1. adapted from the papers of **Schlaich and Schafer (1987, 1991)** demonstrates clearly the outline of the analysis.

Table 2.1. Analysis leading to stresses or strut-and-tie forces

<table>
<tr><td colspan="2" rowspan="2">Analysis \ Structure</td><td colspan="3">Structure consisting of:</td></tr>
<tr><td colspan="2">B- and D-regions
e.g., linear structures, slabs and shells</td><td>D-regions only
e.g., deep beams</td></tr>
<tr><td colspan="2">Overall structural analysis
(Table 2) gives:</td><td>B-regions
Sectional effects
M, N, V, M_T</td><td>D-regions*
Boundary forces:
Sectional effects</td><td>D-regions
Support reactions</td></tr>
<tr><td rowspan="3">Analysis of inner forces or stresses in individual regions</td><td>State I
(uncracked)</td><td>Via sectional values
A, J_s, J_T</td><td colspan="2">Linear elastic analysis*
(with redistributed stress peaks)</td></tr>
<tr><td>State II
(cracked)</td><td colspan="3">Strut-and-tie-models
and/or nonlinear stress analysis*</td></tr>
<tr><td colspan="2">Usually truss</td><td colspan="2"></td></tr>
</table>

* May be combined with overall analysis.

Table 2.2. Structural analysis of statically indeterminate structures

Limit state	Overall structural behavior	Corresponding method of analysis of sectional effects and support reactions	
		Most adequate	Acceptable
Service-ability	Essentially uncracked	Linear elastic	—
	Considerably cracked, with steel stresses below yield	Nonlinear	Linear elastic (or plastic if design is oriented at elastic behavior)
Ultimate capacity	Widely cracked, forming plastic hinges	Plastic with limited rotation capacity or elastic with redistribution	Linear elastic or nonlinear or perfectly plastic with structural restrictions

After the sectional forces of B regions and consequently the boundary forces of the D regions are determined, the struts and ties of the strut and tie model proposed for the D regions have to proportioned. The strut and ties are represented by straight lines and the curvatures are concentrated at the nodes. Consequently the strut and tie forces are calculated so that they satisfy equilibrium. These are the inner forces. The struts and ties are dimensioned taking the crack width limitations into account. The above procedure indicates that the structure is designed according to the lower bound theorem of plasticity. Concrete is a material which allows only limited plastic deformations. For this reason, the strut and tie model has to be selected so that this deformation limit is not exceeded.

In highly stressed regions, dimensioning and arranging the struts and ties according to the theory of elasticity would be adequate to satisfy the ductility requirements. In normally or lightly stressed regions on the other hand, the direction of the struts and ties in the model may differ significantly from the elastic pattern without exceeding the structure's ductility. The ties may be placed according to practical considerations. The acceptance of the principles of the theory of elasticity in strut and tie modelling ignores some of the ultimate load capacity which could be maintained by a pure application of the theory of plasticity. On the other hand, the same model can be used for both the ultimate load and the serviceability check. **Schlaich and Schafer** state that:

"Orienting the geometry of the model to the elastic stress distribution is also a safety requirement because the tensile strength of concrete is only a small fraction of the compressive strength. Prismatic stress fields according to the theory of plasticity (neglecting the transverse tensile stresses due to the spreading of forces in the concrete) are unsafe for plain concrete. This would be unsafe even if both requirements of the lower bound theorem of the theory of plasticity are fulfilled, namely, equilibrium and $F/A<f_c$. Compatibility evokes tensile forces, usually transverse to the direction of the loads which may cause premature cracking and failure. The bottle shaped compressive stress field which is introduced above

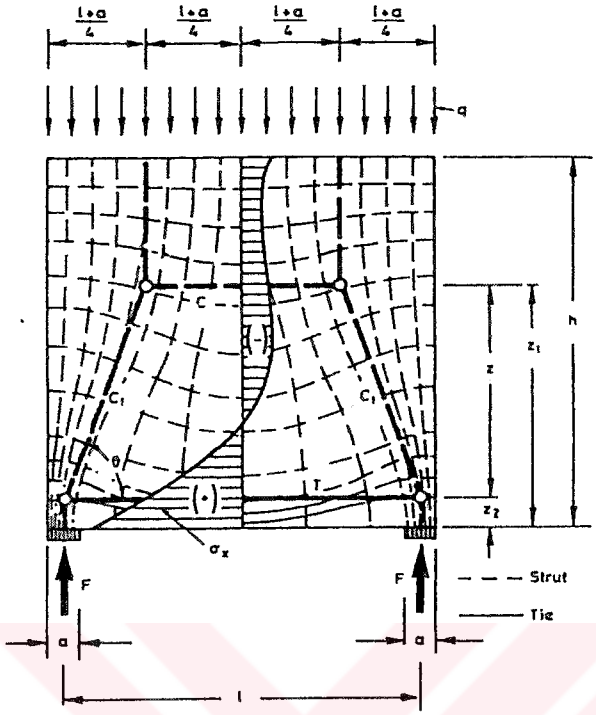

Figure 2.8 : The load paths and the corresponding strut and tie model.

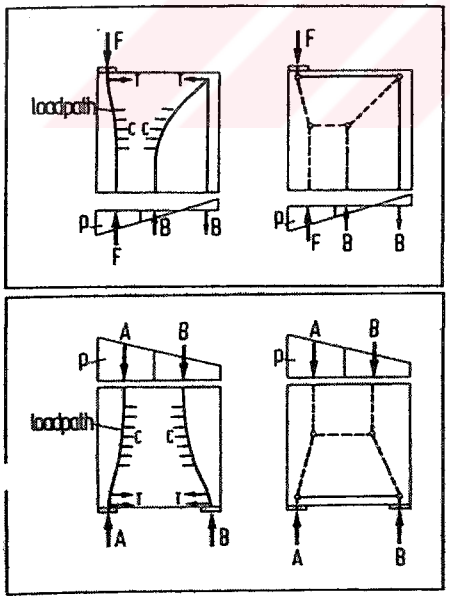

Figure 2.9 : A typical D region with the elastic stress trajectories and the elastic stresses.

eliminates such "hidden" dangers when occasionally the model chosen is too simple."

Strut and tie modelling will be much simplified if the elastic stresses and principal stress directions are obtained. Such an elastic analysis can be carried out by the computer programs available today. The direction of the struts can then be taken as the mean direction of the principal compressive stresses or the important struts or ties can be placed at the centre of gravity of the corresponding stress diagrams. However, if no elastic analysis is available and if there is no time to prepare one, it is easy to prepare one using the so called "load path method". Figure 2.8 demonstrates the load paths and the strut and tie model. A typical D region with the elastic stress trajectories and the elastic stresses are demonstrated in Figure 2.9.

For using the load path method, first, the equilibrium of the boundary forces is maintained. The stress diagram is subdivided in such a way, that the loads on one side of the structure find their counterpart on the other, provided the load paths do not cross each other. The load paths have the direction of the applied loads or reactions and tend to take the shortest possible streamlined way in between. Curvatures concentrate near stress concentrations (support reactions or singular loads). Up to now, only the equilibrium in the direction of the applied loads has been considered. After all the load paths are sketched, further struts and ties must be added for transverse equilibrium acting between the nodes. The ties are arranged parallel to the sides of the concrete surface due to considerations of practicability and of crack distribution requirements. Equilibrium in a given model is possible only for a special loading case.

In the choice of the model, it should be taken into account that loads try to use the path with the least forces and deformations. The model with the least and shortest ties is the best because reinforced ties are much more deformable than concrete struts. In choosing the model between several possible ones, it is important to use the path with the least forces and deformations. Since reinforcement ties can deform more than the struts, the model with the least and shortest ties is the best. **Schlaich and Schafer (1991)** suggested that the criteria for a good model is formulated as

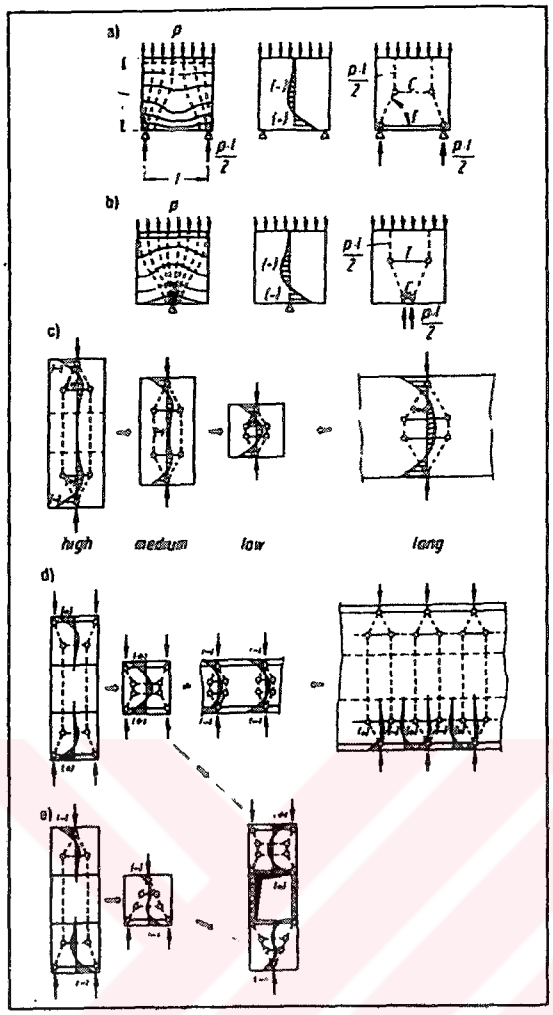

Figure 2.10 : The two most frequent and most useful strut and tie models.

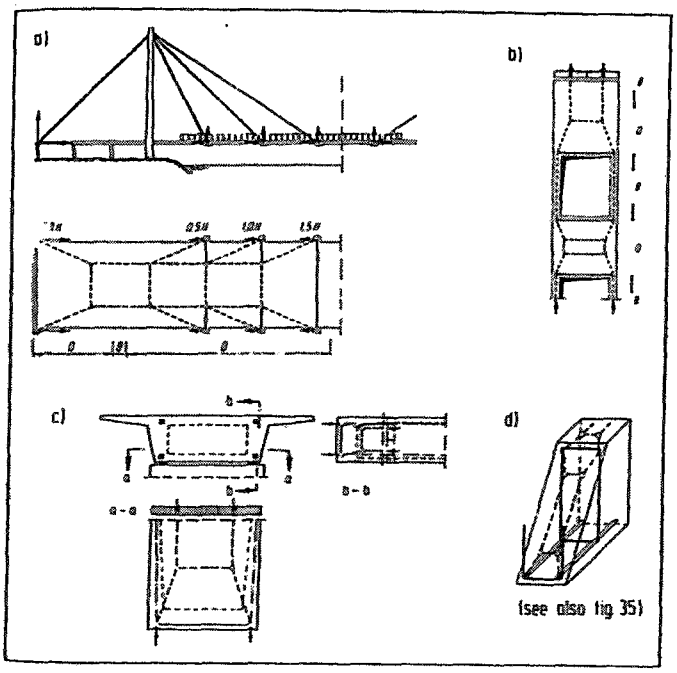

Figure 2.11 : Four examples of strut and tie models

$$F_i \, l_i \, \varepsilon_{mi} = \text{minimum} \qquad (2.1)$$

where

Fi is the force in strut or tie i

li is the length of member i

ε_{mi} is the mean strain of member i

The authors derived this equation from the principle of minimum strain energy for linear elastic behaviour of the struts and ties after cracking. The concrete struts are usually neglected in this procedure because the strains of the struts are usually much smaller than those of the steel ties. This is the main criteria in preventing inappropriate models.

The two most frequent and most useful strut-and-tie models can be viewed in Figure 2.10. One particular strut and tie model can appear in many different structures. Four examples are given in Figure 2.11.

2.7 Dimensioning

2.7.1 Dimensioning the ties

Tie forces are carried by the reinforcement. Crack widths can be analysed if the reinforced tie is considered as a prismatic reinforced bar with an effective concrete area.

2.7.2 Dimensioning the concrete struts or compression stress fields

The struts in the model are the resultant of the stress fields. By the definition of the strut and tie model, it is known that the deformations and the curvatures are concentrated at the nodes. This implies that the struts can be taken as straight. However, in a highly stressed structure, the straight lengths of the struts can be decreased either by refining the model or spreading the node over a substantial

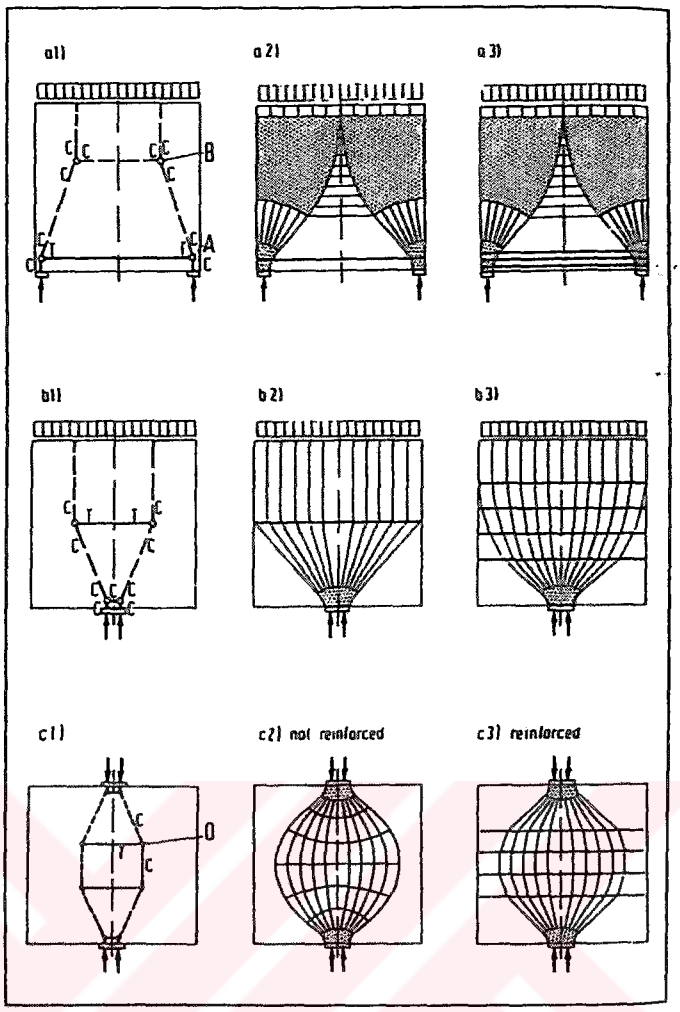

Figure 2.12 : Some typical examples of strut and tie models

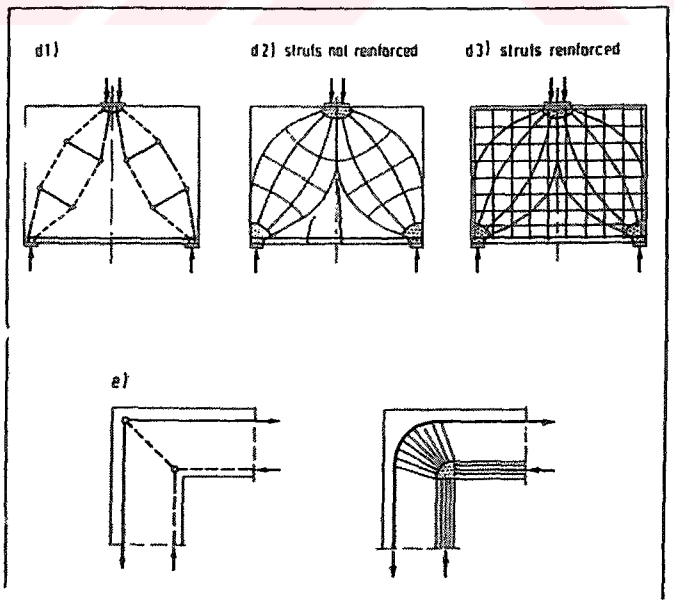

Figure 2.13 : Some typical examples of stress fields, nodes and corresponding reinforcement

length of the strut. The three different compression fields were listed above. These were the fan shaped stress field, the bottle shaped stress field and the prismatic stress field. For dimensioning, the following simplified design strength values for f_{cd} are proposed by **Schlaich and Schafer (1991):**

$f_{cd} = 1.0\ f_c'$ for an undisturbed and uniaxial state of stress. (2.2)

$f_{cd} = 0.8\ f_c'$ for compression fields with cracks parallel to the compression stresses.

$f_{cd} = 0.6\ f_c'$ for compression fields with skew cracks

where

f_{cd} denotes the concrete compressive design strength for uni-axial compression according to the code of practice.

The authors state that the design values which are given above for cracked concrete are for structural concrete. Skew cracks are not expected if the theory of elasticity is followed. The allowable stresses in the concrete will be dealt in more detail in the following paragraphs.

2.7.3 Nodes

Nodes are the intersection points of one or more struts and ties. **Schlaich and Schafer (1987)** classify the nodes into two. They state that:

The nodes of a model are in fact the idealisation of the reality. If one of the struts or ties represent a concentrated stress field, the deviation of forces tends to be locally concentrated also. On the other hand, for wide concrete stress fields joining each other or with tensile ties, which consist of many closely distributed reinforcing bars, the deviation of forces may be smeared (or spread) over some length. Therefore, in the former case the nodes are called singular (or concentrated) nodes, whereas in the latter case they are called smeared (or continuous nodes). Figure 2.12 and 2.13 shows some typical examples of strut and tie models, their stress fields, nodes and corresponding reinforcement. D regions usually contain both smeared nodes as well as singular nodes and the check of stresses in the smeared nodes is usually

unnecessary. However if a smeared node is a CCT (compression-compression-tension) node and if it is assumed to remain uncracked, the tensile stresses of the corresponding concrete stress field need to be checked. For a safe design of smeared or singular nodes, the following rules are necessary:

In smeared nodes, where wide concrete stress fields join each other, it is sufficient to ensure safe anchorage of the reinforcing bars in the smeared node and to catch the outermost fibres of the deviated compressive stress field with reinforcement.

However, the design of singular nodes are very important. They should be carefully designed so that the deformation limits should not be exceeded and the crack widths should be taken into consideration. Three important criteria should be considered.

1. The geometry of the node should be related to the incoming forces and their widths. The reinforcement anchored in a node should be regularly distributed over a height u.
2. The average compressive stresses in the node regions should be less than the following limits according to **Schlaich and others (1991).**

f_{cd}= 1.1 f_c' in nodes where only compression struts meet. (2.3)

f_{cd}= 0.8 f_c' in nodes where tensile bars are anchored and an allowance in strength must be made for bond action.

3. Safe anchorage of ties in the nodes has to be assured. This implies that the minimum radii of the bars and the anchorage lengths will be determined in accordance with the codes.

There are four types of nodes in a reinforced concrete structure. This classification of nodes which is mentioned below depends on the types of struts (C) and ties (T). These nodes are:

CCC- node

CCT-node

T.C. YÜKSEKÖĞRETİM KURULU
DOKÜMANTASYON MERKEZİ

CTT-node

TTT-node

The principles remain the same if more than three struts or ties meet.

Due to cracking, the compressive concrete strength will be reduced naturally. This reduction in concrete strength will be dealt in more detail in the following paragraphs.

2.8 Failure of reinforced concrete structures

It is usually very difficult to calculate the stress state of every strut and tie in the local regions of a reinforced concrete structure. This would imply the incorporation of the complex constitutive relationships to account for the multi-axial stress state of the concrete. For this reason, it is certainly necessary to find some simple criteria regarding the failure of reinforced concrete structures. **Vollum (1998)** and **Park and Paulay (1975)** classify the stress state in the concrete as follows:

2.8.1 Bi-axial and Tri-axial Compression

Transverse compression is beneficial, particularly if the concrete is confined in both directions transverse to the axis of applied stress. This could be in the form of bi-axial or tri-axial compression.

2.8.2. Transverse tension

Transverse tension is harmful due to cracks forming. If this tension is carried by reinforcement and adequately confined, then the extent of this cracking will be not so severe, but still a reduction factor for the concrete strength should be taken into account. This would certainly result in different compressive stresses to be adapted for the cracked and un-cracked concrete.

2.8.3. Cracks which are not parallel to compressive stresses

Schlaich and others (1987) suggest a third type of crack which forms unparallel to the compressive stresses. These types of cracks are also detrimental.

2.9 Design Stresses for Concrete

Most researchers such as **Nielsen (1978), Vecchio and Collins (1982)** have taken this reduction of strength in concrete into account. Some codes such as **CEB Model Code 90** also makes this differentiation. Usually, this cracked concrete strength is chosen some fraction of the uni-axial cylinder strength.

$$f_{cd} = \nu f_c' \qquad (2.4)$$

where

ν is an effectiveness factor that is less than 1.

Based on the tests on beams, **Nielsen (1978)** and his co workers suggested an empirical equation for the cracked concrete strength

$$f_{cd} = (0.7 - f_c' / 200) f_c' \qquad (2.5)$$

where

f_c' is in MPa and $f_c' < 60$ MPa.

Again based on test results, **Ramirez and Breen (1983)** suggested the following formula

$$f_{cd} = 2.82 \ f_c' / \sqrt{f_c'} \qquad (2.6)$$

Marti (1985) suggested the following formula for the stress levels in the struts and nodes

$$f_{cd} = 0.6 f_c' \qquad (2.7)$$

For dimensioning different types of struts and nodes, **Schaich (1987)** and **Mac Gregor (1988)** suggested the following equations:

f_{cd}= 0.85 f_c' for undisturbed and uniaxial state of compressive stress that may exist for prismatic struts. (2.8)

f_{cd}= 0.68 f_c' for tensile strains and/or reinforcement perpendicular to the axis of the strut which may cause cracking parallel to the strut with normal crack width. (2.9)

f_{cd}=0.51 f_c' for tensile strains causing skew cracks and/or reinforcement at skew angles to the strut's axis. (2.10)

f_{cd}= 0.34 f_c' for skew cracks with extraordinary crack width. Skew cracks would be expected if modelling of the struts departs significantly from the theory of elasticity's flow of internal forces. (2.11)

f_{cd}= 0.5 f_c' for isolated compression struts in deep beams or D regions. (2.12)

Based on the test results, **Bergmeister (1991)** proposed the following equation for the cracked concrete strength.

$$f_c = (0.5 + 1.25 / \sqrt{f_c'})\, f_c' \quad (2.13)$$

where:

fc' is in MPa. The above equation is valid for the concrete cylinder strengths of 20 to 80 MPa.

The cracked concrete strength which is recommended by CEB Model Code is also of interest. The author of this thesis preferred the recommendations of CEB Model Code 90 due to the simplicity of these equations. CEB code states that:

f_{cr}= 0.6 f_c (1-f_c/250) the compressive strength for the cracked concrete (2.14)

f_{uncr}=0.85f_c (1-f_c/250) the compressive strength for the un-cracked concrete (2.15)

CEB Model recommends the following rules for the design of strut and tie models:

1. The angles between the struts and ties should be about 60^0 but not less than 45^0.

2. If the model is in accordance with a linear elastic stress field, it is not necessary to check the serviceability limit state.

3. Struts should be placed in the direction of the linear elastic stress field while the ties can be arranged due to practical considerations.

Finally, the recommendations of **Collins and Mitchell** will be mentioned.

$$f_{c2max} = 1 / (0.8+170\ \varepsilon_1)\ f_c < f_c \qquad (2.16)$$

$$\varepsilon_1 = \varepsilon_x + (\varepsilon_x + 0.002)/ \tan^2\theta$$

The recommendations of Mitchell and Collins takes the reduction factor as a function of the transverse strain.

2.10 The Advantages and Disadvantages of Strut and Tie Modelling

2.10.1 The Advantages

1. Strut and tie models are simple.

2. Designers can visualise the flow of forces. Throughout the design process, the designer is fully aware of the stresses and strains and the behaviour of the structure during the successive loading stages.

3. Designers can predict the failure loads with a few iterative calculations.

4. Designers can predict the failure modes with a few iterative calculations.

5. As stated by **Vollum (1998)** a unified approach can be developed for the design of a complete structure, including B and D regions. The model can also account for the design of members loaded to combined shear, torsion and bending.

2.10.2 The Disadvantages

1. The model can not account for detailing.

2. In the hands of inexperienced engineers, unsuitable models can be adapted.

3. There are difficulties in incorporating the seismic forces in to the strut and tie model. This is due to the fact that the strains in the transverse reinforcement in the joint is usually dependent on the number of cycles. Also the extent of damage in the joint is dependent on the magnitude and number of cycles.

3. CYCLICALLY LOADED BEAM COLUMN JOINTS

3.1. Introduction

This chapter reviews the previous research on cyclically loaded beam column joints. The experiments carried out on cyclically loaded beam-column joints are usually on interior joints in the literature. The principles of these studies however, can well be applied on exterior joints. Before reviewing the test data, the differences in the behaviour of exterior and interior joints have to be clarified.

3.2 Comparison Between Interior and Exterior Reinforced Concrete Beam-Column Joint Behaviour

The only published work on the differences between interior and exterior beam column joints is that of **Fuji & Morita's (1991).** The specimen configuration and loading equipment and the details of the joint reinforcement in the tests of Fuji and Morita are given in Figs. 3.1 and 3.2. In Fig. 3.3, the typical crack patterns in the exterior and interior beam-column joints are shown. The comparison of the test results for exterior and interior joints are given in Fig. 3.4. Fuji and Morita have suggested that the shear cracking capacity of the joint concrete is increased with the increase of the column axial load for interior and exterior joints and the shear cracking is not influenced by the amount of joint hoop reinforcement. The effects of column load and the amount of joint hoop on the joint shear strength were more noticeable for exterior joints than for interior joints. In interior joints, the joint hoop reinforcement had no effect on the load-deflection curves and the deflection was caused solely by joint shear, whereas in exterior joints 50% of the total deflection was due to the joint shear strain. Fuji and Morita have proposed a simple model shown in Fig.3.5, to simulate the reduction of joint shear rigidity under cyclic load reversals. Fig.3.6. shows the envelopes of cyclic joint shear stress versus shear strain curves. Fuji and Morita suggested that the joint shear stress versus shear strain

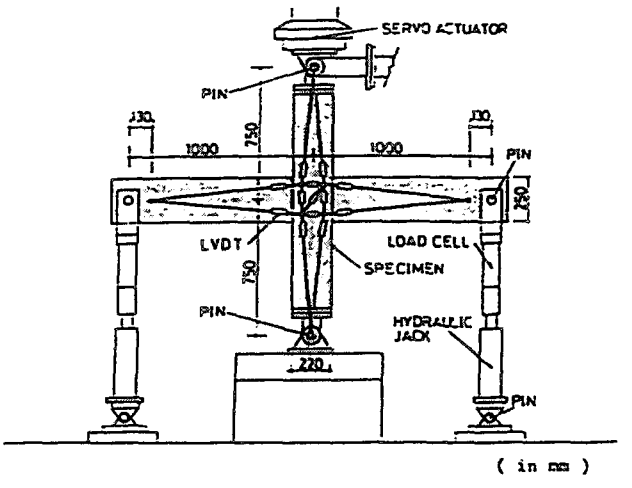

Figure 3.1 : The specimen configuration and loading equipment

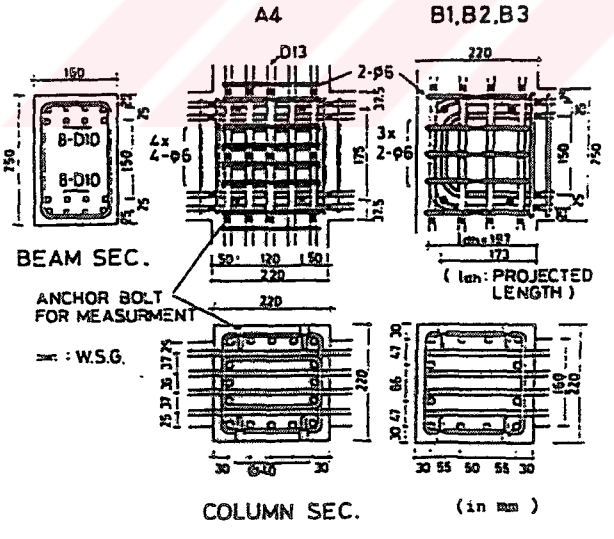

Figure 3.2 : The details of the joint reinforcement

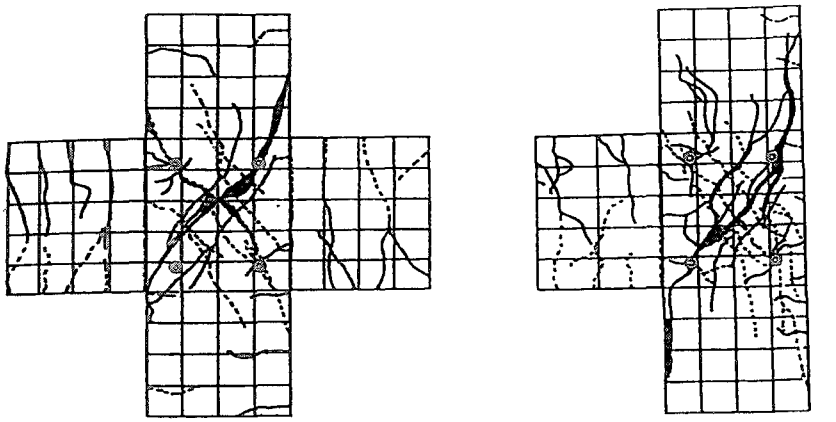

Figure 3.3 : Typical crack patterns in the exterior and interior beam column connections

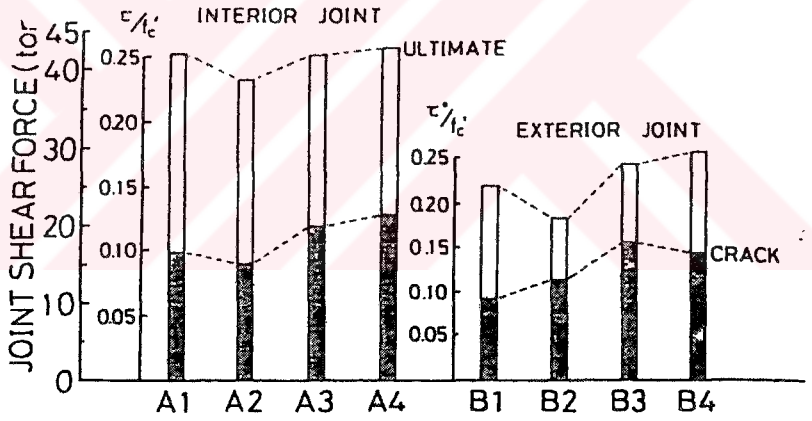

Fig. 6--Comparison of test results

Figure 3.4 : The comparison of the test results for exterior and interior joints.

relationship was strongly influenced by the loading history. The test results have shown that hoop strain increased abruptly with hoop yielding. Even in heavily reinforced joints, hoop strain reached the yield strain. The hoop strain at the maximum load attained yield strain in every specimen, however at lower load levels there was considerable difference in measured hoop strain between specimens with high column load and low column load. This argument clearly indicates the beneficial effect of the column axial load in reducing the amount of joint shear reinforcement. It can be stated that if joint shear failure is prevented and the column axial load is kept constant during disturbance, the shear reinforcement amount can be reduced. The New Zealand Code takes the advantage of column load into account.

Due to the extensive cracking in joint concrete, the linear distribution of strain across the column end section could not be maintained and the stress in every column bar shifted to tension side from the calculated value. This proved that intermediate column bars were ineffective as vertical shear reinforcement. The shear transfer mechanisms of joint reinforcement and the proposed fan shaped mechanism are shown in Fig. 3.7 and 3.8 respectively.

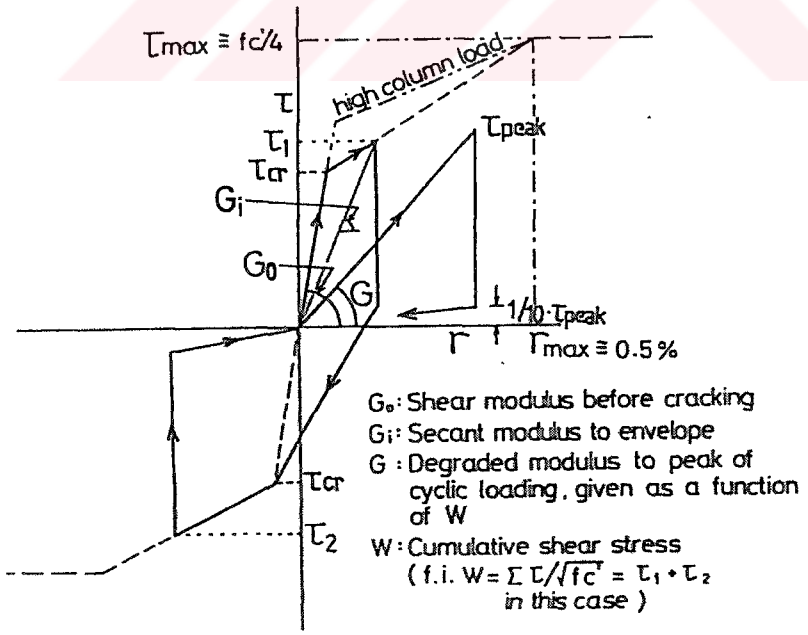

Figure 3.5. Degradation model of shear rigidity.

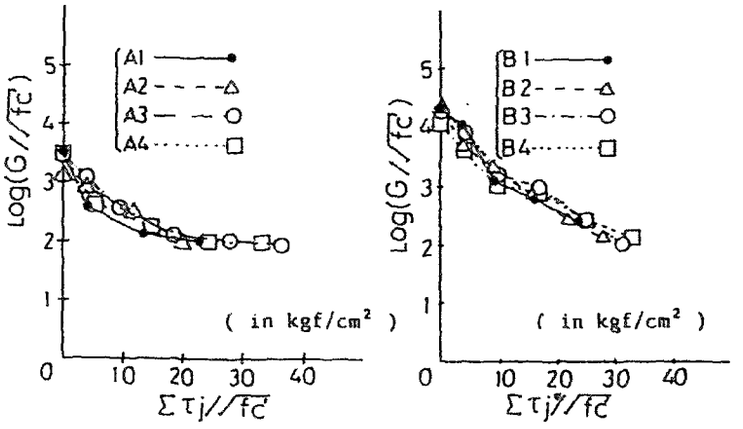

a) Interior joint b) Exterior joint

Figure 3.5b. Degradation model of shear rigidity.

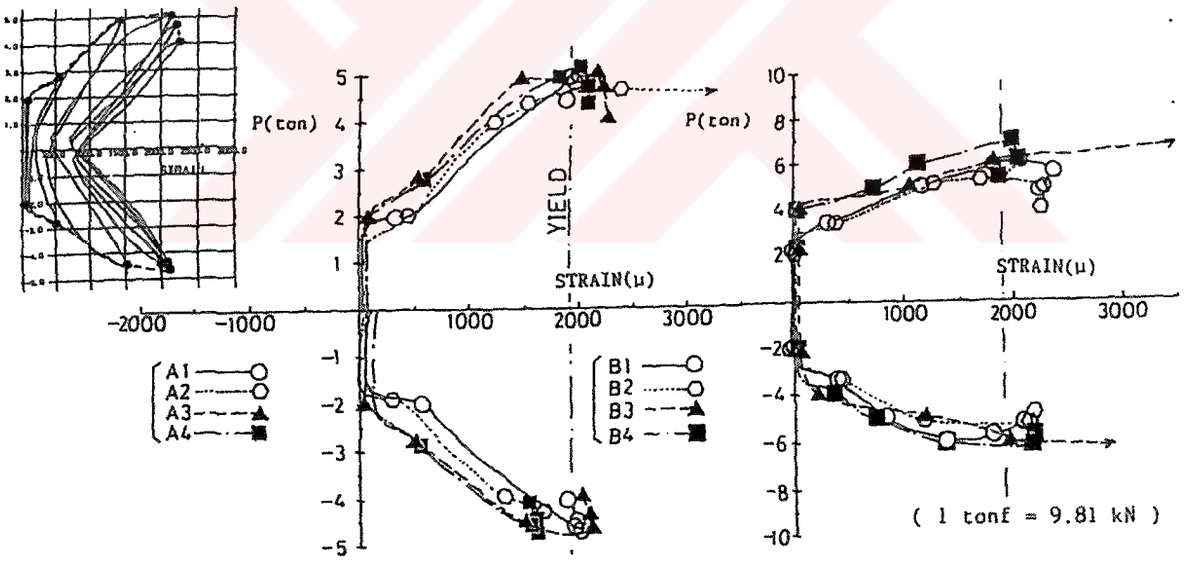

a) Interior joint b) Exterior joint

Figure 3.6. The envelopes of cyclic joint shear stress versus shear strain curves.

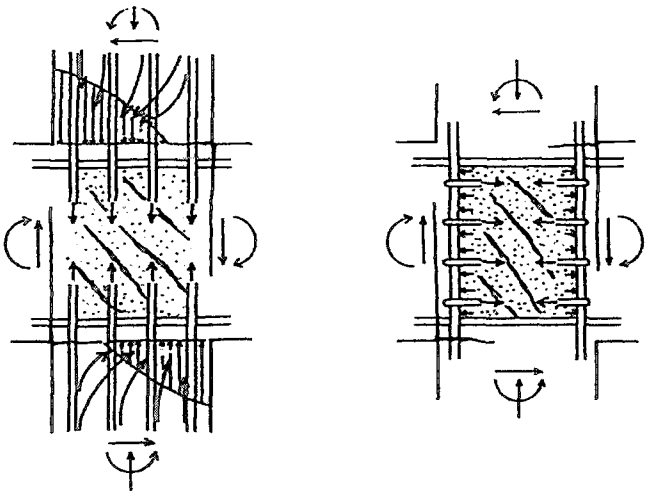

a) Hoop tension b) Column bar tension

Figure 3.7. The shear transfer mechanisms of joint reinforcement

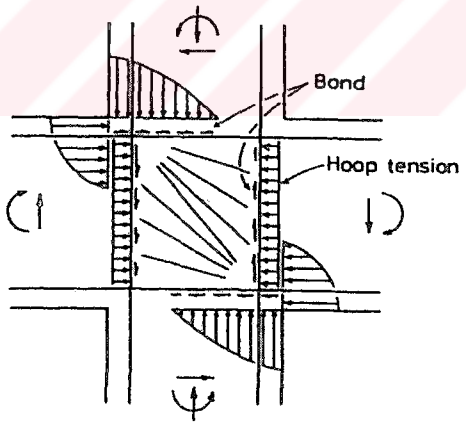

Figure 3.8. The fan shaped mechanism

3.3. The Design Philosophy of Weak Beams Strong Columns

The very first principle in the design of cyclically loaded beam-column joints is that the connections should be designed on the weak beam strong column principle. The seismic design codes all over the world are based on the principle of weak beams and strong columns. However this attitude should have some limits. **Aoyama (1993)** states that there are two earthquake resistant design methods. The first is the strength design, where the structure is designed so that it shall have a large lateral load resisting capacity and the second is the ductility design, where the structure is provided with a large inelastic deformation capacity. If the structure is designed according to the ductility design method, it is important not to end up with brittle failures, such as shear and anchorage failure, even under the most severe earthquake conditions. Obviously, the critical sections will have the need for inelastic deformations and the best is to dissipate the vibrational energy of the structure through stable hysteresis at the plastic hinges. These plastic hinges should be prevented at the columns since it is hard for the large inelastic deformations to form in columns and secondly, the columns support the upper stories. **Aoyama (1993)** states that plastic hinges should form in the beams, because first, large inelastic deformations can easily develop; second, stable and large hysteretic energy can be dissipated without significant loss of resistance; third, failure of some beams will not result in the failure of the whole frame and fourth, plastic hinges can develop at all beam ends simultaneously. As a result, it is desirable to have beam side sway mechanism in a frame rather than column side sway mechanism. This is achieved by either designing the beams to be weaker than columns or designing the columns to be stronger than the beams. This concept is called weak beam strong column frame design.

Aoyama discusses the beam column connections in the context of weak beam strong column criteria. He states that the design of beam column joints is very important since the joints must be designed so as not to fail in shear before the flexural yielding of beams, moreover they should have enough resistance against the yielding of the framing members. It is also necessary that bond deterioration of beam bars passing from the joint should be avoided since this action decreases the capacity of energy dissipation of the total frame.

Kamimura (1993) proposed an empirical equation to determine the ultimate shear strength v_u of the beam column connection.

$$v_u = (0.78 - 0.0016 f_c') f_c' + p_w f_y / 2 \quad (3.1)$$

where

f_c' is the concrete strength (kgf/cm^2)

p_w is the shear reinforcement ratio in the connection

f_y is the yield strength of the shear reinforcement (kgf/cm^2).

In order to investigate the differences allocated in the different codes, half scale interior beam column connections were tested under a constant vertical load and reversals of earthquake loading. **Aoyama (1993)** stated that the tests showed, the protection of the connection against shear at the initial yielding of the framing beams was not sufficient to avert shear failure of the connection. Large amount of horizontal shear reinforcement was effective in connection shear deformation. Therefore higher connection shear capacity could be reached with connection shear reinforcement larger than 1%. As soon as the shear stress at the joint reached a stress level as calculated from Kamimura's equation, connection shear resistance began to decrease by 20-40% after several cycles at story drift angles of 1/50 to 1/15 and the effect of connection shear reinforcement on shear capacity deterioration was small. If column depth was smaller than 20 times the beam longitudinal reinforcement diameter, bond of beam bars was deteriorated at a story drift angle of about 1/200, to cause the deterioration in energy dissipation capacity and finally better energy dissipation capacity was achieved by using beam longitudinal bar diameter smaller than a 1/25 of the column depth.

3.4 Difference in various codes in the design of reinforced concrete beam column joints

The United States **ATC Code (1978)** is based on the ultimate strength design using load factors and strength reduction factors whereas, Japanese code **(Aoyama 1993)** uses the allowable stress design for low level of earthquake loading and the ultimate member strength for estimating the collapse state resistance of the structure for high

earthquake loading. It should be noted that live load is approximately 10 % greater in the United States design procedure. On the contrary, the total weight of a structure for earthquake loading is greater in Japanese design procedure. The Japanese design code requires higher strength and stiffness than the American code.

As stated above, a reinforced concrete building in Japan is traditionally designed for a large earthquake load, which normally resulted in wide columns. However, the use of higher strength materials may decrease the dimensions of columns and the beam column joints may become the weak link of the chain. Therefore joint shear failure and a significant beam bar slippage within a joint should be prevented up to an expected structural deformation.

A striking difference exists in the seismic design provisions for beam column joints between the New Zealand and the United States Code ACI. The New Zealand Code entails a large amount of lateral reinforcement in a joint to resist a dominant part of the joint shear by the truss mechanism. The New Zealand Code Design procedure is based on the assumption that there is good bond stress transfer along the longitudinal reinforcement. The usage of high strength and greater diameter beam bars is restricted in the New Zealand code in order to decrease the bar slippage within a joint. On the contrary, the ACI design procedure is based on the assumption that the concrete strut resists the joint shear. The philosophy of the ACI towards the joint shear resistance can be formulated as 'the diagonal strut mechanism governs the shear resistance and all of the joint shear shall be carried by joint concrete'. The New Zealand Code on the other hand relies on the truss mechanism since large inelastic deformation reversals at beam end plastic hinges are assumed to cause residual tensile strains in beam bars and deteriorate the diagonal strut mechanism under strong seismic motions. Consequently, bond stresses along beam bars passing through the joint shall be strictly limited to develop the truss mechanism and lateral reinforcement be assigned to resist most of the joint shear. Japanese Code relies on both mechanisms and estimates the joint shear strength as the sum of the concrete and reinforcement contributions using experimental formulas. Consequently, the differences in predicting the resistance mechanisms results in different amounts of lateral reinforcements according to different codes. ACI requires a constant amount of lateral reinforcement simply for the purpose of confining the joint concrete. On

the other hand the New Zealand Code requires the amount of lateral reinforcement to increase with the joint shear stress levels. Japanese Code does not require lateral reinforcement until the shear stress level has reached the concrete contribution calculated using the experimental equations. These differences are due to different interpretations of test results and different expectations from the earthquake resistance capacities of the beam column joints.

As indicated above there has been different practices in different countries like Japan, New Zealand and U.S. regarding the beam column joints. **Bonacci and Pantazopoulou (1993)** have investigated the causes of these differences and have suggested that these differences are consequences of different interpretations of test results. For example; specimens constructed and tested in New Zealand and to a lesser extend in Japan are distinguished by large size of columns that lead to a low value for bond index. On the contrary, the specimens tested in the United States all exhibited failure types involving bond failure due to relatively small size of columns allowed in design. The effect of joint hoop reinforcement has also been a matter of dispute. The New Zealand code which is much affected by the works of Park and Paulay states that the effect of hoops in the joint is to form a part of a truss mechanism which resists the joint shear. According to this proposal, hoops carry a significant part of the joint shear while the remainder of the joint shear is resisted by a diagonal compression strut. The alternative argument is proposed by the **ACI-ASCE committee (1985)** which states that the shear forces are primarily resisted by the concrete core and the longitudinal column reinforcement. Therefore the horizontal hoop reinforcement serves the purpose of confining the concrete and increase its compressive resistance in the compressed diagonal and preserve the integrity of the connection. Bonacci and Pantazopoulou have investigated the difference between the maximum joint shear stress factor and the potential of the hoops (v_m-v_p) for all specimens that experienced joint shear failure detected by yielding of hoops. They have concluded that for increasing confinement ratios, the demand on the concrete core diminishes, whereas the fraction of the horizontal shear stress resisted by the hoops increases. The authors also attempted to investigate the failure mechanism in terms of the fraction v_p / v_y, that is the potential of the hoops divided by the input to the joint from the beam reinforcement at yielding. The

Japanese, New Zealand and the US test specimens are compared in order to understand the differences between different design philosophies in different countries. The results showed that joint shear failures are prevented when the joint hoop potential is equal to or greater than that of beams. The authors have also concluded that axial load has no influence on the strength of beam column joints.

The authors explained the different results achieved from beam column joint tests. They concluded that these differences are due to the different design philosophies pursued when designing the test specimens. Moreover the parameters that control the response of the test specimens are the weakest link in the chain and also under severe load conditions, some parameters can interact with each other. Also in most reported experiment results, the overall load displacement curves rather than the breakdown of component responses are published, therefore, although it is possible from these results to see the pinching or yielding occurring in the overall response, it is not possible to identify the factor that limited the resistance of the assembly. The main design objective in the joint, should be to avoid the yielding of hoops in the joint area. Increasing the yield stress of hoops, the amount of hoop reinforcement in the direction of load or the confining axial stress in the longitudinal beam had similar influences of causing hoops to yield at progressively higher joint shear stress and strain. Increasing the uniaxially compressive strength of concrete caused hoops to yield at lower shear strain and only slightly higher shear stress. The joint shear stress at hoop yield is most sensitive to the value of percentage of stirrup reinforcement in direction of the joint shear, column axial load divided by the depth and the breadth of the joint, column longitudinal reinforcement percentage whereas shear strain is most sensitive to yield stress of effective transverse joint reinforcement, percent of stirrup reinforcement in direction of shear through joint, horizontal axial load acting in main beam of connection. Therefore increasing the percentage of stirrup reinforcement in direction of shear through joint, increasing the horizontal axial load in main beam of the connection and the yield stress of effective joint reinforcement are most beneficial to overall response. Test results indicate that increasing the uni-axial joint compressive strength is not an effective design option for joints. Since as the f_c^1 and the percent of total horizontal reinforcement in direction of shear action through joint (including beam reinforcement) and column

axial load divided by the column dimensions is increased, hoops yield at higher force but lower story drift.

3.4.1 Comments on the model of Bonacci and Pantazopulou

Bonacci and Pantazopulou methodology is based on the assumption that there is full bond between the concrete and the reinforcement. In reality, this is not the case and due to the cracking, some bond of beam bars is inevitably lost. The model does not take the influence of different detailing types on the behaviour of beam-column joints.

3.5 The Models Demonstrating the Shear Resistance of a Joint

3.5.1 The Shear Resisting Mechanisms proposed by Ichinose

The only study on interior joints investigating the interaction between bond at beam bars and shear reinforcement in the joint has been that of **Ichinose (1991).** The author's work deals with the modelling of joints taking the bond conditions into account. The details of the author's model will not be given here but can be found in the reference of **Ichinose (1991).**

3.5.1.1. Comments on the Model of Ichonese

The author's model is based on the bond conditions of the beam longitudinal reinforcement. By doing so, the author wants to simulate the actual behavioural mode of the joint. However, he falls into the fallacy of making his model too complex. A designer will only want to use a model, if it is simple and easy to apply.

More seriously, he does not take into account the redistribution of column forces. It is experimentally proved by various researchers that column longitudinal reinforcement forces shift to tension from the assumption of plane sections remain plane. So the effect of this redistribution in column longitudinal reinforcement forces should be taken into account in the model.

The author's model implies that the anchorage strength increases with axial load. This is also experimentally proved by **Minami (1988).**

3.5.2. The Shear Resistance of a Joint with Poor Bond

The effect of various bond conditions are reviewed in the upper paragraphs referring to the work of Ichinose. In the following paragraphs, the shear resistance of a joint with poor bond will be investigated. **Kamimura (1993)** in his doctoral thesis investigated the shear strength of interior beam column joints with poor bond. This implied that the truss mechanism was ineffective due to poor bond conditions. For this purpose, he proposed a macro model consisting of a strut throughout the diagonal of the interior joint. The Figures 3.9 and 3.10 show the actions and resultant stresses of interior beam column joints and proposed shear resistance mechanisms respectively. The model uses some equilibrium equations as stated below. Figure 3.11 shows the mechanisms of shear transfer in beam-column joints.

3.5.2.1 Comments on The Model of Kamimura

Kamimura relates the width of the inclined strut to the width of the compressive stress blocks of the upper and bottom columns unlike **Ortiz (1993)**. The simplicity of the model is another advantage. However, the model is only limited to cases where there is poor bond. Moreover, the tensile shift of column bars and consequently the redistribution of the column forces are not taken into account.

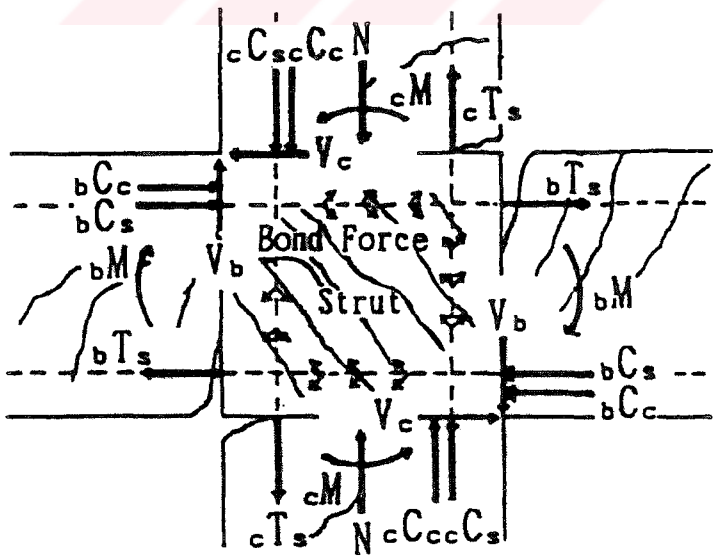

Figure 3.9. The actions of interior beam-column joints

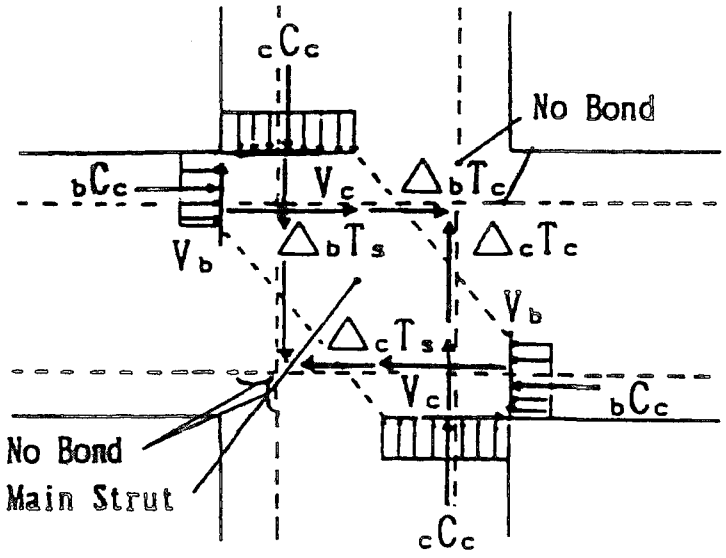

Figure 3.10. Shear resisting mechanisms

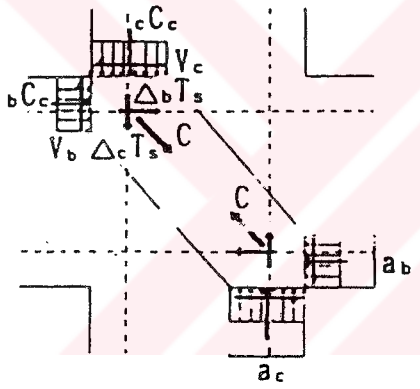

(a) Strut Mechanism

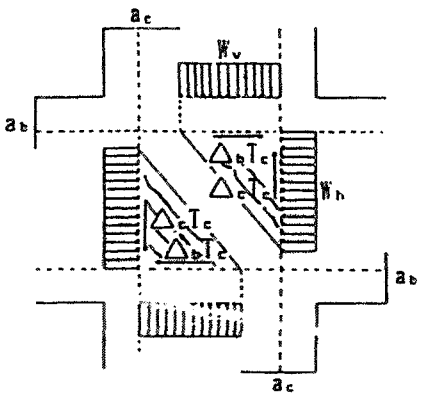

(b) Truss Mechanism with Intermediate Column Longitudinal Reinforcement

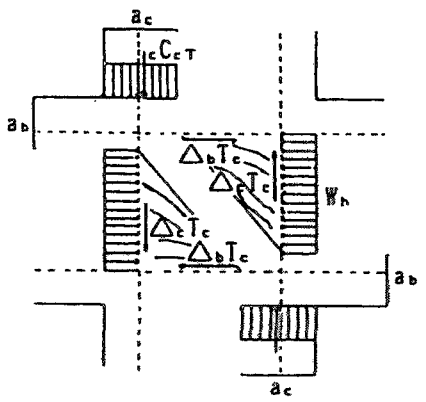

(c) Truss Mechanism without Intermediate Column Longitudinal Reinforcement

Figure 3.11. Mechanisms of shear transfer in beam-column joints

3.5.3 Paulay's strut and truss models

As mentioned previously, The New Zealand Code contradicts the code of U.S. on beam column joints in many ways. The New Zealand Code is influenced by the works of Paulay and Park. They have suggested that the shear is resisted in the beam column joint by means of two mechanisms. These are the strut and the panel truss mechanisms. **Paulay (1989)** has suggested to use the equilibrium in order to investigate the shear resisting mechanism in the joint.

Paulay demonstrated by only considering the equilibrium in a seismically loaded interior beam column joint of a ductile reinforced concrete frame that, internal forces rearrange themselves after the tensile strength of the core concrete is lost because of diagonal cracking. Considerable amount of orthogonal tensile forces within the joint core are necessary to enable shear stresses applied to the boundaries to be transferred by means of a diagonal compression field.

Forces generated in beam or column bars within a joint panel are generally incompatible with those derived from conventional analysis of plane sections at the boundaries of a joint. Therefore the response of plastic hinges next to a joint may be affected considerably by the distribution of internal forces within a joint.

After diagonal cracking, diagonal compression forces transferred by concrete alone are absolute necessities of statically admissible shear transfer within a joint. The aim of transverse reinforcement in the joint is to support such mechanisms.

In order to limit excessive joint expansion, which may considerably increase story drift, orthogonal tensile forces within a joint core must be resisted primarily by reinforcement additional to beam and column bars that pass through the joint.

Joint forces to be considered are those introduced by means of internal actions from adjacent beams and columns. So, a member such as a beam, which is assumed to reach its full strength at an adjacent plastic hinge, can not be used to provide concurrently reactive forces, for example to provide confinement to the concrete core of the joint.

Under seismic effects, beams expand rather than confine joint cores. Paulay therefore concludes that provided the major fraction or the entire flexural

reinforcement in a beam passes through or is anchored within the column, the width of the beam relative to the width of the column which is limited in the ACI Code and The Canadian Code is an inapplicable quantity in terms of joint performance.

Beams will provide some useful confinement for joint cores when they are aligned in the transverse direction to the earthquake load provided their strength can not be mobilised by earthquake generated story drift in the transverse direction. This occurs when seismic resistance in the direction transverse to frames is provided entirely by considerably stiff structural walls.

In the interior beam column joints, at the interior rectangular columns of the buildings, plastic beam hinges are assumed to develop in all four sides of the joint. If subjected to skew earthquake effects, beams will cause a joint core to expand concurrently in both horizontal directions. Due to the above factor, the conditions in such joint cores are more severe than the situation in joints of one way frames. Experimental evidence suggests that the performance of interior joints in two way frames were considerably inferior to the performance of identically reinforced joints of corresponding one way frames.

The tensile strength of the concrete is neglected in the Paulay's model. Paulay has stated that joint shear mechanism in a joint is based on a diagonal strut mechanism and a truss mechanism **(Paulay, 1989).** The strut mechanism develops as the resultant of the horizontal and vertical compression stresses and the shear stresses at the beam and column critical sections. In the truss mechanism, reinforcing bars as well as diagonal struts resist shear in the joint. Paulay claims that joint shear reinforcement is necessary in both the horizontal and the vertical directions. This consequently means that in addition to the horizontal stirrup ties, intermediate column bars are also required in the joint as a means of vertical shear reinforcement. Paulay bases the idea of using intermediate column bars in columns on tests performed by **Park and Keong (1979).** In another study **(Keong, 1978),** vertical shear reinforcement in the form of intermediate column bars were used in specimens. The result was a spectacular improvement in the hysteretic behaviour of the joint.

The diagonally cracked concrete in the joint core sustains all the compressive diagonal forces in the joint. Forces from the beam or column reinforcement are

transferred to this strut mechanism through bond stresses and the remainder by the bend portion of the tensile reinforcement. These actions are shown in Figure 3.12 in detail. During the first inelastic loading of the beam, the greater part of the flexural compressive forces in the beam are transferred to the joint by compressive stresses. The rest of the compressive forces are sustained by the bottom beam bars where excellent bond conditions exist. The tension force from the beam bars are transferred to the joint core primarily by bond stresses and the remainder are transferred by the bend in the joint. However, the yield strains in the joint will eventually transfer to the joint core decreasing and finally diminishing the bond stresses along the straight portion of the beam bars. This will cause the tensile force in the beam bars to be sustained by the bend portion of the beam tensile reinforcement.

3.5.3.1.Comments on Paulay's Model

Paulay has done a significant contribution to the design of beam column connections. His model is the basis of all the models suggested later, on the design of beam column connections. However, the model has the following theoretical inconsistencies. First, the research data of Fuji and Morita had suggested that intermediate column bars are ineffective in resisting joint shear. This is because, there is a considerable amount of tensile shift in the joint from the assumptions of plane sections remain plane. Paulay does not take this redistribution of column forces into account. The model erroneously relies on the intermediate column bars for the vertical shear resistance. Second, the model does not make clear where the failure of the joint will take place. In other words no failure criteria is adapted for the model. Third, the model does not discriminate between the cyclically and monotonically loaded joints and assumes that in both kinds of loading, stirrups increase the joint shear strength. The shear strength however, is not increased by the stirrups in cyclically loaded joints. Fourth, the model assumes that all the stirrups yield at failure. This however, is not the case in monotonically loaded beam-column joints.

FORCES ACTING ON A JOINT CORE

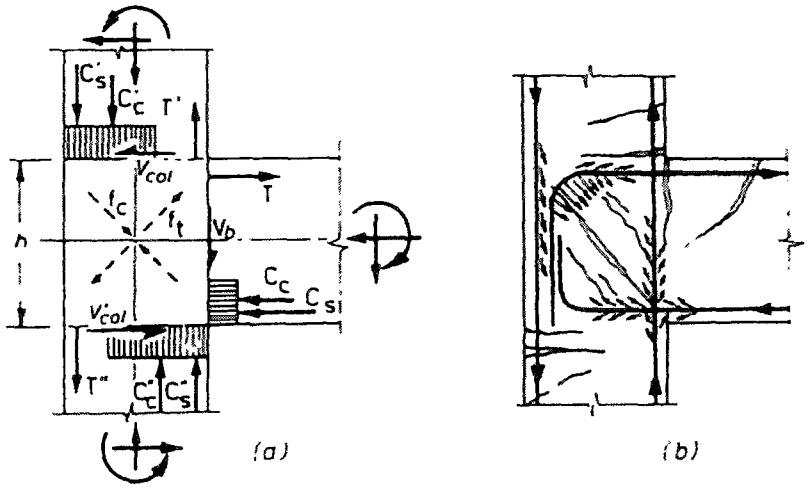

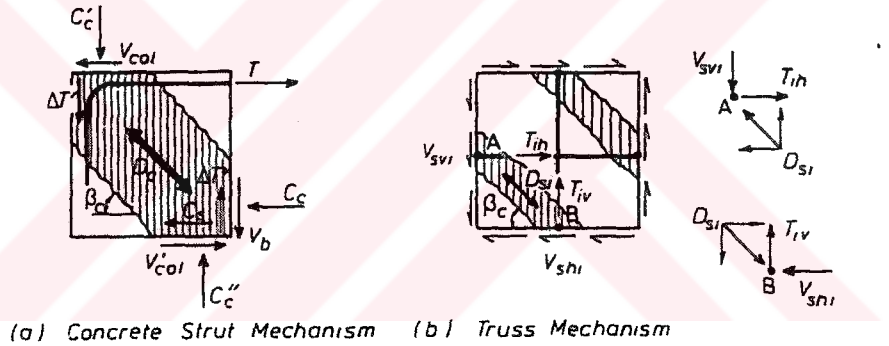

Figure 3.12. Mechanisms of joint shear resistance

3.6. Review of Cyclic Tests on Interior Beam Column Joints

3.6.1.Effect of Bond Along Beam Longitudinal Reinforcement on the Joint Shear Strength

Kamimura (1993) carried out an experimental work to study the effect of bond along beam longitudinal reinforcement. Two joints were tested, one with good bond, other with poor bond. The beam shear versus the story drift angle hysteresis loop shows pinched characteristics with poor energy dissipation for specimen with poor bond because of the slippage of the beam longitudinal reinforcement in the joint.

Kamimura makes similar observations with Fuji and Morita and says that there is a considerable amount of tensile shift in the column bars within the joint core of the specimen with good bond from the assumption of plane sections remain plane due to the shear crack width in the specimen with good bond which was greater than the specimen with poor bond.

Although there was difference in the maximum strength between the specimens with good and poor bond, the strut force C in the joint was nearly same at the maximum strength. So it appeared that the joint shear strength depends on the compressive strength of the concrete strut in the strut mechanism. The joint hoop strains for the specimen with good bond were larger than those with poor bond.

The strains at the column tensile reinforcement at the column critical region were greater than those that are calculated by the flexural theory. This was due to restraining effect against the lateral bulging of column cracked sections and the resisting bond force acting along column longitudinal reinforcement in the outer concrete of the strut. Kamimura tried to predict the failure mode of the beam column joints depending on the softening coefficient v, which accounted for the concrete compressive strength reduction. In other words, the author defined this coefficient as the ratio of the strut stress to that of the compressive stress in the concrete. Kamimura classified the failure modes of beam column joints as follows;

$0.68 \leq v \leq 0.88$: Joints fail before and after beam flexural yielding

$0.01 \leq v \leq 0.78$: Beam flexural failure

Both specimens of Kamimura failed in joint shear, the maximum strength being lower in a poor bond specimen then a good bond specimen. But surprisingly at the ultimate load, the compressive strut resultant force in the joint was not related to the bond condition of beam longitudinal reinforcement. The resultant strut forces were almost same for both of the specimens which implied that the joint shear strength depends on the compressive strength of the concrete strut in the proposed model.

Another interesting observation of Kamimura was that the beam tensile reinforcement was in good agreement from the assumption of plane sections remain plane, however the beam compressive reinforcement was shifted to tension from the assumption of plane sections remain plane.

Ishibashi (1993) investigated whether or not the bond behaviour in a joint would affect the shear strength in the joint region and whether or not the effect of the shear reinforcement in a joint is less than significant under poor bond condition. He came to the conclusion that the ultimate bond strength develops in the joint core where severe shear failure of concrete occurs. It is considerably lower than the maximum bond strength in undamaged concrete. Ishibashi suggests that the joint with sufficient shear reinforcement tends to fail in compression along the diagonal strut concrete.

Kitayama (1993) investigated the effect of beam bar bond deterioration within a joint on earthquake response of reinforced concrete frame structures. If bond deterioration of beam bars within a joint occurs, the energy dissipation at beam ends decreases by pinching in a hysteresis shape and the diagonal compressive stresses increase with a change in the joint shear transfer mechanism after beam yielding. the beam deformations also increase due to the slippage of beam bars within a joint. Kitayama defined the following equation for joints:

$$h_c / d_b \geq f_y / (9 \sqrt{f_c}) \qquad (3.2)$$

Halim (1993) investigated the effect of bi-directional lateral loading on the bond behavior of beam longitudinal reinforcement. Based on his tests, the author reached the following conclusions;

First, an average bond stress along beam bars in a joint decreases under lateral reversal loading. Second under bi-directional lateral loading, the concrete in joints is subjected to bi-axial stress transferred from beam longitudinal reinforcement in two directions by bond resulting in a decrease in the capability of bond stress transfer of beam bars in a joint due to severe stress condition of the concrete in the joint. Finally under bi-directional lateral loading, when the specimen is subjected to unidirectional forced displacement first, and then to a forced displacement perpendicular to the first loading direction by maintaining the displacement amplitude of the first loading direction, the stresses of beam longitudinal reinforcement and lateral reinforcement in the joint become large, although the load in the first loading direction decreases.

The work of **Roberto Leon (1989)** is also of concern. Leon tested four half scale reinforced concrete interior beam column joints to evaluate the validity of current anchorage provisions for interior beam column joints. He tested the validity of the the ACI-ASCE Committee Recommendations which, stipulates three constraints on the beam column joints. First, in order to maintain stability and prevent story mechanisms, the columns must be considerably stronger than the beams framing in at any joint. Second, the nominal joint shear stress must be kept low so that excessive joint shear deformation is prevented. Third, it is recommended that the anchorage length of the beam longitudinal reinforcement must be at least 20 bar diameters. These requirements eventually lead to large columns. The anchorage length is a problem for the designer because he or she is faced with either usage of many small bars or great column sizes in order to satisfy this criterion. As mentioned in the above references, compared with the New Zealand Code which requires at least 35 bar diameters of anchorage, American code requires only 20 bar diameters of anchorage which the author suggests, should be supported by extensive experiments. Leon defined a term "bond efficiency" as the average bond stress, measured by the strain gages at the beam column interfaces and centre of the column, divided by the bond stress required to bring the bar from yielding (or whatever force is present in the beam) in tension on one side to zero force at the

other side. As a result, it is concluded that the bond efficiency increases as the anchorage length increases. The other important conclusion the author reached by interpreting the strain gage data was that, the bars at the compressive side of the joint only picked up minimal amounts of compression in BCJ4. The shear is carried by the joint either through a strut or a panel truss mechanism, depending on the anchorage conditions. The absence of any compression strains in these bars indicates that a panel truss mechanism did not seem to be active for these specimens. Most of the load was transferred by a strut mechanism even when the anchorage lengths reached 28 bar diameters. Thus the author suggested that it is not justifiable to ask for larger anchorage lengths than 28 d_b, or to require large amounts of joint transverse steel to sustain a hypothetical truss mechanism. Leon finally concluded that an anchorage length of 28 bar diameters is necessary to make sure that a weak beam strong column mechanism is maintained through a severe load history. He also discovered that strut mechanism was solely efficient in the shear resisting mechanism of the joint and due to the absence of transverse steel in the joint, the truss mechanism did not develop. So it appeared from test results that for beam column joints with sufficiently large anchorage lengths (24 bar diameters), only a minimum amount of transverse steel was sufficient in the joint. The contribution of column inelastic rotation was proportional to the moment ratio. When the anchorage length was small such as in BCJ2, the column inelastic rotation became significant after yielding. As the anchorage length is increased (BCJ3), column rotation was significant after a ductility ratio of 2 was imposed. For BCJ4, which had the highest anchorage length, there was insignificant column inelastic rotation. This observation led the author to the fact that, increasing the moment ratio could be a good choice for design in order to decrease the anchorage length.

As evident from the above sections, there are radical differences in the design methods of several different codes. These differences result partly from the differences in the required ductility levels. The other important reason is the inadequate understanding of the shear resisting mechanisms in the joint. It appears that the interaction between bond at beam longitudinal reinforcement and shear reinforcement in reinforced concrete joints has to be studied in full detail.

3.6.2 The influence of concrete compressive strength, stirrups, column axial load and hooked bar development on the joint shear strength

A brief review on the experiments of **Kurose (1993)** as part of the United States, New Zealand and Japanese cooperative research programme revealed that the maximum joint shear had a tendency to increase with the concrete strength and with the amount of lateral reinforcement. The column axial load however, did not seem to affect the joint shear stress. The diagonal strut in the exterior joint extends from the compressive joint end to the bend of hooked beam bars and becomes steeper as the horizontal development length is made shorter. The examination of the test data showed that the truss mechanism can resist a small amount of joint shear although the diagonal strut mechanism dominates the joint shear resistance, and that the shear strength for exterior joints is influenced by horizontal development length of hooked beam bars. According to the author, the shear strength evaluation recommended by ACI 352 estimated experimental strength fairly well but was expected to estimate joint shear strength more precisely, if these points were taken into account. The ratio of V_j (Calculated joint shear strength) to V_u (Beam Moment Flexural Capacity) can be used to judge whether or not the joint will exhibit shear failure prior to beam flexural yielding under strong seismic actions. The majority of specimens with the V_j /V_u value of less than 1 exhibited joint shear failure and those with the V_j/ V_u value of greater than one developed beam flexural yielding. The author suggests that premature shear failure in beam-column joints can be avoided if frames are designed to have sufficient stiffness and moment capacities and dissipate seismic energy at beam end plastic hinges without excessive inelastic deformation reversals and if the joints are designed to have shear strength in excess of beam moment capacities and provided with a nominal amount of lateral reinforcement. A lateral reinforcement ratio of 0.3 % is recommended as the nominal amount based on the test data described.

3.6.3 Effect of Slab on the Flexural Behaviour of a Beam

Suzuki (1993) investigated a half scale three-dimensional reinforced concrete interior beam column subassembly with slab subject to uni-directional earthquake loading in order to examine the effect of slab on the flexural behaviour of a beam. In order to evaluate the stiffness and strength of a beam cast monolithically with slab, it

is imperative to make clear how much width of the slab could contribute to the flexural stiffness and the strength of the beam. The author came to the conclusion that the slabs can contribute to the stiffness as well as the strength of the beams. The effective width of slab increases with the deformation of the beam, and can be as large as the entire width at the ultimate stage of the beam. The test results showed that the torsional moment in a transverse beam caused by forces acting in slabs can not be large enough to cause torsional failure in an interior beam column connection. However the torsional moment and shear in a transverse beam can be significant to cause failure, if the beam is connected to an exterior beam-column connection.

3.7.Cyclic Tests on Exterior Reinforced Concrete Joints

3.7.1.1.The Behaviour Of Exterior Beam Column Joints with Low Axial Load

Megget's (1971) tests on the behaviour of cyclically loaded exterior beam column joints with low axial load are also of interest in the understanding the development of the New Zealand and ACI Codes of today. Megget tested three exterior beam-column joints and suggested that the anchorage requirements of the then ACI Code were adequate, provided that the joint remained intact. He also added that all the failure was caused due to the insufficient amount of stirrups which could not confine the concrete resulting in disruption in the joint after the hoops yielded. This was succeeded by the deterioration of the anchorage of the longitudinal beam reinforcement. **Megget** also suggested that the need for increased amount of joint hoops could also be due to absence of the transverse beams or axial load, which, he assumes increases the anchorage of the beam reinforcement and the shear resistance of the joint.

3.7.1.2 Comments on Megget's conclusions by the author

The author is of the opinion that U bars as well as L bars bent up into the upper column should not be used in the joints. Not only Megget's experiments confirm this but there is also proof for this from **Taylor's (1976)** as well as **Scott's (1992)** tests. The author is also of the opinion that hoops are essential for the confinement of the joint and it is unnecessary to increase the yield strength of the hoops as the more number of hoops you provide in the joint, the better confinement you get. The author

does not agree on the effect of transverse beams in the joint. The reason for this is that in all the tests with transverse beams, the loading is from one direction only. In reality earthquakes can occur in various directions, resulting in possible hinges in the transverse beams as well as the beam on the plane of the joint. The possible plastic hinges lead to weak beams in two directions eliminating the possibility of confinement from these transverse beams. Regarding the column axial load, Megget says that the column axial load improves the anchorage conditions for the beam longitudinal reinforcement. This suggestion is undoubtedly confirmed by other tests. However he goes on to say that column axial load increases the shear resisting capacity of the beam column joints which is not confirmed by tests.

3.7.2 Anchorage Behaviour Of Bent Bar In Exterior Beam-Column Joints Under Seismic Loading

Marques and Jirsa (1975) have tested twenty-two exterior reinforced concrete joint specimens provided with varying degrees of confinement at the joint in order to estimate the performance of the anchored beam reinforcement.

The authors concluded that the results of this study indicated; tail extensions beyond those of a standard hook were not effective for providing development length. In all cases, failure was observed by side splitting of the joint and not by the pullout of the hooked bar. The authors also suggested that the tail extensions did not increase the anchorage strength where side splitting occurred. Lateral restraint provided by the lateral beams might have beneficial effect and improve the effectiveness of tail extensions.

The anchorage behaviour of bent bar in exterior beam-column joints has been investigated by **Nishimura and Minami (1988).**

It is apparent that the anchorage of the beam bars in exterior joints is closely related to the shear resisting mechanisms of the joint. If short lead embedment lengths are provided for the beam bars, equilibrium can not be maintained in the joint. The tensile forces can not be equilibrated which shows that the behaviour of short lead embedment length is not satisfactory. The conclusions of Jirsa and Marques can be summarised in the following three paragraphs:

First, the authors have suggested that strength of hooks is increased as the restraint against side splitting is increased.

Second, much higher strengths than those specified by the codes could be permitted. For small bar sizes these values were unrealistically restrained. However for larger bar sizes higher stresses could only be allowed if minimum straight embedments before the hook are provided.

Third, no distinction was made between the strength of 90 deg and 180 deg standard hooks.

3.7.2.1 Commentary on the works of Marquez and Jirsa and that of Nishimura and Minami

The author's tests have been carried out almost twenty five years ago.Later tests by Nishimura and Minami suggests that the column axial load significantly increase the bond of beam bars opposite to Marquez and Jirsa who state that the column axial load has no significant effect on the bond conditions for cyclically loaded joints.

4. DESIGN AND ANALYSIS OF MONOTONICALLY LOADED EXTERIOR BEAM COLUMN CONNECTIONS

4.1. Introduction

There are three alternative methods for the design of exterior beam column joints. The first one is using empirical design equations, while the second one is using semi-rational models such as strut and tie models. The third alternative is using finite element models. The non-linear finite element analysis has the disadvantage of being overly complex. The principle aim of this thesis however, is to propose simple design equations and models for exterior beam-column joints.

The joints are classified into two. The third chapter was principally concerned with the design of cyclically loaded beam-column joints while this chapter will be on monotonically loaded joints.

In this chapter, the previous tests on monotonically loaded exterior beam-column joints are reviewed with a commentary at the end of each, and this is followed by the analysis of the test specimens in order to find the effects of several parameters such as column longitudinal reinforcement ratio, beam bar detailing, joint aspect ratio, column axial load, and beam longitudinal reinforcement ratio on the normalized joint shear strength. Finally, an empirical design equation will be developed. The previously suggested strut and tie models are reviewed and criticized with a commentary at the end of each. There are difficulties in applying the strut and tie models on the cyclically loaded joints because the strains in the stirrups are dependent on the number of cycles. Stirrups do not increase the joint shear strength in cyclically loaded joints but are provided in the joint area to prevent the degradation of stiffness and to increase the ductility. Therefore, it is more sensible to base the design of cyclically loaded joints on direct strut mechanism rather than strut and truss models together. The monotonically loaded exterior beam-column joints on the other hand can be satisfactorily designed by strut and tie models as in monotonically

loaded beam-column joints, the joint shear strength is considerably increased by the provision of stirrups.

4.2.The review of tests on monotonically loaded exterior beam column connections

4.2.1. Calculation of Joint Shear Strength

The procedure used for determining the normalized joint shear strength is as follows:

1. The reported failure loads of the tests are used to calculate the moment developing at the boundary of the joint.
2. No factors of safety are adapted for the mean concrete strength.
3. A value for the strain in the most compressed fiber is assumed. This assumed value can be between zero and ε_{cu} which is the maximum strain that the most compressed fiber can have. For a systematic approach a value as low as 0.0003 is adapted.
4. The neutral axis depth is estimated from the force equilibrium and moment equilibrium conditions at the cross sections of beam and the columns. The strains in the reinforcement are calculated in terms of the neutral axis depth. From each determined ε_{ci} value, the stresses are calculated and checked against yielding.

$$\sigma_{si} = \varepsilon_{si} E_s \leq f_y \tag{4.1}$$

5. Consequently, the forces at the boundary of the joint are determined. The forces were estimated by multiplying the area of the steel with the corresponding stress in that reinforcement.

$$F_{si} = A_{si}\ \sigma_{si} \tag{4.2}$$

Similarly, the force in the concrete compressive stress block is calculated.

7. The joint shear force is determined from the following equation:

$$V_j = T\text{-}R \tag{4.3}$$

where:

T is determined from the section analysis mentioned above.

$$R = P_{applied} (L + 0.5\ h_c) / H \qquad (4.4)$$

L is the distance from the applied loading to the face of the column

h_c is the height of the column

H is the distance between the horizontal restraints.

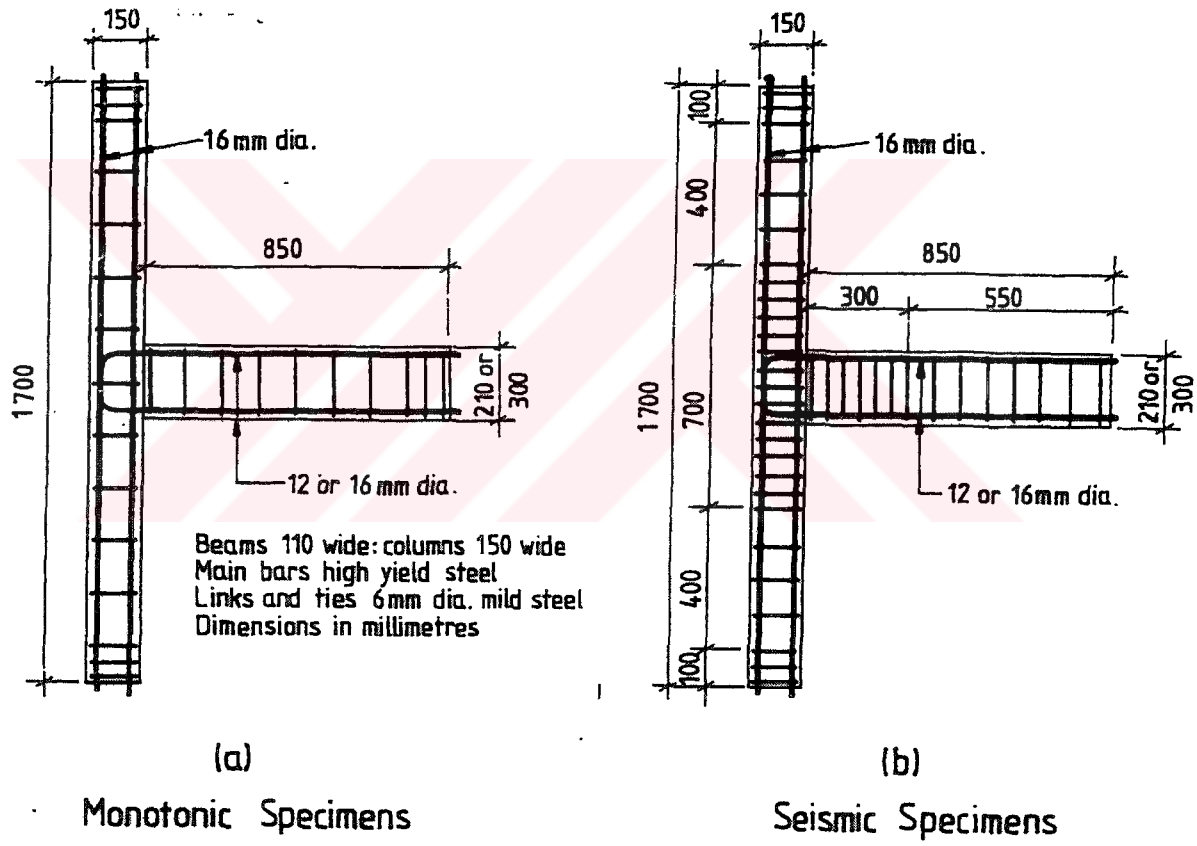

Figure 4.1 : Layout of the test specimens of Scott.

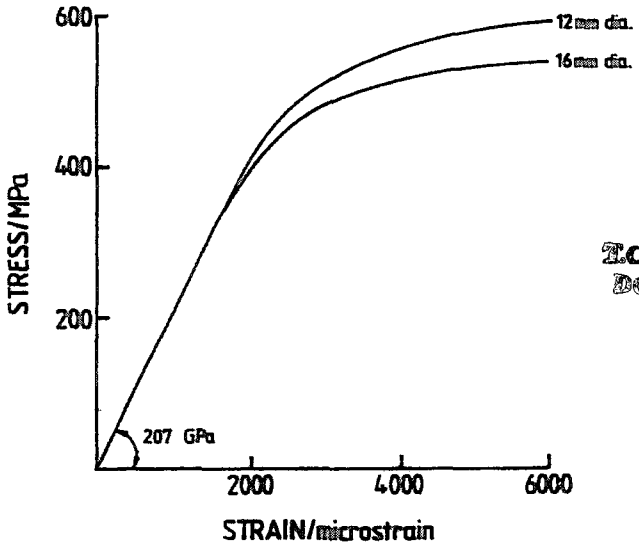

T.C. YÜKSEKÖĞRETİM KURULU
DOKÜMANTASYON MERKEZİ

Figure 4.2 : Stress-strain relationships for the specimens of Scott

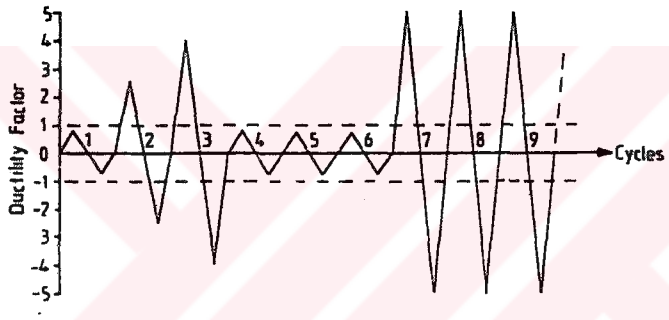

Figure 4.3 : Earthquake representation of the tests of Scott

A computer program is written for the above procedure by the author. The program increases the strain assumed for the concrete strain in each column and the beam in small increments up until the moment equilibrium is satisfied. For each column and beam $1x10^6$ iterations is carried out.

4.2.2. Scott's tests

4.2.2.1.The effect of detailing

The effect of detailing on reinforced concrete beam column joints behavior is also very important. Scott (1992) tested fifteen exterior beam column connections. The

layout of the test specimens is shown in Figure 4.1. The stress-strain relationships and the earthquake representation are in Figures 4.2 and 4.3. **Scott** used three reinforcement details - bending beam tension steel up or down into the column and the 'U' bars. **Scott** aimed at testing the recommendations suggested by **Taylor (1976)** who had been a great influence on the design of exterior type reinforced concrete joints to British design practice. The specimen details are shown in Table 4.1. and the experimental beam moments as percentages of theoretical values at ultimate and failure modes and shear stresses are shown in Tables 4.2. and 4.3. In general the overall specimen behavior was consistent with that observed in other investigations; flexural cracking in the beam during early load stages, followed by growth of a diagonal crack in the connection zone. Further loading led to specimen failure, either by a plastic hinge forming in the beam at the face of the column or by extensive joint cracking in the connection zone, depending on the relative influences of beam steel percentage, reinforcement detail, and column load. Taylor identified a 1.2 % beam tension reinforcement a criterion for determining failure modes of external beam column joints. According to **Taylor**, a beam longitudinal reinforcement ratio below 1.2 % gave a beam failure (plastic hinge in beam), above 1.2 % gave a joint failure (extensive joint cracking). **Scott** investigated the above criterion by the tests he carried out on exterior beam column joints. The latter category beam column joints he tested, all failed by joint cracking regardless of the column load or reinforcement detail. However the former category beam column joints with a detailing of bending beam bars down into the column or the U bars detail, which would be expected to exhibit beam failure, achieved this only when a high column load was applied. When subjected to a low column load, these same details gave a joint failure, as did the detail of bars bent up. **Taylor** did not examine the beam column joints subjected to low column load and beam steel percentage of less than 1.2. This study implies that column load may be more substantial in affecting the failure mode than had previously been thought, indicating that, in a multi-story frame, the behavior of a joint may be influenced by its position. **Scott** concluded that the beam bars bent down detail were the most successful of the three details tested.

Table 4.1. Specimen details

Specimen	Beam depth (mm)	Diameter of beam tension reinforcement (mm)	% beam tension reinforcement	Detailing type
C1	210	12	1.0	L bars bent down detail
C1A	210	12	1.0	Same
C1AL	210	12	1.0	Same
C2	210	12	1.0	L bars up
C3	210	12	1.0	U bars
C3L	210	12	1.0	Same
C4	210	16	1.9	L bars bent down detail
C4A	210	16	1.9	Same
C4AL	210	16	1.9	Same
C5	210	16	1.9	L bars up
C6	210	16	1.9	U bars
C6L	210	16	1.9	U bars
C7	300	16	1.3	L bars bent down detail
C8	300	16	1.3	L bars up
C9	300	16	1.3	U bars

Table 4.2. Experimental beam moments as percentages of theoretical values at ultimate

Specimen	Initial joint cracking	Specimen failure
C1	80	>100
C1A	95	>100
C1AL	55	100
C2	90	100
C3	100	>100
C3L	60	100
C4	55	85
C4A	50	85
C4AL	35	80
C5	30	40
C6	40	60
C6L	40	70
C7	40	55
C8	45	50
C9	40	50

Table 4.3. Failure modes and shear stresses

Specimen	Failure mode	Shear stress at failure, MPa	Ratio column/beam flexural strength
C1	B	6.3	1.1
C1A	B	6.5	1.2
C1AL	J	5.3	1.2
C2	J	5.2	1.1
C3	B	6.2	1.2
C3L	J	5.2	1.2
C4	J	7.7	0.7
C4A	J	8.3	0.7
C4AL	J	7.4	0.7
C5	J	3.6	0.7
C6	J	5.7	0.7
C6L	J	6.8	0.7
C7	J	5	0.4
C8	J	4.3	0.4
C9	J	4.4	0.4

L bars bent down detail gave a significant load increment between joint cracking and failure regardless of reinforcement percentage or the column load. This type of detailing employed the vertical leg in order to accommodate the changes in the load transfer once the bond around the bend had been lost. The U bar detail followed the same performance, but without reaching the same high strain levels. Although it has performed quite satisfactorily, if ductility is the main criteria in order to determine the performance, the bending down detail will be preferable. Bending bars up gave a small load increment between joint cracking and failure inhibiting the overall performance of a specimen, which led to brittle behavior, with low strains generated as a consequence.

4.2.2.2. Analysis of Scott's tests

Lateral sway was prevented in all of Scott's tests by the provision of a horizontal prop. The beam of each specimen was 850 mm long and either 210*110 or 300*110 cross-sections. The columns had square cross sections of 150*150. The distance between the lateral restraints in the upper and lower column was 1700 mm. The column longitudinal reinforcement was 4T16 high yield bars.

Table 4.4. Yield strength of the reinforcement in Scott's tests

Yield strengths of the reinforcement in Scott's tests	Yield Strength (MPa)
Bar Diameter	
16	540
12	590
6	not measured

Anchorage Lengths of Beam Longitudinal Reinforcement:

Anchorage lengths for beam tension longitudinal reinforcement were generally the minimum recommended by BS8110, however they were increased by 365 mm and 390 mm respectively for specimens C1 and C4.

4.2.2.3. Analysis of Scott's tests

The results of the analysis of Scott's tests by the author are given in Table 4.5.

Table 4.5. Analysis of Scott's tests

Specimen	Cylinder Strength	Type of Detailing of the Beam Bars	Failure Mode	Effective Joint Stirrups	Column Axial Stress/f_c'	Joint Shear Strength $v_j = V_j / b_e h_c \sqrt{f_c'}$	Ratio of Tensile Reinforcement	Joint Aspect Ratio
Units	MPa	-	-	-	-	MPa	-	
Scott								
C1	39.92	1	B	1T6	0.306	0.907	1.11	1.4
C1A	48	1	B	1T6	0.255	0.762	1.11	1.4
C1AL	33.36	1	J	1T6	0.066	0.839	1.11	1.4
C4	41.44	1	J	1T6	0.295	1.042	1.976	1.4
C4A	44.32	1	J	1T6	0.275	1.075	1.976	1.4
C4AL	35.76	1	J	1T6	0.062	1.086	1.976	1.4
C7	35.2	1	J	1T6	0.347	0.755	1.33	2
Mean	39.71				0.229	0.968		1.4
C3L	35.52	2	J	1T6	0.062	0.795	1.11	1.4
C6	39.84	2	J	1T6	0.307	0.775	1.976	1.4
C6L	45.84	2	J	1T6	0.266	0.855	1.976	1.4
C9	35.92	2	J	2T6	0.340	0.649	1.33	2
C3	36	2	B	1T6	0.339	0.95	1.11	1.4
Mean	38.624				0.263	0.888		1.4
C8	44.48	3	J	2T6	0.274	0.561	1.33	2
C5	33.04	3	J	1T6	0.369	0.543	1.976	1.4
C2	49.36	3	J	1T6	0.247	0.652	1.11	1.4
Mean	42.29				0.297	0.703		1.4
Total Mean	39.87				0.254	0.888		1.4

Notes:

1. The normalized joint shear strengths are calculated according to section 4.2.1.
2. The type of detailing 1 denotes: the L bars bent down into the column detail; Type 2 denotes: the U bar specimens; Type 3 denotes: the L bars bent up into the column detail

The author has also inspected the specimens C1 and C1A with C1AL. Specimen C1 and C1A are identical except the fact that C1 has got greater anchorage length than C1A. This is possibly why the normalized joint shear strength of C1A is 16% less than C1. The comparison of specimen C1AL however, does not give any idea regarding the effect of low column axial load because:

Specimens C1 and C1A exhibited beam failure and they had higher beam failure loads than specimen C1AL. C1AL on the other hand, exhibited joint shear failure and the joint region of this specimen was severely cracked. If two specimens exhibit different failure modes, their joint shear strengths can not be compared. It can be concluded that, increasing the column axial load would increase the load at which beam cracking will occur and change the failure mode of specimens.

If concrete cylinder strength of a specimen is significantly less than other specimens with higher concrete cylinder strengths, there will be more extensive damage in the

joint region of that specimen. This would change the failure mode of that specimen. Typical example to the above argument is Scott specimens C1, C1A and C1AL that had concrete cylinder strengths of 39.92, 48 and 33.36 respectively. The above matter is taken into account in the simple methodology suggested in the later sections for predicting the failure modes of test specimens. The methodology predicts that the limiting beam bar ratio is given by the following formula:

$$\rho_{blim} = \alpha h_c (b_c+b_b) f_c (1-f_c/250) / \tan\theta \; b_b \; d_b \; f_y \qquad (4.5)$$

where

α is a constant

h_c is the height of the column

b_c is the breadth of the column

b_b is the breadth of the beam

f_c is the concrete cylinder strength (MPa)

$\tan\theta$ is the ratio given by height of the beam to the height of the column

d_b is the depth of the beam

f_y is the yield stress of the longitudinal reinforcement

It is apparent from the above formula that as the concrete cylinder strength decreases, the limiting value for the beam longitudinal reinforcement ratio decreases. This means that unless very low amount of beam longitudinal reinforcement is used, failure of the joint by joint shear failure or column hinge will be more likely.

The specimens C4, C4A and C4AL are also analyzed. It was stated in the upper paragraphs that specimen C4 had significantly higher anchorage length than C4A or C4AL. In spite of this, it had lower normalized joint shear strength compared to C4A and C4AL. In the total series of tests, C4A has the highest beam failure load. The relative joint shear strengths and failure loads are shown in Figures 4.4 and 4.5 which show that increasing column axial load will increase the beam failure load. The column axial load increases the normalized joint shear strength of monotonically loaded exterior beam column joints only when a column hinge is expected in the upper column. However, if the joint is expected to exhibit joint shear failure, this effect is invisible. Vollum is of the same opinion. The column axial load only is influential on the failure modes of joints.

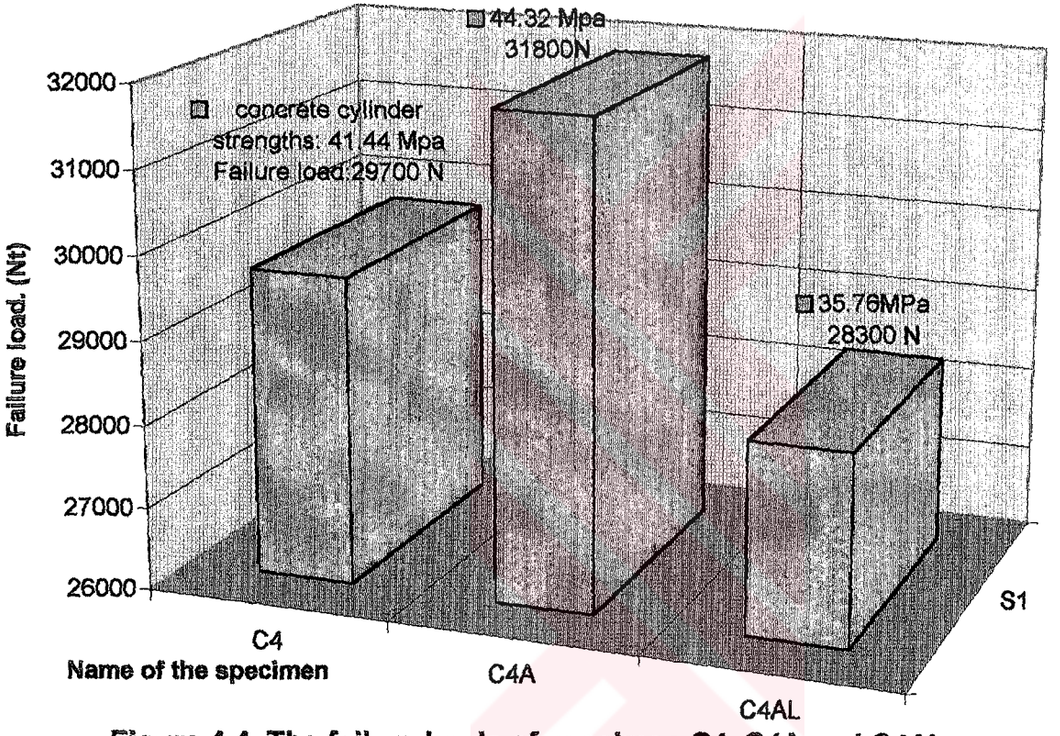

C4 and C4A has 275 kN column axial load while C4AL has 50 kN.

Figure 4.4. The failure loads of specimen C4, C4A and C4AL

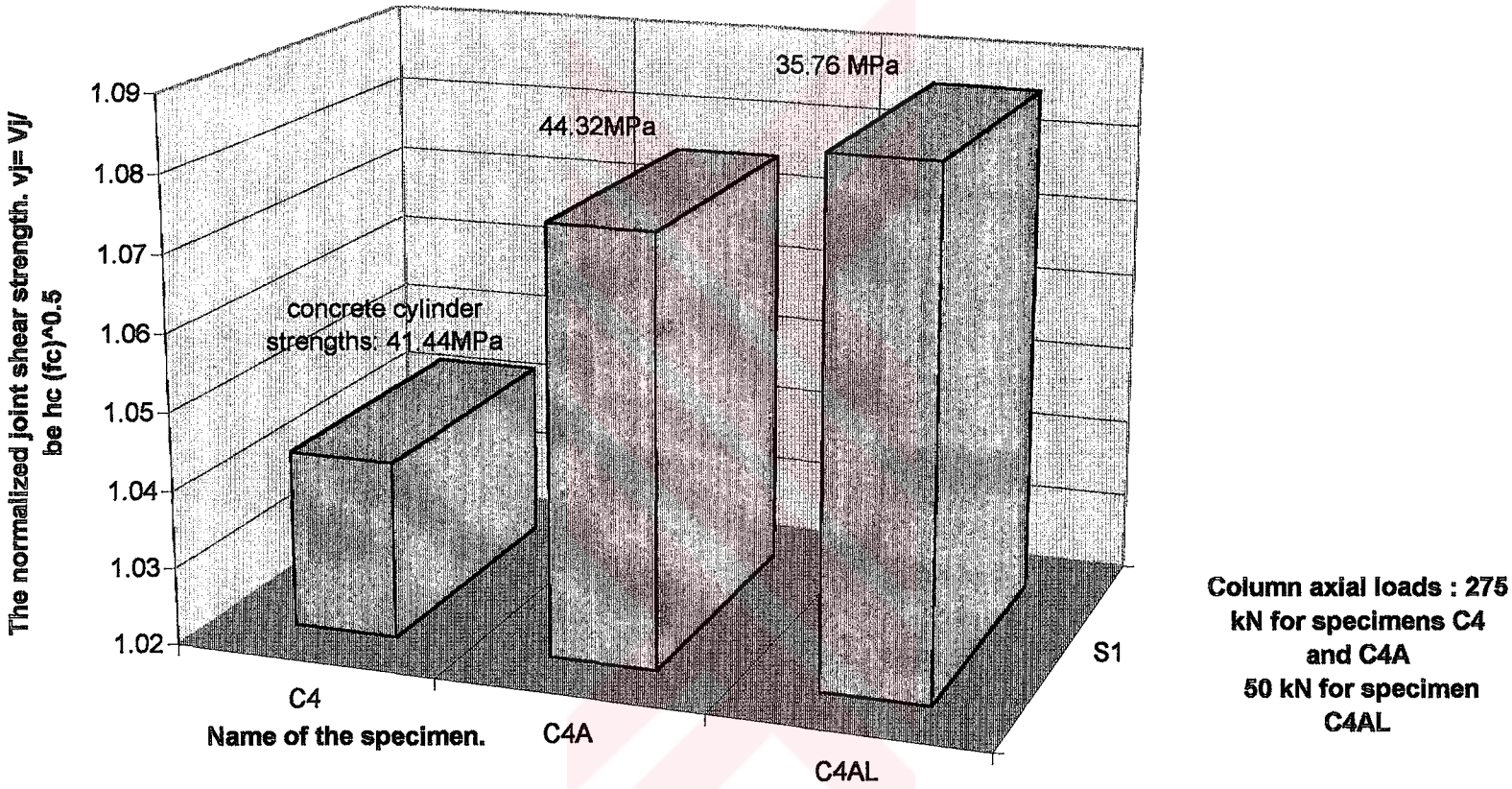

Figure 4.5.The normalized joint shear strengths of Scott specimens C4, C4A and C4AL.

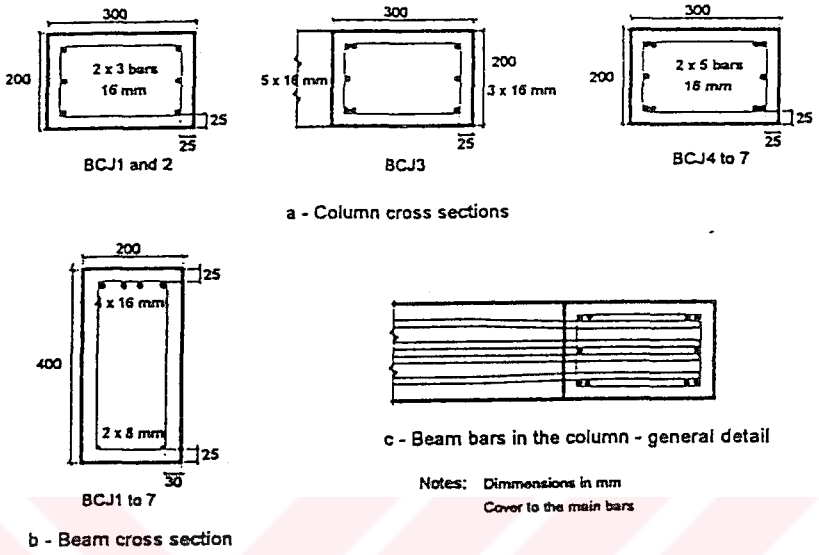

Figure 4.6 : The details of the cross sections of Ortiz specimens.

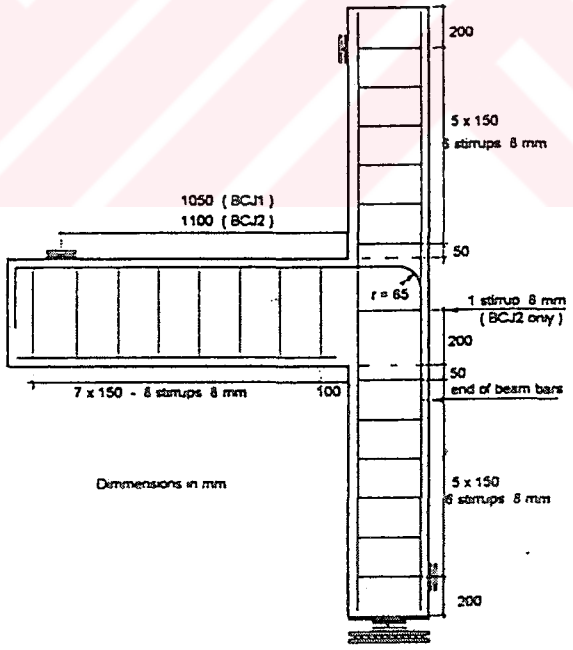

Figure 4.7 : The details of the beam column joints 1 and 2 respectively.

The analysis of C7 and C4A of Scott is also of concern. Inspection of specimen C7 clearly shows that, it has got the lowest normalized shear strength of all the beam bars bent down detail specimens. Nevertheless, it has the same column axial load, same type of detailing, same amount of beam and column reinforcement as well as effective stirrups as that of C4A. The only difference between the two specimens is that, the joint aspect ratio of C4A is 30 % less than that of C7. The joint shear strength of C4A is 29.7 % greater than C7. This shows a relationship between the normalized shear strength and the joint aspect ratio.

4.2.3. The Experimental work of Ortiz

Ortiz has made seven tests on exterior monotonically loaded beam column joints. The variables of her tests were the joint stirrups, column axial load and detailing of beam reinforcement on the strength of monotonically loaded connections. The Figures 4.6 and 4.7 shows the detail of the cross sections of Ortiz specimens and details of the beam column joints 1 and 2 respectively. The details of the beam column joints 3, 4 and 6 are shown in Figure 4.8 and the properties of the test specimens 5 and 7 are shown in Figure 4.9.

4.2.3.1.Reinforcement Properties:

The beam reinforcement details and Column reinforcement details are shown in Tables 4.6 and 4.7 respectively. The concrete splitting and crushing strengths are shown in Table 4.8, whereas the shear reinforcement details are shown in Table 4.9. Table 10 shows the radius of bends of beam bars.

Table 4.6. Beam reinforcement

BCJ	Diameter ϕ mm	Total area A_s mm^2	Reinforc. Percentage A_s/bd %	Yield strength f_y MPa	Bend Radius mm	Straight anchorage mm
1& 2	16	804	1.1	720	65	420
3	16	804	1.1	720	130	420
4& 5	16	804	1.1	720	65	290
6& 7	16	804	1.1	720	130	220

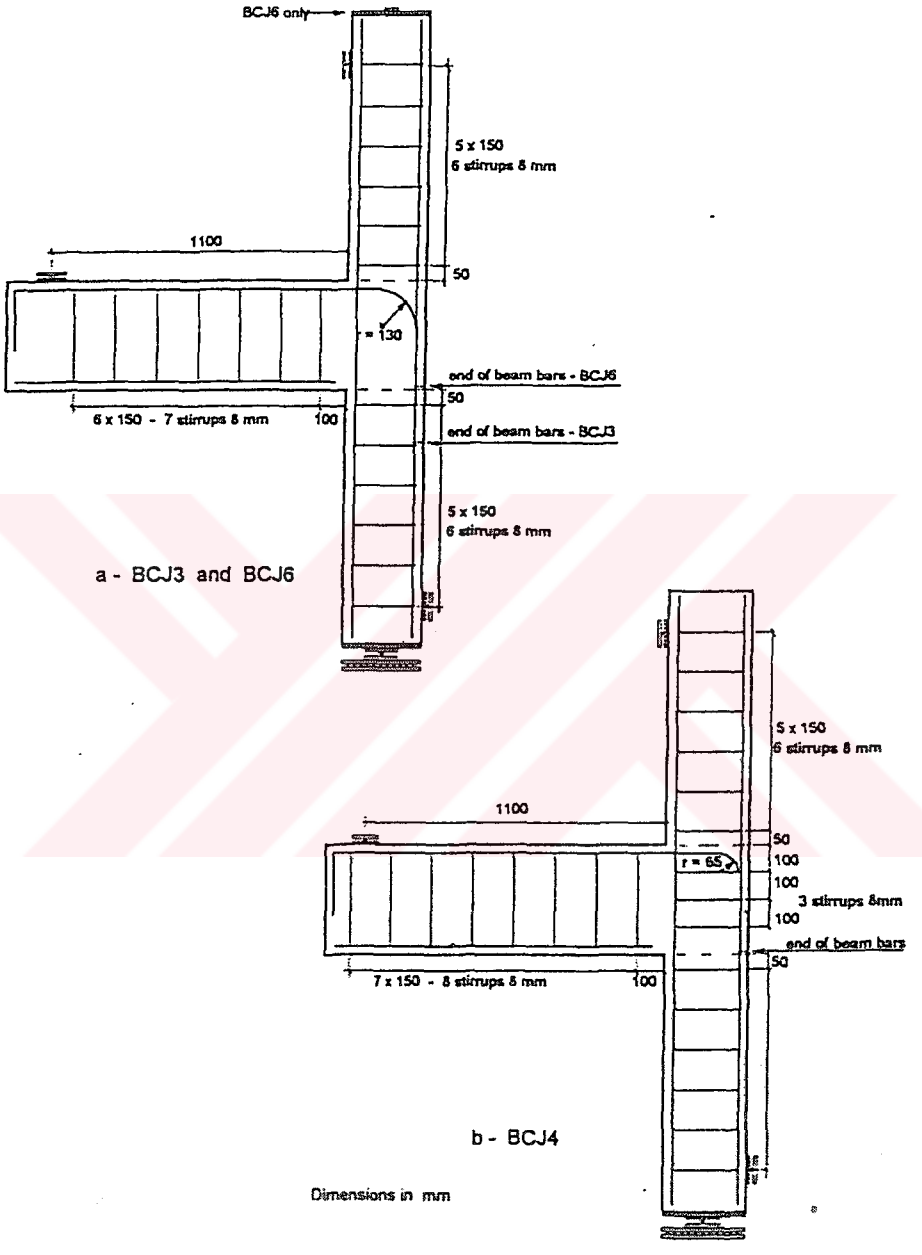

Figure 4.8 : The details of the beam column joints 3, 4 and 6.

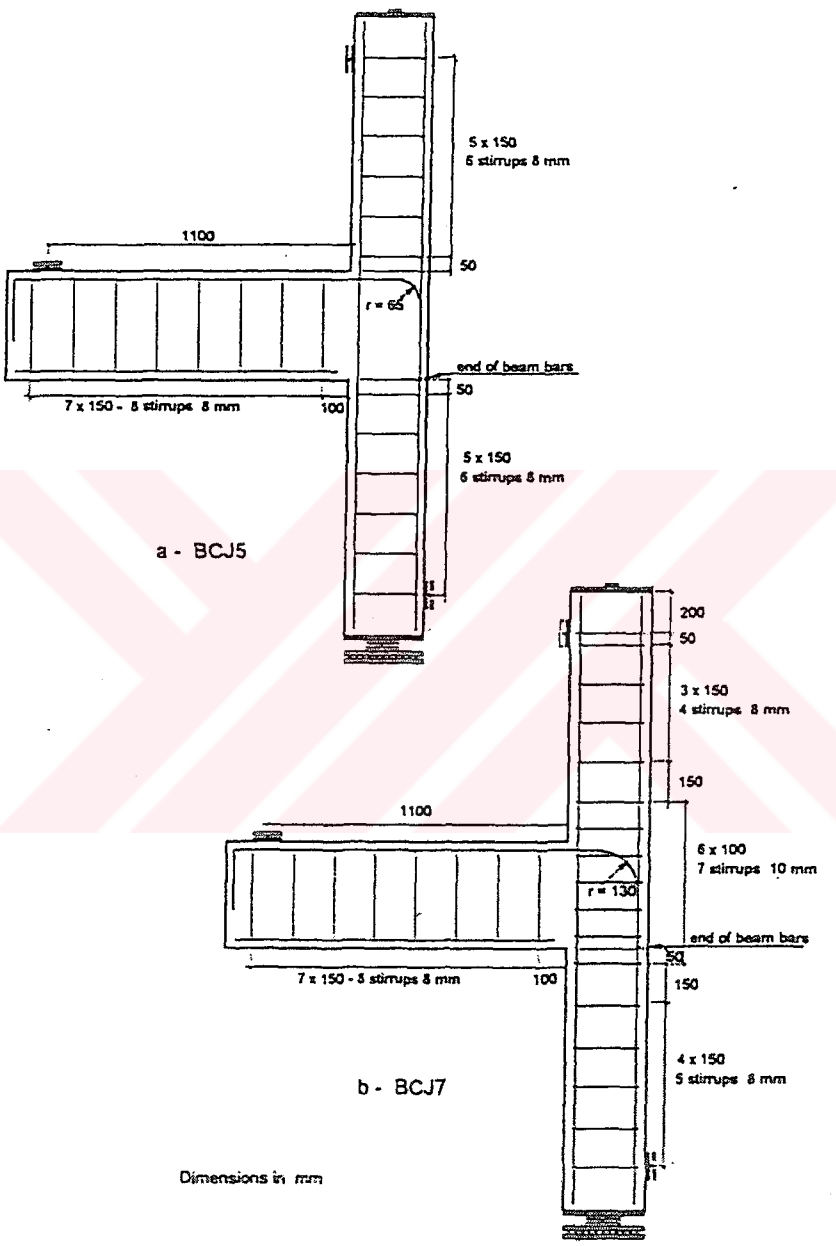

Figure 4.9 : The properties of the test specimens 5 and 7.

Table 4.7. Column reinforcement

BCJ	Diameter ϕ mm	Total area A_s mm^2	Reinforc.Percentage A_s / bd %	Yield strength f_y MPa
1& 2	16	1206	2.01	720
3	16	1608	2.68	720
4 to 7	16	2010	3.35	720

Table 4.8. Concrete splitting and crushing strengths

BCJ	Splitting strength f_{sp} MPa	Cube strength f_{cu} MPa	Cylinder strength f_c MPa
1	2.77	42.3	34
2	3.68	47.2	38
3	3.31	41.3	33
4	2.98	42	34
5	3.29	47.4	38
6	3.43	43.7	35
7	3.23	44	35

Table 4.9. Shear reinforcement

BCJ	No of joint stirrups	Joint stirrup diameter mm	Column stirrup diameter mm	Beam stirrup diameter mm	Yield strength f_y MPa
1	-	-	8	8	571
2	1	8	8	8	571
3	-	-	8	8	571
4	3	8	8	8	571
5	-	-	8	8	571
6	-	-	8	8	571
7	4	10	8 10	8	571 556

4.2.3.2.Test Results

In BCJ1, the widened cracks ran further along the column bars spalling off the cover above the joint. At failure, the central crack was wide open and the concrete crushed near its lower end. The concrete spalled off in a large area around the column bars at the beam side of the joint, at middle height of the beam. These column bars were highly stressed and the high bond stresses were the probable cause of the spalling. In BCJ2, BCJ5, BCJ6 and BCJ3, as load was increased, new cracks developed parallel to the proposed strut direction following the column bars above the joint. Failure occurred with wide opening of these cracks and spalling of the cover of the column bars. BCJ4 showed a similar behavior to BCJ3 and BCJ2 at failure. However in addition to this, two stirrups yielded. At BCJ7 on the other hand, with stirrups tying the core of the joint, no bond deterioration occurred and failure occurred in the beam by yielding of the beam bars and crushing of the horizontal beam chord at the corner of the joint.

Table 4.10. The radius of bend of beam bars and corresponding failure modes of Ortiz specimens

Specimen	Column load	Beam load at cracking Pcr	Beam load at failure Pu	Radius of the bend of beam bar	Failure Mode
Units	kN	kN	kN	mm	-
BCJ1	0	40	118	65	joint shear
BCJ2	0	50	125	65	joint shear
BCJ3	0	50	118	130	joint shear
BCJ4	0	50	130	65	joint shear
BCJ5	300	80	115	65	joint shear
BCJ6	300	80	115	130	joint shear
BCJ7	300	70	170	130	joint shear

4.2.3.2.1.Influence of Column Axial Load

No axial load was present on Ortiz specimens BCJ1 to BCJ4. In BCJ4, BCJ5 and BCJ7 on the other hand, the column axial load was increased to 300 kN. The test specimens of Ortiz do not give an idea about the effect of column axial load on the joint shear strength of exterior beam column joints. The main reason for this is the specimens, which have different column axial loads, different vertical anchorage length for beam bars and different radius of bends. The characteristics of the specimens are given in Table 4.11.

Table 4.11. Normalized joint shear strengths of Ortiz specimens and corresponding vertical anchorage lengths.

Specimen	Radius of bend	Length of vertical leg	Column axial load	$Vj/ b_e h_c f_c$	$Vj/b_e h_c\sqrt{f_c}$	$100A_{scol}/b_c/d_c$
Units	mm	mm	kN	-	$MPa^{0.5}$	mm^2
BCJ1	65	420	0	0.156	0.909	2.01
BCJ3	130	420	0	0.168	0.968	2.68
BCJ5	65	290	300	0.14	0.865	3.35
BCJ6	130	200	300	0.1535	0.908	3.35

The above specimens are not reinforced by transverse reinforcement. Inspection of BCJ1 and BCJ5 shows that there is 5% decrease in the normalized joint shear strength of BCJ5 with respect to BCJ1 although the column axial load is increased from 0 to 300 kN and the column longitudinal reinforcement ratio is increased from 2.01 to 3.35. Analysis of the experimental data of Scott suggests that the column load is unlikely to decrease the joint shear strength, it can either increase the joint shear strength or it won't affect it. This means that decreasing the length of the vertical leg of beam bars is the cause of the decrease in the joint shear strength.

Inspection of BCJ3 and BCJ6 again shows that the normalized joint shear strength is decreased by 6 % due to the decrease in the anchorage length.

As a result, Ortiz data provides no useful information regarding the effect of column axial load on the joint shear strength of monotonically loaded exterior beam column joints.

Inspection of the above table shows another trend. BCJ1 and BCJ5 are compared in terms of beam cracking load. It is clear that the load at which cracking occurred increased when the column axial load is increased from 0 to 300 kN. The same trend exists for BCJ3 and BCJ6. However, the beam loads at failure are unchanged by increasing the column axial load. The failure modes are also unchanged.

Table 4.12. Anchorage lengths and normalized joint shear strengths of Ortiz specimens

Specimen	Column Load	Beam Load at Cracking	Beam Load at Failure	Radius of bend of the beam bar	Length of vertical leg of the beam bar	Failure Mode	Normalized Joint Shear Strength $v_j=V_j/b_e h_c\sqrt{f_c}$	Ratio of Tensile Reinforcement
Units	kN	kN	kN	mm	mm	-	$MPa^{0.5}$	-
BCJ1	0	40	118	65	420	Joint Shear	0.909	1.00
BCJ2	0	50	125	65	420	Joint Shear	0.944	1.00
BCJ3	0	50	118	130	420	Joint Shear	0.968	1.00
BCJ4	0	50	130	65	290	Joint Shear	1.05	1.00
BCJ5	300	80	115	65	290	Joint Shear	0.865	1.00
BCJ6	300	80	115	130	225	Joint Shear	0.908	1.00
BCJ7	300	70	170	130	225	Beam Failure	1.33	1.00

4.2.3.2.2. Influence of Column Longitudinal Reinforcement Ratio

Ortiz specimens can not be directly compared regarding the influence of column longitudinal reinforcement ratio because the factors affecting the joint shear strength such as the radius of bend, the anchorage lengths and the column loads are all different in specimens.

4.2.3.2.3. Influence of the Radius of Bend

Inspection of BCJ1 and BCJ3 shows that there is 6% increase in the normalized joint shear strength if the radius of the bend is increased from 65mm to 130 mm.

Inspection of BCJ5 and BCJ6 also shows that there is a 4.7 % increase in the joint shear strength if the radius of the bend is increased from 65 mm to 130 mm. The relative decrease from 6 to 4.7 % shows that 90 mm decrease in the vertical anchorage length of BCJ6 decreases the joint shear strength.

4.2.3.2.4. Influence of the vertical anchorage length

Inspection of BCJ1 and BCJ5 shows that there is 5% decrease in the normalized joint shear strength of BCJ5 with respect to BCJ1 although the column axial load is increased from 0 to 300 kN and the column longitudinal reinforcement ratio is increased from 2.01 to 3.35. This means that decreasing the length of the vertical leg of beam longitudinal reinforcement decreases the joint shear strength. The column axial load and the increase in the column bar ratio are quite low to change this trend. The comparison of BCJ3 and BCJ6 shows the same trend. The author is of the opinion that, the decrease in the shear strength of BCJ5 with respect to BCJ1 and BCJ6 with respect to BCJ3 is mainly due to the decrease in the anchorage length.

4.2.3.2.5. Influence of Joint Stirrups

The stirrup forces calculated from the measured stirrup strains of Ortiz are shown in Table 4.13. First, the joint shear strength of BCJ1 and BCJ2 will be compared. The beam-cracking load is increased by 20 % by the provision of stirrups and the beam failure load is increased by 5.6 %. The increase of joint shear strength due to stirrups can be neglected if the joint tie ratio is 0.002. The joint shear strength of BCJ2 is increased by 3.7 % relative to BCJ1 by the provision of 1T8 tie in which is situated just at the middle of the joint. The BCJ2 and BCJ4 have same radius of bends. However the vertical anchorage length is 130 mm less for BCJ4 compared to BCJ2. The column axial loads are zero for both BCJ2 and BCJ4. Because of this, the beam loads at cracking for BCJ2 and BCJ4 are same. The failure load is 3.8% higher for BCJ4 than BCJ2. The joint shear strength on the other hand is 10 % higher in BCJ4 compared with BCJ2. The only possible reason for this could be the increased stirrup ratio. The joint stirrup ratio is 0.001 in BCJ2; 0.003 in BCJ4. This 50 % increase in the stirrup ratio resulted in 10% increase in the joint shear strength.

Table 4.13. Stirrup forces reported by Ortiz

Specimen	Reported Stirrup Strains	Stirrup Force	Total Stirrup Force	Normalized Joint Shear Strength $v_j=V_j/b_e h_c\sqrt{f_c}$	Length of Vertical Length of Beam Bar	Beam Load at Cracking	Beam Load at Failure	Radius of bend of the beam bar
Units	* (10^*6)	kN	kN	$MPa^{0.5}$	mm	kN	kN	mm
BCJ1		-	-	0.909	420	40	118	65
BCJ2	y7584	57	57	0.944	420	50	125	65
BCJ3		-	-	0.968	420	50	118	130
BCJ4	1887 y2990 y3003 1139	38 57 57 22	114	1.052	290	50	130	65
BCJ5		-	-	0.865	290	80	115	65
BCJ6		-	-	0.908	225	80	115	130
BCJ7	1445 1942 1442 1826 305	48 64 48 60 10	172	1.33	225	70	170	130

when the stirrup ratio is increased to 0.005, the joint shear strength of BCJ7 will be 21% higher than BCJ4 and 29% higher than BCJ2. The possible increase of the shear strength could be due to the effect of the increase in the radius of bend of the beam longitudinal reinforcement in BCJ7 with respect to BCJ4 and BCJ2.

4.2.3.2.6. The Effect of the Concrete Cylinder Strength on the Joint Shear Strength

As will be explained in the following sections, the joint shear strength of exterior beam column joints is proportional to the square root of the concrete cylinder strength. The author found this relation to be:

$$V_j \approx \sqrt{f_c}\, b_e\, h_c \qquad (4.6)$$

The average of Ortiz specimens is $V_j = 0.91\sqrt{f_c}\, b_e\, h_c$

4.2.3.3.Conclusions from the Analysis of Ortiz

1. The joint shear strength is proportional to the square root of the concrete cylinder strength.
2. An increase in the radius of bend of the beam longitudinal reinforcement will result in an increase in the joint shear strength of monotonically loaded exterior beam column connections. This increase will be around 5%.
3. Reducing the vertical anchorage length will decrease the joint shear strength. But the extent of this can not be deduced from the specimens of Ortiz as it is difficult to separate the influences of different variables chosen by Ortiz that are interacting with each other.
4. Stirrups increase the joint shear strength but at different rates for different stirrup ratios. If stirrups such as in BCJ2 are provided, the joint shear strength is not increased possibly because:

   a) The number of stirrups provided is insufficient to provide confinement for the joint.

   b) The amount of stirrup is not sufficient to increase the joint shear strength of joints. There is 10% increase in the joint shear strength of BCJ4 relative to BCJ2.

   c) If stirrups such as BCJ7 are provided, all the stirrups do not yield. The joint shear strength is increased by 29% with respect to BCJ2.
5. There are no conclusive data in the tests of Ortiz regarding the effect of the column axial load on the joint shear strength of the monotonically loaded exterior beam column joints. But the cracking load of the beam is considerably increased by the provision of column axial load.
5. There is no conclusive data regarding the effect of the amount of the column longitudinal reinforcement ratio on the joint shear strength of exterior beam column joints.

Specimen[1]	Concrete cube strength	Concrete tensile strength f_t	Cracking load	Failure load	Failure mode[2]
Units	MPa	MPa	kN	kN	-
C6LN0	64	3.4	18.5	23.9	S
C6LN1	64	3.3	18.1	24.6	S
C6NL3	61	3.2	17.8	28.7	S
C6NL5	46	2.7	14.7	33.9	S
C6LH0	126	4.7	25.4	36.1	S
C6LH1	127	4.9	22.2	37.1	S
C6LH3	121	3.7	23.3	41.2	S
C6LH5	125	5.2	25.5	51.4	B
C4ALN0	53	2.7	13.2	26.5	C
C4ALN1[4]	57	3.2	18.7	33.5	S
C4ALN3[5]	52	2.9	13.3	35.2	S
C4ALN5	63	3.2	14.1	39.5	S
C4ALH0	130	4.9	20.6	43.2	C
C4ALH1[6]	119	3.7	19.6	43.4	B
C4ALH3	132	5.5	24.8	46.1	B
C4ALH5	123	5.0	27.4	48.7	B

Notes

1. All beams 210 mm deep and reinforced with 2T16 bars. Beams denoted C6 are reinforced with U bars and beams denoted C4 with L bars. Number (i.e. 0, 1, 3 or 5) refers to number of joint stirrups.
2. Failure modes as follows; S shear, C connection zone reinforcement pull out, B beam failure.
3. Column load was 50 kN for normal strength specimens and 100 kN for high strength specimens with exception of C6LN1 which was loaded to 100 kN.
4. Maximum stirrup strain 2080 microstrain at failure. Average strain 1530 microstrain at failure.
5. Maximum stirrup strains at failure 2100 top, 2880 middle, 2340 bottom.
6. Stirrup strains of over 22000 microstrain were observed.

Table 4.14. The details of Scott and Hamill tests adapted from . Vollum.

4.2.4. Scott and Hamill Specimens

Scott and Hamill specimens have also got beam prop forces around 2 to 10 kN. Scott and Hamill have made 16 experiments with the same geometry of Scott's tests. The depth of the beam was 210 mm in all of Scott tests. No information is provided regarding the yield stress of stirrups in Scott's tests. The steel used for the stirrups in Scott's and later in Scott and Hamill tests were provided by different manufacturers. The stirrups in the specimens of Scott and Hamill are as follows: The joints were reinforced by 0, 1, 3 or 5 stirrups Table 4.14 shows the details of Scott and Hamil's tests adapted from Vollum.

4.2.4.1.The analysis of Scott and Hamill tests

The analysis of Scott and Hamill tests is made according to section 4.2.1. The results are shown in Table 4.15.

The analysis of specimens C4ALHO and C4ALH1 of Scott and Hamill is of concern. These two specimens are high strength concrete specimens. C4ALHO has got no joint stirrups, has very low column axial stress and high concrete strength. C4ALH1 on the other hand is almost identical to C4ALHO, however it is provided by a single stirrup at the center of the joint. Inspection of the two specimens shows that provision of a single stirrup in the joint results in 5% increase in the normalized joint shear strength.

Table 4.15. The analysis of Scott and Hamill tests

Specimen	Cylinder Strength	Type of Detailing of the Beam Bars	Failure Mode	Effective Joint Stirrups	Column Axial Stress/fc	Joint Shear Strength $v_j = V_j / b_c h_c \sqrt{fc}$	Ratio of Tensile Reinforcement	Joint Aspect Ratio
Units	MPa	-	-	-	-	MPa	-	-
C4ALN3	41.6	1	J	2T6	0.053	1.245	1.976	1.4
C4ALH0	104	1	P	0	0.021	0.919	1.976	1.4
C4ALN5	50.4	1	J	3T6	0.044	1.250	1.976	1.4
C4ALH3	105.6	1	B	2T6	0.042	0.935	1.976	1.4
C4ALH5	98.4	1	B	3T6	0.045	0.960	1.976	1.4
C4ALNO	42.4	1	P	0	0.062	0.910	1.976	1.4
C4ALN1	45.6	1	J	1T6	0.058	1.116	1.976	1.4
C4ALH1	95.2	1	B	1T6	0.046	0.967	1.976	1.4
Mean (L Bars)	70.489				0.047	1.115		1.4
Mean (Total)	73.15				0.050	1.009		1.4

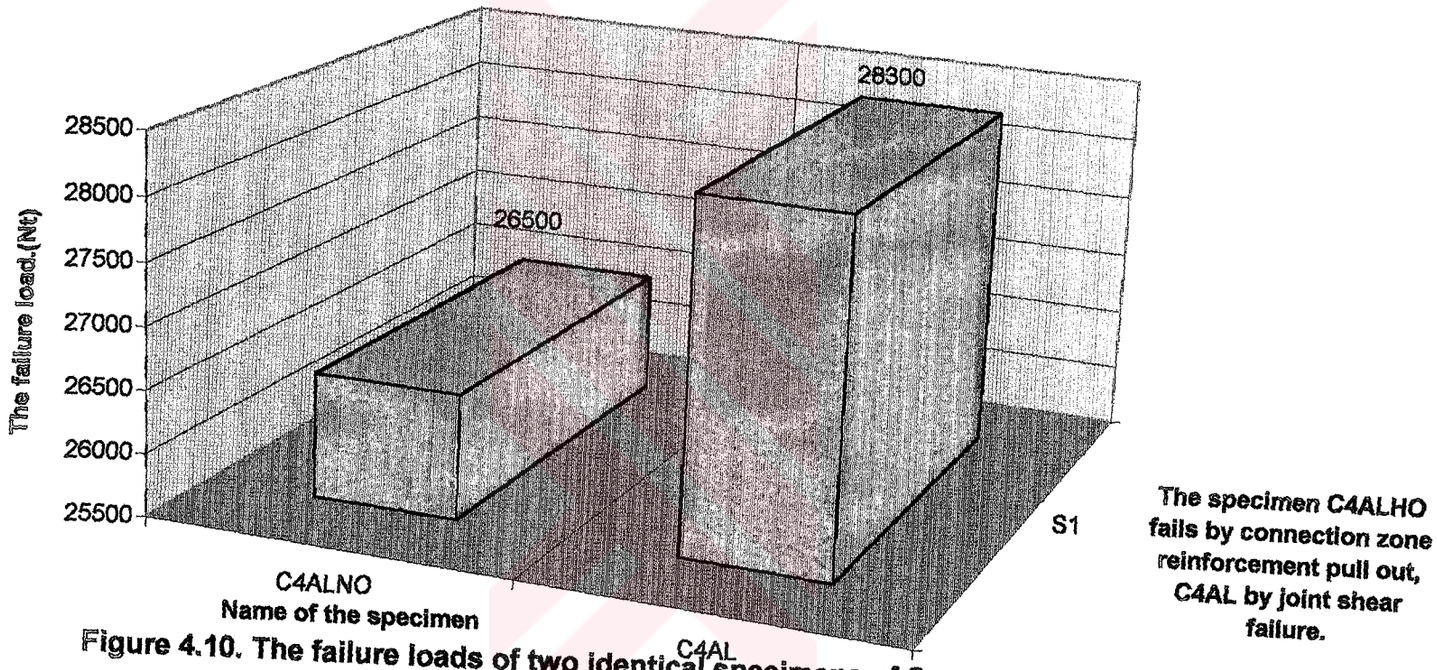

Figure 4.10. The failure loads of two identical specimens of Scott and Scott and Hamill which fail by different failure modes.

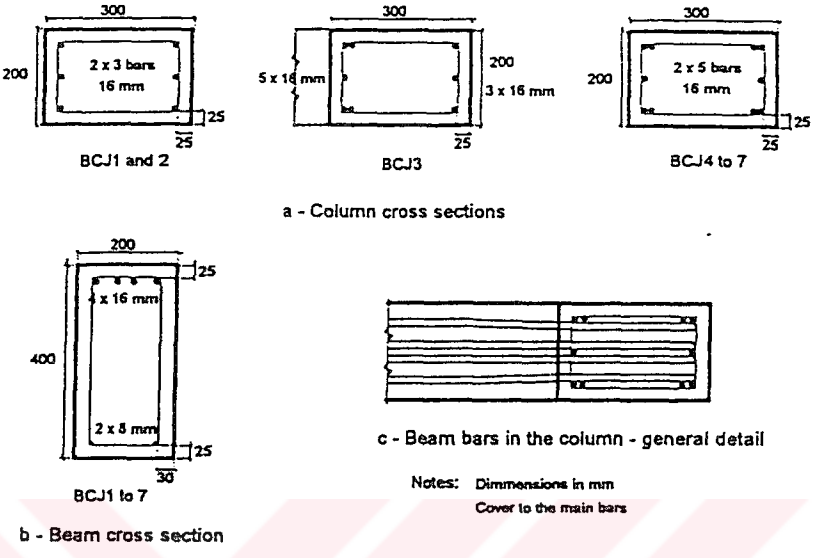

Figure 4.6 : The details of the cross sections of Ortiz specimens.

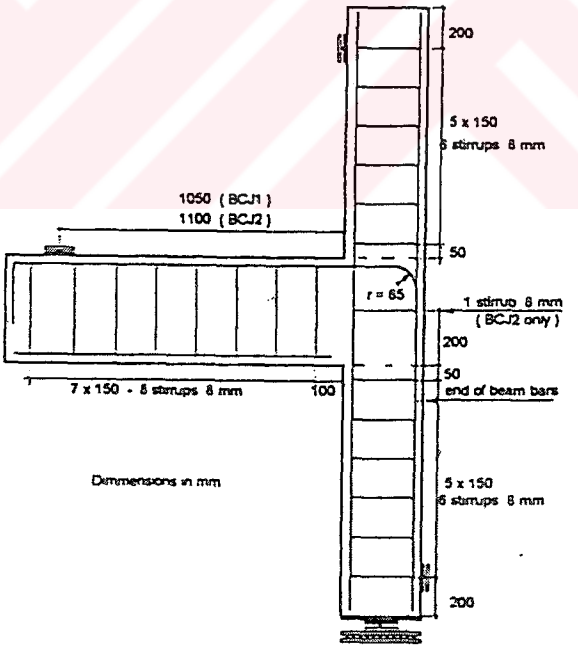

Figure 4.7 : The details of the beam column joints 1 and 2 respectively.

The analysis of C7 and C4A of Scott is also of concern. Inspection of specimen C7 clearly shows that, it has got the lowest normalized shear strength of all the beam bars bent down detail specimens. Nevertheless, it has the same column axial load, same type of detailing, same amount of beam and column reinforcement as well as effective stirrups as that of C4A. The only difference between the two specimens is that, the joint aspect ratio of C4A is 30 % less than that of C7. The joint shear strength of C4A is 29.7 % greater than C7. This shows a relationship between the normalized shear strength and the joint aspect ratio.

4.2.3. The Experimental work of Ortiz

Ortiz has made seven tests on exterior monotonically loaded beam column joints. The variables of her tests were the joint stirrups, column axial load and detailing of beam reinforcement on the strength of monotonically loaded connections. The Figures 4.6 and 4.7 shows the detail of the cross sections of Ortiz specimens and details of the beam column joints 1 and 2 respectively. The details of the beam column joints 3, 4 and 6 are shown in Figure 4.8 and the properties of the test specimens 5 and 7 are shown in Figure 4.9.

4.2.3.1.Reinforcement Properties:

The beam reinforcement details and Column reinforcement details are shown in Tables 4.6 and 4.7 respectively. The concrete splitting and crushing strengths are shown in Table 4.8, whereas the shear reinforcement details are shown in Table 4.9. Table 10 shows the radius of bends of beam bars.

Table 4.6. Beam reinforcement

BCJ	Diameter ϕ mm	Total area A_s mm^2	Reinforc. Percentage A_s/bd %	Yield strength f_y MPa	Bend Radius mm	Straight anchorage mm
1& 2	16	804	1.1	720	65	420
3	16	804	1.1	720	130	420
4& 5	16	804	1.1	720	65	290
6& 7	16	804	1.1	720	130	220

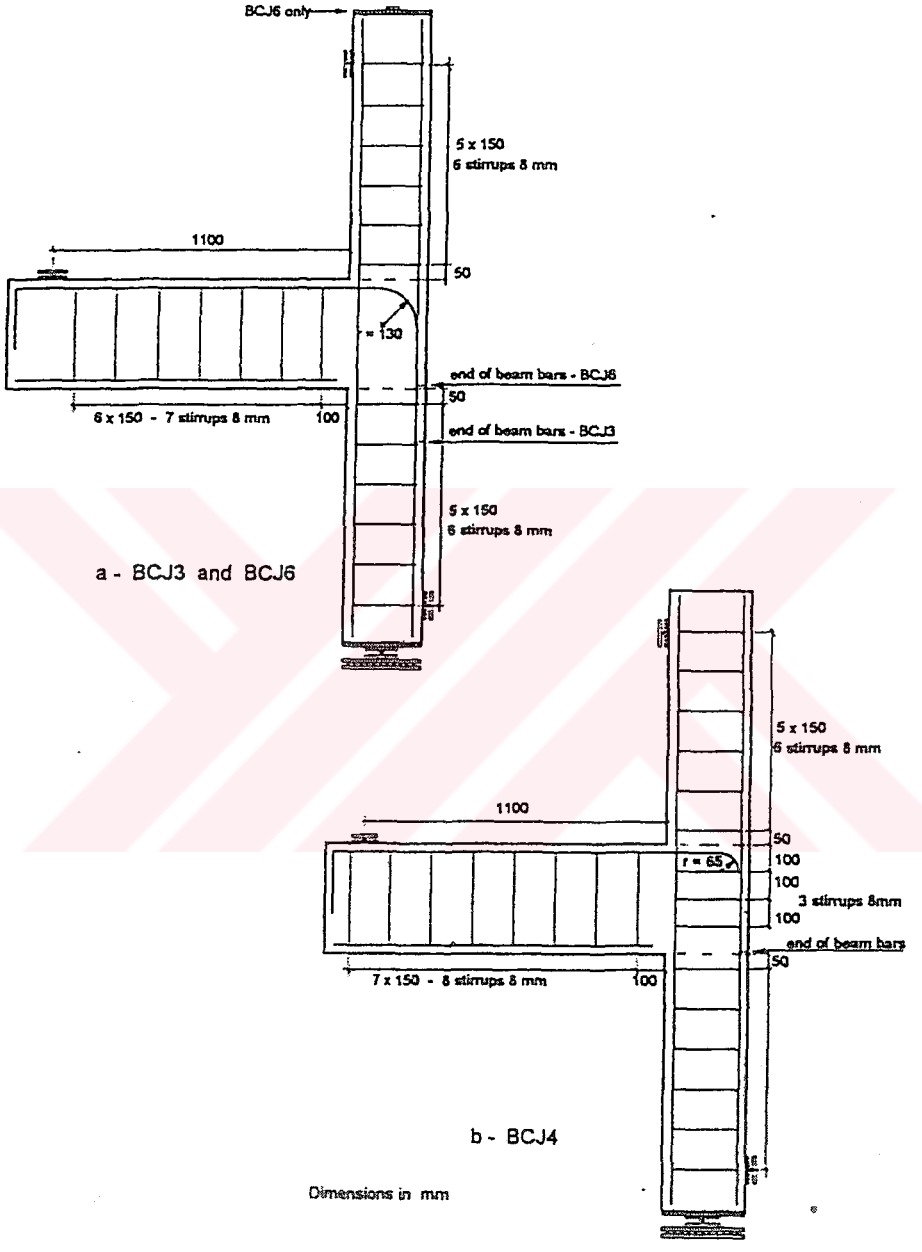

Figure 4.8 : The details of the beam column joints 3, 4 and 6.

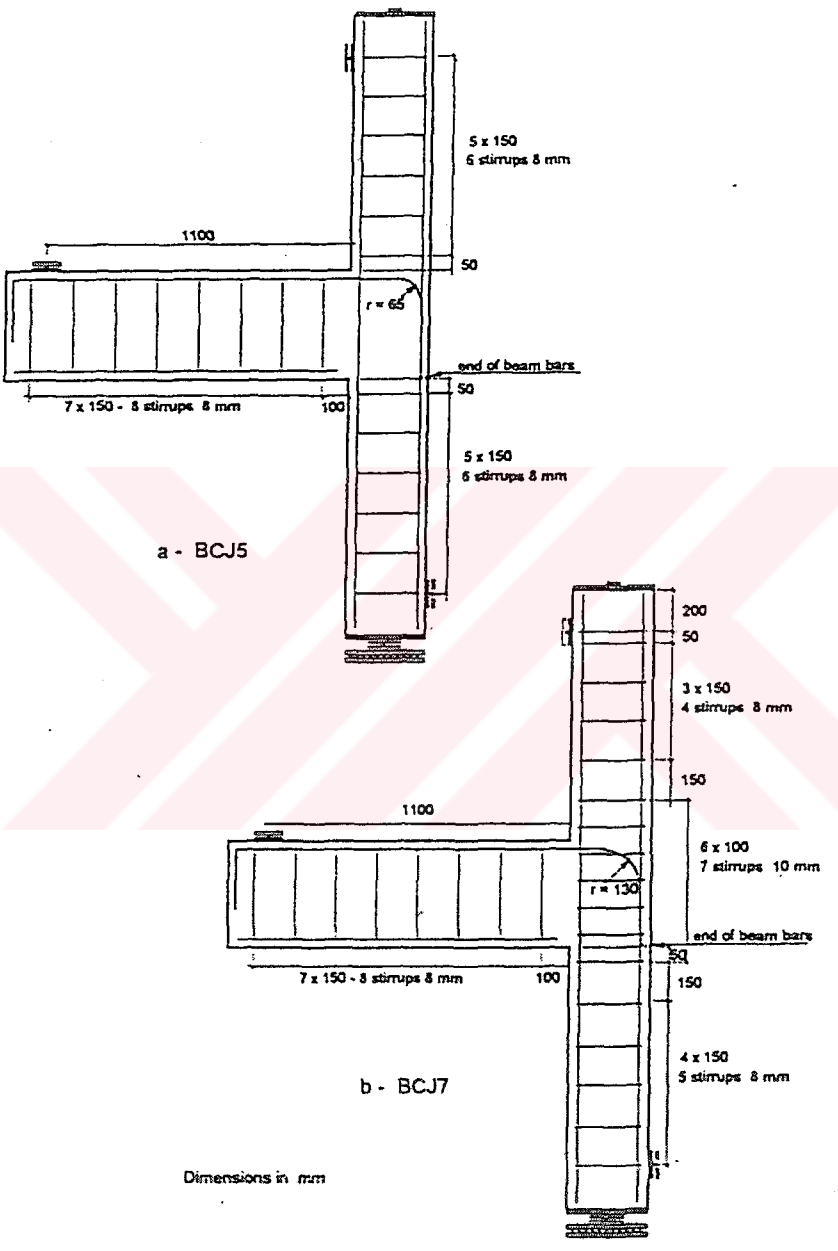

Figure 4.9 : The properties of the test specimens 5 and 7.

Table 4.7. Column reinforcement

BCJ	Diameter ϕ mm	Total area A_s mm^2	Reinforc.Percentage A_s / bd %	Yield strength f_y MPa
1& 2	16	1206	2.01	720
3	16	1608	2.68	720
4 to 7	16	2010	3.35	720

Table 4.8. Concrete splitting and crushing strengths

BCJ	Splitting strength f_{sp} MPa	Cube strength f_{cu} MPa	Cylinder strength f_c MPa
1	2.77	42.3	34
2	3.68	47.2	38
3	3.31	41.3	33
4	2.98	42	34
5	3.29	47.4	38
6	3.43	43.7	35
7	3.23	44	35

Table 4.9. Shear reinforcement

BCJ	No of joint stirrups	Joint stirrup diameter mm	Column stirrup diameter mm	Beam stirrup diameter mm	Yield strength f_y MPa
1	-	-	8	8	571
2	1	8	8	8	571
3	-	-	8	8	571
4	3	8	8	8	571
5	-	-	8	8	571
6	-	-	8	8	571
7	4	10	8 10	8	571 556

4.2.3.2.Test Results

In BCJ1, the widened cracks ran further along the column bars spalling off the cover above the joint. At failure, the central crack was wide open and the concrete crushed near its lower end. The concrete spalled off in a large area around the column bars at the beam side of the joint, at middle height of the beam. These column bars were highly stressed and the high bond stresses were the probable cause of the spalling. In BCJ2, BCJ5, BCJ6 and BCJ3, as load was increased, new cracks developed parallel to the proposed strut direction following the column bars above the joint. Failure occurred with wide opening of these cracks and spalling of the cover of the column bars. BCJ4 showed a similar behavior to BCJ3 and BCJ2 at failure. However in addition to this, two stirrups yielded. At BCJ7 on the other hand, with stirrups tying the core of the joint, no bond deterioration occurred and failure occurred in the beam by yielding of the beam bars and crushing of the horizontal beam chord at the corner of the joint.

Table 4.10. The radius of bend of beam bars and corresponding failure modes of Ortiz specimens

Specimen	Column load	Beam load at cracking Pcr	Beam load at failure Pu	Radius of the bend of beam bar	Failure Mode
Units	kN	kN	kN	mm	-
BCJ1	0	40	118	65	joint shear
BCJ2	0	50	125	65	joint shear
BCJ3	0	50	118	130	joint shear
BCJ4	0	50	130	65	joint shear
BCJ5	300	80	115	65	joint shear
BCJ6	300	80	115	130	joint shear
BCJ7	300	70	170	130	joint shear

4.2.3.2.1.Influence of Column Axial Load

No axial load was present on Ortiz specimens BCJ1 to BCJ4. In BCJ4, BCJ5 and BCJ7 on the other hand, the column axial load was increased to 300 kN. The test specimens of Ortiz do not give an idea about the effect of column axial load on the joint shear strength of exterior beam column joints. The main reason for this is the specimens, which have different column axial loads, different vertical anchorage length for beam bars and different radius of bends. The characteristics of the specimens are given in Table 4.11.

Table 4.11. Normalized joint shear strengths of Ortiz specimens and corresponding vertical anchorage lengths.

Specimen	Radius of bend	Length of vertical leg	Column axial load	$V_j/ b_e h_c f_c$	$V_j/b_e h_c\sqrt{f_c}$	$100A_{scol}/b_e/d_c$
Units	mm	mm	kN	-	$MPa^{0.5}$	mm^2
BCJ1	65	420	0	0.156	0.909	2.01
BCJ3	130	420	0	0.168	0.968	2.68
BCJ5	65	290	300	0.14	0.865	3.35
BCJ6	130	200	300	0.1535	0.908	3.35

The above specimens are not reinforced by transverse reinforcement. Inspection of BCJ1 and BCJ5 shows that there is 5% decrease in the normalized joint shear strength of BCJ5 with respect to BCJ1 although the column axial load is increased from 0 to 300 kN and the column longitudinal reinforcement ratio is increased from 2.01 to 3.35. Analysis of the experimental data of Scott suggests that the column load is unlikely to decrease the joint shear strength, it can either increase the joint shear strength or it won't affect it. This means that decreasing the length of the vertical leg of beam bars is the cause of the decrease in the joint shear strength.

Inspection of BCJ3 and BCJ6 again shows that the normalized joint shear strength is decreased by 6 % due to the decrease in the anchorage length.

As a result, Ortiz data provides no useful information regarding the effect of column axial load on the joint shear strength of monotonically loaded exterior beam column joints.

Inspection of the above table shows another trend. BCJ1 and BCJ5 are compared in terms of beam cracking load. It is clear that the load at which cracking occurred increased when the column axial load is increased from 0 to 300 kN. The same trend exists for BCJ3 and BCJ6. However, the beam loads at failure are unchanged by increasing the column axial load. The failure modes are also unchanged.

Table 4.12. Anchorage lengths and normalized joint shear strengths of Ortiz specimens

Specimen	Column Load	Beam Load at Cracking	Beam Load at Failure	Radius of bend of the beam bar	Length of vertical leg of the beam bar	Failure Mode	Normalized Joint Shear Strength $v_j=V_j/b_e h_c\sqrt{f_c}$	Ratio of Tensile Reinforcement
Units	kN	kN	kN	mm	mm	-	$MPa^{0.5}$	-
BCJ1	0	40	118	65	420	Joint Shear	0.909	1.00
BCJ2	0	50	125	65	420	Joint Shear	0.944	1.00
BCJ3	0	50	118	130	420	Joint Shear	0.968	1.00
BCJ4	0	50	130	65	290	Joint Shear	1.05	1.00
BCJ5	300	80	115	65	290	Joint Shear	0.865	1.00
BCJ6	300	80	115	130	225	Joint Shear	0.908	1.00
BCJ7	300	70	170	130	225	Beam Failure	1.33	1.00

4.2.3.2.2. Influence of Column Longitudinal Reinforcement Ratio

Ortiz specimens can not be directly compared regarding the influence of column longitudinal reinforcement ratio because the factors affecting the joint shear strength such as the radius of bend, the anchorage lengths and the column loads are all different in specimens.

4.2.3.2.3. Influence of the Radius of Bend

Inspection of BCJ1 and BCJ3 shows that there is 6% increase in the normalized joint shear strength if the radius of the bend is increased from 65mm to 130 mm.

Inspection of BCJ5 and BCJ6 also shows that there is a 4.7 % increase in the joint shear strength if the radius of the bend is increased from 65 mm to 130 mm. The relative decrease from 6 to 4.7 % shows that 90 mm decrease in the vertical anchorage length of BCJ6 decreases the joint shear strength.

4.2.3.2.4. Influence of the vertical anchorage length

Inspection of BCJ1 and BCJ5 shows that there is 5% decrease in the normalized joint shear strength of BCJ5 with respect to BCJ1 although the column axial load is increased from 0 to 300 kN and the column longitudinal reinforcement ratio is increased from 2.01 to 3.35. This means that decreasing the length of the vertical leg of beam longitudinal reinforcement decreases the joint shear strength. The column axial load and the increase in the column bar ratio are quite low to change this trend. The comparison of BCJ3 and BCJ6 shows the same trend. The author is of the opinion that, the decrease in the shear strength of BCJ5 with respect to BCJ1 and BCJ6 with respect to BCJ3 is mainly due to the decrease in the anchorage length.

4.2.3.2.5. Influence of Joint Stirrups

The stirrup forces calculated from the measured stirrup strains of Ortiz are shown in Table 4.13. First, the joint shear strength of BCJ1 and BCJ2 will be compared. The beam-cracking load is increased by 20 % by the provision of stirrups and the beam failure load is increased by 5.6 %. The increase of joint shear strength due to stirrups can be neglected if the joint tie ratio is 0.002. The joint shear strength of BCJ2 is increased by 3.7 % relative to BCJ1 by the provision of 1T8 tie in which is situated just at the middle of the joint. The BCJ2 and BCJ4 have same radius of bends. However the vertical anchorage length is 130 mm less for BCJ4 compared to BCJ2. The column axial loads are zero for both BCJ2 and BCJ4. Because of this, the beam loads at cracking for BCJ2 and BCJ4 are same. The failure load is 3.8% higher for BCJ4 than BCJ2. The joint shear strength on the other hand is 10 % higher in BCJ4 compared with BCJ2. The only possible reason for this could be the increased stirrup ratio. The joint stirrup ratio is 0.001 in BCJ2; 0.003 in BCJ4. This 50 % increase in the stirrup ratio resulted in 10% increase in the joint shear strength.

Table 4.13. Stirrup forces reported by Ortiz

Specimen	Reported Stirrup Strains	Stirrup Force	Total Stirrup Force	Normalized Joint Shear Strength $v_j=V_j/b_e h_c\sqrt{f_c}$	Length of Vertical Length of Beam Bar	Beam Load at Cracking	Beam Load at Failure	Radius of bend of the beam bar
Units	* (10^*6)	kN	kN	$MPa^{0.5}$	mm	kN	kN	mm
BCJ1		-	-	0.909	420	40	118	65
BCJ2	y7584	57	57	0.944	420	50	125	65
BCJ3		-	-	0.968	420	50	118	130
BCJ4	1887 y2990 y3003 1139	38 57 57 22	114	1.052	290	50	130	65
BCJ5		-	-	0.865	290	80	115	65
BCJ6		-	-	0.908	225	80	115	130
BCJ7	1445 1942 1442 1826 305	48 64 48 60 10	172	1.33	225	70	170	130

when the stirrup ratio is increased to 0.005, the joint shear strength of BCJ7 will be 21% higher than BCJ4 and 29% higher than BCJ2. The possible increase of the shear strength could be due to the effect of the increase in the radius of bend of the beam longitudinal reinforcement in BCJ7 with respect to BCJ4 and BCJ2.

4.2.3.2.6. The Effect of the Concrete Cylinder Strength on the Joint Shear Strength

As will be explained in the following sections, the joint shear strength of exterior beam column joints is proportional to the square root of the concrete cylinder strength. The author found this relation to be:

$$V_j \approx \sqrt{f_c}\, b_e\, h_c \qquad (4.6)$$

The average of Ortiz specimens is $V_j = 0.91\sqrt{f_c}\, b_e\, h_c$

4.2.3.3.Conclusions from the Analysis of Ortiz

1. The joint shear strength is proportional to the square root of the concrete cylinder strength.
2. An increase in the radius of bend of the beam longitudinal reinforcement will result in an increase in the joint shear strength of monotonically loaded exterior beam column connections. This increase will be around 5%.
3. Reducing the vertical anchorage length will decrease the joint shear strength. But the extent of this can not be deduced from the specimens of Ortiz as it is difficult to separate the influences of different variables chosen by Ortiz that are interacting with each other.
4. Stirrups increase the joint shear strength but at different rates for different stirrup ratios. If stirrups such as in BCJ2 are provided, the joint shear strength is not increased possibly because:

   a) The number of stirrups provided is insufficient to provide confinement for the joint.

   b) The amount of stirrup is not sufficient to increase the joint shear strength of joints. There is 10% increase in the joint shear strength of BCJ4 relative to BCJ2.

   c) If stirrups such as BCJ7 are provided, all the stirrups do not yield. The joint shear strength is increased by 29% with respect to BCJ2.
5. There are no conclusive data in the tests of Ortiz regarding the effect of the column axial load on the joint shear strength of the monotonically loaded exterior beam column joints. But the cracking load of the beam is considerably increased by the provision of column axial load.
5. There is no conclusive data regarding the effect of the amount of the column longitudinal reinforcement ratio on the joint shear strength of exterior beam column joints.

Specimen[1]	Concrete cube strength	Concrete tensile strength f_t	Cracking load	Failure load	Failure mode[2]
Units	MPa	MPa	kN	kN	-
C6LN0	64	3.4	18.5	23.9	S
C6LN1	64	3.3	18.1	24.6	S
C6NL3	61	3.2	17.8	28.7	S
C6NL5	46	2.7	14.7	33.9	S
C6LH0	126	4.7	25.4	36.1	S
C6LH1	127	4.9	22.2	37.1	S
C6LH3	121	3.7	23.3	41.2	S
C6LH5	125	5.2	25.5	51.4	B
C4ALN0	53	2.7	13.2	26.5	C
C4ALN1[4]	57	3.2	18.7	33.5	S
C4ALN3[5]	52	2.9	13.3	35.2	S
C4ALN5	63	3.2	14.1	39.5	S
C4ALH0	130	4.9	20.6	43.2	C
C4ALH1[6]	119	3.7	19.6	43.4	B
C4ALH3	132	5.5	24.8	46.1	B
C4ALH5	123	5.0	27.4	48.7	B

Notes

1. All beams 210 mm deep and reinforced with 2T16 bars. Beams denoted C6 are reinforced with U bars and beams denoted C4 with L bars. Number (i.e. 0, 1, 3 or 5) refers to number of joint stirrups.
2. Failure modes as follows; S shear, C connection zone reinforcement pull out, B beam failure.
3. Column load was 50 kN for normal strength specimens and 100 kN for high strength specimens with exception of C6LN1 which was loaded to 100 kN.
4. Maximum stirrup strain 2080 microstrain at failure. Average strain 1530 microstrain at failure.
5. Maximum stirrup strains at failure 2100 top, 2880 middle, 2340 bottom.
6. Stirrup strains of over 22000 microstrain were observed.

Table 4.14. The details of Scott and Hamill tests adapted from . Vollum.

4.2.4. Scott and Hamill Specimens

Scott and Hamill specimens have also got beam prop forces around 2 to 10 kN. Scott and Hamill have made 16 experiments with the same geometry of Scott's tests. The depth of the beam was 210 mm in all of Scott tests. No information is provided regarding the yield stress of stirrups in Scott's tests. The steel used for the stirrups in Scott's and later in Scott and Hamill tests were provided by different manufacturers. The stirrups in the specimens of Scott and Hamill are as follows: The joints were reinforced by 0, 1, 3 or 5 stirrups Table 4.14 shows the details of Scott and Hamil's tests adapted from Vollum.

4.2.4.1.The analysis of Scott and Hamill tests

The analysis of Scott and Hamill tests is made according to section 4.2.1. The results are shown in Table 4.15.

The analysis of specimens C4ALHO and C4ALH1 of Scott and Hamill is of concern. These two specimens are high strength concrete specimens. C4ALHO has got no joint stirrups, has very low column axial stress and high concrete strength. C4ALH1 on the other hand is almost identical to C4ALHO, however it is provided by a single stirrup at the center of the joint. Inspection of the two specimens shows that provision of a single stirrup in the joint results in 5% increase in the normalized joint shear strength.

Table 4.15. The analysis of Scott and Hamill tests

Specimen	Cylinder Strength	Type of Detailing of the Beam Bars	Failure Mode	Effective Joint Stirrups	Column Axial Stress/fc	Joint Shear Strength $v_j = V_j / b_c h_c \sqrt{fc}$	Ratio of Tensile Reinforcement	Joint Aspect Ratio
Units	MPa	-	-	-	-	MPa	-	-
C4ALN3	41.6	1	J	2T6	0.053	1.245	1.976	1.4
C4ALH0	104	1	P	0	0.021	0.919	1.976	1.4
C4ALN5	50.4	1	J	3T6	0.044	1.250	1.976	1.4
C4ALH3	105.6	1	B	2T6	0.042	0.935	1.976	1.4
C4ALH5	98.4	1	B	3T6	0.045	0.960	1.976	1.4
C4ALNO	42.4	1	P	0	0.062	0.910	1.976	1.4
C4ALN1	45.6	1	J	1T6	0.058	1.116	1.976	1.4
C4ALH1	95.2	1	B	1T6	0.046	0.967	1.976	1.4
Mean (L Bars)	70.489				0.047	1.115		1.4
Mean (Total)	73.15				0.050	1.009		1.4

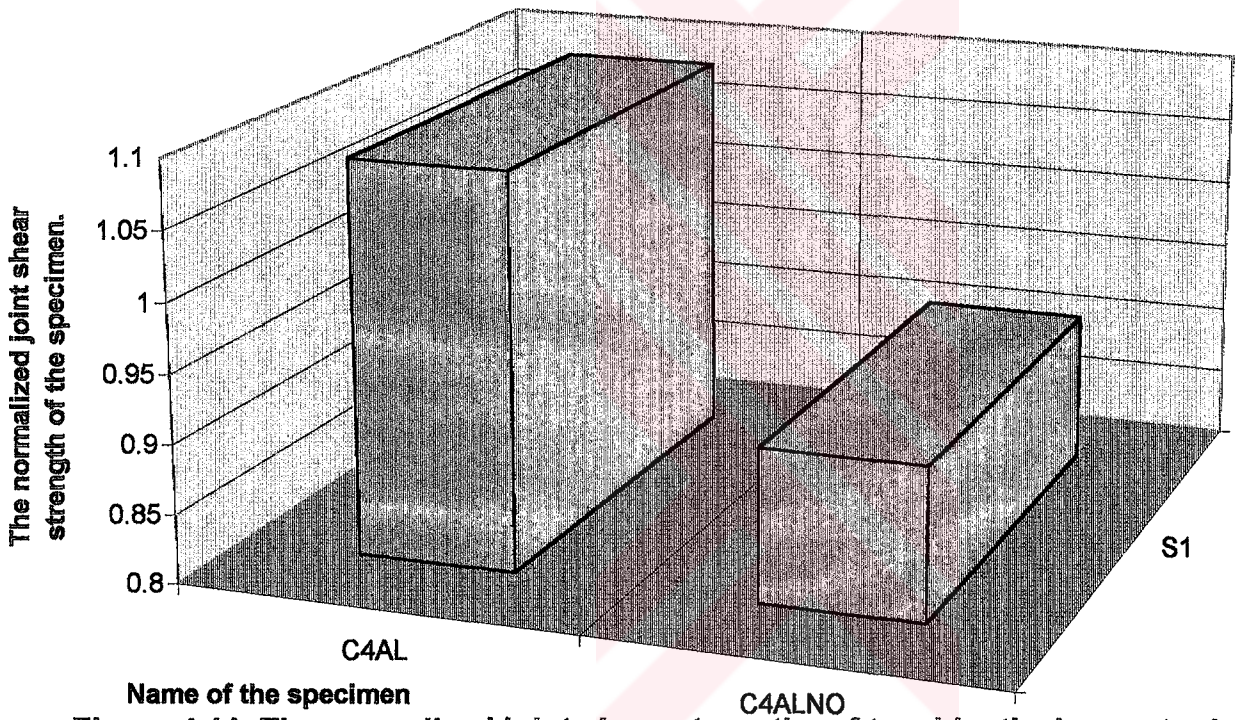

Figure 4.11. The normalized joint shear strengths of two identical monotonically loaded exterior beam column connections which fail by different failure modes.

The specimens C4ALNO and C4ALN1 of **Scott and Hamill** are analyzed. These two specimens are normal strength concrete specimens. C4ALNO has got no joint stirrups, very low column axial stress and high concrete strength. C4ALN1 on the other hand is almost identical to C4ALNO, however it is provided by a single stirrup at the center of the joint. Inspection of these two specimens shows that provision of a single stirrup results in 18% increase in the normalized joint shear strength of monotonically loaded exterior beam column connections. The specimen C4ALN1 exhibits joint shear failure, while C4ALNO exhibits connection zone reinforcement pull out. As mentioned previously, the model adapted determines the normalized shear strength of monotonically loaded exterior beam-column joints, which exhibit joint shear failure accurately. However, the specimens' normalized joint shear strengths which exhibit beam or connection zone reinforcement pull out failures are determined on the basis that beam longitudinal reinforcement yield. It is clear that, provision of even a single stirrup increases the normalized joint shear strength of monotonically loaded exterior beam column joints. However, the extent of this is not clear from the above data because, the failure modes are different.

The specimens C4ALNO and C4AL of **Scott and Hamill** are analyzed. These specimens are two identical specimens except that C4ALNO has got 42.4 MPa concrete cylinder strength, C4AL has got 35.76 MPa. In spite of that, the failure modes are different. C4ALNO exhibited connection zone reinforcement pull out, while C4AL exhibited joint shear failure. Figures 4.10 and 4.11 show that the type of failure modes also affect the failure loads and the normalized joint shear strengths.

The specimen, which has the highest normalized joint shear strength, is specimen C4AL5. The possible reason for this is that the specimen has the highest amount of joint stirrups.

The specimens C4ALN1 and C4ALN3 are identical except the number of effective joint stirrups. The normalized joint shear strength increases by only 10.36% by the increasing the ratio of stirrups from 0.003 to 0.006.

The specimens C4ALN5 and C4ALN3 are identical except the number of effective joint stirrups. The normalized joint shear strength increases by only 0.4% by the increase in the ratio of stirrups from 0.006 to 0.009.

4.2.5. The tests of Parker and Bullmann

Parker and Bullman (1997) conducted twelve experiments on monotonically loaded exterior beam column connections. The layout of the specimens is shown in Figure 4.12. The details of the tests and the material properties are shown in Table 4.16 and Table 4.17 respectively. Six of the specimens had no links in the joint while the other six had T12 links, which were, provided in 150 mm spacing for specimens 5a, 5b and 5c. The spacing of the stirrups was 100 mm for specimens 5d, 5e and 5f. The radius of the bend of the beam bars was 3ϕ for all specimens. The radius of the bend was 75 mm for specimens from 4a to 5d. Specimens 5d, 5e and 5f had radius of bend of 96 mm. Table 4.18 shows the normalized joint shear strength of **Parker and Bullman** specimens calculated by the author

4.2.5.1. Analysis of Parker and Bullman specimens

4.2.5.1.1.The influence of column axial load

The only difference between specimen 4a and 4b seems to be the column axial load. The column axial load is increased to 300 kN for specimen 4b. Increasing the column axial load resulted in 14.5% increase in the joint shear strength. The beam failure load is also increased by 15% when 300 kN column axial load was applied. The beam longitudinal reinforcement ratio was 0.88%. The column axial load was influential on the failure mode. Increase in the column axial load changed the failure mode from column failure to joint shear failure. Increasing the column axial load to 570 kN increased the joint shear strength of specimen 4c by 33% with respect to 4a. The same trend can be viewed in Table 4.18 for specimens 4d, 4e, 4f as well as 5a, 5b, 5c and 5d, 5e, 5f. The possible reasons for the low joint shear strengths in **Parker and Bullman** tests are discussed in the following sections.

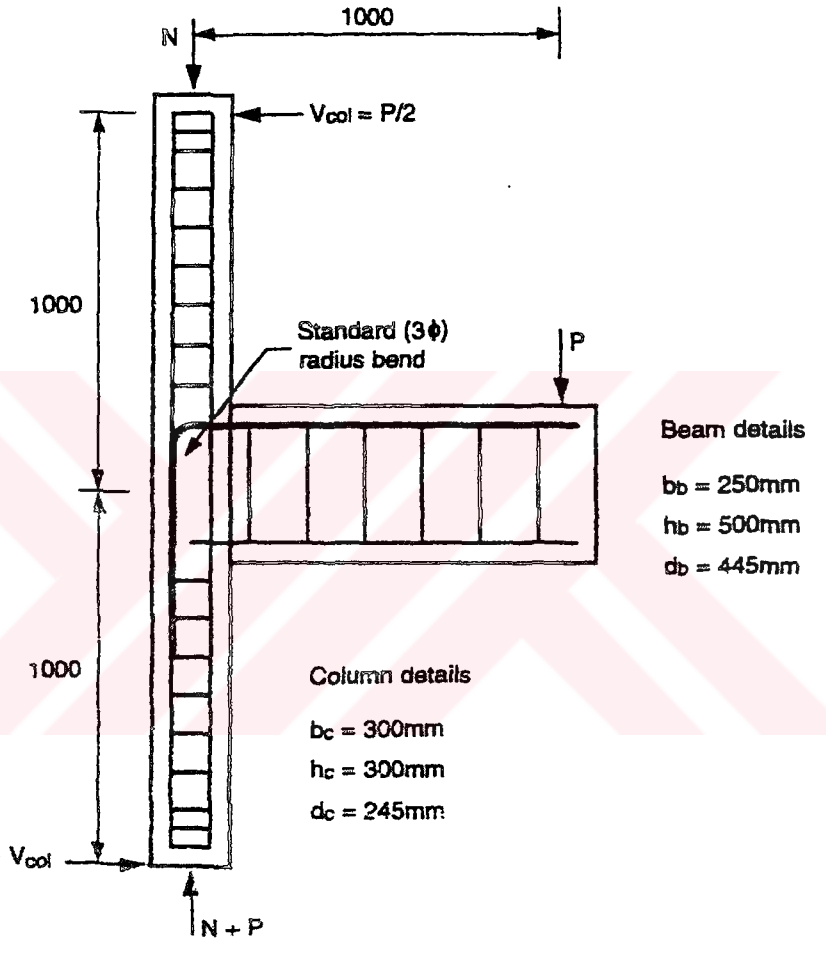

Figure 4.12 : The layout of the specimens of Parker and Bullman..

Table 4.16. Details of tests

Test ref.	Column steel	Beam steel	Links in joint	Axial load N (kN)	Failure load P (kN)
4a	4T16	2T25	–	0	118
4b	4T16	2T25	–	300	138
4c	4T16	2T25	–	570	170
4d	4T32	2T25	–	0	150
4e	4T32	2T25	–	300	160
4f	4T32	2T25	–	600	183
5a	4T25	2T25	T12@150	0	213
5b	4T25	2T25	T12@150	300	236
5c	4T25	2T25	T12@150	600	242
5d	4T25	2T32	T12@100	0	226
5e	4T25	2T32	T12@100	300	295
5f	4T25	2T32	T12@100	600	322

Table 4.17. Material properties

Test ref.	Column steel (N/mm^2)	Beam steel (N/mm^2)	Link steel (N/mm^2)	Concrete cubes (N/mm^2)
4a	550	570	560	49
4b	550	570	560	49
4c	550	570	560	46
4d	580	570	560	49
4e	580	570	560	50
4f	580	570	560	47
5a	485	485	480	53
5b	485	485	480	54
5c	485	485	480	54
5d	485	515	480	54
5e	485	515	480	56
5f	485	515	480	54

Table 4.18. Normalized joint shear strengths and failure loads of Parker and Bullman specimens

Specimen	Concrete Cylinder Strength	Failure Mode	Transverse Reinforcement	Column axial stress /f_c	vj= $Vj/b_e h_c \sqrt{f_c}$	100Asb/ db bb	Joint aspect ratio	100 A_{sc}/d_c b_c
Parker & Bullmann								
4a	39.2	C	0	0	0.403	0.882	1.667	1.094
4b	39.2	J	0	0.085	0.471	0.882	1.667	1.094
4c	36.8	J	0	0.172	0.604	0.882	1.667	1.094
4d	39.2	J	0	0	0.512	0.882	1.667	4.377
4e	40	J	0	0.083	0.540	0.882	1.667	4.377
4f	37.6	J	0	0.177	0.642	0.882	1.667	4.377
Mean	38.66				0.563		1.667	
5a	42.4	C	2T12	0	0.618	0.882	1.667	2.67
5b	43.2	J	2T12	0.077	0.679	0.882	1.667	2.67
5c	43.2	B	2T12	0.146	0.677	0.882	1.667	2.67
5d	43.2	C	3T12	0	0.820	1.440	1.667	2.67
5e	44.8	C	3T12	0.074	0.859	1.440	1.667	2.67
5f	43.2	J	3T12	0.154	0.962	1.440	1.667	2.67
Mean	43.3				0.769		1.667	

4.2.5.1.2.Increase in Column Longitudinal Reinforcement Ratio

Comparison of specimens 4a and 4d, 4b and 4e, 4c and 4f reveal that increasing the column longitudinal reinforcement ratio increases the normalized joint shear strength. The normalized joint shear strength of 4d with respect to 4a is increased by 21% when the column longitudinal reinforcement ratio is increased by 75%; the normalized joint shear strength of 4e is increased by 12.8% with respect to 4b when the column longitudinal reinforcement ratio is increased by 75%; the normalized joint shear strength of 4f is increased by 6% with respect to 4c when the column longitudinal reinforcement ratio is increased by 75%. As the column axial load is increased, the increase in the normalized joint shear strength due to increasing the ratio of column longitudinal reinforcement in the joint decreases. Figure 4.13 shows the interactions between the column longitudinal reinforcement ratio and the column axial load.

4.2.5.1.3.The Influence of Joint Stirrups

Inspection of specimens without stirrups shows clearly that their joint shear strength is relatively low with respect to the specimens with stirrups. The author is of the

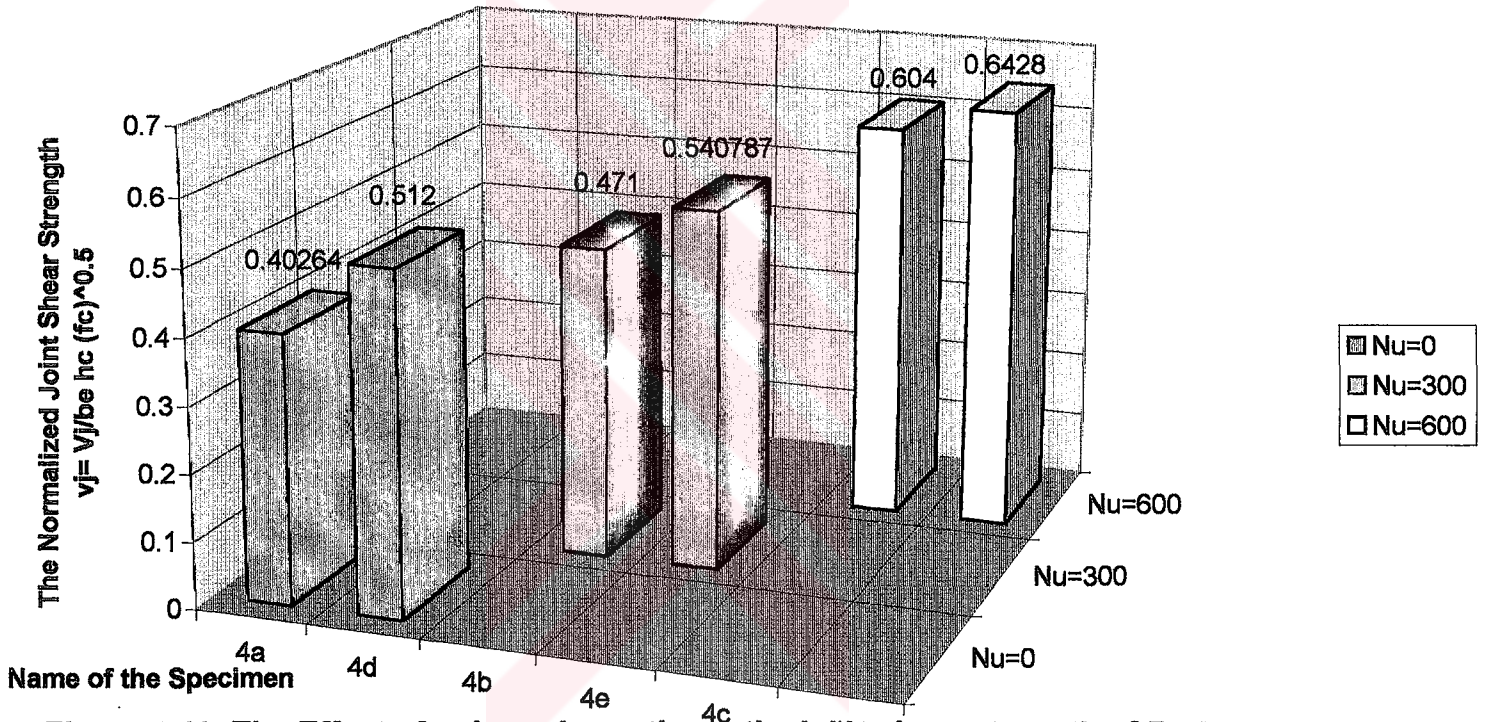

Figure 4.13. The Effect of column bar ratio on the joint shear strength of Parker and Bullman's monotonically loaded exterior beam column connections.

opinion that the increase of joint shear strengths of specimens 5d, 5e, 5f with respect to 5a, 5b, 5c has two main reasons:

1.The radius of the bend of the beam longitudinal reinforcement are increased to 96 mm for specimens 5d, 5e and 5f which increased the joint shear strength.

2.The effective stirrups in the joint are increased to 2T12 from 3T12.

4.2.5.1.4.The Influence of Beam Bend Radius

Careful inspection of the specimens 5d, 5e and 5f with respect to 5a, 5b and 5c show that the joint shear strength is considerably increased by increasing the radius of bend of the beam longitudinal reinforcement. However, the extent of this increase can not be deduced due to the increase in the amount of stirrups and the beam longitudinal reinforcement.

4.2.5.2. Summary

The author came to the following conclusions by inspecting Parker and Bullman tests.

1.The joint shear strength is increased by increasing the column longitudinal reinforcement ratio. However the increase in the normalized joint shear strength of exterior beam column joints decrease as the column axial load is increased.

2.The author came to the conclusion that Parker and Bullman's data does not provide information on the separate effects of the parameters such as column longitudinal reinforcement ratio, column axial load, beam longitudinal reinforcement ratio and the radius of the bend of beam bars. The reason for this is that several parameters are varied in one single specimen and these variables have interactions within each other as stated in the previous paragraph. Some parameters such as column axial load for example inhibit the increase in joint shear strength due to the column bar ratio at high column axial loads. However if we speak in general terms, the following parameters seem to increase the joint shear strength.

a. The beam longitudinal reinforcement ratio.

b. The column axial load.

c. The beam bar bend radius.

d. The transverse reinforcement provided.

e. The column longitudinal reinforcement ratio.

3. As will be stated later, the most apparent conclusion from the investigation of the normalized joint shear strengths of Parker and Bullman is that the joint shear strengths are extremely low compared to the normalized joint shear strengths of Ortiz. The possible reasons for this could be:

a. The beam longitudinal reinforcement is concentrated at the corners of the cross sections. They are not distributed regularly.

b. The joint aspect ratios of Parker and Bullman specimens are higher than that of Ortiz. However this is unlikely to result in 38% increase in the joint shear strength of Ortiz specimens. The author made a parametric study to investigate the effect of the joint aspect ratio on the normalized joint shear strength of monotonically loaded exterior beam column connections. The results showed that as the joint aspect ratio is increased, the normalized joint shear strength decreases.

c. The concrete cylinder strengths could be lesser than they are thought to be, or alternatively the concrete cylinder strengths of Ortiz could be higher than that is assumed.

d. The beam longitudinal reinforcement ratio of Parker and Bullman is 12.6% less than Ortiz specimens.

e.The radius of the bend of beam bars is standard 3ϕ for Parker and Bullmann specimens. The radius of the bend of beam bars on the other hand for Ortiz specimens is 4 and 8ϕ. As was stated in the previous sections, increasing the radius of the bend of beam bars from 4 to 8ϕ had resulted in 5% increase in the joint shear strength. The decrease due to this radius of bend could at most be 2.5%.

f.The average concrete cylinder strengths of Ortiz specimens is 35 MPa while that of Parker and Bullman is 38 MPa. The analysis the details of which will be given in the following sections suggest that in joints without stirrups, the joint shear strength is proportional to the square root of the concrete cylinder strength. This would mean that the normalized joint shear strengths of the specimens of Parker and Bullman should be 4% higher than that of Ortiz.

In beam-column joints, the preferred failure mode is beam flexural failure. In Parker and Bullman's specimens only specimen 5c exhibited beam failure. Joint 5c had the following characteristics:

1.Specimen 5c had the highest column load.

2.Specimen 5c had been sufficiently reinforced by stirrups.

3.The beam longitudinal reinforcement ratio was lower compared to the specimens 5d, e, and f.

When the beam longitudinal reinforcement ratio is increased, failure should be expected in the joint. This shows clearly that there should be an upper limit for the beam longitudinal reinforcement. If this limit is exceeded, failure is more likely to occur outside the beam. The above criterion is considered when developing the simple model to predict the failure modes of monotonically loaded exterior beam-column joints the details of which will be given in the following sections.

4.2.5.3.The Possible Reasons for the low normalized joint shear strengths of Parker and Bullman

The possible reasons for the low strengths are mostly stated in the preceding paragraphs. At first, it was regarded that the most probable reason of the low normalized joint shear strengths of Parker was the concentration of bars in the corners of the joints. This would result in a non-uniform introduction of stresses into the joint which, would decrease the transverse bursting tensile strains in the direct strut, and as suggested by Mitchell and Collins would decrease the concrete strength. **Vollum (1998)** gives a similar explanation as quoted below:

"The very low joint shear strength of Parker and Bullman's specimens may arise from the detailing arrangement adapted. Both the column and beam of Parker and Bullman's specimens were only reinforced with a single bar in each corner, whereas Ortiz's specimens were reinforced with a minimum of three bars in each column face and four bars in the tension face of the beam. Therefore, the forces in the beam bars would have been introduced into the joint much less uniformly in Parker and Bullman's tests than Ortiz's. The effect of introducing the forces into the joint non-uniformly from the reinforcement is to increase the transverse bursting tensile strains

in the direct strut, and consequently to reduce the strength of the concrete in the joint. The spalling stresses, in the cover zone, would also have been greater in Parker and Bulmann's tests. Bearing this in mind, the lack of intermediate column and beam bars may account for the fact that the joint shear strength of Parker and Bullman specimens 4b to 4f increased considerably with column axial load. As the column load is increased, a greater proportion of the resultant vertical shear force at the external face of the column, F_{ve} would have been introduced into the direct strut via direct compression through the concrete. This would have had the effect that stresses would have been introduced into the direct strut more uniformly across its width. Bond conditions would also have been improved for the beam bars. Both these effects would have enhanced the joint shear strength."

Scott specimens had also a single bar in each corner of the beams and the columns. Analysis showed that the normalized shear strengths of Scott's specimens were not as low as that of Parker and Bullman's.

4.2.5.4.Objections to Vollum's suggestions for the low joint shear strength of Parker and Bullman

Vollum erroneously states that the very low joint shear strengths of Parker and Bullman specimens is due to the detailing arrangement adapted by Parker and Bullman However, inspection of the whole database of experiments showed that Scott specimens have also got a bar at each corner of the cross sections of the beam and the columns. In spite of this, the normalized joint shear strengths of Scott specimens are significantly higher than the specimens of Parker and Bullman. The author is of the opinion that the low beam longitudinal reinforcement ratio and the high joint aspect ratios of Parker and Bullman specimens result in these low values of normalized joint shear strengths.

4.2.6.Kordina

4.2.6.1. The tests of Kordina

Kordina (1984) tested ten exterior beam column connections. His specimens are important due to the different variables tried. The variables Kordina tested were:

-Different beam bar anchorage types such as U Bars, beam bars anchored by steel plates outside the joint or different beam bar detailing such as inclined bars.

-Different radius of beam bar bend.

-Different amounts of stirrups.

-Different column axial loads.

-Different joint aspect ratio

All of the specimens of Kordina exhibited joint failure. The details of Kordina's specimens are shown in Figure 4.14 and Table 4.19, which are adapted from Vollum. Table 4.20 shows the failure loads of Kordina specimens.

4.2.6.2. Analysis of the Specimens by the Author

The specimen RE3 has medium amount of joint stirrups while RE4 has low amount of stirrups. Previous analysis of test data had shown that the stirrups in joints, which are reinforced by low amount of stirrups, would not increase the joint shear strength of joints much. Therefore it is prudent to expect that the joint shear strength of RE4 is not increased by the provision of a single tie. Moreover, the placement of the single tie is just under the top bars of the beam. The author is of the opinion that if a single tie will be provided in the joint, it will be best to place it theoretically just at the middle of the distance between the top of the beam compressive chord and under the beam top bars. If it is situated just under the top beam longitudinal reinforcement, it will not increase the joint shear strength.

The normalized joint shear strength of RE4 is 25.8% less than RE3. The possible reasons for this are:

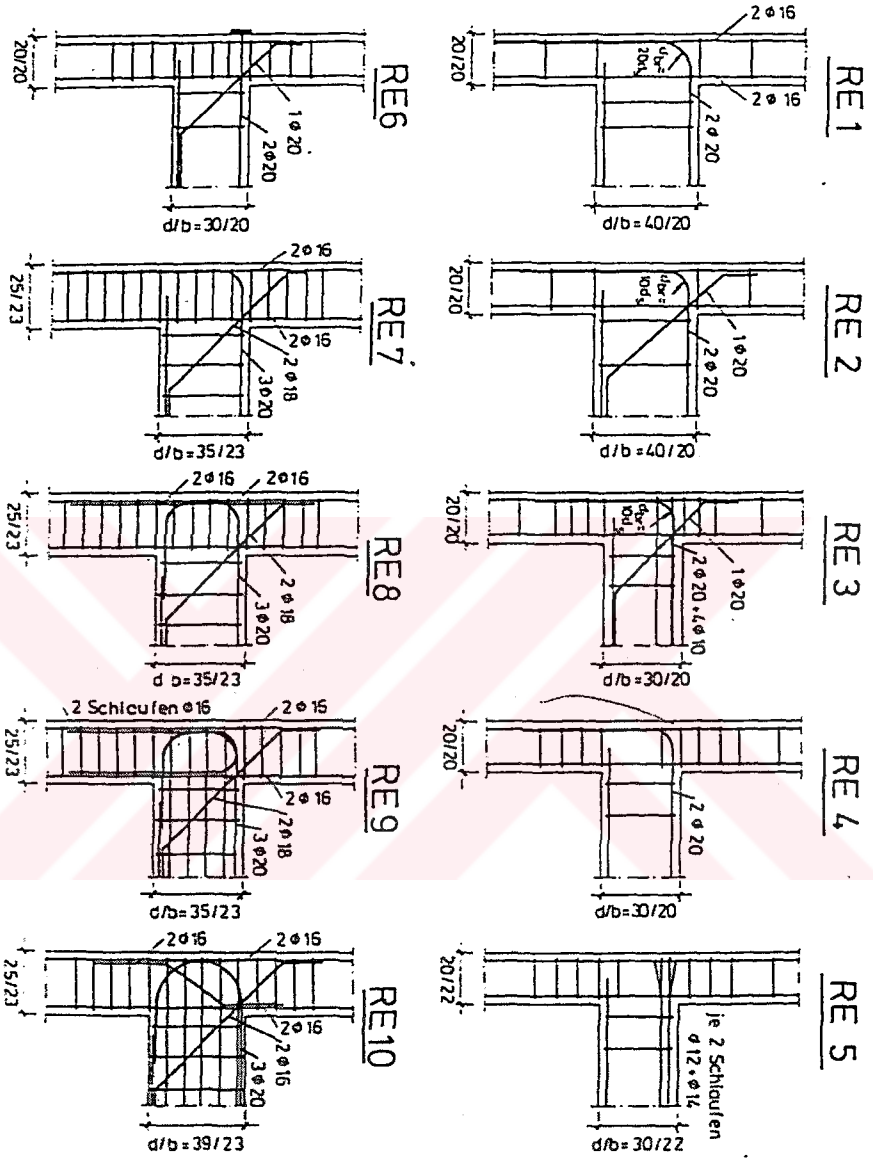

Figure 4.14 : The details of Kordina specimens.

Specimen	Column steel	Beam steel	Links in joint	Yield strength T16	Yield strength T20	Equivalent 150 mm cube strength
Units	-	-	-	MPa	MPa	MPa
RE2	4 T16	2 T20	Nil	420	420	31.6
RE3	4 T16	2T20+2T10	1 T10 UB	420	420	50.5
RE4	4T16	2 T20	1 T8	420	420	40.3
RE5	4T16	2 T12+2T10	Nil	420	420	36.9
RE6	4T16	2 T20	3 T8	490	463	39.5
RE7	4T16	3 T20	4 T8	454	448	32.1
RE8	4T16	3 T20	4 T8	454	464	35.0
RE9	4T16	3 T20	4 T8 UB	406	454	35.6
RE10	4T16	3 T20	5 T8 UB	440	459	29.7

Table 4.19. Details of Kordina's specimens.

Specimen	Column load	Failure load	Theoretical beam failure load
Units	kN	kN	kN
RE2	240	67	86.9
RE3	400	80	91.3
RE4	51	51	62.8
RE5	46	46	97.3
RE6	213	66	70.1
RE7	650	117	117
RE8	525	105	125
RE9	770	110	122
RE10	551	100	138

Notes

1. All values taken from Table 4, Reference [33]

Table 4.20. Failure loads of Kordina's specimens.

1.The provision of T10 tie in RE3.

2.The provision of an inclined bar.

3. The high column axial load in specimen RE3.

The joint shear strength of a monotonically loaded exterior beam column connection will decrease if the confinement regions of the upper and lower columns of a joint are adequately confined by closely spaced stirrups, but the joint is not.

Specimen RE7 had the highest normalized joint shear strength of the entire beam bar bent down detail specimens. The reasons are listed below:

Detailing is the most influential factor in increasing the joint shear strength. RE7 had the highest amount of inclined bars. It also had a beam bar bent down detail. It had the highest column axial load and had regularly distributed stirrups throughout the joint region and the stirrups are arranged closely spaced in the confinement regions of the upper and lower columns. The joint aspect ratio of RE7 was the smallest which in other words meant that if every other variables' effect were neglected, the normalized joint shear strength of RE7 would be the highest. RE7 had the highest stirrup ratio of all and the stirrups were regularly distributed throughout the joint region. These all increased the normalized joint shear strength of RE7 with respect to others.

The joint shear strength of RE7 is 32.9% higher than that of RE2. If every other variable were constant, the normalized joint shear strength of RE7 would be 19 % higher than that of RE2. There is only 13.9 % more joint shear strength due to 3T8. This alone shows that the separate effects of the different variables can not be superimposed without taking the interaction of these into account. In other words a designer can not mathematically add the separate effects of different variables. Some variables govern the behavior of exterior beam column connections more than the others. Table 4.21 shows an analysis of Kordina's specimens.

The specimens RE2 and RE3 are analyzed. RE2 and RE3 have got same radius of bend of beam bars. However specimen RE3 has an inclined beam bar and a single 10 mm stirrup in the joint. The joint aspect ratio is higher in RE2, which theoretically means that it will have 15 % less joint shear strength than RE3. The test data does not provide any information regarding the separate effects of the variable(s) or interactions of variables because:

There are too many variables including column axial load, ratio of the beam bars, different joint aspect ratio, different beam bar detailing, different amount of joint stirrups, different concrete cylinder strengths. Therefore it is impossible to separate the relative effects or interactions of these variables.

Table 4.21. Analysis of Kordina specimens

Specimen	Cylinder Strength	Type of Detailing of the Beam Bars	Failure Mode	Column Axial Stress/fc	Joint Shear Strength $v_j = V_j / b_c h_c \sqrt{f_c}$	Ratio of Tensile Reinforcement	Joint Aspect Ratio
Units	MPa	-	-	-	MPa	-	
Kordina							
RE2	25.28	1	J	0.237	0.918	0.785	2.125
RE3	40.4	1	J	0.247	1.182	0.982	1.625
RE4	32.24	1	J	0.039	0.876	1.047	1.625
RE7	25.7	1	J	0.439	1.32	1.17	1.5
Mean	30.905			0.240	1.074		1.6
RE6	31.6	Beam bar anchored by steel plates outside the joint	J	0.168	1.156	1.047	1.625
RE5	29.52	unusual	-	0.033	0.574	0.581	1.36
RE8	28	2	J	0.326	1.12	1.17	1.625
RE9	28.55	2	J	0.469	1.16	1.17	1.5
RE10	23.8	2	J	0.402	1.014	1.17	1.66
Mean (U Bars)	26.78			0.399	1.098		1.453
Mean (Total)	29.45			0.262	1.035		1.513

The author is of the opinion that the most influential parameter here is again detailing rather than the joint aspect ratio. This is because RE4 has got the same joint aspect ratio with RE3. In spite of this, it has much less normalized joint shear strength. The amount of inclined bars is greater than RE2 and the stirrups in the confinement regions of the columns have been increased in specimen RE3. This type of detailing made the effect of joint aspect ratio on joint shear strength perceptible rather than conceive it. Therefore it can be concluded that the joint aspect ratio increases the normalized joint shear strength of monotonically loaded exterior beam column connections only if the connection is adequately detailed.

The specimens RE2 and RE4 are compared. The amount of stirrup provided for RE4 is quite low and its contribution to the shear strength of the joint can be neglected. The joint aspect ratio of RE2 is 23.5% higher than RE4, which in other words indicate that the joint shear strength of RE4 will be 11 % higher than RE2. However the joint shear strength of RE4 is 4.5% less than RE2. The possible reasons for this could be:

1.The provision of inclined bars increased the normalized shear strengths of RE2.

2.The column axial load of RE2 is 240 kN while that of RE4 is 51 kN. The previous data of Parker and Bulmann had indicated an increase in joint shear strength with increasing column axial load. However the data of Scott had shown an invisible effect of column axial load on the normalized joint shear strength.

3.The concrete cylinder strength of specimen RE2 could be less than that is assumed.

Result: It seems likely that beam bar detailing, or provision of inclined bars specifically is a more dominant parameter than provision of transverse reinforcement or joint aspect ratio. The author believes that with adequate beam bar detailing, the joint shear strength could be increased significantly. (4.5% in the comparison of RE2 and RE4 although RE2 should have 11% less normalized joint shear strength theoretically due to the higher joint aspect ratio it had). Specimen RE4 has closely spaced stirrups in the confinement region of the upper and lower columns of the connection. In spite of this, it has got a single stirrup, which is situated just under the top beam bars in the joint. These lead us to the following conclusions:

1.If a joint has got a single tie, placing it just under the top beam bars will not increase the normalized joint shear strength.

2. If a joint has closely spaced stirrups in the confinement regions of the upper and lower columns of a connection, and if it does not have regularly distributed closely spaced stirrups in the joint, then that joint's normalized joint shear strength will decrease.

RE5 is the specimen, which has the lowest normalized joint shear strength of all specimens. Understanding the reasons for this would highlight the interactions between different variables. The author is of the opinion that the most probable reasons for the low normalized joint shear strength of Kordina RE5 were:

1. The beam longitudinal reinforcement was very badly anchored.
2. It had no inclined bars.
3. The single stirrup provided was situated in the compressive chord of the beam, which in other words meant that it was ineffective in contributing to the shear resistance of the joint.

4. RE5 had very low column axial load.

5. RE5 had the lowest joint aspect ratio, which indicates that it would, if every other variable were kept constant, have the highest normalized joint shear strength of all specimens. However we see that it has the lowest. This in other words means that the joint aspect ratio is not a dominant parameter but beam bar detailing and anchorage are more effective in resisting shear. The above reasons are deliberately written in the order of dominance. Thus, the most influential parameter is number 1 and the least is number 4.

The main difference of specimen RE6 is the anchorage of the beam bars. A steel plate at the outside of the joint anchors the beam bars. However, inspection of the L bar bent down detail specimen RE7 with regularly distributed joint stirrups suggests that this type of detailing is not as effective as beam bars bent down detail. It only has slightly higher normalized joint shear strength with respect to U bar details. We should also add that specimen RE6 can not be directly compared to specimen RE7 because RE7 has got higher amount of inclined bars and less joint aspect ratio which makes direct comparison of these two specimens difficult.

The specimen, which has the highest normalized joint shear strength between RE8, RE9 and RE10, is expectedly RE9. Quick inspection of this specimen shows that it has the lowest joint aspect ratio. As stated previously, joint aspect ratio is not a dominant parameter and it's effect can only be conceived if the connection is adequately detailed. RE9 has been reinforced by a U bar specimen. The comparison of two identical (except the fact that RE7 is reinforced with beam bars bent down and RE8 with U bars) specimens RE7 and RE8 shows that the normalized joint shear strength of U bar specimens will be 15% less than beam bars bent down detail specimens. The average normalized joint shear strength of U bar specimens with high amount of stirrups are lesser than the single specimen RE7 which has high amount of stirrups and with beam bars bent down into the column detail. The only difference between specimen RE8 of Kordina and RE9 is the provision of the U bars into the lower column of the connection. Comparison of this type of detailing (double U) with the beam bars bent down detail of specimen RE7 of Kordina showed that, beam bars bent down detail increases the normalized joint shear strength of monotonically loaded exterior beam column connections above that of the double U bar detail.

Nevertheless, it should be stated that this double U type of detailing (RE9) gave better normalized joint shear strength with respect to the U bar specimen RE8. Inspection of specimen RE9 of **Kordina** shows that another characteristic of this specimen is the provision of several layers of beam bars. If specimen RE10 was not analyzed, it could be suggested that the increase in the normalized joint shear strength of RE9 was possibly due to the several layers of beam bars. However, inspection of the **Kordina** specimen RE10 shows that although this specimen has been provided with several layers of beam longitudinal reinforcement, its normalized joint shear strength is the least of all the other U bar specimens. RE10 is reinforced by two set of inclined bars, one crossing the diagonal of the joint and the other set perpendicular to the first one. This in other words means that the type of detailing as in RE10 is not much effective in resisting the joint shear.

4.2.6.3. Summary

The average normalized joint shear strength of **Ortiz** specimens is 0.99, which is 7.2 % less than average of the **Kordina** specimens with L bar bent down detail. The possible reasons are:

1. The radius of bends of the beam bars is 10d compared with 5 or 8d of **Ortiz** specimens. This could have increased the normalized joint shear strength of **Kordina** specimens.
2. **Kordina** used inclined bars and closely spaced stirrups such as RE7 which increased the shear strength above that of **Ortiz.**
3. The joint aspect ratio was 1.33 average in **Ortiz** specimens, while 1.6 in **Kordina** specimens. Increase in joint aspect ratio is more likely to decrease the normalized joint shear strength rather than increase it. It is possible therefore that different detailing adapted for **Kordina** specimens such as high radius of bends of beam bars, inclined bars conceived the effect of joint aspect ratio.

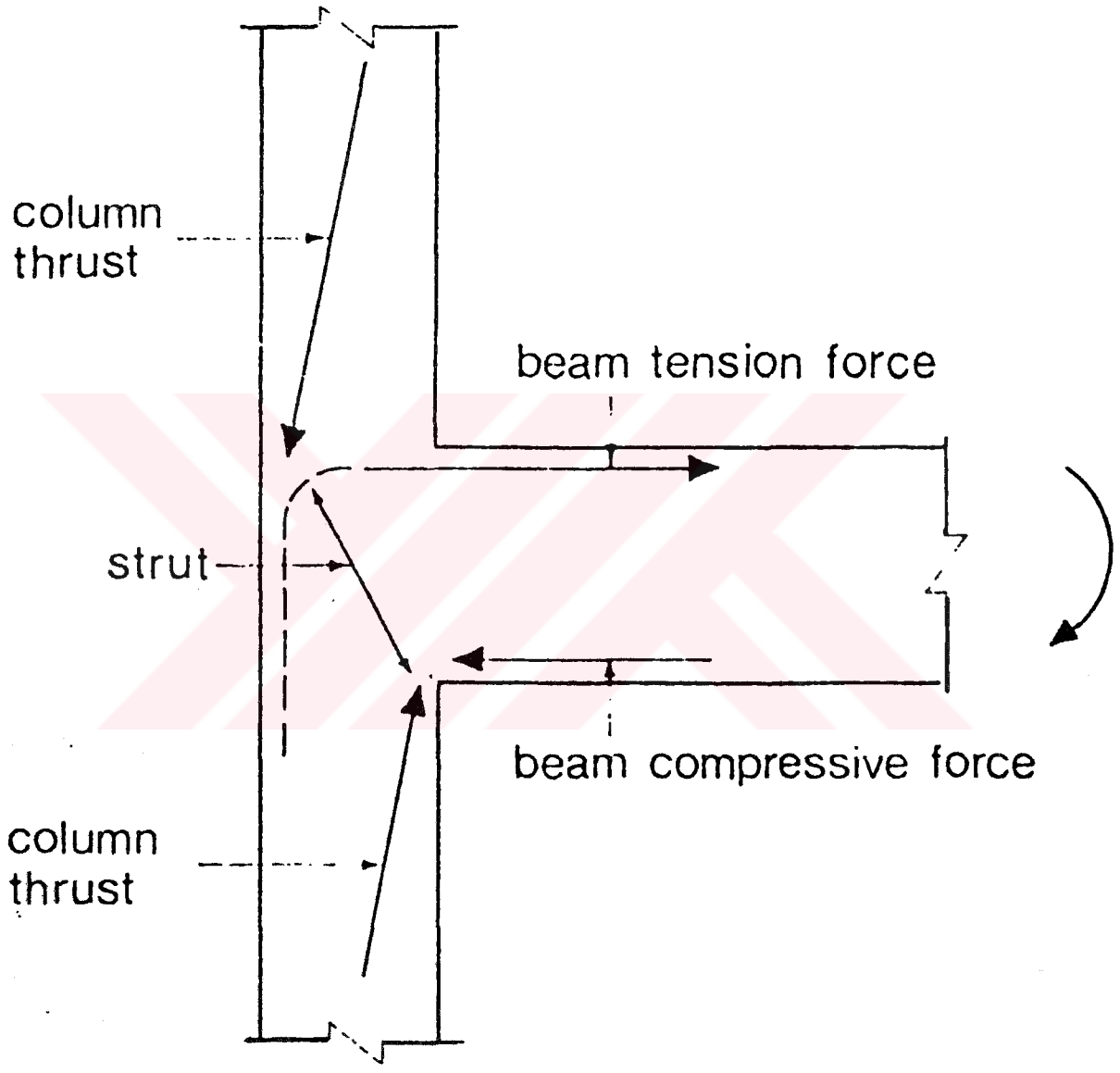

Figure 4.15 :The internal forces in the joint zone in Taylor's tests

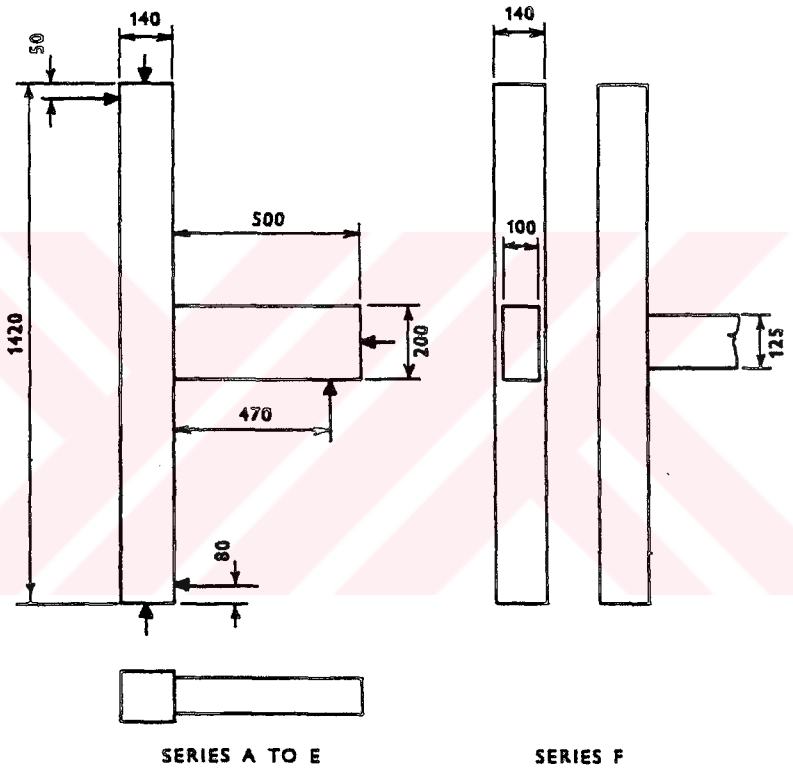

Figure 4.16 : The layout of the test specimens of Taylor.

4.2.7.Taylor

Taylor (1974, 1976) is the most influential person in UK design practice on the behavior of beam column joints. He carried out many experiments on exterior beam column connections during his years in The Cement and Concrete Association. This experimental work at the Cement and Concrete Association, in which 26 joints were tested, covered a range of the important parameters such as; the detail type, beam steel percentage, joint geometry, column load, provision of additional column ties and beam thrust.

4.2.7.1. Internal Forces in the Joint Zone

Figure 4.15. shows the internal forces in the joint zone while the Figure 4.16 shows the layout of the test specimens. The inspection of Figure 4.15 suggests that Taylor also assumed that there was an inclined strut, which resisted shear in the joint. At right angles to this strut, there was a tensile stress field, which was the main cause of the diagonal cracking. Taylor also states that the reinforcement arrangement was made so that the internal forces in Figure 4.15 could be achieved. Figure 4.17 shows the reinforcement details of the test specimens. Taylor comments that the beam bar bent up into the column detail was not so efficient because the diagonal joint thrust can not lock onto the bend of the beam steel. As can be viewed in Figure 4.17, it is really difficult to develop the internal force system with this kind of detailing.

4.2.7.2.Cracking Analysis

Figure 4.18 shows the boundary forces acting outside the joint. Figure 4.19 shows the notation used in preparation of the design formula. The main forces were:

N_1 = The column load

N_b = The beam thrust

V_d = The shears which are provided by dividing the beam moment by the lever arm

V_b = The vertical beam shear.

N_2 = Column load below the joint.

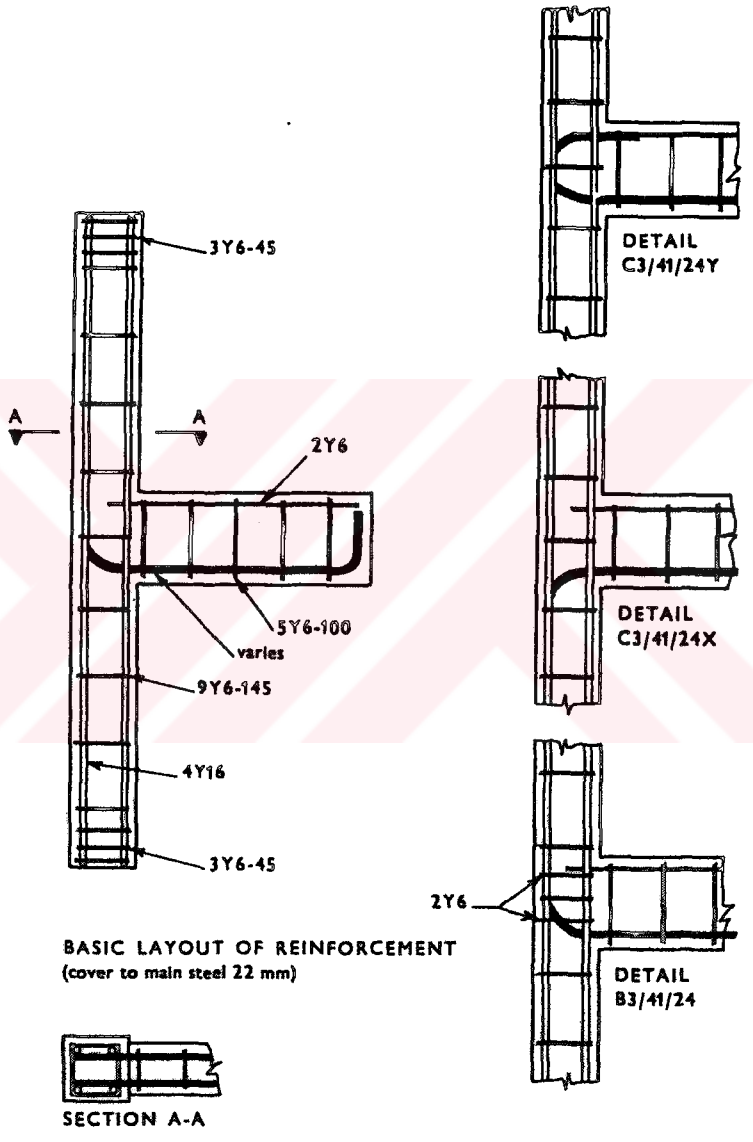

Figure 4.17 : The reinforcement details of the test specimens of Taylor

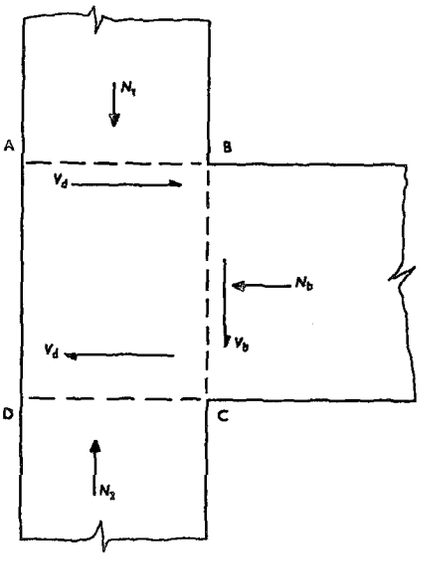

Figure 4.18 : The boundary forces acting outside the joint.

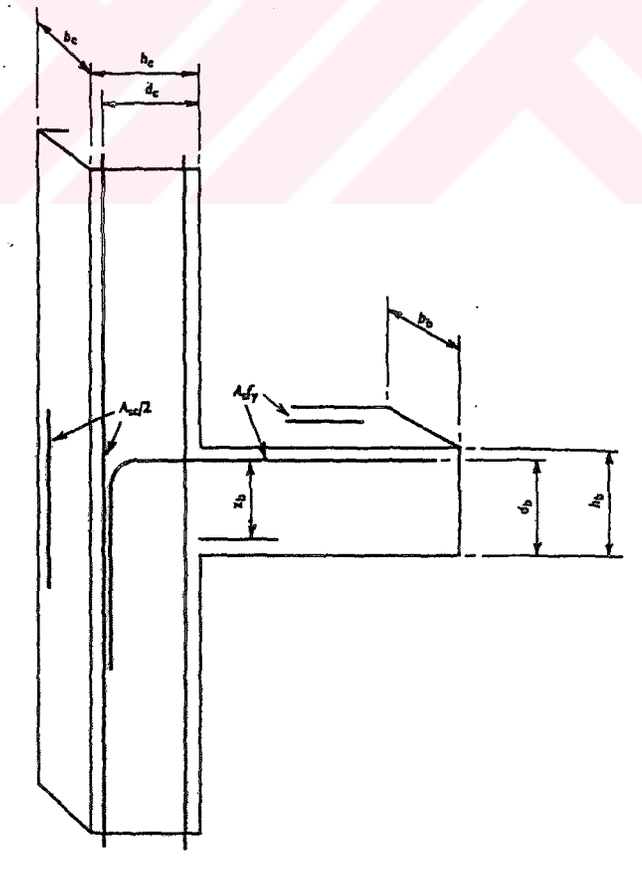

Figure 4.19 : The notation used in preparation of the design formula.

For the analysis, Taylor assumed the stress in the joint from the columns to be a normal stress f_c

where:

$$f_c = N_1 / b_c h_c \qquad (4.7)$$

Taylor added that this lower value of N gives a higher principal tensile stress. The beam thrust was assumed to provide a stress

$$f_b = N_b / b_c h_b \qquad (4.8)$$

and the tensile strength of the concrete f_t was assumed to be one tenth of f_u

$$v_d = 0.67 \sqrt{(f_{ct}^2 + f_c f_{ct} + f_b f_{ct} + f_c f_b)} \qquad (4.9)$$

Taylor then stated that the effect of f_b in the analysis should be neglected, as the beam thrust was very small. The equation then simplifies to:

$$V_d = 0.67 \sqrt{(f_{ct}^2 + f_c f_{ct})} \qquad (4.10)$$

4.2.7.3.The Ultimate Limit State Design Approach

Taylor developed an ultimate limit state design approach considering the shears acting on the joint zone. Figure 4.20 shows the relation between shear on a short beam and in a joint zone and Figure 4.21 shows the plot of ultimate joint shear compared with nominal shear stress in CP110. Taylor plotted the shear test results with concentrated loads all with a_v/d, the shear spans to the effective depth ratios less than 4. The results are in Figure 4.22. In constructing the graph, the partial safety factor was removed from the shear stresses by multiplying the reported concrete strength for the test by 1.5 and looking up the shear stress corresponding to that value. From the inspection of Figure 4.25, it can be said that this equation gives a lower bound for all the tests. Taylor suggests that equation should be used, as a design equation to ensure that diagonal cracking does not occur at the serviceability limit state, since this crack, if allowed to form, can be very wide.

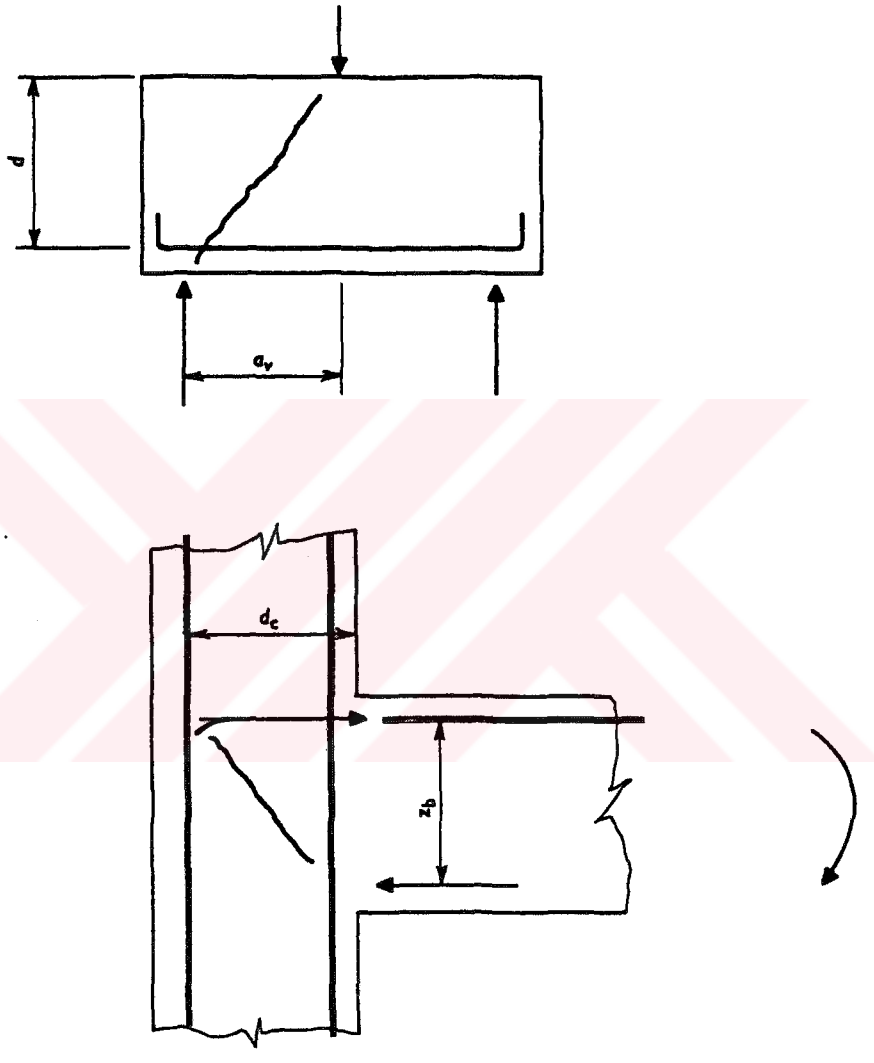

Figure 4.20 : The relation between shear on a short beam and in a joint zone..

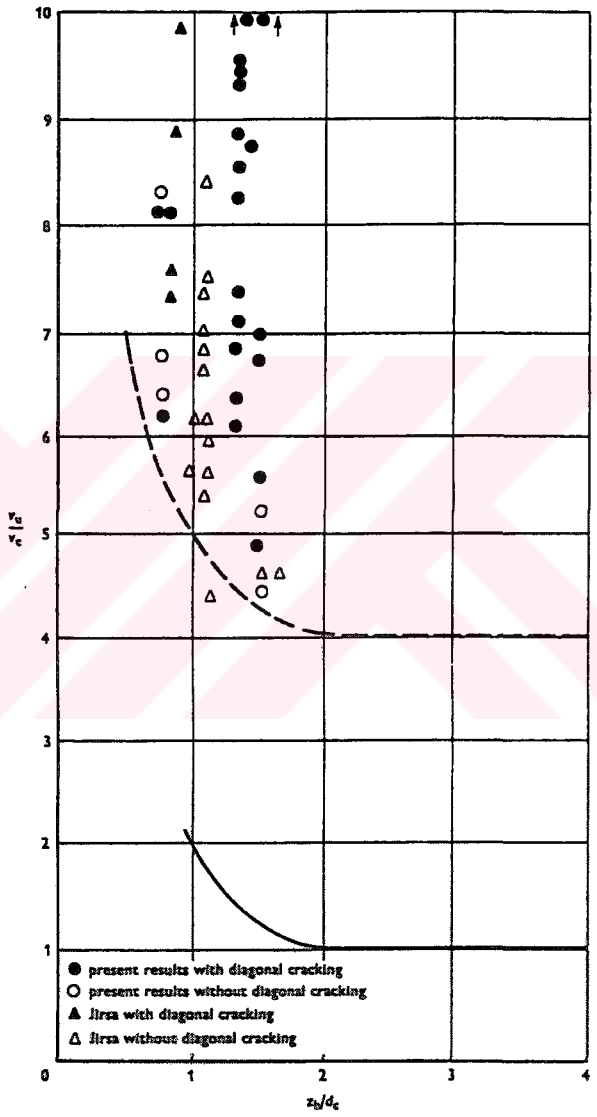

Figure 4.21 : Plot of ultimate joint shear compared with nominal joint shear compared with nominal shear stress in CP110.

The previous British Code used to recognize that very short members, subject to certain loading and steel anchorage requirements, have a shear capacity higher than that predicted by Table 5 of the code. For short members, CP110 recommends the shear stresses of Table 5 to be enhanced.

Taylor comments that the force system in a short beam is quite similar to a beam column connection. Figure 4.20 of Taylor demonstrates this similarity very clearly.

The CP110 enhancement clause recommends the shear stress from Table 5 to be multiplied by $2d / a_v$ where $a_v / d < 2$. The plot of ultimate joint shear stress compared with nominal shear stress in CP110 was shown in Figure 4.21.

The solid line in Figure is the Code line and the broken line is the lower bound to all the test results. The Code line on the figure is the expression.

$$v_u / v_c = 2d / a_v \tag{4.11}$$

when:

$$a_v / d_c < 2 \tag{4.12}$$

The lower bound line demonstrated by the broken line in the figure is:

$$v_u / v_c = 3 + 2d_c / z_b \tag{4.13}$$

The lower bound line in Figure, is a lower bound to all the test data regardless of the failure mode of the specimen.

If it is assumed that the total shear force in the joint is $0.87 A_s f_y$ in design, which is the beam steel tension capacity, the other column shears can be ignored as they are of a lower order magnitude. Then:

$$A_s f_y / b_c d_c = (3+ 2d_c /z_c) v_c \tag{4.14}$$

The previous British Code recommends that the beam should be designed for the un-redistributed bending moments. Taylor therefore suggests that the above principle is also relevant to beam column joint design. The simplest way of doing so according to Taylor is to divide the steel force by a constant β where;

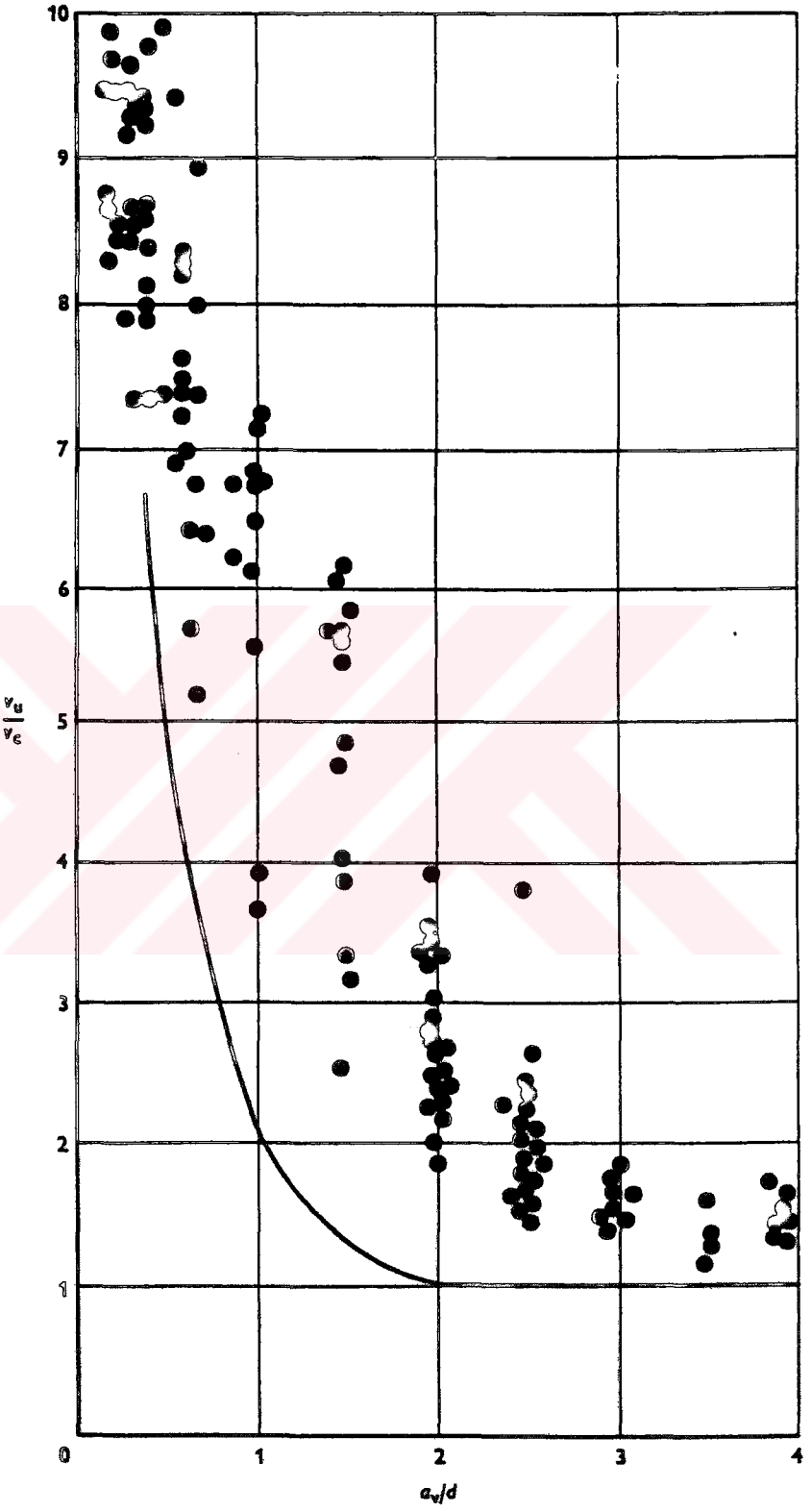

Figure 4.22 : Plot of shear test results with concentrated loads.

β = 1- percent redistribution / 100

The equation then simplifies to:

$A_s f_y / \beta\ b_c d_c = (3 + 2d_c / z_c)\ v_c$

Taylor states that this equation can be satisfactorily be used in design to limit the beam bar ratio. The equation then takes the following form;

$$100\ \rho_b = 100\ (3 + 2d_c / z_b)\ b_c d_c \beta\ v_c / b_b d_b\ 0.87 f_y \qquad (4.15)$$

where:

v_c is the value of nominal shear stress for the column section using the steel percentage at the outer tension face of the column.

$100\ A_{sc} / 2\ b_c d_c$

$100\ \rho_b$ is the beam steel percentage, $100\ A_s / b_b d_b$

Taylor comments that the applicability of the above formula has not been proved for z_b/d_c ratios greater than 2. However, it is unlikely that beam column joints that have zb/dc ratios greater than 2 will ever occur in practice.

4.2.7.4. Inspection of the Specimens of Taylor in More Detail

The Tables 4.22 and 4.23 show the details of the test specimens and the test results. The analysis of the tests is given in Table 4.24.

4.2.7.4.1. The Loading

Initially, the beam was loaded by applying a vertical load at the point of contra-flexure. The column was loaded by a jack on rollers through ball joints at each end to a load that was equivalent to the dead load only acting on the structure. The test instrumentation is shown in Figure 4.23. Failure occurred as either a beam failure, in the case of the beams with low steel percentages, or as a joint failure in the column with crushing in the same direction as the inclined joint crack. Taylor placed a single stirrup at the center of each beam-column joint so that the buckling of the beam bars is prevented. He did not mention the shear resisting capacity of the stirrups or the confinement they provide. Figure 4.24 shows the stress-strain curves for steel.

Table 4.22. The details of the test specimens of Taylor.

Specimen	Series	Variable	Strut type	Beam steel percentage	Column steel percentage	Concrete strength (N/mm^2)
P1/41/24	P	Preliminary	1	2.4	4.1	33
P2/41/24			2	2.4	4.1	29
P2/41/24A			2	2.4	4.1	46.5
P1/41/09			1	0.9	4.1	37
A3/41/24	A	Beam steel percentage	3	2.4	4.1	27
A3/41/13			3	1.3	4.1	45
A3/41/09			3	0.9	4.1	43.5
A3/41/06			3	0.6	4.1	27.5
B3/41/24	B	Column ties	3	2.4	4.1	22
C3/41/24X	C	Beam steel detail	3	2.4	4.1	50.5
C3/41/24BY			3	2.4	4.1	31.7
C3/41/13Y			3	1.3	4.1	28.2
C3/41/24Y			3	2.4	4.1	59.5
D3/41/24	D	Column load	3	2.4	4.1	53
D3/41/13			3	1.3	4.1	55.5
D3/41/09			3	0.9	4.1	42.5
D3/41/06			3	0.6	4.1	21.0
E3/41/24A	E	Beam thrust	-	2.4	4.1	42.8
E3/41/24B			-	2.4	4.1	44.5
E3/41/24C			-	2.4	4.1	41.6
F3/41/24A	F	Beam thrust, steel percentage, column load, all with small beam size	3	2.3	4.1	37.2
F3/41/16A			3	1.6	4.1	21.1
F3/41/24B			3	2.3	4.1	34.2
F3/41/16B			3	1.6	4.1	23.9
F3/41/24C			-	2.3	4.1	34.4
F3/41/16C			-	1.6	4.1	37.7

Table 4.23. The test results of Taylor specimens.

Specimen	Column load (kN)	Beam thrust (kN)	Concrete strength (N/mm^2)	M_{flex} (kN m)	M_d (kN m)	M_u (kN m)
P1/41/24	240	0	33	26.7	14	18.8
P2/41/24	240	13.4	29	25.2	11.7	18.8
P2/41/24A	240	20.6	46.5	29.9	16.43	25.25
P1/41/09	240	0	37	13.3	12.28	17.54
A3/41/24	240	7.2	27	24.2	11.69	18.71
A3/41/13	240	15.4	45	21.6	18.71	22.39
A3/41/09	240	7.3	43.5	14.6	11.7	12.9
A3/41/06	240	8.3	27.5	9.3	-	12.80
B3/41/24	240	6.8	22	20.9	11.72	16.31
C3/41/24X	240	2.13	50.3	30.4	14.61	16.08
C3/41/24BY	240	4.9	31.7	22.8	11.69	15.49
C3/41/13Y	240	8.3	28.2	15.9	14.41	14.41
C3/41/24Y	240	14.3	59.5	31.7	19.88	24.20
D3/41/24	60	14.0	53	30.8	16.37	26.95
D3/41/13	60	9.1	55.5	20.6	12.86	20.64
D3/41/09	60	14.5	42.5	14.0	14.03	15.96
D3/41/06	60	5.8	21	8.85	-	10.17
E3/41/24A	240	5.0*	42.8	28.9	11.69	14.41
E3/41/24B	240	2.5*	44.5	29.0	16.37	16.37
E3/41/24C	240	15.0*	41.6	28.7	18.71	21.66
F3/41/24A	240	3.9	37.2	7.72	9.94	10.03
F3/41/16A	240	4.2	21.1	4.95	-	8.24
F3/41/24B	240	4.6	34.2	7.48	7.6	9.82
F3/41/16B	240	3.2	23.9	5.50	7.31	7.77
F3/41/24C	60	2.5	34.4	7.46	-	10.14
F3/41/16C	60	2.5	37.7	5.80	-	7.98

*constant thrust throughout test

4.2.7.4.2. Test Results

The analysis of Taylor can be viewed in Table 4.23 and 4.24.

Table 4.24. Analysis of Taylor's results

Specimen	Cylinder Strength	Detail	Failure Mode	Effective Joint Stirrups	N/bhfc	$v_j = V_j / b_c h_c \sqrt{fc}$	ρ_b	h_b/h_c
Units	MPa	-	-	-	-	MPa	-	
Taylor								
P1/41/24	33	4	J	1T6	0.371	1.045	2.01	1.428
P2/41/24	29	4	J	1T6	0.422	1.079	2.01	1.428
P2/41/24A	46.5	4	J	1T6	0.263	1.076	2.01	1.428
A3/41/24	27	4	J	1T6	0.45	1.15	2.01	1.428
A3/41/13	45	4	B	1T6	0.272	0.807	2.01	1.428
D3/41/24	53	4	B	1T6	0.0577	1.09	2.01	1.428
D3/41/13	55.5	4	B	1T6	0.055	0.738	1.178	1.428
E3/41/24A	42.8	4	J	1T6	0.286	0.657	2.01	1.428
E3/41/24B	44.5	4	J	1T6	0.275	0.088	2.01	1.428
E3/41/24C	41.6	4	J	1T6	0.294	0.99	2.01	1.428
F3/41/24A	37.2	4	B	1T6	0.329	0.98	1.884	0.893
F3/41/24B	34.2	4	B	1T6	0.358	0.984	1.884	0.893
F3/41/24C	34.4	4	B	1T6	0.0898	0.979	1.884	0.893
C3/41/24BY	31.7	2	J	1T6	0.386	0.855	2.01	1.428
C3/41/13Y	28.2	2	J	1T6	0.4342	0.801	1.178	1.428
C3/41/24Y	59.5	2	J	1T6	0.206	0.066	2.01	1.428
Mean	40.1937				0.284	0.837		1.328

Notes for Table 4.24: 1. 4 indicates beam longitudinal reinforcement that is not anchored at the joint.

4.2.7.5. Commentary on Taylor's tests

Taylor considered joints only from the point of the efficiency in detailing in joints and incorrectly suggested that stirrups do not increase the joint shear resistance or confine the joint. According to him, the stirrups were only necessary to prevent the buckling of the columns. Therefore he decided that a single stirrup would satisfy this demand. Today it is apparent from recent tests that stirrups confine the joint core by decreasing the principal tensile strain in the joint and consequently increasing the concrete strength. Thus, the joint shear strength is considerably increased by the provision of stirrups. Taylor developed a simple design equation that predicts the failure mode of the specimen. He suggested that, if the beam bar ratio were higher than this limit, the joint would necessarily exhibit joint shear failure. If the beam longitudinal reinforcement ratio is less than this limit, the joint will exhibit beam flexural failure. However, Taylor did not examine the beam column joints subjected to low column load and beam steel percentage of less than 1.2. These kind of specimens were later tested by Scott and they all exhibited joint shear failure. The author is of the opinion that Taylor could not evaluate the influence of the column axial load and the transverse reinforcement on the behavior of the joints adequately.

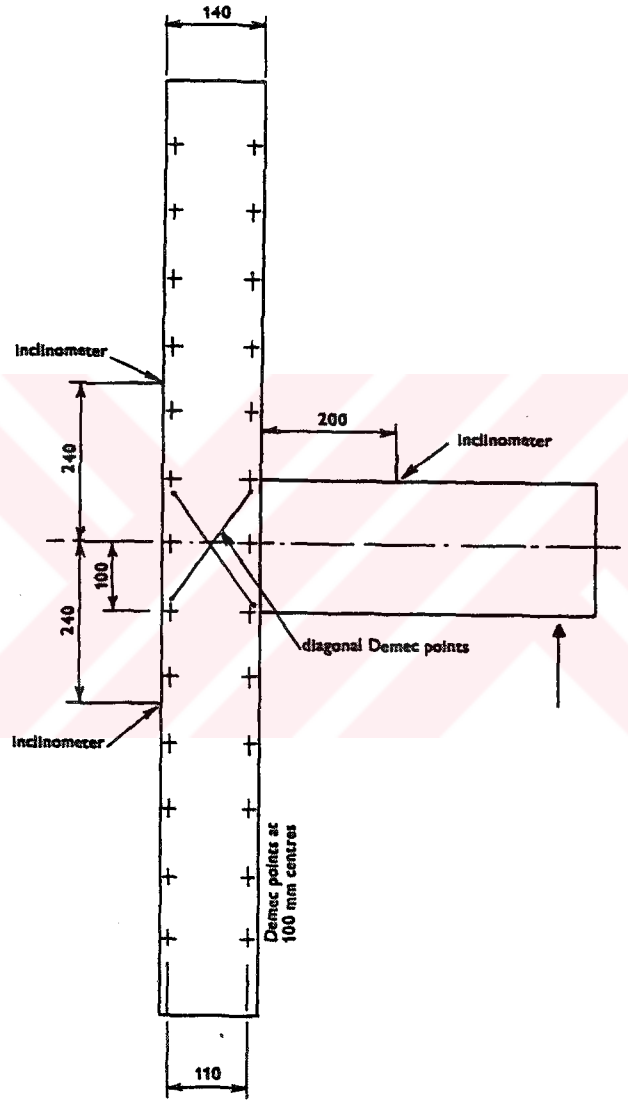

Figure 4.23 : The test instrumentation of Taylor specimens.

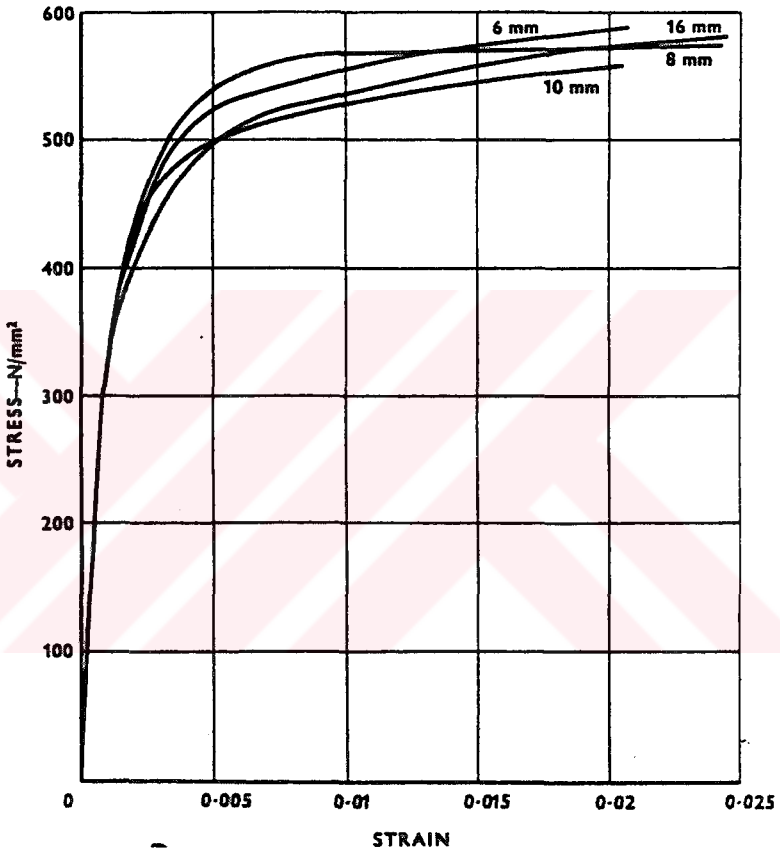

Figure 4.24 : Stress strain curves for the steel.

4.3. The Parameters Affecting the Joint Shear Strength of Monotonically Loaded Specimens

The joint shear strength of reinforced concrete beam column joints are affected by many parameters including beam bar detailing, concrete strength, joint aspect ratio beam bar ratio and the amount of transverse reinforcement. These parameters can also have interactions with each other. In the preceding sections, the tests of different researchers had been discussed. In this section, all the experimental database will be evaluated. The effects of the parameters on each of these tests will be discussed in the following paragraphs. The failure modes will also be taken into consideration because the specimens, which exhibit different failure modes, can not be directly compared.

Table 4.25. Analysis of Ortiz and Parker and Bullman specimens

Specimen	f_c	Detailing	Failure	Stirrups	$N/f_c b_c h_c$	$v_j = V_j / b_c h_c$	ρ_{beam}
Units	MPa	-	-	-	-	MPa	-
Ortiz							
BCJ1	34	L bent down	Joint Shear	0	0	5.287	1.005
BCJ2	38	Same	JS	1T8	0	5.819	1.005
BCJ3	33	Same	JS	0	0	5.561	1.005
BCJ4	34	Same	JS	2T8	0	6.136	1.005
BCJ5	38	Same	JS	0	.131	5.335	1.005
BCJ6	35	Same	JS	0	0.142	5.374	1.005
BCJ7	35	Same	B	3T8	0.142	7.877	1.005
Mean	35.28					5.913	

Table 4.26. Analysis of Parker and Bullman specimens

Specimen	f_c	Detailing	Failure	Stirrups	$N/f_c b_c h_c$	$v_j = V_j / b_c h_c$	ρ_{beam}
Units	MPa	-	-	-	-	MPa	-
Parker and Bullman							
4a	39.2	L bent down	C	0	0	2.52	0.785
4b	39.2	same	JS	0	0.085	2.950	0.785
4c	36.8	same	JS	0	0.172	3.665	0.785
4d	39.2	same	JS	0	0	3.207	0.785
4e	40	same	JS	0	0.083	3.420	0.785
4f	37.6	same	JS	0	0.177	3.940	0.785
Mean	38.66					3.500	
5a	42.4	same	C	2T12	0	4.027	0.785
5b	43.2	same	JS	2T12	0.077	4.465	0.785
5c	43.2	same	B	2T12	0.146	4.450	0.785
5d	43.2	same	C	3T12	0	5.395	1.287
5e	44.8	same	same	3T12	0.074	5.755	1.287
5f	43.2	same	JS	3T12	0.154	6.320	1.287
Mean	43.3					5.069	
Total Mean	40.98					4.284	

Notes: 1. The breadth of the joint is calculated as follows: $b_e = 0.5 (b_c + b_b)$, where: b_b is the width of the beam, b_c is the width of the column

2. The maximum concrete stress was calculated as $0.85 f_c (1 - f_c / 250)$ as recommended by the CEB Model Code 90.

4.3.1. Concrete Cylinder Strength

The concrete strength significantly affects the shear strength of joints. It is well known that cracking would reduce the compressive concrete cylinder strength of joints. The **CEB Code 90** assumes that there is a linear relationship between the cracked concrete strength and the cylinder strength of the joint. This would imply that the relationship between the cracked concrete strength and the joint shear strength is linear. In order to examine the effect of concrete cylinder strength on the joint shear strength of monotonically loaded beam column joints, the tests of **Parker and Bullman, Kordina, Scott & Hamill** and **Ortiz** are analyzed. The joint shear strengths are calculated according to the procedure stated in Section 4.2. of this thesis. The cylinder strengths are the mean cylinder strengths reported by researchers and no factors of safety are adapted. The analysis of the **Ortiz** and **Parker & Bullman** specimens are shown in Table 4.26. The results of the analysis of the specimens of **Kordina** and **Scott** are shown in Table 4.27. As the place is limited the rest of the tables are given in Appendix B of the thesis. Table B-1 in appendix B shows the results of the analysis of **Scott and Hamill's** tests carried out by the author.

4.3.1.1.Analysis of Tables 4.26 and 4.27

In order to investigate the effect of concrete cylinder strength on joint shear strength of beam column joints, a parametric study using the Tables 4.26, 4.27, Table B-1 and Table B-2 is carried out as shown in Figure 4.26a. In order to exclude the effects of transverse reinforcement, column axial stress and joint aspect ratio, similar specimens that had no transverse reinforcement, with low or no column axial load and with similar joint aspect ratios were analyzed. The specimens chosen were **Ortiz** specimen BCJ1 and **Scott & Hamill's** C4ALHO and C4ALNO. It is clear that the joint shear strength will be proportional to $\alpha(f_c)^n$. The results of the analysis of the above three test specimens showed that the relation between the concrete cylinder strength and joint shear strength is:

$$v_j \approx (f_c)^{0.5} \qquad (4.16)$$

Table 4.27. Analysis of the specimens of Kordina and Scott

Specimen	Cylinder Strength	Type of Detailing of the Beam Bars	Failure Mode	Effective Joint Stirrups	Column Axial Stress/f_c	Joint Shear Strength $v_j = V_j / b_c h_c$	Ratio of Tensile Reinforcement
Units	MPa	-	-	-	-	MPa	-
Kordina							
RE2	25.28	L bent down	Joint Shear	0	0.237	4.615	0.785
RE3	40.4	same	JS	1T10	0.247	7.500	0.981
RE4	32.24	same	JS	1T8	0.039	4.977	1.047
RE7	25.7	same	JS	3T8	0.439	6.695	1.17
Mean	30.905				0.240	5.946	
RE6	31.6	Beam bar anchored by steel plates outside the joint	JS	2T8	0.168	6.498	1.047
RE5	29.52	unusual	-	0	0.033	3.119	0.580
RE8	28	U Bars	JS	3T8	0.326	5.928	1.170
RE9	28.55	U Bars	JS	3T8	0.469	6.210	1.170
RE10	23.8	U Bars	JS	3T8	0.402	4.95	1.170
Mean (U bars)	26.78				0.399	5.696	
Mean (Total)	29.45				0.262	5.61	
Scott							
C1	39.92	L bent down	B	1T6	0.306	5.728	0.979
C1A	48	same	B	1T6	0.254	5.278	0.979
C1AL	33.36	same	JS	1T6	0.066	4.84	0.979
C4	41.44	same	JS	1T6	0.294	5.524	1.740
C4A	44.32	L bent down	JS	1T6	0.275	7.155	1.740
C4AL	35.76	Same	JS	1T6	0.062	6.494	1.740
C7	35.2	L bent down	JS	2T6	0.347	7.413	1.740
Mean	39.71				0.229	6.06	
C3L	35.52	U Bar	JS	1T6	0.062	4.738	0.979
C6	39.84	U Bar	JS	1T6	0.307	4.895	1.740
C6L	45.84	U Bar	JS	1T6	0.266	5.787	1.740
C9	35.92	U Bar	JS	2T6	0.340	6.398	1.740
C3	36	U Bar	B	1T6	0.339	5.72	0.979
Mean	38.624				0.263	5.507	
C8	44.48	L bent down	JS	2T6	0.274	6.099	1.740
C5	33.04	same	JS	1T6	0.369	3.124	1.740
C2	49.36	same	JS	1T6	0.247	4.584	0.979
Mean	42.29				0.297	4.6	
Total Mean	39.87				0.254	5.585	

It is apparent that in joints without stirrups, the joint shear strength is directly proportional to the square root of the concrete cylinder strength. This in turn shows that when investigating the effects of different parameters on the joint shear strength of monotonically loaded exterior beam column joints, it will be best to normalize the joint shear strength with the square root of the concrete cylinder strength rather than the cylinder strength itself, in order to exclude the effect of the concrete cylinder strength on the joint shear strength of the joint.

4.3. 2.The Effect of the Ratio of Beam Height to Column Height

The following tables show the effect of the joint aspect ratio on the joint shear strength. The joint shear strength of each specimen is calculated in the tables as

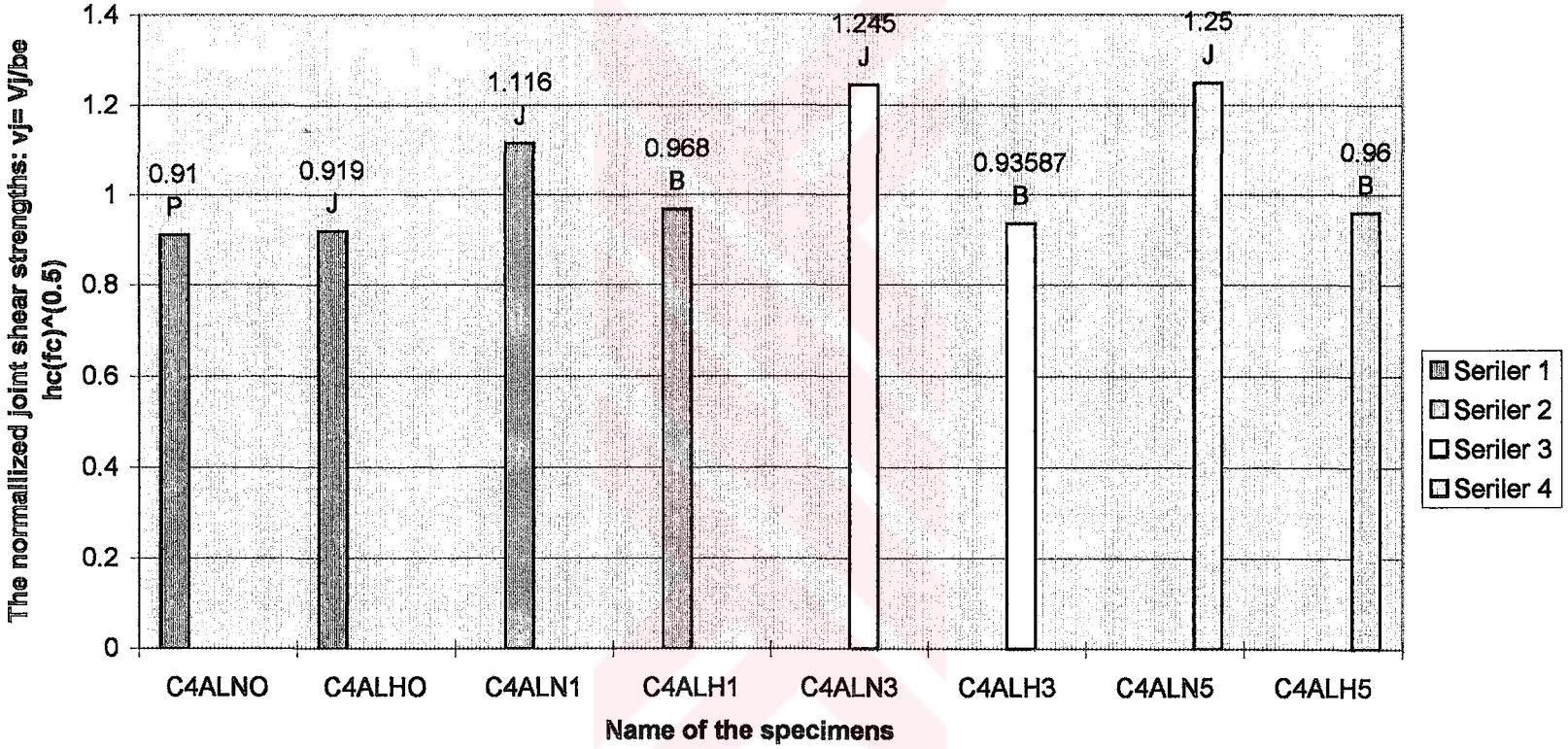

Figure 4.25a : The normalized joint shear strength of exterior beam-column joints with high and normal concrete strength

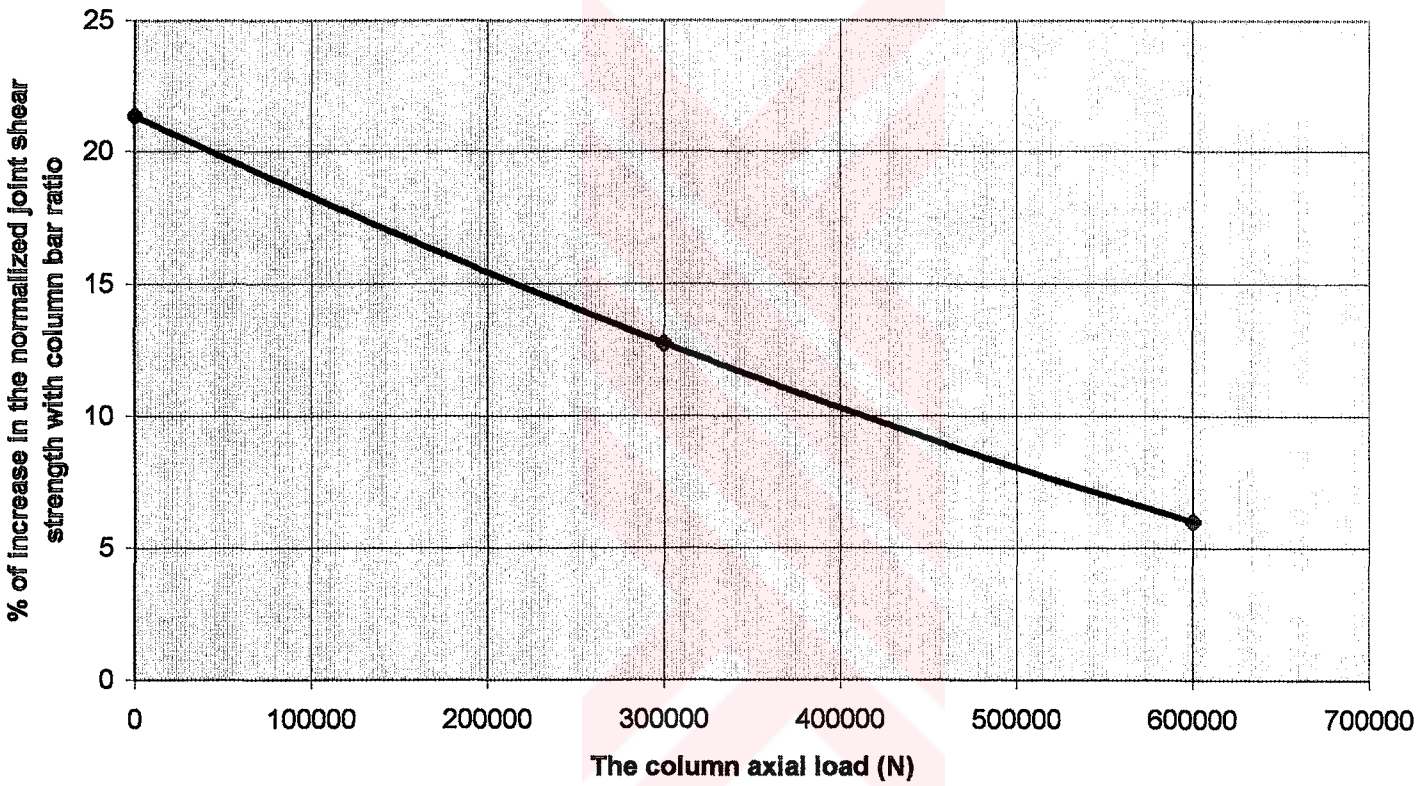

Figure 4.25b : The percentage of increase in the normalized joint shear strength with column longitudinal reinforcement ratio versus the column axial load.

explained in Section 4.2. The results showed clearly that as the joint aspect ratio is increased, the normalized joint shear strength decreases. Table 4.28 shows the normalized joint shear strength of the test specimens of **Ortiz** and **Parker & Bullman** with different joint aspect ratios. The results of the complete analysis can be found in Appendix B, Tables B-3 and B-4.

4.3.3.Influence of Column Axial Load

In the tests of **Ortiz**, it is apparent that the first four beam column joints, BCJ1, BCJ2, BCJ3, BCJ4 has no axial load in the columns. In the rest of the specimens, the axial load was increased to 300 kN. The column loads **Ortiz** took into account were so low that it will be incorrect to reach some conclusions from these very low column loads. The beam column joints of 1 and 3 can not be compared with 5 and 6, because the anchorage length of the beam reinforcement was less in the specimens BC5 and BCJ6. The reduction in joint shear strength of specimen 5 compared to BCJ1 and BCJ6 compared with BCJ3 was due to anchorage failure rather than the increase in column load. **Parker and Bullman** specimens suggest an increase in the normalized joint shear strength with increasing column axial load. However, this increase can be misleading because the specimen 4a of **Parker and Bullman**, which had no column axial stress, exhibited column hinge while that of 4b exhibited joint shear failure. The increase in the column axial stress changes the failure mode of a specimen. Careful inspection of **Scott**'s specimens reveals that the column axial load does not increase the normalized joint shear strength. Table 4.29 shows the calculated normalized shear strengths of the tests of **Ortiz** and **Parker and Bullman** with the column axial stresses of each specimen.

4.3.4. Comparison of the tests of Ortiz and Parker and Bullman

Ortiz specimens' normalized joint shear strengths are significantly higher than **Parker and Bullman** specimens. This is because the joint aspect ratio of **Ortiz** specimens are 1.33 while that of **Parker and Bullman** are 1.67. The author stated in the previous sections that the joint aspect ratio would decrease the normalized joint shear strength of monotonically loaded exterior beam

Table 4.28. The Analysis of Ortiz and Parker & Bullman Specimens

Specimen	Cylinder Strength	Detailing	Failure Mode	Effective Stirrups	$N/b_c h_c f_c$	$v_j=V_j/b_c h_c\sqrt{f_c}$	ρ_b	h_b/h_c
Units	MPa	-	-	-	-	$MPa^{0.5}$	-	-
Ortiz								
BCJ1	34	1	J	0	0	0.909	1.005	1.333
BCJ2	38	1	J	1T8	0	0.944	1.005	1.333
BCJ3	33	1	J	0	0	0.968	1.005	1.333
BCJ4	34	1	J	2T8	0	1.052	1.005	1.333
BCJ5	38	1	J	0	0.131	0.865	1.005	1.333
BCJ6	35	1	J	0	0.143	0.908	1.005	1.333
BCJ7	35	1	B	3T8	0.143	1.330	1.005	1.333
Mean	35.28					0.996		1.333
Parker &Bullmann								
4a	39.2	1	C	0	0	0.402	0.785	1.667
4b	39.2	1	J	0	0.085	0.471	0.785	1.667
4c	36.8	1	J	0	0.172	0.604	0.785	1.667
4d	39.2	1	J	0	0	0.512	0.785	1.667
4e	40	1	J	0	0.083	0.540	0.785	1.667
4f	37.6	1	J	0	0.177	0.642	0.785	1.667
Mean	38.66					0.563		1.667
5a	42.4	1	C	2T12	0	0.618	0.785	1.667
5b	43.2	1	J	2T12	0.077	0.679	0.785	1.667
5c	43.2	1	B	2T12	0.146	0.677	0.785	1.667
5d	43.2	1	C	3T12	0	0.820	1.287	1.667
5e	44.8	1	C	3T12	0.074	0.859	1.287	1.667
5f	43.2	1	J	3T12	0.154	0.962	1.287	1.667
Mean	43.3					0.769		1.667
Total Mean	40.98					0.666		1.667

Notes: The beam detailing type 1 denotes the specimens that have beam bars bent down into lower column.

column joints. This means that the joint shear strength of Parker and Bullman specimens should be 12% less than the specimens of Ortiz if both are adequately detailed. This does not explain the 33% difference in the normalized joint shear strength of Parker and Bullman and Ortiz. However, as stated by the author in the previous sections, this relationship could only be obtained if both specimens are adequately detailed. The specimens of Parker and Bullman have been reinforced by only a single bar at each corner of the cross sections of the beam and the columns. The bars in the beam and column cross sections of Ortiz specimens on the other hand have been regularly distributed throughout the cross section. The analysis of the two sets of tests can be found in Table B5.

4.3.4.1.Comparison of Parker and Bullman specimens 4a, 4d and Ortiz specimen BCJ1

These specimens were deliberately chosen because three of the specimens had got no joint stirrups or column axial stress. By doing so, the interactions or influence of the column axial stress or stirrups were eliminated. The comparison of Parker and

Bullman specimen 4a and Ortiz specimen BCJ1 reveal that the possible increase of the normalized joint shear strength of BCJ1 with respect to specimen 4a is due to:

1.The relatively low joint aspect ratio of Ortiz specimens.

2.The beam and column longitudinal reinforcement of Parker and Bullman are concentrated at the corners of the cross sections of the beam and the columns.

3.Ortiz specimen BCJ1 a higher beam longitudinal reinforcement ratio. (Ortiz specimen has a beam longitudinal reinforcement ratio of 1.005, while that of Parker and Bullman's is 0.785).

4.Ortiz specimen BCJ1 has got a higher column longitudinal reinforcement ratio. (Ortiz specimen has a column longitudinal reinforcement ratio of 2.19, while Parker and Bullman specimen has a column longitudinal reinforcement ratio of 1.094.)

5.The normalized joint shear strength of Parker and Bullman 4a is 52% less than that of Ortiz BCJ1. The failure mode of specimen 4a is column failure, while that of Ortiz's is joint.

Table 4.29. The specimens of Ortiz and Parker & Bullman

Specimen	f_c	Detailing	Failure Mode	Effective Stirrups	$N/b_c h_c f_c$	$v_j = V_j / b_c h_c$	ρ_b
Units	MPa	-	-	-	-	MPa	-
Scott &Hamill							
C6NL3	48.8	U Bars	JS	2T6	0.045	6.360	1.74
C6ALN5	36.8	U Bars	JS	3T6	0.060	7.840	1.74
C6ALH3	96.8	U Bars	JS	2T6	0.045	8.940	1.74
C6ALH5	100	U Bars	B	3T6	0.044	9.480	1.74
C6ALH0	100.8	U Bars	JS	0	0.044	9.380	1.74
C6ALH1	101.6	U Bars	JS	1T6	0.043	8.015	1.74
C6ALN0	51.2	U Bars	JS	0	0.043	5.252	1.74
C6ALN1	51.2	same	JS	1T6	0.10	5.988	1.74
Mean(Bars)	73.4				0.053	7.657	
C4ALN3	41.6	L Bars bent down	JS	2T6	0.053	8.030	1.74
C4ALH0	104	same	P	0	0.025	10.370	1.74
C4ALN5	50.4	same	JS	3T6	0.044	10.410	1.74
C4ALH3	105.6	same	B	2T6	0.042	9.617	1.74
C4ALH5	98.4	same	B	3T6	0.045	9.550	1.74
C4ALNO	42.4	same	P	0	0.062	6.580	1.74
C4ALN1	45.6	same	JS	1T6	0.058	8.339	1.74
C4ALH1	95.2	same	B	1T6	0.046	9.440	1.74
Mean (Lbars)	70.489				0.047	9.042	
Mean (Total)	73.15				0.050	8.349	

4.3.4.2. Comparison of the tests of Scott and Parker & Bullman

The specimens of Scott and Parker & Bullman are compared because the specimens of both of the series of tests have been reinforced by one single bar at each corner of

the joint. Scott and Parker & Bullman specimens have got 31% difference in their normalized joint shear strengths for beam bars bent down detail specimens. Detailing can not explain the very low normalized joint shear strength of Parker and Bullman specimens when compared to Scott specimens, which have got similar detailing.

4.3.4.3.Comparison of the specimens of Scott and Scott & Hamill

The comparison of the specimens of Scott and Scott & Hamill showed that the normalized joint shear strength of Scott specimens which are reinforced by a single stirrup are 6.7 % less than the specimens of Scott & Hamill as shown in Table B4. The author considered only the specimens, which have, beam bars bent down detail. The reason for this is as follows:

1.The beam bars bent down detail specimens have significantly higher joint shear strength than the U bar or L bars bent up into the column specimens.

Table 4.30. The Comparison of the tests of Scott and Parker & Bullman

Specimen	f_c'	Failure Mode	Effective Stirrups	$N/b_c/f_c/h_c$	$v_j = V_j / b_c h_c \sqrt{f_c'}$	ρ_b	h_b/h_c	$A_{stot}/b_c/h_c$
Units	MPa	-	-	-	MPa	-		
Scott								
C1	39.92	B	1T6	0.306	0.907	1.110	1.400	4.289
C1A	48.00	B	1T6	0.254	0.762	1.110	1.400	4.289
C1AL	33.36	J	1T6	0.066	0.839	1.110	1.400	4.289
C4	41.44	J	1T6	0.294	1.042	1.976	1.400	4.289
C4A	44.32	J	1T6	0.275	1.075	1.976	1.400	4.289
C4AL	35.76	J	1T6	0.062	1.086	1.976	1.400	4.289
C7	35.20	J	1T6	0.347	0.755	1.330	2.000	4.289
Mean	39.71			0.229	0.968		1.400	
4a	39.20	C	0	0	0.402	0.882	1.667	1.094
4b	39.20	J	0	0.085	0.471	0.882	1.667	1.094
4c	36.80	J	0	0.172	0.604	0.882	1.667	1.094
4d	39.20	J	0	0	0.512	0.882	1.667	4.377
4e	40.00	J	0	0.083	0.540	0.880	1.667	4.377
4f	37.60	J	0	0.177	0.642	0.880	1.667	4.377
Mean	38.66			0.086	0.563		1.667	
5a	42.40	C	2T12	0	0.618	0.880	1.667	2.67
5b	43.20	J	2T12	0.077	0.679	0.880	1.667	2.67
5c	43.20	B	2T12	0.146	0.677	0.880	1.667	2.67
5d	43.20	C	3T12	0	0.820	1.440	1.667	2.67
5e	44.80	C	3T12	0.074	0.859	1.440	1.667	2.67
5f	43.20	J	3T12	0.154	0.962	1.440	1.667	2.67
Mean	43.30				0.769		1.667	

2.In terms of ductility, Scott's experiments showed that the most ductile specimens are the beam bars bent down detail. The beam bars bent up into column detail

specimens are the worst in terms of ductility. The author is therefore of the opinion that this kind of detailing should not be used.

The specimens of **Scott** and the specimens of **Scott and Hamill** are compared regarding the effect of the concrete cylinder strength on the normalized joint shear strength. The results are depicted in Figure 4.25a which shows that increasing the concrete cylinder strength does not necessarily increase the normalized joint shear strength of monotonically loaded exterior beam column connections.

4.3.5. Development of Design Equations for Monotonically Loaded Exterior Beam Column Connections

4.3.5.1. Effect of Concrete Cylinder Strength

The author made a parametric study in order to investigate the relation between the concrete cylinder strength and the normalized joint shear strength of monotonically loaded exterior beam column connections. The specimens investigated were; C4ALHO of **Scott**, C4ALNO of **Scott**, BCJ1 of **Ortiz**. These specimens were deliberately chosen because they had the following characteristics:

1.They had no stirrups.

2.They had no column axial load.

3.They had similar joint aspect ratios.

The analysis gave the following result:

$$v_j = 0.88 (f_c)^{0.5} \qquad (4.16)$$

where

$v_j = V_j / b_e h_c$

$b_e = (b_b + b_c) / 2$

f_c is the concrete cylinder strength taken directly as the average cylinder strength without any factors of safety.

The analysis shows that the joint shear strength of monotonically loaded exterior beam-column joints is proportional to the square root of concrete cylinder strength.

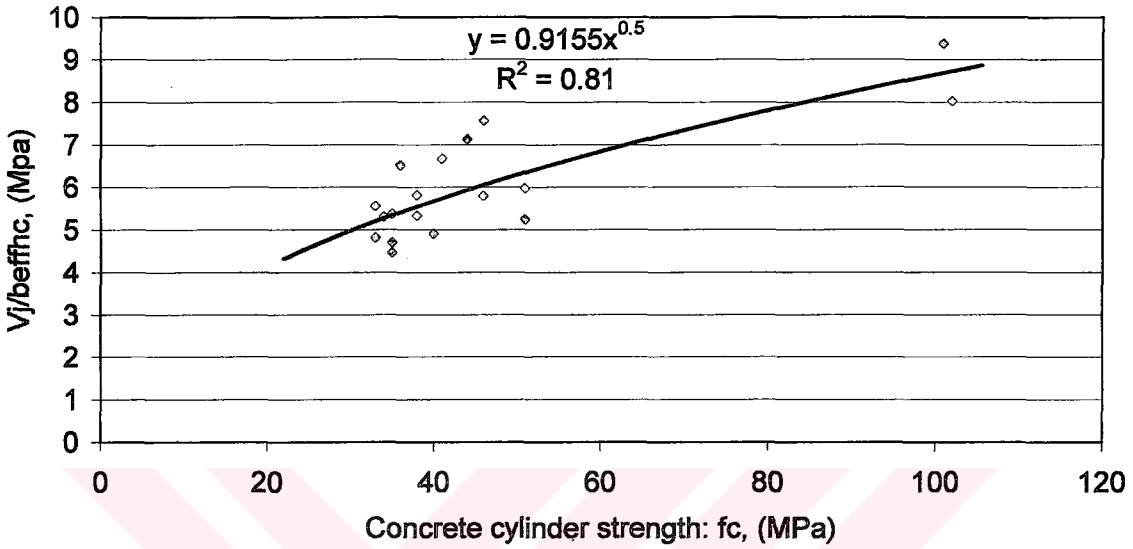

Figure 4.26a. The influence of concrete cylinder strength on joint shear strength of joints with low amount of stirrups

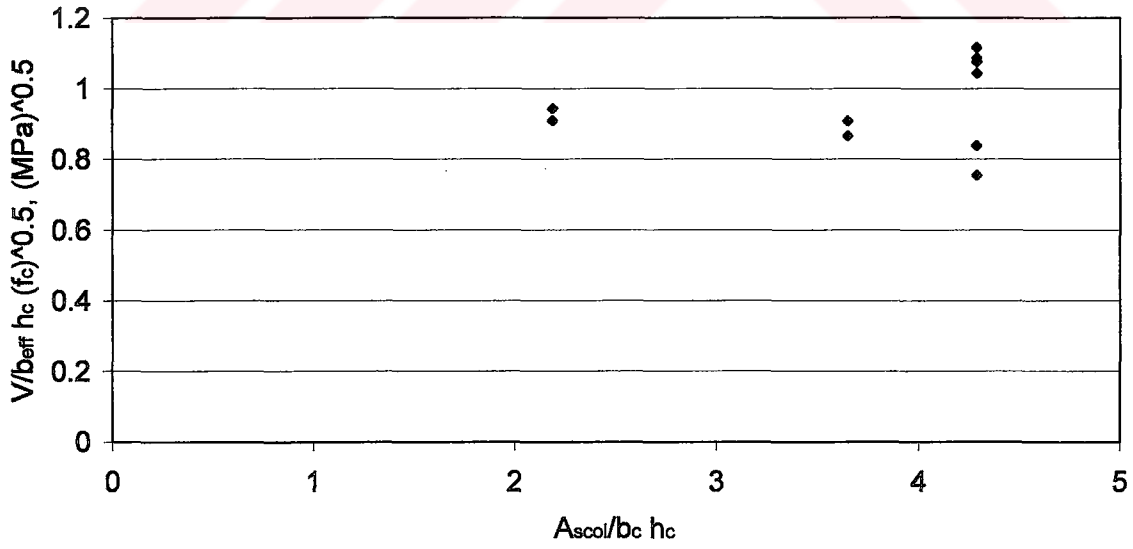

Figure 4.26b: The influence of the column longitudinal reinforcement ratio on the normalised joint shear strength

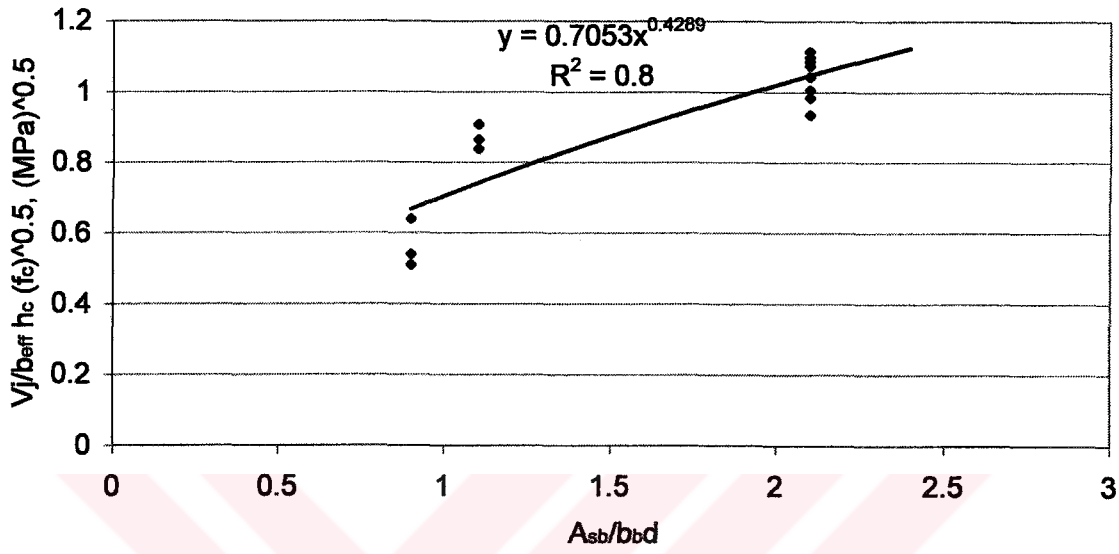

Figure 4.26c: The influence of the beam longitudinal reinforcement ratio on the normalised joint shear strength

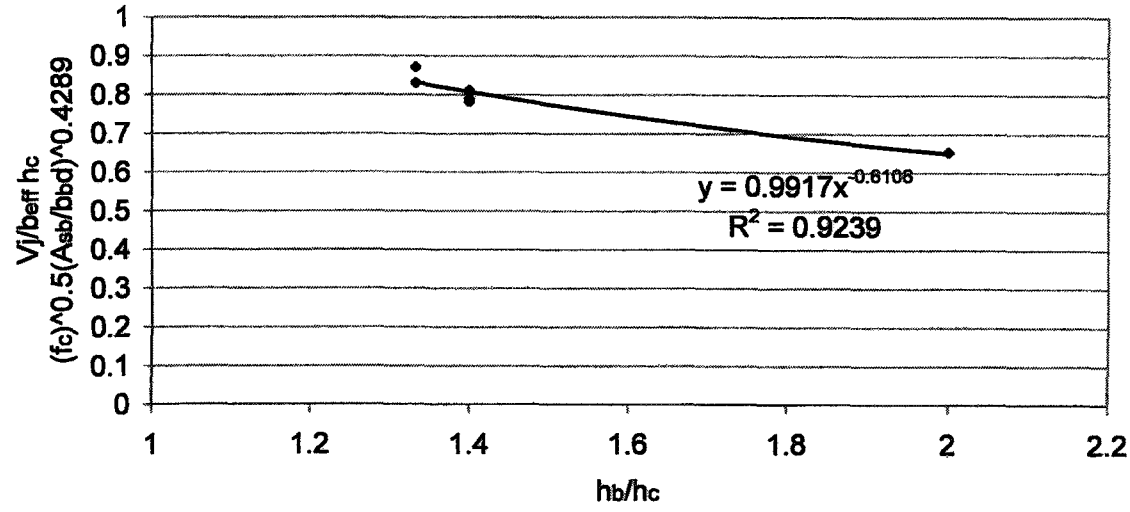

Figure 4.26d: The influence of the joint aspect ratio on the joint shear strength normalised by the concrete cylinder strength and the beam reinforcement ratio

DOKUMANTASYON MERKEZI

made a parametric study in order to investigate the relationship between the column longitudinal reinforcement ratio, column axial stress and the normalised joint shear strength of monotonically loaded exterior beam column connections. The specimens were 4a, 4d, 4b, 4e, 4c and 4f. First, the relationship between the column longitudinal reinforcement ratio and the normalised joint shear strength is considered for specimens with no column axial load. i.e. specimens 4a and 4d. **In Parker and Bullman** specimens, it is apparent that the normalised joint shear strength is proportional to

$$v_j \approx (\rho_{col})^{(0.173)} \qquad (4.17)$$

It is demonstrated in Figure 4.25b that the increase in the normalized joint shear strength of monotonically loaded exterior beam column joints due to column longitudinal reinforcement ratio decrease as the column axial load is increases in **Parker and Bullman** tests. A parametric study carried out by the author showed that the relationship between the column axial load, column longitudinal reinforcement ratio and the normalized joint shear strength for **Parker and Bullman** specimens should have the form of:

$$v_j \approx (\rho_{col})^{(0.173-1.8067\,(P\,/\,bc\,dc))} \qquad (4.18)$$

The author having applied this relationship on specimen C7 of **Scott** found out that the above relationship can not be applied on specimens other than those of **Parker and Bullman**. When applied, it gives unrealistic results. It seems likely that **Parker and Bullman** specimens are very sensitive to the changes in the column axial load. This trend is not present in the other tests of the experimental database used for the development of the design equation. The possible reasons could be as follows:

1. **Parker and Bullman** had very high joint aspect ratio.
2. **Parker and Bullman** specimens had very low radius of bend.
3. The bars were not regularly distributed throughout the cross section. **Parker and Bullman** specimens had a bar at each corner of the cross section.
4. **Parker and Bulmann** specimens exhibited column failure by a hinge forming in the upper column.

The authors have plotted the column longitudinal reinforcement ratio versus the normalized joint shear strength of all the joints without significant stirrups as shown

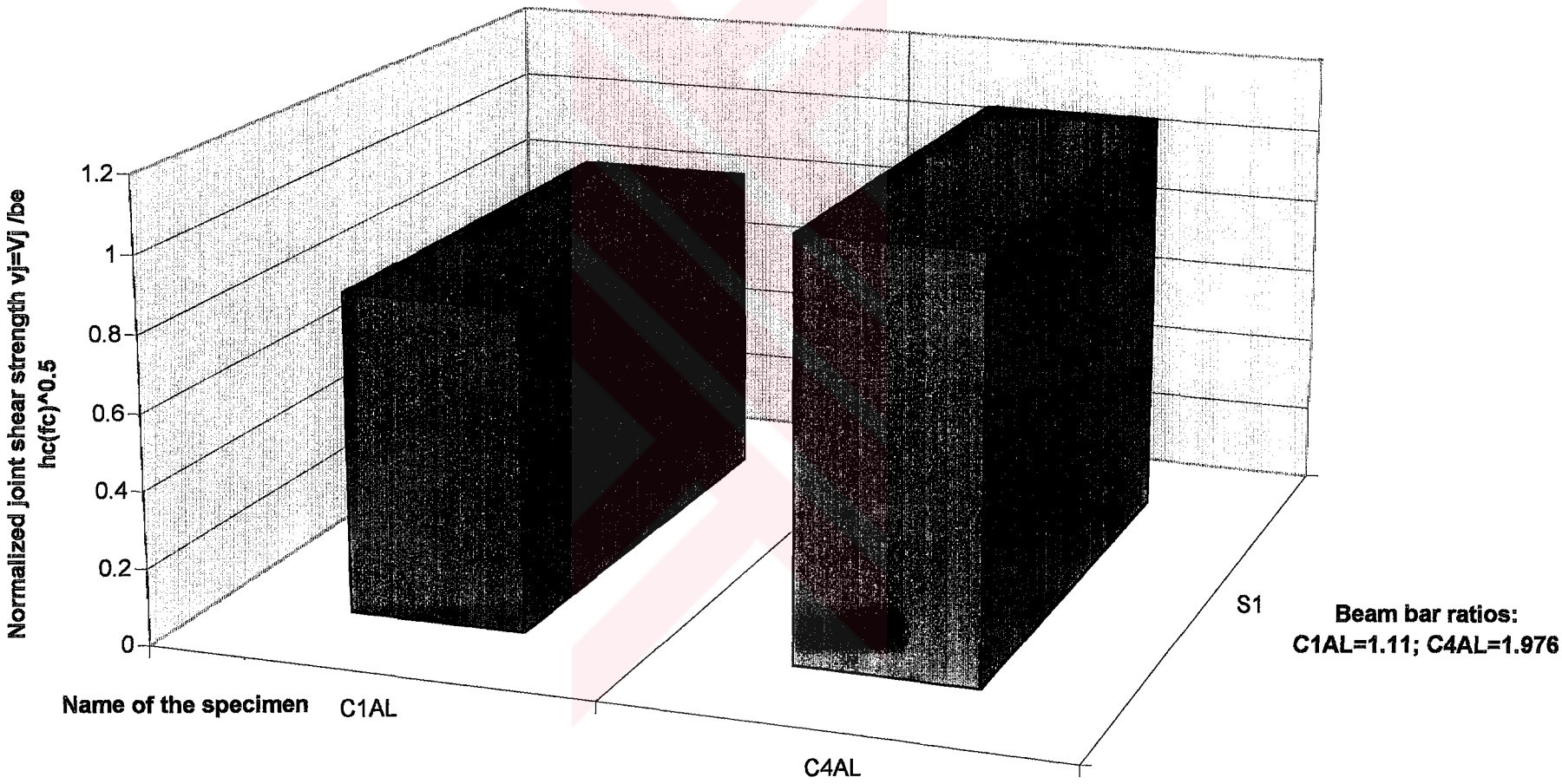

Figure 4.27. Increase in the normalized joint shear strength with increase in beam bar ratio

in Figure 4.26b. The regression analysis showed no relation between the column longitudinal reinforcement ratio and the normalized joint shear strength.

4.3.5.3.Beam Longitudinal Reinforcement Ratio

The author having investigated Parker and Bullman specimens decided that the possible reason for the very low strength of Parker and Bullman specimens apart from detailing and beam column joint aspect ratio could be the ratio of beam longitudinal reinforcement. In order to investigate the relationship between the beam longitudinal reinforcement ratio and the normalized joint shear strength, the author made a parametric study. The specimens chosen by the author were C1AL and C4AL, which were nearly identical, except the beam longitudinal reinforcement ratios they had. Both of the two specimens had low column axial load and low amount of stirrups. A quick inspection of these specimens' normalized joint shear strengths showed that the normalized joint shear strengths increased with beam longitudinal reinforcement ratio.

The results of the author's parametric study showed that the beam longitudinal reinforcement ratio is related to the normalized joint shear strength with the below equation:

$$v_j \approx (A_{sb}/bd)^{0.4289} \qquad (4.19)$$

The regression analysis, whose details are shown in Figure 4.26c, confirmed the above finding. Figure 4.27 shows the difference in the normalized joint shear strengths with different beam longitudinal reinforcement ratios.

4.3.5.4. Column Axial Stress

The analysis of Parker and Bullman tests showed that the column axial load increased the normalized joint shear strength of joints. However this effect was invisible for Scott specimens. Scott specimens and the specimens of Parker and Bullman had same type of detailing; a bar at each corner of the cross sections of the

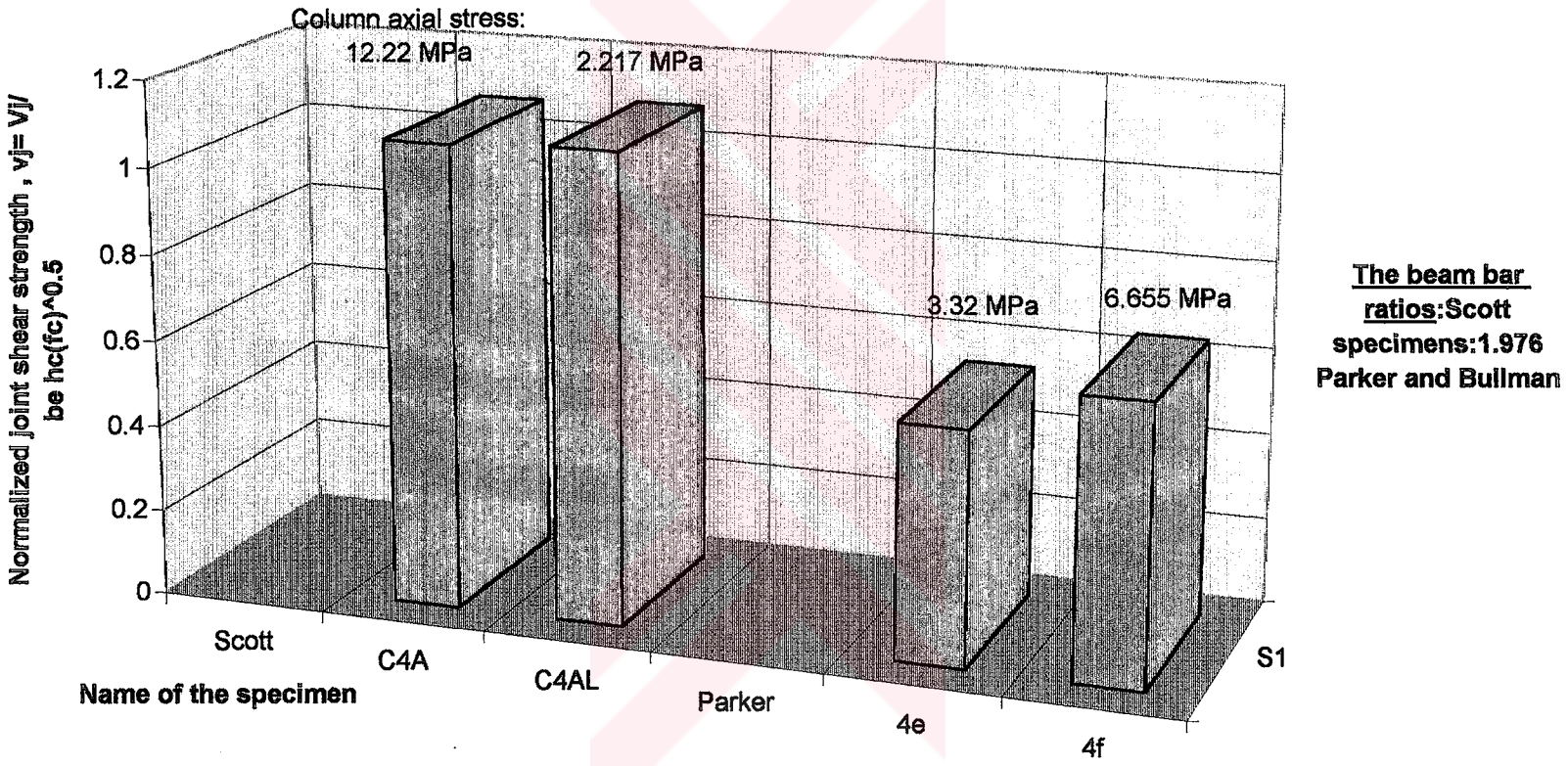

Figure 4.28. The increase in normalized joint shear strength with column axial load.

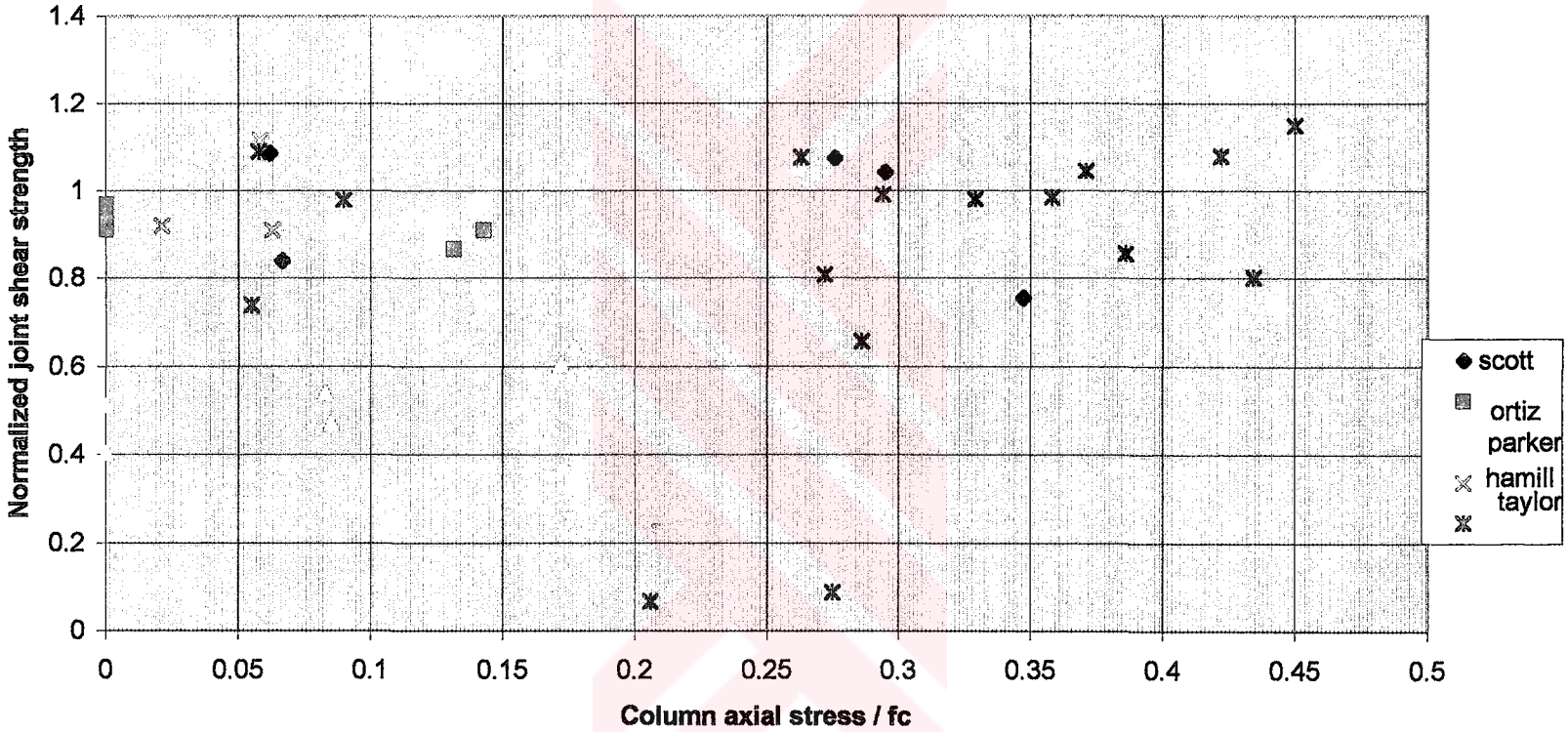

Figure 4.29.The effect of column axial load on the normalized joint shear strength of monotonically loaded exterior beam column connections.

beam and the columns. Thus, detailing of the beam longitudinal reinforcement could not be the reason why Parker and Bullmann exterior beam-column joint specimens had significantly lower joint shear strengths with respect to the exterior beam-column joints of Ortiz, Scott, Scott and Hamill, Taylor and Kordina. The joint aspect ratios of Parker and Bullman specimens were significantly higher than the joint aspect ratios of Scott specimens. Joint aspect ratio is defined as the ratio of the cross-sectional height of the beam to the cross-sectional height of the column. Moreover, the beam longitudinal reinforcement ratio of Parker and Bullman were significantly lower than the beam longitudinal reinforcement ratio of Scott specimens.

Figure 4.28 clearly demonstrates that the increase in the normalized joint shear strength of monotonically loaded exterior beam column joints decreased as the beam longitudinal reinforcement ratio increased and the joint aspect ratio decreased. The author carried out a parametric study to understand the effect of column axial stress on the normalized joint shear strength of monotonically loaded exterior beam column connections. The specimens excluded from the database were:

1.All the specimens which have more than one transverse reinforcement in the joint.

2.The specimens which exhibited beam failure.

The specimens with different failure modes other than the joint shear failure were excluded from the parametric study. This is because the joint shear strength of joints that exhibit different failure modes will be different and it will be illogical to compare the joints that exhibit different failure modes. The results are shown in Figure 4.29. Figure 4.29 shows no correlation between the column axial stress and the normalized joint shear strength of monotonically loaded exterior beam-column joints. The author having investigated the database in detail came to the conclusion that the relationship between column axial stress and the normalized joint shear strength could be as follows:

1.No affect of column axial load on the normalized joint shear strength as suggested by Figure 4.29.

2.The column axial stress increased the normalized joint shear strength at low column axial stress, but at higher column axial stress ratios this effect was invisible.

3.The column axial stress increased the joint shear strength only in joints where column failures were expected.

The results show that more experiments are needed to investigate the relationship between the normalized joint shear strength and the column axial stress. In the design equation developed, it will be assumed that the column axial load does not effect the normalized joint shear strength.

4.3.5.5. Joint Aspect Ratio

The only test data available that investigates the joint aspect ratio is the tests of Scott. His specimen C7 has a joint aspect ratio of 2, while a similar specimen C4AL has a joint aspect ratio of 1.4. The specimen C7 apart from the difference in joint aspect ratio has one more stirrup than the specimen C4AL. The author assumed that the effect of this extra stirrup is negligible because:

1. The normalized joint shear strength of specimen C7 is not significantly increased by the provision of this extra stirrup with respect to C4AL.
2. We are not informed by Scott where this extra stirrup is placed. Bearing the first cause in mind, it is more likely that this extra stirrup is placed outside the effective region, which is defined by the top of the beam compressive chord up to the top beam longitudinal reinforcement.

Vollum incorrectly predicted that the joint aspect ratio has a linear relationship with the normalised joint shear strength because he did not take the influence of the beam longitudinal reinforcement into account. The author taking the beam longitudinal reinforcement ratio into account made a parametric study to investigate the effect of the joint aspect ratio on the normalised joint shear strength of monotonically loaded exterior beam column connection and found that the regression analysis whose details are given in Figure 4.26d confirms the below equation.

$$v_j \approx (h_b/h_c)^{-0.61} \qquad (4.20)$$

4.3.5.6. Effect of Joint Stirrups

The author made a parametric study on the effect of joint stirrups to the normalized joint shear strength of beam-column joints. Throughout the study it is assumed that

the effective stirrups are those that are situated under the top beam bars and above the beam compressive chord. Park and Paulay have made a similar assumption. In joints without stirrups, it is found out that the joint shear of joints is given by the equation

$$V_c = \frac{0.71\,\beta\gamma\,(100 * \frac{A_{sb}}{b_b d_b})^{0.4289}}{(\frac{h_b}{h_c})^{0.61}}\,(\frac{b_c + b_b}{2})h_c\sqrt{f_c} \qquad (4.21)$$

where $\beta = 0.85$ for joints detailed by U bars and $\beta = 1$ for joints detailed by L bars. γ=1.37 for joints with inclined bars and 1 for others. The constant 0.664 is a capacity reduction factor determined empirically.

4.3.5.6.1. Determining the Contribution of Joint Stirrups

The previous studies of the author have shown that not all the stirrups yield at failure. Therefore the traditional $V_j = V_c + A_{sw}\,f_y$ equation which is adapted by many researchers in the past including Ortiz, Sarsam and Phillips, Parker and Bullman should not be used. The author made a parametric study to investigate the effect of stirrup ratio on the normalized joint shear strength. Wight has previously stated that the yield stress of stirrups does not increase the normalized joint shear strength of beam column connections. Therefore the author does not take the effect of the yield stress of stirrups into account.

4.3.5.7. Stirrup index versus the normalized joint shear strength

The author used the above tables given in this chapter and the Appendix B to investigate the relationship between the normalized joint shear strength $v_j=V_j/b_e\,h_c\,(f_c)^{\wedge}0.5$ and the parameter named stirrup index by Vollum; that is $A_{sw}\,f_y\,/b_e\,h_c\,(f_c)^{\wedge}0.5$. The results are demonstrated in Figure 4.30.

There are two lines in the figure. The below line is drawn by the author as a lower bound to all the tests. The figure shows very clearly that the minimum stirrup index to increase the normalized joint strength is 0.4. for Parker and Bullman specimens. The author made other parametric studies to investigate the effects of a.The stirrup ratio on the normalized joint shear strength; .b.The stirrup index versus the parameter $(V_j - A_{sw}\,f_y)/\,b_e\,h_c\,\sqrt{f_c}$. The influence of the stirrup ratio on the normalized joint shear strength is demonstrated in Figure 4.31. Parker and Bullman specimens are excluded

from the database. The figure shows that the relationship is best described by a tri-linear graph. For stirrup ratios below 0.003, the normalized joint shear strength does not increase. Therefore, the author suggests that the minimum stirrup ratio to increase the normalized joint shear strength should be 0.003. The stirrup ratios below this value will be classified as low amount of stirrups. The figure shows that for stirrup ratios between 0.003 & 0.0055%, the normalized joint shear strength increases significantly. No change in the shear strength should be expected for stirrup ratios above 0.0055. The stirrup ratio in this region will be classified as high. Parker and Bullman specimens are excluded from the database due to the reasons listed in the preceding paragraphs. Figure 4.32 shows the relationship between the stirrup index and the $(V_j\text{-}A_s f_y)/ b_e h_c \sqrt{f_c}$.

4.3.5.8. Formulation of the Contribution of Joint Stirrups

The formulation of the contribution will be as in Eq. (4.22)

$$\frac{V_j}{b_{eff}\, h_c \sqrt{f_c}} = v_c + \frac{\alpha \quad A_{sje}\, f_y}{b_e h_c \sqrt{f_c}} \tag{4.22}$$

The final equation will be:

$$V_j = \frac{0.71 \;\; \beta \;\; \gamma (100 \;\; * \frac{A_{sb}}{b_b d_b})^{0.4289} (\frac{b_c + b_b}{2}) \;\; h_c \sqrt{f_c}}{(\frac{h_b}{h_c})^{0.61}} + \alpha \;\; A_{sje} f_y \tag{4.23}$$

where $\alpha = 0.664$ for joints with low amount of stirrups, $\alpha = 0.600$ for joints with medium amount of stirrups, $\alpha = 0.370$ for joints with high amount of stirrups

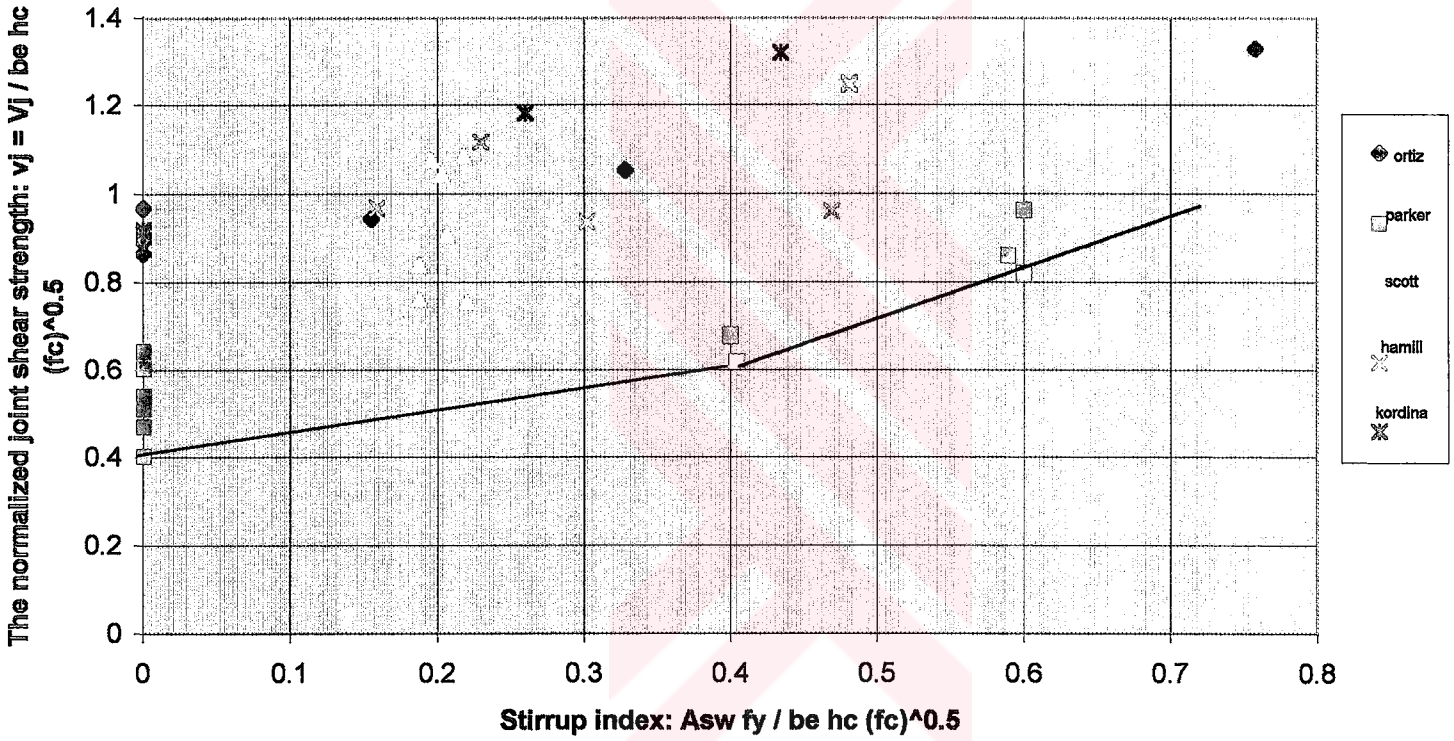

Figure 4.30. Stirrup index vs the normalized joint shear strength

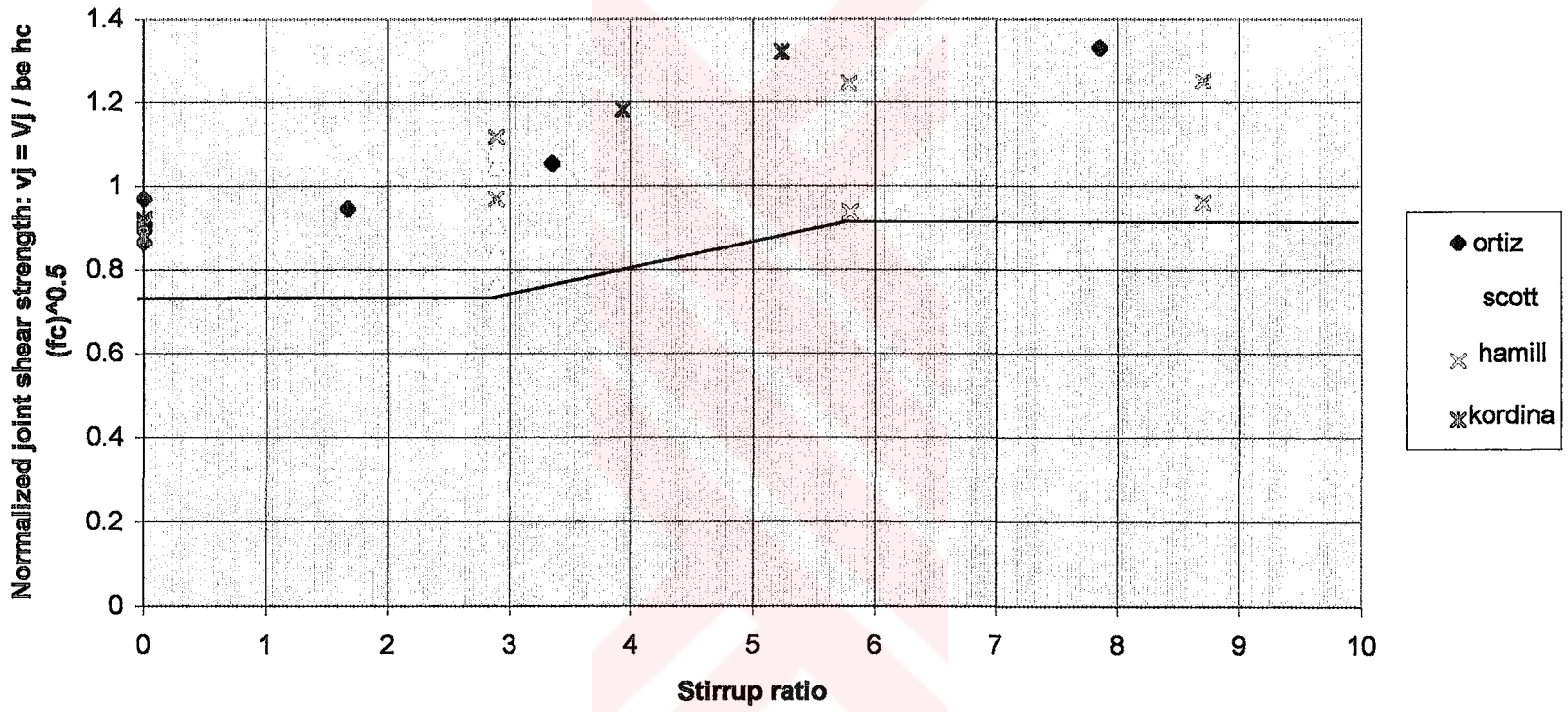

Figure 4.31 The stirrup ratio vs the normalized joint shear strength

4.3.5.9. Results

1. The beam longitudinal reinforcement detailing is the most influential parameter on the joint shear strength. If a joint's top beam longitudinal reinforcement is bent down into the lower column and moreover if that joint is provided by inclined beam bars, the joint shear strength is increased considerably.
2. Some parameters conceal the effect of others. The greatest example is that of column axial load. Column longitudinal reinforcement ratio increases the normalized joint shear strength, but as the column axial load increases, the increase in normalized joint shear strength due to the column longitudinal reinforcement ratio decreases or if a connection is adequately detailed, it's normalized joint shear strength can be well above that of a specimen with less adequately detailed and having a less joint aspect ratio. This means that the effect of joint aspect ratio is conceived by better detailing adapted.
3. The joint aspect ratio increases the normalized joint shear strength as mentioned in Eq. (4.20) only if the connection is adequately detailed. (From the inspection of Kordina specimen RE7 and RE5)
4. If a single stirrups is provided in the joint, it will be best to place it theoretically just at the middle of the distance between the top of the beam compressive chord and under the beam top longitudinal reinforcement. If it is situated just under the top beam longitudinal reinforcement, it will not increase the joint shear strength. (Conclusion from the inspection of RE4). If the single tie is situated in the beam compressive chord, it will not be effective in resisting shear. (Inspection of specimen RE5 of Kordina)
5. The joint shear strength of a joint will decrease if the confinement regions of the upper and lower columns of a joint are adequately confined by closely spaced stirrups, but the joint stirrups are not closely spaced.. (Conclusion from the inspection of RE4)
6. The separate effects of the different variables can not be superimposed without taking the interaction of these into account. In other words a designer can not mathematically add the separate effects of different variables. Some variables are

more influential than the others. (From the comparison of Kordina specimens RE2 and RE7)

7. The comparison of two identical (except the fact that RE7 is reinforced with beam bars bent down and RE8 with U bars) specimens RE7 and RE8 shows that the normalized joint shear strength of U bar specimens will be 15% less than beam bars bent down detail specimens as shown in Figure 4.33. Anchoring the beam bars by steel plates outside the joint as in specimen RE6 of Kordina will provide better joint shear strength than U bar specimens and slightly less normalized joint shear strength with respect to the beam bar bent down detail specimens.

8. The U bars are detailed by three different detailing types in the tests of Kordina which are listed below:

a. The provision of two sets of U bars, one for the beam, the other for the lower column and a single set of inclined bars. (as in RE9)

b. The provision of a single set of U bars for the beam and a single set of inclined bars. (as in RE8)

a. The provision of double set of inclined bars perpendicular to each other. (as in RE10)

The normalized joint shear strengths of the U bar specimens show that the most effective type of detailing in resisting shear is type a and the least effective type of detailing is type c.

9. The specimen failure mode affects the failure load and the normalized joint shear strengths. Inspection of Scott specimen C4AL and Stephan and Hamill specimen C4ALNO showed that C4AL which exhibited joint shear failure had higher normalized joint shear strength and higher failure load with respect to C4ALNO which exhibited connection zone reinforcement pull out.

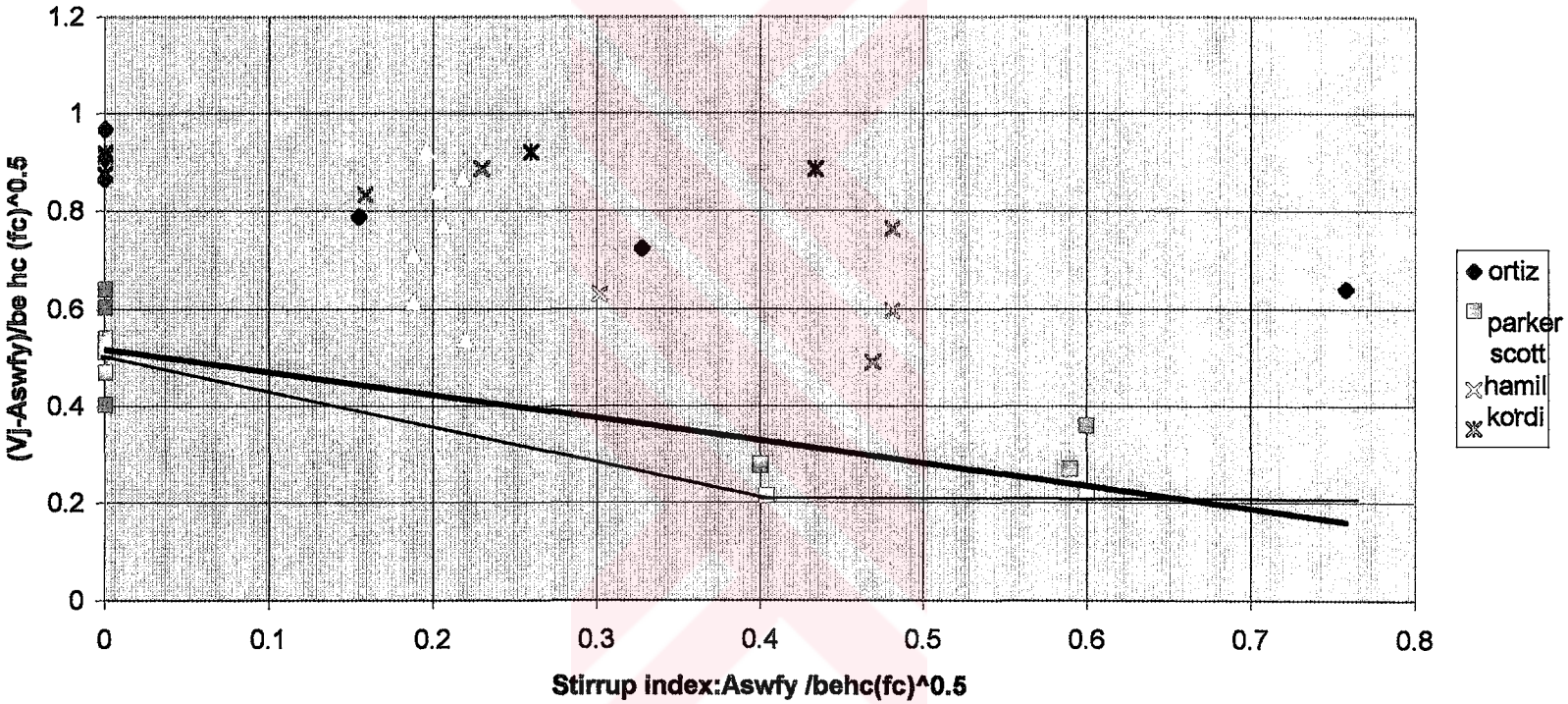

Figure 4.32.The stirrup index vs (Vj-Asw fy)/behc(fc)^0.5

Comparison between Scott specimens C1, C1A and C1AL suggests that, increasing the column axial load would increase the load at which beam cracking will occur and change the failure mode of specimens.

10.If the anchorage length of beam longitudinal reinforcement is increased as in two identical specimens C1 and C1A with beam bars bent down details, the normalized joint shear strength will considerably increase.

Table 4.31. The yield capacity of stirrups and the normalized joint shear strengths of the test specimens of Ortiz and Parker and Bullman.

Specimen	$\rho_{stirrup}*1000$	Effective Stirrups	$N/f_c b_c h_c$	$v_j = V_j / b_c h_c \sqrt{fc}$	ρ_b	h_b/h_c	Asw fy /be hc √fc	(Vj-Asw fy)/ be hc √fc
Units	-	-	-	$MPa^{0.5}$	-	-		
Ortiz								
BCJ1	0	0	0	0.909	1.072	1.333	0	0.909
BCJ2	1.6	1T8	0	0.944	1.072	1.333	0.155	0.789
BCJ3	0	0	0	0.968	1.072	1.333	0	0.968
BCJ4	3.3	2T8	0	1.052	1.072	1.333	0.328	0.724
BCJ5	0	0	0.131	0.865	1.072	1.333	0	0.866
BCJ6	0	0	0.142	0.908	1.072	1.333	0	0.908
BCJ7	7.8	3T8	0.142	1.330	1.072	1.333	0.758	0.640
Mean				0.996		1.333		
Parker &Bullm								
4a	0	0	0	0.402	0.882	1.667	0	0.402
4b	0	0	0.085	0.471	0.882	1.667	0	0.470
4c	0	0	0.172	0.604	0.882	1.667	0	0.604
4d	0	0	0	0.512	0.882	1.667	0	0.512
4e	0	0	0.083	0.540	0.882	1.667	0	0.540
4f	0	0	0.177	0.642	0.882	1.667	0	0.640
Mean				0.563		1.667		
5a	5.4	2T12	0	0.618	0.882	1.667	0.404	0.214
5b	5.4	2T12	0.077	0.679	0.882	1.667	0.400	0.279
5c	5.4	2T12	0.146	0.677	0.882	1.667	0.400	0.277
5d	8.2	3T12	0	0.820	1.440	1.667	0.600	0.220
5e	8.2	3T12	0.074	0.859	1.440	1.667	0.589	0.270
5f	8.2	3T12	0.154	0.962	1.440	1.667	0.600	0.360
Mean				0.769		1.667		
Total Mean				0.666		1.667		

4.4.Designing the joints

4.4.1.The strut and tie models

4.4.1.1. The Strut and Tie Model of Ortiz

Ortiz was the first in UK to propose a strut and tie model for exterior beam column connections which determines the failure loads. Her model was the superposition of the direct strut model to the truss model proposed earlier by Paulay, which all together combined to form a strut and tie model. This simple prediction of the failure

loads and modes of exterior beam column connections by strut and tie models raised great attention in UK and increased the research done on exterior beam column connections again which was once led by Taylor. In this section the model of Ortiz will be investigated in full detail and will be applied on the experiments, which were performed by Scott and Hamill, Parker and Bullman. It will be shown that Ortiz model besides its simplicity has some important theoretical inconsistencies.

4.4.1.1.1.The Model

Ortiz model consisted of a micro-model and a simplified macro-model, which are given in Figures 4.34 and 4.35. She never used the micro-model to predict the failure loads or modes saying that it was too complicated and instead offered a macro model in which one parameter was taken from experiments. The formulation of the model is as follows:

4.4.1.1.2. Horizontal Shear in the Joint

Ortiz assumed that one edge of the beam strut extended from the top of the beam chord at the column face at an angle of θ with the horizontal direction. The shear in the joint is calculated by the formula that is previously used in all models in the exterior beam column joints.

$$V_j = T_{bb} - V_{ct} = C_{be} - V_{cb} \qquad (4.24)$$

where

T_{bb} is the total force in the beam bars,

C_{be} is the force in the beam's compression chord,

V_{ct} is the shear force in the column above the joint; in the present tests R_t+F, R_t being the reaction at the horizontal support of the column above the joint and F the friction force developed at the top of the column, when a vertical load was applied before the beam loading,

V_{cb} is the shear force in the column below the joint and in the present tests equals the reaction at the horizontal support of the column below the joint.

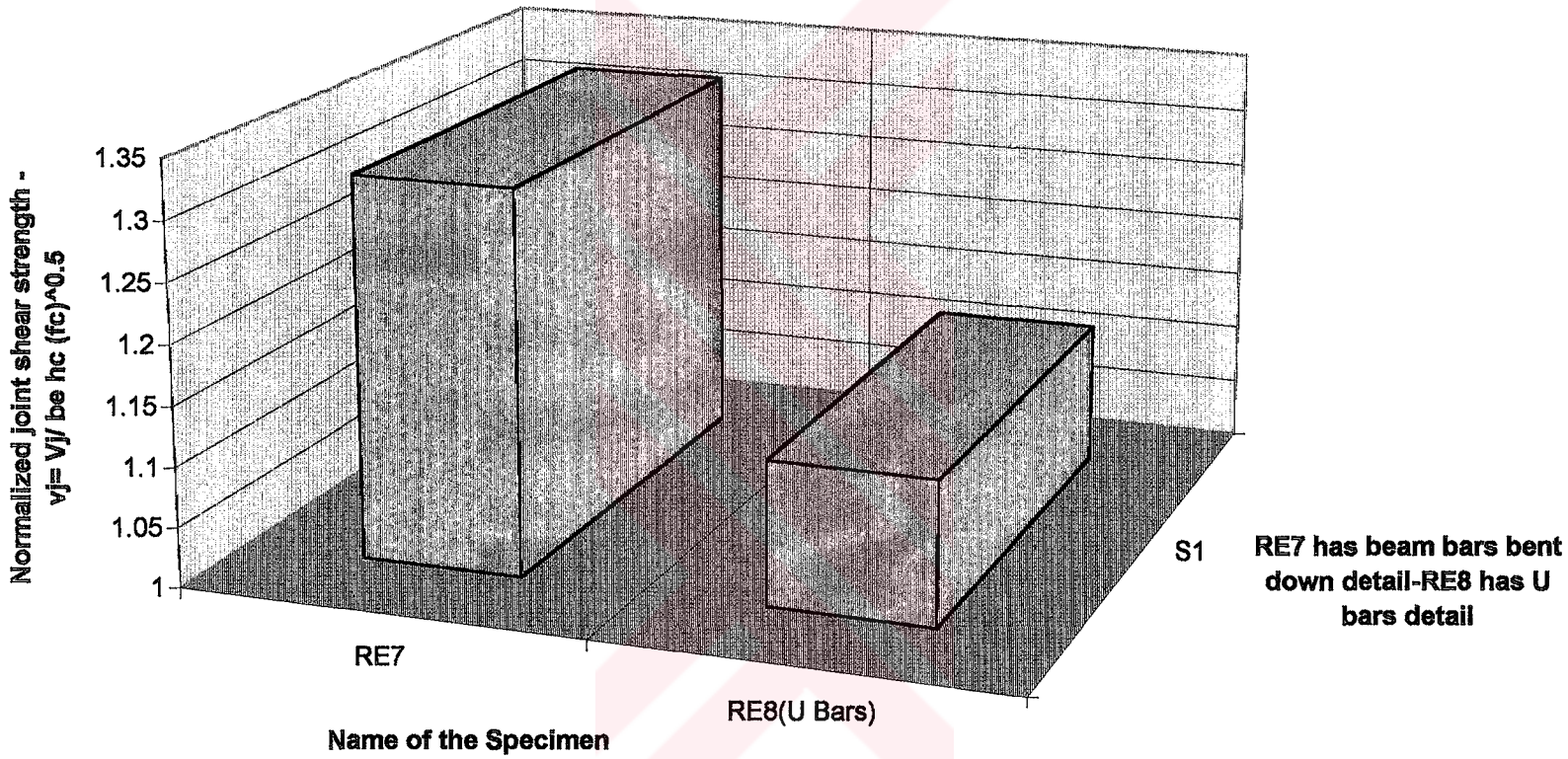

Figure 4.33 The normalized joint shear strength of identical specimens with different beam bar detailing

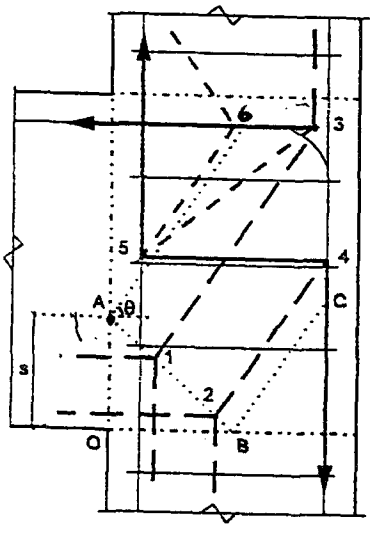

Figure 4.34 : Micromodel of Ortiz.

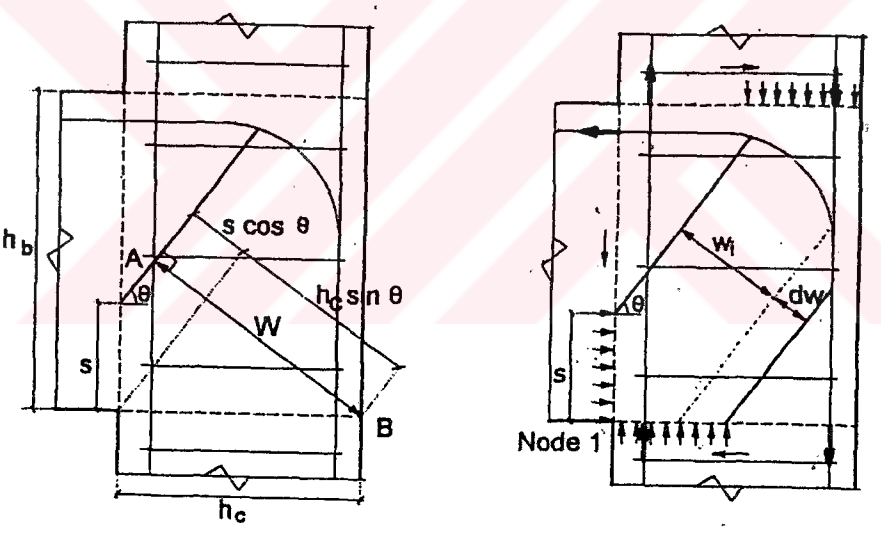

Figure 4.35 : Simplified macromodel of Ortiz.

4.4.1.1.3. Cracking Analysis

As all the previous models, this model determines the forces in the bars and the compressive chord of the column and beam sections that are close to the joint by means of iterative methods. The concrete and steel stress-strain diagrams that are depicted in Figure 4.36 are taken into account throughout the design. For the cracking analysis, the model adapts Taylor's approach. The average stress is thus:

$$v_{cr}=0.67\sqrt{(f_{ct}^{2}+\sigma_c f_{ct}+\sigma_b f_{ct})} \qquad (4.25)$$

where

f_{ct} is the tensile strength of the concrete

σ_c is the normal stress in the column

σ_b is the normal stress in the beam provided by the beam thrust.

The satisfactory correlation between the shear at cracking determined by Taylor's approach and the shear at cracking during the test proved that Taylor's approach was very good at predicting the shear at cracking.

4.4.1.1.4. Vertical Shear

As in all other previous models, the forces acting at the boundary of the D region of the joint, has to be determined. As stated previously, this procedure is highly iterative. Linear stress distribution is considered throughout this iterative procedure. The vertical resultants of the beam shear force and the column forces in each side of the joint F_v are

$$F_v=F_{ti}+F_{bi}+C_{cb}-V_{be}=F_{te}+F_{be}+C_{ct} \qquad (4.26)$$

where F_v is the vertical shear in the joint,

F_{ti} is the force in the bars in tension

F_{bi} is the force in the bars in compression in the bottom column

C_{cb} is the force in the concrete strut in the bottom column,

V_{be} is the shear force in the beam

F_{te} is the force in the bars in compression

F_{be} is the force in the bars in tension

C_{ct} is the force in the concrete strut

Ortiz names the angle between the diagonal strut and the horizontal direction as θ, and the diagonal force is named as D. The height of node 1 is assumed to be equal to the beam chord depth s. Figure 4.37 defines the diagonal strut.

4.4.1.1.5. Equilibrium and The Angle of Inclination

The equilibrium is fulfilled by the following equations.

$$D \sin\theta = F_v \quad (4.27)$$

$$D \cos\theta = V_j \quad (4.28)$$

where D is the total force in the diagonal strut.

F_v is the vertical force introduced at each side of the joint.

V_j is the joint shear force.

In other words θ can be determined as;

$$\theta = \arctan (F_v / V_j) \quad (4.29)$$

4.4.1.1.6. The Width of the Direct Strut

The diagonal strut width w_i is the strut width when the connection does not have any transverse reinforcement. The value of w_i was determined by Ortiz so that it could fit the experimental results on joints without stirrups.

$$w_i = 0.45\ W \quad (4.30)$$

$$W = h_c \sin\theta + s\cos\theta \quad (4.31)$$

W is the maximum width available for the strut inside the joint. It is the distance from point B to the upper side of the strut. This W is a geometric limit and depends on the dimensions of the joint.

4.4.1.1.7. The Axial Force in the Diagonal Strut

Near failure the joint is cracked and the force D carried by the diagonal strut is taken as:

$$D = \alpha_2 f_c b_c w \quad (4.32)$$

where $\alpha_2 = 0.6 (1 - f_c / 250)$; b_c is the column width;w is the strut width.

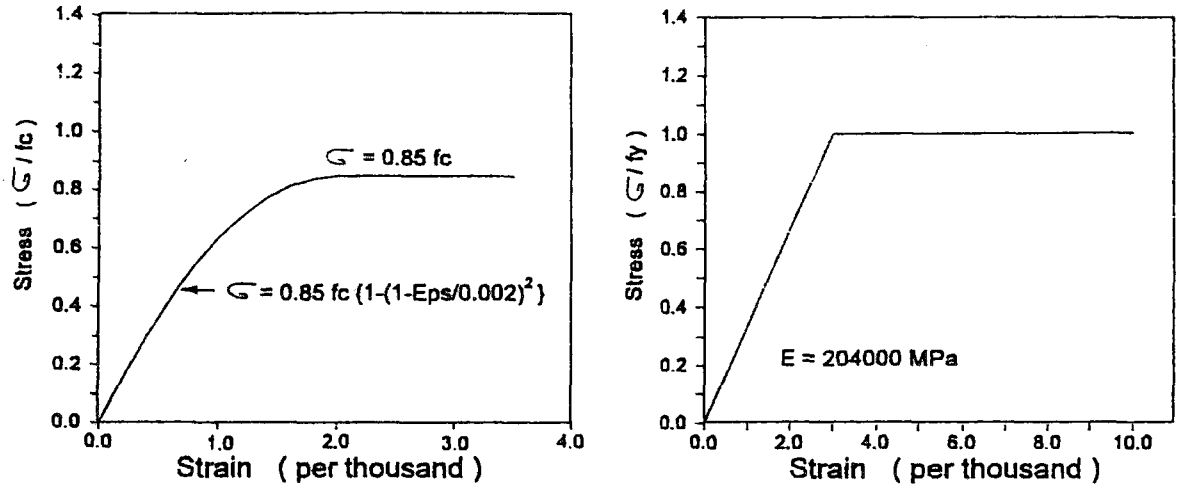

Figure 4.36 : The concrete and steel stress strain diagrams.

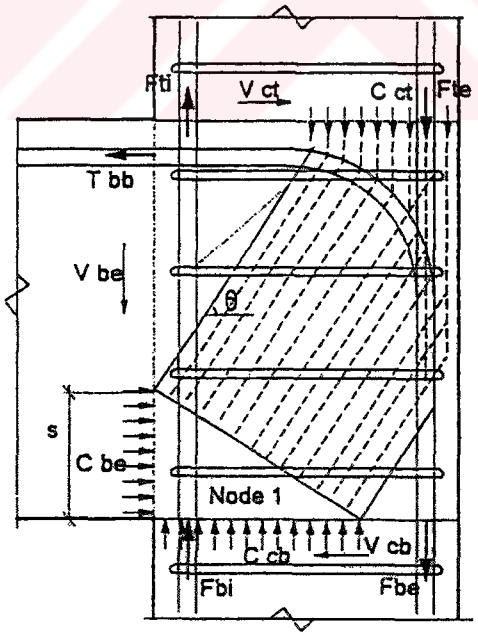

Figure 4.37 : The diagonal strut definition.

Ortiz states that the stress distribution on the cross section of the strut is not uniform, but for simplification, she has preferred to assume it so throughout the area $b_c w$ of the strut.

4.4.1.1.8. The Width of the Indirect Strut

In joints with stirrups, she chooses to increase the strut width by an amount of δw which corresponds to the increase in shear force $\delta V_j = \delta D \cos\theta$ provided by the stirrups, that equals the force they are able to resist with the total area As and tensile strength f_y.

$$\delta V_j = T_s = A_{sv} f_y = \delta D \cos\theta \quad (4.34)$$

$$D+\delta D = \alpha_2 f_c b_c (w+\delta w) = D + A_{sv} f_y / (\cos\theta) \quad (4.35)$$

Therefore the total strut width is:

$$w = 0.45 W + A_{sv} f_y /(\cos\theta \alpha_2 f_c b_c) < W \quad (4.36)$$

$T_s = A_{sv} f_y$ is the force resisted only by the stirrups that are placed between the beam longitudinal reinforcement and the beam chord.

4.4.1.1.9. The Joint Failure Load

The joint failure load is then,

$$V_{ju} = w \cos\theta \alpha_2 f_c b_c \quad (4.37)$$

$$V_{ju} = 0.45 W \cos\theta \alpha_2 f_c b_c + A_{sv} f_y \quad (4.38)$$

Where $A_{sv} f_y < \alpha_2 f_c b_c 0.55 W \cos\theta$

4.4.1.1.10. Design Method

The angle of inclination of the diagonal strut is determined from the following equation;

$\theta = \arctan (F_v / V_j)$

where $V_j = T_{bb} - V_{ct} = C_{be} - V_{cb}$

$F_v = F_{ti} + F_{bi} + C_{cb} - V_{be} = F_{te} + F_{be} + C_{ct}$

The necessary strut width should be determined bearing in mind that the strut force must equal the shear force introduced in the joint.

$w = D/(\alpha_2 f_{cd} b_c) = V_j /(\alpha_2 f_{cd} b_c \cos\theta) \leq W$

The required w must be compared to the maximum W given by the following equation.

$W = h_c \sin\theta + s \cos\theta$

If w >W, the design must be reviewed.

$Vj/(\alpha_2 f_{cd} b_c \cos\theta) = 0.45\ W + A_{sv} f_y/(\alpha_2 f_{cd} b_c \cos\theta)$

4.4.1.1.11. The Micro -model of Ortiz

We need three data to sketch the strut and tie model of Ortiz. These are; the depth of the beam chord s; the angle of inclination of the strut (θ); the strut width defined as:

$0.45\ W + A_s f_y /(\alpha_2 f_c b_c \cos\theta)$

4.4.1.1.12. The procedure followed in micro model

From the top of the beam chord (point A), sketch a line with an angle equal to the angle of inclination of the direct strut as shown in Figure 4.34. Draw a parallel line at a distance w from the first line. Find point B, which is the intersection point of the perpendicular line to the border of the direct strut with the border of the bottom column. Draw the line of action the direct strut at a distance of half w_i from the first line. Draw the line of action of the secondary strut at a distance of half δw_i from line BC. Ortiz states that AOB triangle shown in Figure 4.34 is the main node in the model.

4.4.1.1.13. Application of the Model on Experiments

The author of this thesis applied Ortiz model on the test data, published after Ortiz completed her Ph.D and predicted the failure loads by Ortiz model. The tests used are the tests of Scott and Hamill, and the tests of Parker and Bullman. The characteristics of the test specimens are shown in the following tables.

4.4.1.1.14. Comments on Ortiz Model by the Author

1. There is a clear inconsistency in the load paths of the macro and the micro models regarding the upper node. It is not clear how the upper node is equilibrated in the

macro model. But from Figure 4.35, it seems that both the truss and the strut mechanism are equilibrated by the upper compressive rectangular stress block. In the micro model on the other hand, it is demonstrated clearly that the force in the top secondary strut is equilibrated in the upper region of the joint by another strut coming from the upper column. There is a clear inconsistency in the definition of the top node and the equilibrating mechanisms in the micro and macro models.

Table 4.32. The predicted failure loads of Ortiz's tests

Specimen	Detailing	Actual Failure Mode	Predicted Failure Mode	Cylinder Strength	Ppred/Pfail
Units	-	-	-	**MPa**	-
Ortiz					
BCJ1	L Bar	JS	JS	33.8	0.949
BCJ2	L Bar	JS	JS	37.8	1.152
BCJ3	L Bar	JS	JS	33	0.898
BCJ4	L Bar	JS	JS	34	1.184
BCJ5	L Bar	JS	JS	37.9	1.026
BCJ6	L Bar	JS	JS	35	1.026
BCJ7	L Bar	B	B	35	1.015
				Average wos	1.010
				Averagews	1.061
				Total Average	1.035

2. Ortiz in her micro model shows a secondary strut coming from the upper column however she does not take into account that this secondary strut coming from the upper column also resists the joint shear. If that strut is there, its contribution to the joint shear resistance should be taken into account.

Table 4.33. The predicted failure loads of Parker & Bullman's tests

Specimen	Detailing	Actual Failure Mode	Predicted Failure Mode	Cylinder Strength	Ppred/Pfail
Units	-	-	-	**MPa**	-
Parker & Bullmann					
4a	L Bar	CF	C	39.2	1.720
4b	L Bar	J	J	39.2	1.507
4c	L Bar	J	J	36.8	0.940
4d	L Bar	J	J	39.2	1.408
4e	L Bar	J	J	40	1.400
4f	L Bar	J	J	37.6	0.928
				Average	1.317
5a	L Bar	C	B	42.4	1.626
5b	L Bar	JS	B	43.2	1.478
5c	L Bar	B	B	43.2	1.440
5d	L Bar	C	C	43.2	1.540
5e	L Bar	C	C	44.8	1.278
5f	L Bar	C	C	43.2	1.229
				Average	1.430
				Total Average	1.374

3. She suggests that the maximum width available for the strut inside the joint is

$W = h_c \sin\theta + s \cos\theta$

This geometrical limit suggested by Ortiz is clearly incorrect. The geometrical limit to the width of the strut can only be constrained by the widths of the compressive stress blocks of the beam and the column. Otherwise equilibrium of the joint will be destroyed because there is no compressive force to equilibrate the diagonal force in the strut outside the compressive stress block of the lower column.

Table 4.34.The predicted failure loads of Scott & Hamill's tests

Specimen	Detailing	Actual Failure Mode	Predicted Failure Mode	Cylinder Strength	Ppred/Pfail
Units	-	-	-	MPa	-
Scott & Hamill					
C4ALN0	L Bar	P	J	42.4	0.940
C4ALN1	L Bar	J	J	45.6	1.014
C4ALHO	L Bar	P	B	104	1.497
C4ALH1	L Bar	B	B	95.2	1.430
C6LH0	U Bar	J	J	100.8	1.110
C6LN1	U Bar	J	J	101.6	1.626
C6LN0	U Bar	J	J	51.2	1.460
C6NL3	U Bar	JS	B	48.8	1.620
C6NL5	U Bar	JS	B	36.8	1.250
C6LH3	U Bar	JS	B	96.8	1.519
C4ALN3	L Bar	J	J	41.6	1.264
C4ALH3	L Bar	B	B	105.6	1.410
C6LH5	U Bar	B	B	100	1.235
C4ALN5	L Bar	JS	B	50.4	1.190
C6LH1	L Bar	JS	B	101.6	1.725
C4ALH5	L Bar	B	B	98.4	1.295
			Average wos		1.350
			Average ws		1.540
			Total Average		1.349

Notes for Table 4.34:

1. The following abbreviations are used for the failure modes.

B : Beam failure

JS: Joint shear failure

P : Beam bar pullout

4. She assumes that all the stirrups yield at failure, which is not true. Even Ortiz test results reveal that in her specimen BCJ7, not all the stirrups yield. The product $A_{sv} f_y$ can only be an upper bound of the contribution of the secondary strut to the joint shear. Because of this, her model incorrectly predicts that all the specimens of Scott and Hamill, which have more than one stirrup except C4ALN3, exhibit beam flexural

failure. Table 4.34 can be referred to for these incorrect predictions of the failure modes.

5. The angle of inclination θ is accepted as the ratio of the total vertical shear to the total horizontal shear. This assumption can lead to illogical results. F_v and V_j are the total vertical and horizontal shears correspondingly. V_j is in reality, the summation of the horizontal component of the axial force in the primary strut to the force in the stirrups, which should be calculated, from the strains in the stirrups at failure. The relative contributions of the strut and truss mechanisms have different values for their contributions to the vertical shear and the horizontal shear. The above argument leads us to think that the angle of inclination predicted by Ortiz model does not reflect the actual magnitude of the angle of inclinations of the strut and truss mechanisms.

6.The secondary strut, in Figure 4.34, extending from point 5 to 3 is meaningless. There is no proof or reason that the secondary strut extending from point 3 to 5 will intersect with the primary strut and the upper column longitudinal reinforcement.

7.The model predicts the failure modes and failure loads incorrectly. The average ratio of the predicted failure loads to the actual failure loads is greatly overestimated for the specimens of Scott and Hamill and Parker and Bullman. As stated previously, the failure modes are usually predicted as beam flexural failure for specimens with more than one stirrup because the model overestimates the contribution of the joint stirrups to the shear strength of exterior beam column connections. This results in the overestimation of the failure loads in joints with stirrups in Scott and Hamill, Parker and Bullman tests.

8.Ortiz model of strut and tie has the advantage of being simpler than the models of Ichinose and Vollum.

9.In all the strut and tie models, in order to find the stress and the load paths in the D regions, firstly the forces at the boundary of these non-uniform stress fields should be determined. This would to a great extent help us in developing a good strut and tie model. The above argument implies that if the D region to be analyzed is a joint, then the forces in the beam and the columns, which are adjacent to the joint, should be

considered. This would eventually lead the designer to relate the struts and ties in the joint to the compressive stress blocks and tensile stress fields in the columns and the beam. However Ortiz does not make any effort to relate the struts of her model to the compressive stress blocks in the columns above the joint.

10. She without checking assumes that failure occurs in the direct strut rather than the nodes. However it is commonly known in structural engineering that the most prone regions to failure are the most stressed regions. This would lead us to think that failure would occur in the top node, which are the most stressed node rather than the direct strut. Therefore the width adapted for the failure analysis should be the width of the compressive stress block of the upper column. Vollum makes similar remarks.

11.She does no effort to analyze the top and bottom node. She also does not give the geometry of these.

12. The micro strut and tie model she suggests is also obscure. The geometries of the so-called secondary struts and their angle of inclination and their effect on the behavior of the joint is not clear. It is not easy to understand why they are there.

13.It is experimentally proved by many researchers including Ortiz that the bar forces and the concrete compressive force in the upper column shifts to the tension side from that of the calculations performed based on the hypothesis of plane sections remain plane. This redistribution is also mentioned by Vollum (1998) The tensile shift in the upper column bar and concrete compressive forces are not taken into account in Ortiz model.

14.Most importantly, she assumes in her macro model that the angle of inclination of the direct and indirect struts are same. But in her micro model she assumes that they are different. If the angle of inclination of the direct and indirect struts is same as proposed by her macro model, she should have demonstrated clearly how this force is equilibrated in the vertical direction.

4.4.1.1.15. The Parametric Studies on Ortiz Model

This section investigates the influence of the parameters including concrete cylinder strength, column axial load, joint aspect ratio and column longitudinal reinforcement ratio on Ortiz model of strut and tie. In the preceding sections, the author had criticized the theoretical inconsistencies of the model. In this paper, the influence of the parameters that are counted above are investigated in two parts: one for joints without stirrups and the other for joints with stirrups.

The model of Ortiz was applied on the test specimens of Scott and Hamill and Parker and Bullman and criticized in full detail in the first paper of this section. In this section, the effect of the various parameters including the concrete cylinder strength, column axial load, joint aspect ratio and column bar ratio on Ortiz model will be investigated. The effect of each parameter will be investigated for both the joints with and without stirrups.

4.4.1.1.15.1.Analysis of tests

The author investigated the influence of parameters such as column longitudinal reinforcement ratio, concrete cylinder strength, column axial stress and the joint aspect ratio in the preceding sections. She found that these parameters influenced the behavior of exterior beam column connections as below:

1. The column longitudinal reinforcement ratio did not affect the normalized joint shear strength.
2. The normalized joint shear strength increased when the joint aspect ratio decreased.
3. The joint shear strength increased proportional to the square root of the concrete cylinder strength.
4. The joint shear strength was independent of the column axial stress.

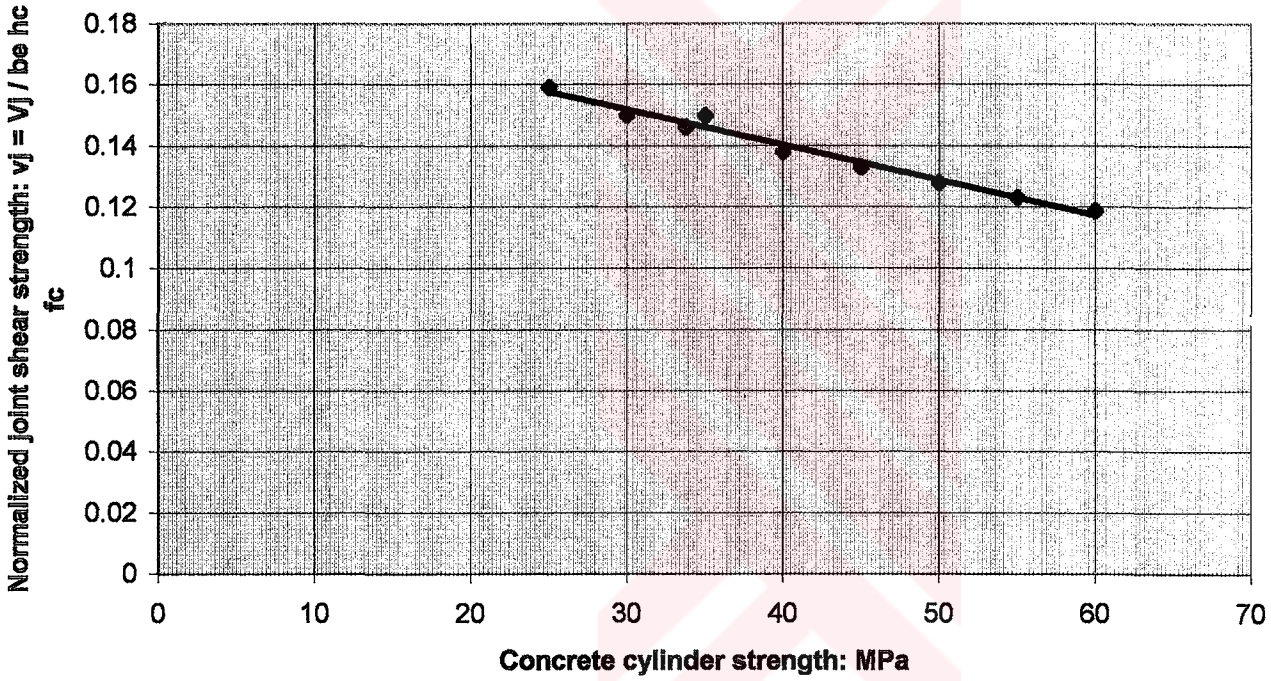

Figure 4.38. The effect of concrete cylinder strength on the predicted normalized shear strength of Ortiz model without stirrups

4.4.1.1.15.2. Joints without Stirrups

A joint very similar to the specimen BCJ1 of Ortiz is investigated. The specimen has no stirrups and no column axial stress. The parameters to be investigated are column axial stress, column longitudinal reinforcement ratio, concrete cylinder strength and the joint aspect ratio.

4.4.1.1.15.3. Influence of Concrete Cylinder Strength in Joints without Stirrups

The author investigated the influence of concrete cylinder strength for concrete cylinder strengths of 25 to 60 MPa. The results are shown in Figure 4.38. The model incorrectly predicts that the normalized joint shear strength decreases with increasing concrete cylinder strength. This can be due to the normalization process. The author found out that the average of the normalized joint shear strengths for Ortiz specimens shows the following trend:

$V_j / b_c h_c f_c = 0.154$

Therefore we can state that the normalized joint shear strength increases with the concrete cylinder strength.

4.4.1.1.15.4. Influence of Column Axial Stress in Joints without Stirrups

The author investigated the effect of the column axial stress on the normalized joint shear strength predicted by Ortiz model. The normalized column axial stresses ($=N / b_c h_c f_c$) investigated were between 0 to 0.25. The results are shown in Figure 4.39. They show that the model incorrectly predicts a decrease in the normalized joint shear strength with increasing normalized column axial stress. In reality the joint shear strength is independent of the column axial stress.

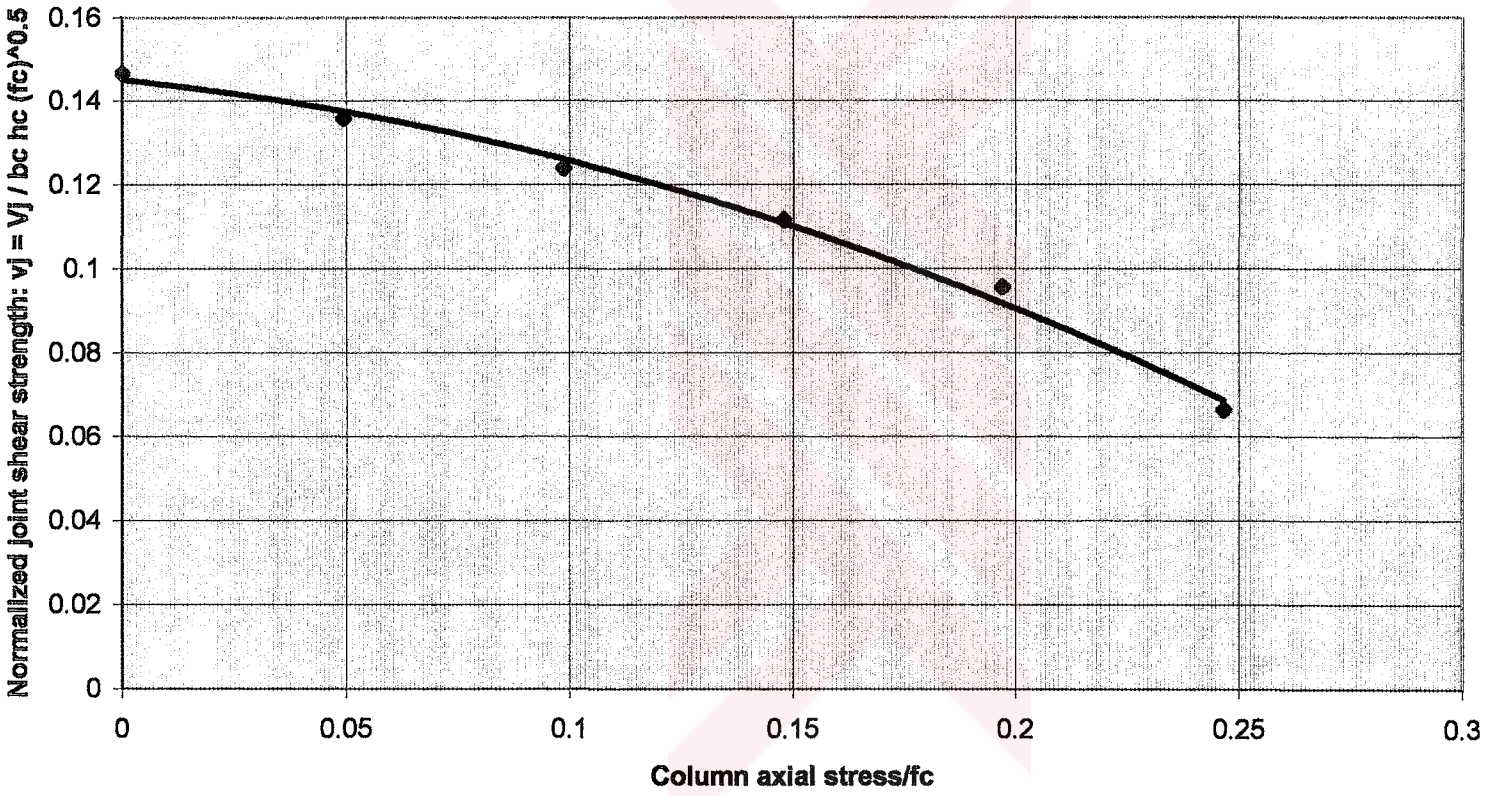

Figure 4.39 The effect of column axial stress on the normalized joint shear strength predicted by Ortiz model for joints without stirrups

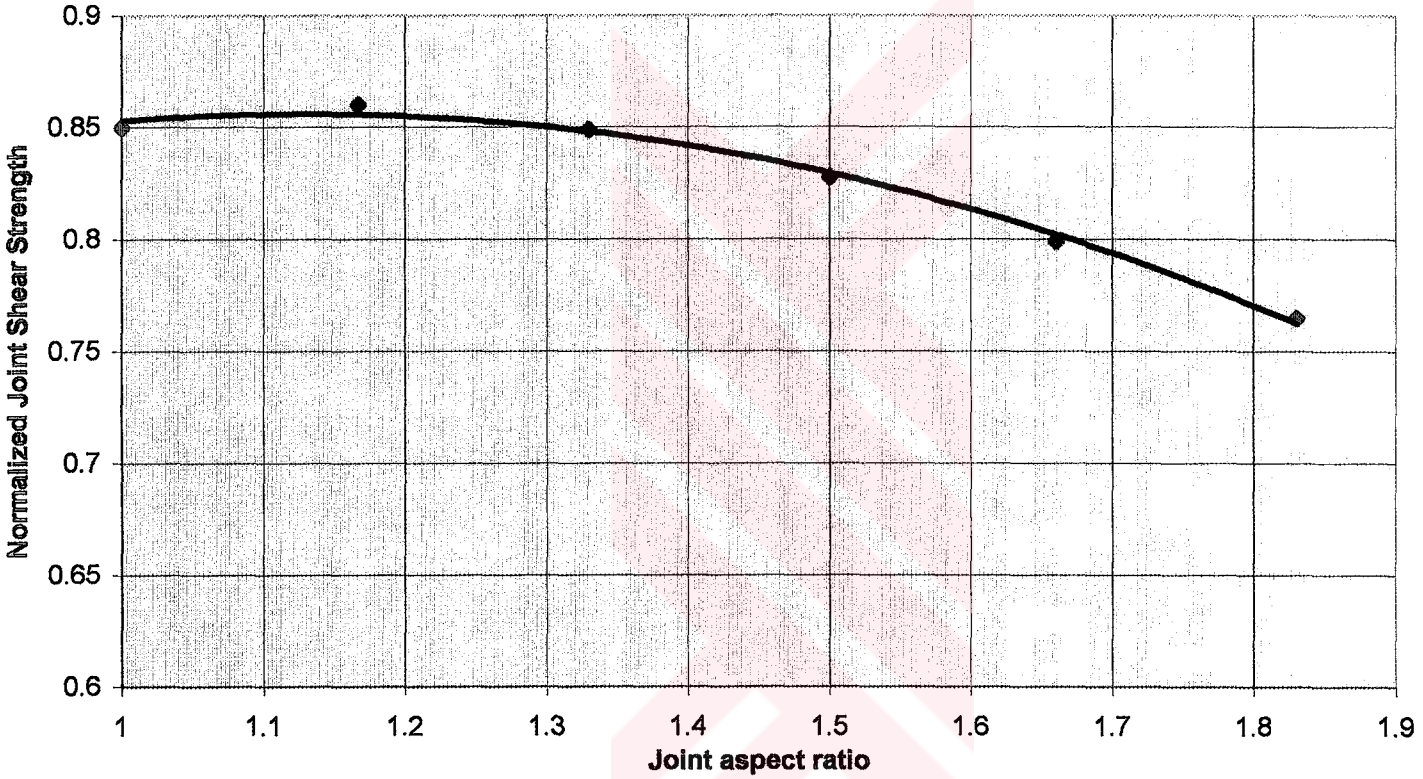

Figure 4.40 The influence of joint aspect ratio on the normalized joint shear strengths predicted by Ortiz model without stirrups

4.4.1.15.5. Influence of Joint Aspect Ratio in Joints without Stirrups

Figure 4.40 shows that the model predicts a decrease in the normalized joint shear strength with increasing joint aspect ratio. This is consistent with the parametric study of authors given in Figure 4.26d.

4.4.1.15.6. Influence of Column Longitudinal Reinforcement Ratio in Joints without Stirrups

The author investigated the normalized joint shear strength of a specimen similar to BCJ1 of Ortiz for different column longitudinal reinforcement ratios. The results are given in Figure 4.41. It is clear from the figure that the model predicts an increase in the normalized joint shear strength with increasing column bar ratio. It is apparent that Ortiz model contradicts with the parametric studies of authors given in Figure 4.26b regarding the influence of the column longitudinal reinforcement ratio. As apparent from Figure 4.26b, the joint shear strength is independent of the column longitudinal reinforcement ratio.

4.4.1.15.7. Joints with Stirrups

The author investigated a specimen similar to BCJ4 of Ortiz.

4.4.1.15.7.1. The Effect of Concrete Cylinder Strength in Joints with Stirrups

The author investigated the effect of concrete cylinder strength on the normalized joint shear strength of joints with stirrups. The range of concrete cylinder strengths was from 25 MPa to 60 MPa. (Please refer to Figure 4.43)

Figure 4.43 clearly shows that likewise the joints without stirrups, there is a clear contradiction with the model's predictions and the test results. Figure shows that the model predicts a decrease in the normalized joint shear strength of exterior beam column connections with increasing concrete cylinder strength.

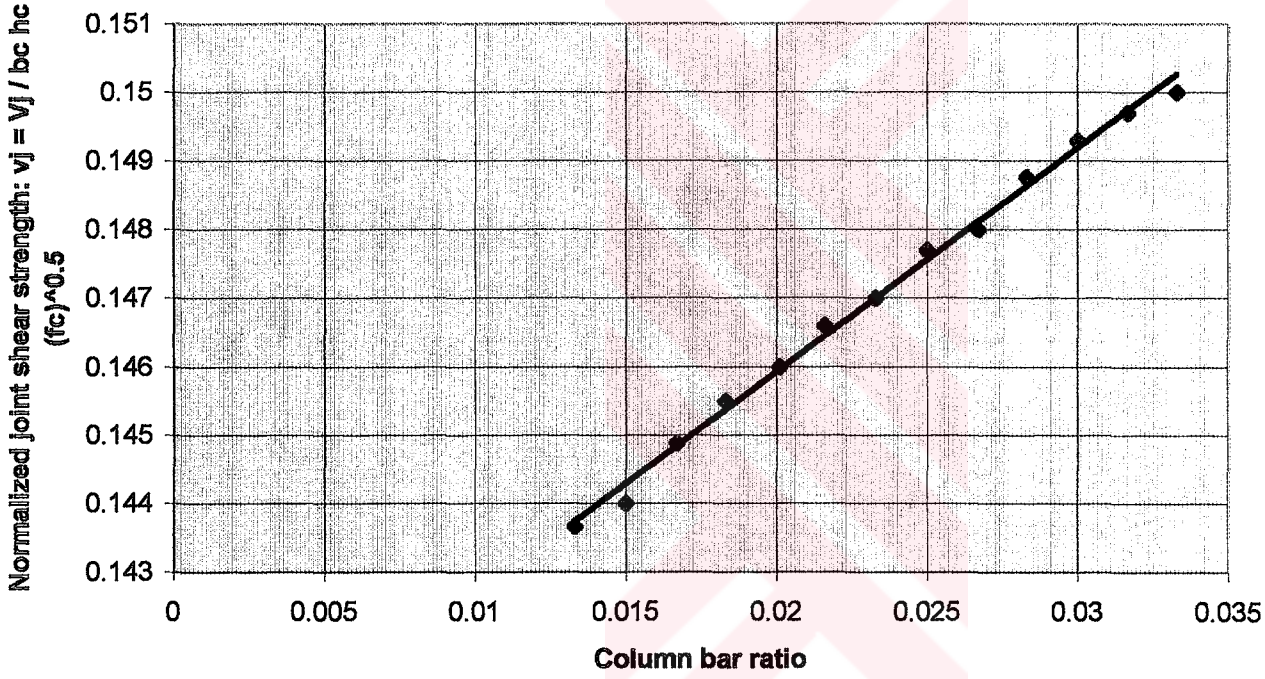

Figure 4.41. The effect of the column bar ratio on the normalized joint shear strength predicted by Ortiz model

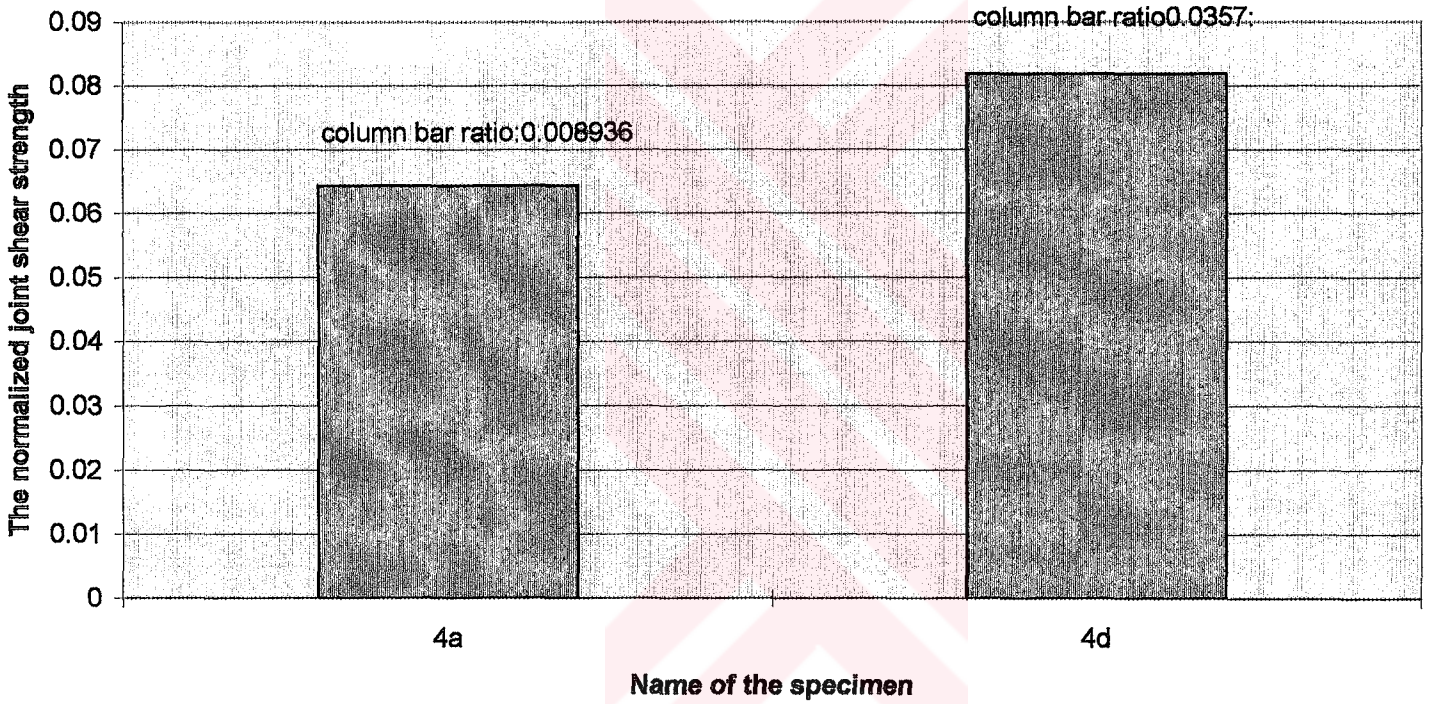

Figure 4.42. The influence of column bar ratio on the normalized joint shear strength

4.4.1.15.7.2. The Effect of Column Axial Stress in Joints with Stirrups

The author made a parametric study to investigate the effect of normalized column axial stress on the normalized joint shear strength as shown in Figure 4.44. The model predicts that the normalized joint shear strength decreases with increasing column axial stress. As apparent, **Ortiz** model contradicts with the parametric study of authors given in Figure 4.29.

4.4.1.15.7.3. The Effect of Joint Aspect Ratio in Joints with Stirrups

The effect of the joint aspect ratio on the predicted normalized joint shear strength of exterior beam column connections is determined for aspect ratios between 1 and 2. The results can be viewed in Figure 4.45. The results of the tests had showed that the normalized joint shear strength increases with decreasing joint aspect ratio. **Ortiz** model's predictions are in agreement with the parametric study of the authors given in Figure 4.26d.

4.4.1.15.7.4. The Effect of Column Longitudinal Reinforcement Ratio in Joints with Stirrups

The author investigated the influence of column bar ratio on the predicted joint shear strength by **Ortiz** model in Figure 4.46. **Ortiz** model predicts an increase in the normalized joint shear strength with increasing column longitudinal reinforcement ratio. Thus, the model is in contradiction with the parametric study of the authors given in Figure 4.26 b.

4.4.1.15.8. Results

The influence of the parameters such as the normalized column axial stress, joint aspect ratio, column longitudinal reinforcement ratio and concrete cylinder strength on the normalized joint shear strength of exterior beam column connections predicted by **Ortiz** model are investigated in this section for joints with and without stirrups. The results of the analysis shows that the model's predictions regarding the effect of the column axial stress, concrete cylinder strength and the column

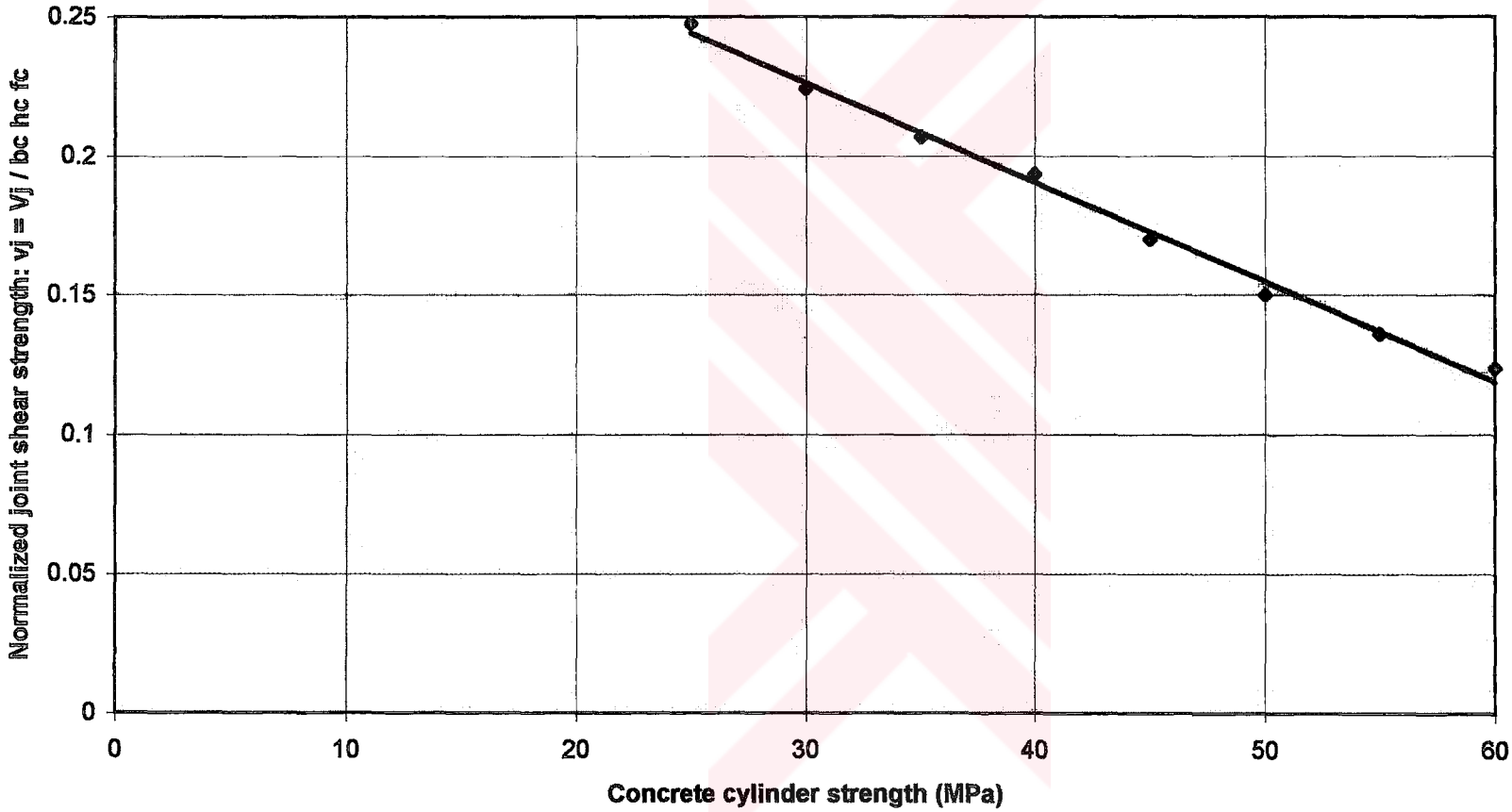

Figure 4.43. The effect of concrete cylinder strength on the normalized joint shear strength of joints with stirrups predicted by Ortiz model

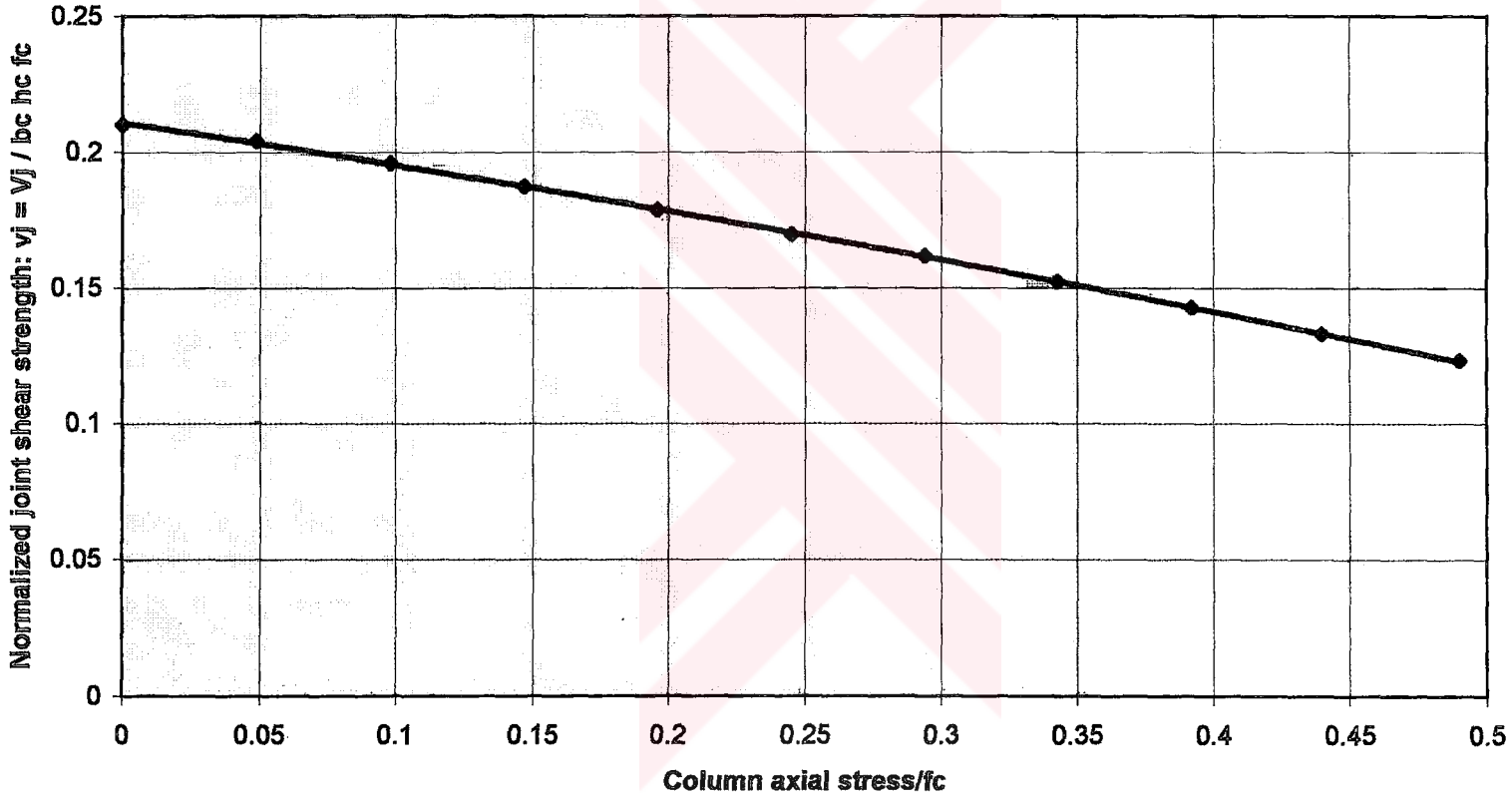

Figure 4.44. The effect of column axial stress on the normalized joint shear strength of exterior beam column connections predicted by Ortiz model

longitudinal reinforcement ratio do not agree with the test results, while the joint aspect ratio are in agreement with what is obtained from tests. The above investigation showed that the possible reasons for the incorrect predictions of the model could be attributed to the fact that the model does not take into account the actual width of the strut which is related to the width of the upper and lower column's concrete compressive stress blocks but instead uses a value which is presumably taken from the results of the experiments.

4.4.1.2. The Strut and Tie Model of Vollum

4.4.1.2.1. Introduction

Vollum suggests the most powerful model. His model is in fact identical to the fan mechanism proposed previously by **Fuji and Morita**. Figure 4.47 shows the model of **Vollum**. The details of the model of **Vollum** will not be given here. Interested readers are encouraged to refer to his doctoral thesis.

Comments on Vollum's model by the author:

The author of this thesis wrote a computer program to evaluate the model of **Vollum** given in Appendix A. The key objection to **Vollum** model is that it is very complex. Designers will only use a strut and tie model because it is simple and therefore more advantageous than non-linear finite element analysis. However, a model like **Vollum**'s, although it is said to give excellent predictions of failure load and superb results of parametric studies comparing the model in various ways to the experimental results, has the disadvantage of defeating the purpose of doing a strut and tie analysis in the first place because of its complexity.

In joints with stirrups, the model of **Vollum** predicts that joints fail not by the failure of the fan mechanism **Vollum** proposed, but by the joint shear reaching two upper limits. If the criterion for failure is so simple, why would a designer use so complex procedures suggested by **Vollum**?

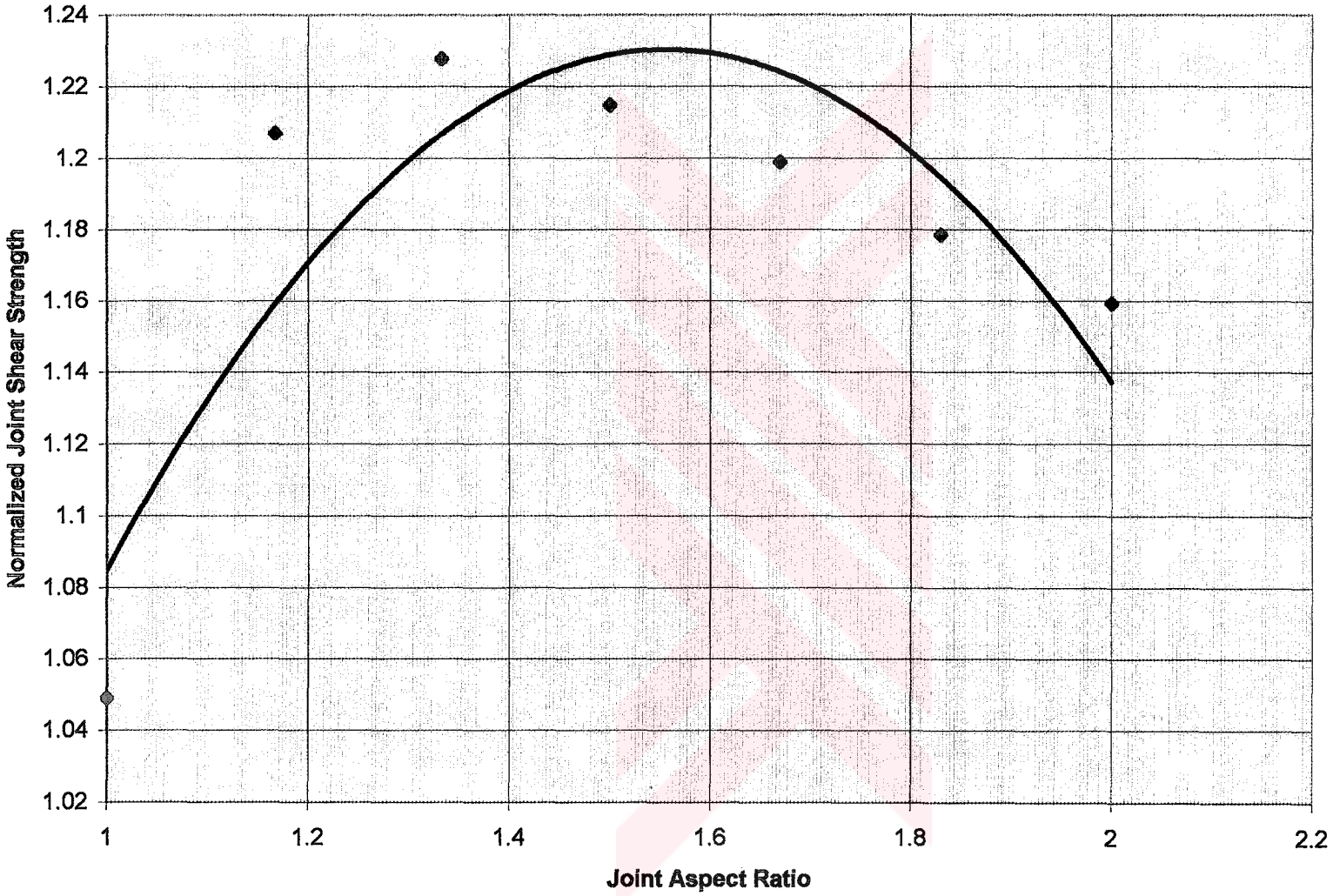

Figure 4.45. The influence of joint aspect ratio on the predicted joint shear strength of Ortiz model with stirrups

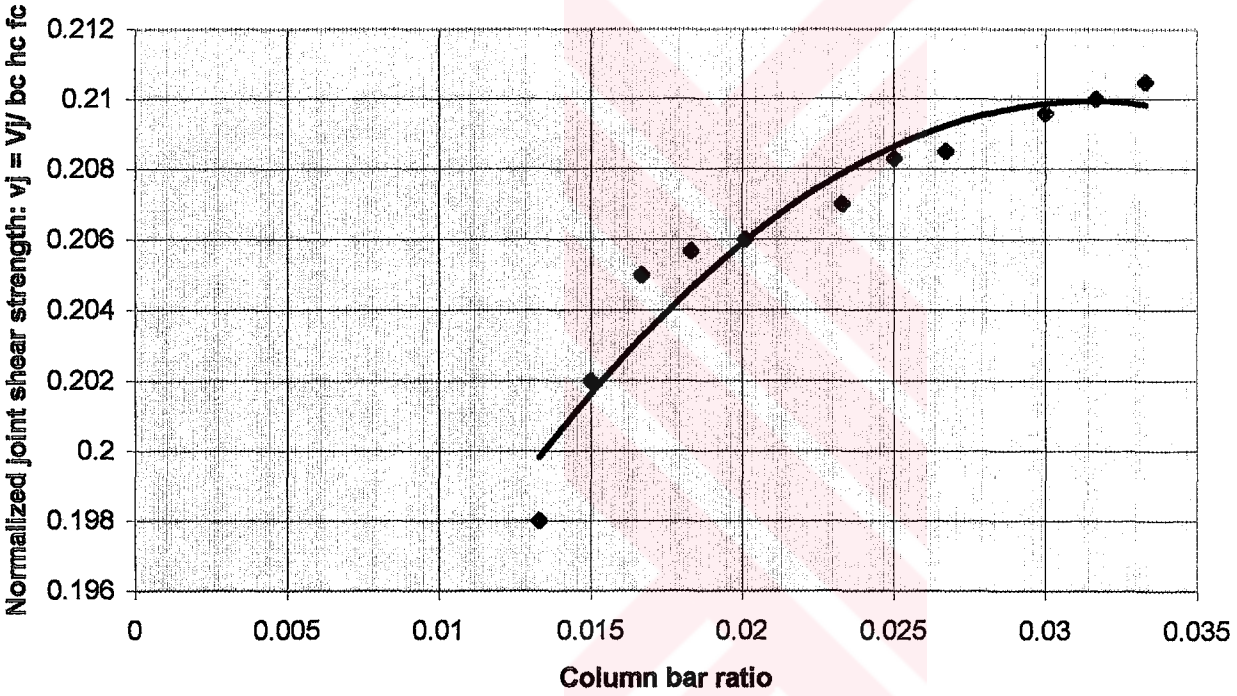

Figure 4.46. The effect of column bar ratio on the normalized joint shear strength of joints with stirrups predicted by Ortiz model

4.5.Overview of the design equations suggested for exterior beam column connections

The author, in this section, will review the previous empirical design equations suggested for monotonically loaded exterior beam column connections 4.5.1. Finally a comparison between the existing design equations and the author's design equation will be made.

4.5.1. The Empirical Equation of Sarsam and Phillips

Sarsam and Phillips (1985) proposed the following equation for the design of exterior beam column connections.

$$V_{col} = 5.08\ (f_{cu}\ \rho_c\ )\ 0.33\ (d_c/d_b)\ 1.33\ (1+ 0.29\ N_u / A_g)^{0.5}\ b_c\ d_c \qquad (4.38)$$

where:

$\rho_c = A_{so} / b_c\ d_c$

A_{so} is the area of the layer of steel furthest from the maximum compression face in a column.

A_g is the gross cross-sectional area of the column at the joint.

N_u is the axial column load.

The shear force resisted by the links is taken as :

$$V_{sd} = 0.87\ A_{js}\ f_{yv} \qquad (4.39)$$

$$V_{ud} = V_{cd} + V_{sd} \qquad (4.40)$$

All the joint stirrups are considered to be effective in increasing the joint shear capacity.

Sarsam and Phillips proposed the following upper limits:

$$\rho_c \leq 0.02 \qquad (4.41)$$

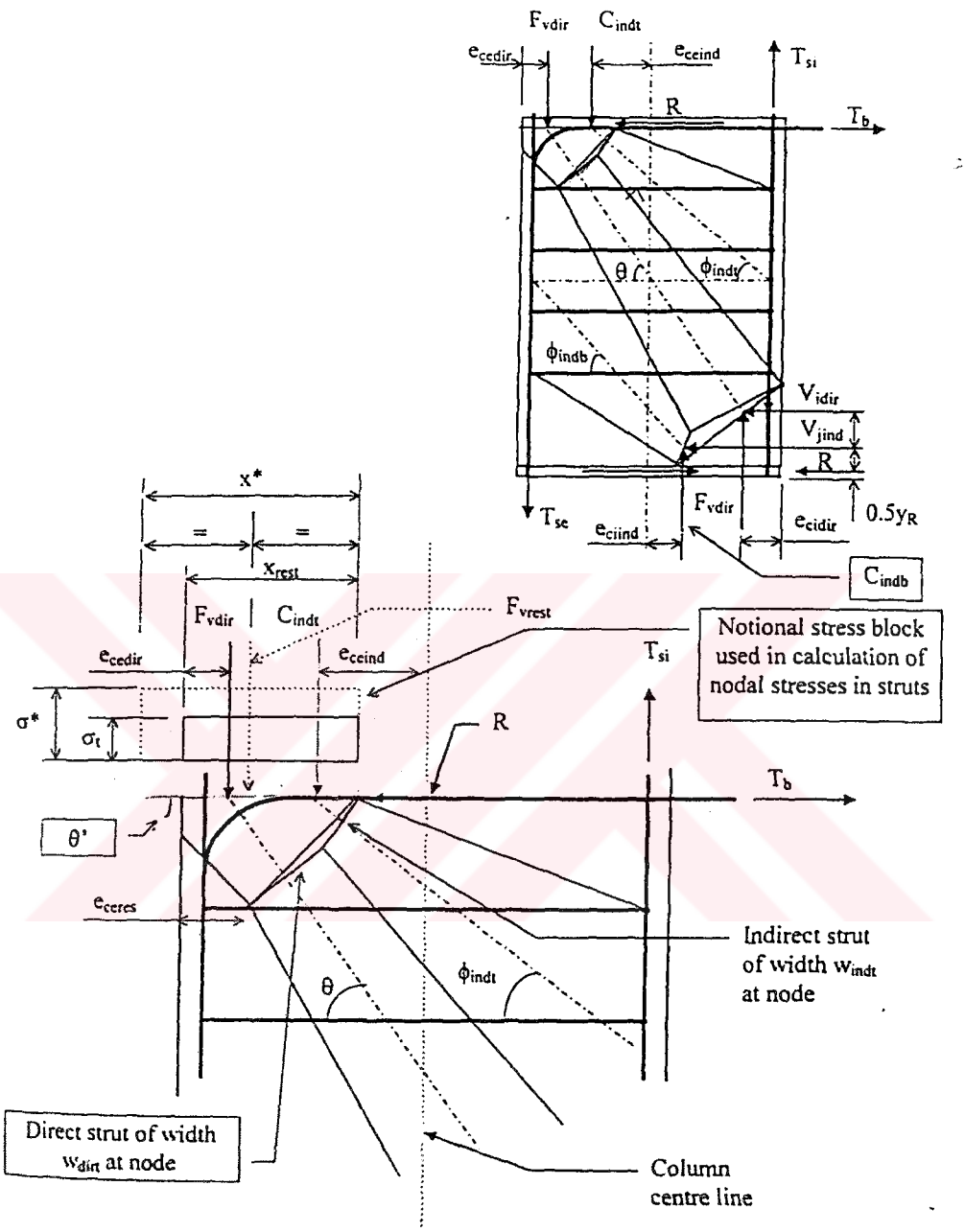

Figure 4.47 : The model of Vollum.

$$N_u / A_g \leq f_{cu} /3 \quad (4.42)$$

$$V_u \leq 2.4 \, (fcu)^{0.33} \, b_c \, d_c \text{ with } f_{cu} \leq 70 \text{ MPa} \quad (4.43)$$

Sarsam and Phillips suggest that, to allow for the effects of strain hardening, the design joint shear force should be higher than:

$$V_{ud} = 1.25 \, V_y \quad (4.44)$$

where; V_y is the joint shear force corresponding to yielding of beam reinforcement. **Sarsam and Phillips** suggested that the column ties should be placed at the same spacing with the joint ties in the upper and lower column. They also suggested that diagonal hairline cracking is allowable in the joint because it is a sign that the joint is loaded and this kind of cracking does not represent flexural cracking in beams. They comment that only structures with special requirements should be designed for no diagonal cracking in joints.

4.5.1.1. Comments on Sarsam and Phillips design equation by the author of this thesis.

Sarsam and Phillip's equation takes into account the contribution of so many parameters such as column axial load, column longitudinal reinforcement ratio, joint stirrups and joint aspect ratio. The equation contradicts the test data as explained below:

1. The author showed in the preceding sections by analyzing the existing test data that the column axial load and column longitudinal reinforcement ratio do not affect the joint shear strength. **Sarsam and Phillip's** equation on the other hand is based on the assumption that as the column axial load and the column longitudinal reinforcement ratio is increased, the joint shear strength increases.
2. **Sarsam and Phillip's** equation assumes that all the stirrups are effective in resisting joint shear strength. The inspection of **Ortiz** test data showed that the stirrups which are effective are those that are situated between the top of the compressive chord of the beam and below the beam longitudinal reinforcement. Moreover, the strain data published by **Ortiz** revealed that not all the stirrups

yield at failure. However, **Sarsam and Phillips** fall into the fallacy that all the stirrups in the joint yield at failure and contribute to shear resistance of the joint.

3. Sarsam and Phillips equation overestimates the influence of the concrete strength on the joint shear strength. In reality, the joint shear strength is related to the square root of the concrete cylinder strength.

4.5.2. The Design Equation of Vollum

Vollum proposed the following equation on the basis of analysis of the test data.

$$V_j = 0.642\ \beta\ (\ 1 + 0.555\ (\ 2 - h_b / h_c\ ))b_e\ h_c\ \sqrt{f_c} \qquad (4.45)$$

where; β is 1.0 for connections with L bars and 0.9 for connections with U bars.
The joint shear strength is then:

$$V_j = V_c + (\ A_{sje}\ f_y - \alpha\ b_e\ h_c\ \sqrt{f_c}\ ) \qquad (4.46)$$

where; A_{sje} is the cross-sectional area of the joint stirrups within the top five-eighths of the beam depth below the main beam reinforcement
α is a coefficient that depends on factors including column load, concrete strength, stirrup index, and joint aspect ratio. **Vollum** chose this value to be 0.2.
V_c is the joint shear strength without stirrups, which is given by equation 4.45.
The joint shear strength should be limited to:

$$Vj < 0.97\ b_e\ h_c\ \sqrt{f_c}\ (1 + 0.555\ (2 - h_b / h_c\ )) < 1.33\ b_e\ h_c\ \sqrt{f_c} \qquad (4.47)$$

The above equations suggest that the joint shear strength reduce linearly by 25 % as the joint aspect ratio is increased from 1.4 to 2.0.

4.5.2.1. The commentary on the design equation of Vollum by the author

The main criticism on the design equation of **Vollum** is that it does not take the influence of the influence of the beam longitudinal reinforcement ratio into account. The author had shown in the preceding sections that the two identical specimens of Scott C1AL and C4AL had 33 % difference in their joint shear strengths due to the different beam longitudinal reinforcement ratios they had. **Vollum**'s equation on the

The stirrups' influence is taken into account as the stirrup index subtracted by a constant 0.2. Adapting a constant 0.2 necessarily overestimates the joint's shear strengths with high amount of joint stirrups. When a joint is provided with high amount of stirrups, the stirrups in the joint do not yield. This makes the equation unsafe for joints such as BCJ7. The author applied the equation of Vollum on BCJ4 and BCJ7 of Ortiz. The results showed that the equation overestimated the joint shear strength of BCJ7 8 % while it underestimated the joint shear strength of BCJ4 by 5 %.

It is unclear how the constant β adapted for the equation is chosen. Does it differ from test to test? How does the equation adjust itself for the tests, which have joint shear strength as low as that of Parker and Bullman?

The basis of the upper limits chosen by Vollum is unclear. What is the basis of the constant 0.97? Moreover the other limit 1.33 $\sqrt{f_c}\ b_e\ h_c$ is chosen because it is the highest shear strength of the database Vollum used. So the accuracy of the above constraint is limited by the experimental database used. More experiments are needed with different joint aspect ratios, slabs and transverse beams reflecting the true boundary conditions in a joint to propose such an equation.

4.5.3. The Design Equation of the author of this thesis

The author's design equation is given by:

$$V_j = \frac{0.71\ \beta\ \gamma(100\ * \frac{A_{sb}}{b_b d_b})^{0.4289}\ (\frac{b_c + b_b}{2})\ h_c \sqrt{f_c}}{(\frac{h_b}{h_c})^{0.61}} + \alpha\ A_{sje}\ f_y \qquad (4.21)$$

where $\alpha = 0.664$ for joints with low amount of stirrups

$\alpha = 0.600$ for joints with medium amount of stirrups

$\alpha = 0.370$ for joints with high amount of stirrups

The equation is an improvement to other equations because:

1. It realistically models the contribution of stirrups in the joint.
2. It takes the influence of the beam longitudinal reinforcement ratio into account.

3. It realistically models the influence of the joint aspect ratio.

4. It realistically models the influence of concrete cylinder strength.

5. The equation is simple.

Therefore it is widely advocated that the author's design equation should be used for monotonically loaded exterior beam column connections to avoid joints with bad detailing and low joint shear strengths such as the tests of Parker and Bullman.

Table 4.31 shows the equation of the author applied on the experimental database. The established principles of joint mechanics

In order to investigate the reliability of the proposed design equation, the author investigated the established equations on the basic mechanics of reinforced concrete beam-column joints. This has been also previously discussed by Paulay and by Bonacci & Pantazopoulou for interior joints who have also taken into account the joint deformations. Both of the authors use the average stresses for equilibrium as shown in Figure 4.49. The typical loading system considered in analysis of exterior beam-column joints is shown in Figure 4.48. Figure 4.49 depicts the equilibrium of vertical and horizontal forces and shows that equilibrium of forces in the horizontal direction require the average transverse compressive stress in the joint σ_x defined as:

$$\sigma_x = -\frac{A_{sb}}{b_{eff} h_b} f_s - \frac{A_{sje}}{b_{eff} h_b} f_w \qquad (4.48)$$

where f_s is the average stress in the beam reinforcement,

f_w is the average stress in the transverse reinforcement

Consequently, the average normal concrete stress in the y direction σ_y can be expressed as :

$$\sigma_y = -\frac{A_{scol}}{b_{eff} h_c} f_{scol} - \frac{N}{b_{eff} h_c} \qquad (4.49)$$

where f_{scol} is the average stress in the column reinforcement

N is the column axial load

Defining the average joint shear stress in the joint as τ_{av}, the maximum principal stress associated with the stress tensor is given as;

$$\sigma = \begin{bmatrix} \sigma_x & \tau_{av} & 0 \\ \tau_{av} & \sigma_y & 0 \\ 0 & 0 & \sigma_z \end{bmatrix} \tag{4.50}$$

where σ_z is the confining stress provided by stirrups in the *z* direction.

In order to determine the principal stresses, Eq. (4.51) has to be solved;

$$\sigma^3 - I_1\sigma^2 + I_2\sigma - I_3 = 0 \tag{4.51}$$

where $I_1=\sigma_x+\sigma_y+\sigma_z$

$I_2=\sigma_x \sigma_y+\sigma_y \sigma_z+ \sigma_x \sigma_z-\tau_{av}^2$

$I_3=\sigma_x \sigma_y \sigma_z - \sigma_z \tau_{av}^2$

The tensile stress in the concrete is negligible and therefore $\sigma_1=0$, which consequently gives ;

$$\sigma_y = \frac{\tau_{av}^2}{\sigma_x} \tag{4.52}$$

From the Mohr's circle,

$$\tan 2\theta = \frac{2\tau_{av}}{\sigma_x - \sigma_y} \tag{4.53}$$

If Eq. (4.52) is substituted into Eq. (4.53), the following quadratic equation ensues;

$$\tau_{av}^2 + \left(\tan\theta + \frac{1}{\tan\theta}\right)\sigma_x\tau_{av} - \sigma_x^2 = 0 \tag{4.54}$$

which gives;

$$\tau_{av} = -\frac{\sigma_x}{\tan\theta} \tag{4.55}$$

Using Eq. (4.52), we have;

$$\sigma_y = -\frac{\tau_{av}}{\tan\theta} \tag{4.56}$$

Collins and Mitchell suggest the following equation for the maximum stress in concrete panels;

$$f_{2\max} = \frac{f_c}{0.8 + 170\varepsilon_1} \langle f_c \tag{4.57}$$

The principal compressive stress is given by;

$$\sigma_2 = \left(2\left(\frac{\varepsilon_2}{-0.002}\right) - \left(\frac{\varepsilon_2}{-0.002}\right)^2\right) f_{2\max} \tag{4.58}$$

σ_2 is also given from Mohr's circle as;

$$\sigma_2 = \sigma_x + \sigma_y = -\tau_{av}\left(\tan\theta + \frac{1}{\tan\theta}\right) \tag{4.59}$$

Thus the average joint shear stress can be expresses as;

$$\tau_{av} = -\frac{\sigma_2}{\left(\tan\theta + \frac{1}{\tan\theta}\right)} \tag{4.60}$$

T.C. YÜKSEKÖĞRETİM KURULU
DOKÜMANTASYON MERKEZİ

Equations 4.57 to 4.60 show very clearly that as the principal tensile strain increases, the average joint shear stress decreases. Thus it is necessary to express the principal tensile strain in terms of the strains in the x and y directions in order to investigate the factors that influence the joint shear strength. From Mohr's circle, it is known that;

$$\tan 2\theta = \frac{\gamma}{\varepsilon_x - \varepsilon_y} \tag{4.61}$$

From Mohr's circle, the principal tensile strain will be;

$$\varepsilon_1 = \frac{(\varepsilon_x + \varepsilon_y)}{2} + \sqrt{(\frac{\varepsilon_x - \varepsilon_y}{2})^2 + (\frac{\gamma}{2})^2} \tag{4.62}$$

If Eq. (4.61) is substituted into Eq. (4.62) and appropriate trigonometric transformations are carried out, Eq. (4.63) given by Bonacci and Pantazopoulou is obtained.

$$\varepsilon_1 = (\frac{\varepsilon_x - \varepsilon_y \tan^2\theta}{1 - \tan^2\theta}) \tag{4.63}$$

The next step will be to express the strains in the x and y directions in terms of the stresses.

$$\sigma_x = -\tau_{av} \tan\theta = -\frac{A_{sh} f_s}{b_{eff} h_b} - \frac{A_{sje} f_w}{b_{eff} h_b} = -(\frac{A_{sh}}{b_{eff} h_b}\mu + \frac{A_{sje}}{b_{eff} h_b}) f_w \tag{4.64}$$

Where $\mu = f_S / f_W$

The strain in the x direction can therefore be expressed as;

$$\varepsilon_x = \frac{f_w}{E_s} = \frac{\tau_{av} \tan\theta}{E_s(\frac{A_{sh}\mu}{b_{eff} h_b} + \frac{A_{sje}}{b_{eff} h_b})} \tag{4.65}$$

The strain in the y direction can similarly be expressed as;

$$\varepsilon_y = \frac{f_{scol}}{E_s} = (\frac{\tau_{av}}{\tan\theta} - \frac{N}{b_{eff} h_c}) \frac{b_{eff} h_c}{A_{scol} E_s} \tag{4.66}$$

If Eqs.(4.65) and (4.66) are substituted into Eq. (4.63),

$$\varepsilon_1 = \frac{1}{E_s(1-\tan^2\theta)}((\tau_{av} \tan\theta(\frac{1}{\frac{A_{sb}}{b_{eff} h_b}\mu + \frac{A_{sje}}{b_{eff} h_b}} - \frac{1}{\frac{A_{scol}}{b_{eff} h_c}})) + \frac{N\tan^2\theta}{b_{eff} h_c \frac{A_{scol}}{b_{eff} h_c}}) \tag{4.67}$$

It is evident from the inspection of experiments that cracks extend throughout the diagonal of the joint. So the angle of principal stresses can be expressed as;

$$\tan\theta = \frac{h_b}{h_c} \tag{4.68}$$

If Eq. (4.68) is substituted into Eq. (4.67),

$$\varepsilon_1 = \frac{1}{E_s(1-(\frac{h_b}{h_c})^2)}(\tau_{av} \frac{h_b}{h_c}(\frac{1}{\frac{A_{sb}\mu}{b_{eff} h_b} + \frac{A_{sje}}{b_{eff} h_b}} - \frac{1}{\frac{A_{scol}}{b_{eff} h_c}}) + \frac{N(\frac{h_b}{h_c})^2}{A_{scol}} \tag{4.69}$$

The above equation shows that the principal tensile strain is increased by the joint aspect ratio and column longitudinal reinforcement ratio and the axial load on the column whereas it is decreased by increasing beam longitudinal reinforcement ratio and the stirrup ratio. The shear stress in the joint is dependent on the principal tensile strain as evident from Eqs.(4.57) and (4.60). It is therefore evident from Eqs.(4.48), (4.49) and (4.69) that the joint shear strength increases as the beam bar ratio and the stirrup ratio increases. Eq. (4.49) shows that the joint shear strength increases as the column load and the column longitudinal reinforcement increases but Eq.(4.69) shows that as the longitudinal column reinforcement and the column load increases, the principal tensile stresses increase which consequently decreases the joint shear strength. Th the increase in the joint shear strength due to Eq. (4.49) is offset by the increase in the principal tensile strain. The above conclusions are totally in accordance with the predictions of the author's equation.

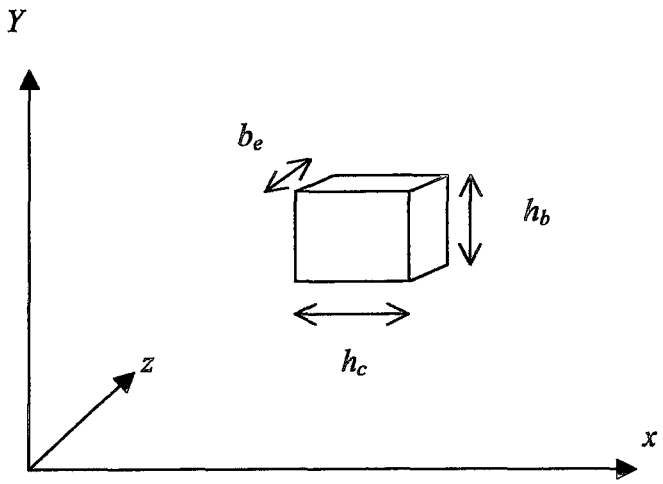

Figure 4.48: Joint geometry

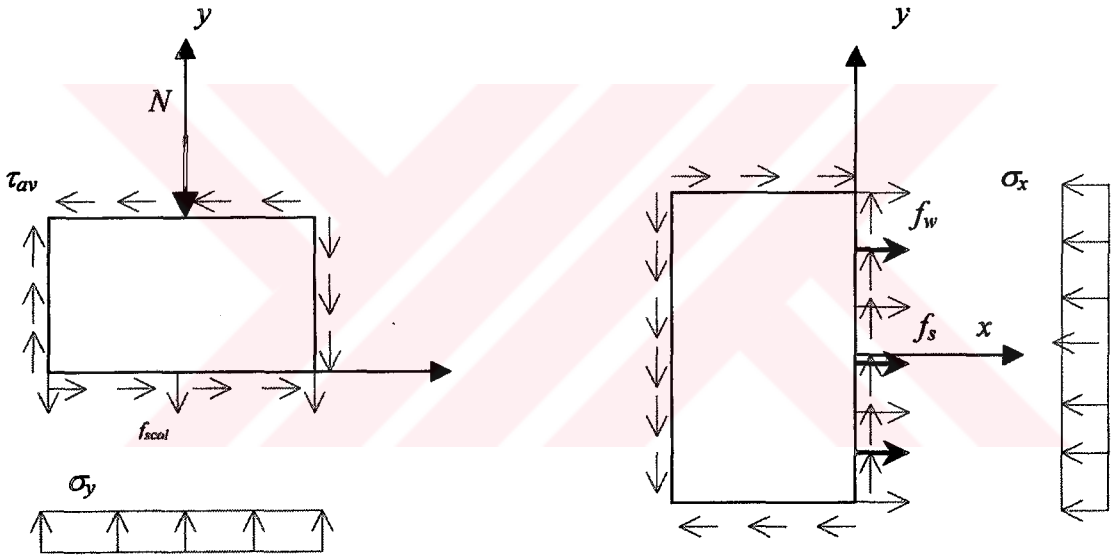

Figure 4.49 : The stress equilibrium

Table 4.35: The design equation of author applied on the experimental database

Investigator	specimen	detail	H (mm)	L (mm)	hb/hc	beam rein.ratio	column rein.ratio	fc(Mpa)	column axial load lkN)	SI (Mpa)^0.5	Vjpredicted/Vjactual
Ortiz	BCJ 1	L bar	2000	1050	1.33	1.1	2.19	34	0	0	0.68
	BCJ 2	L bar	2000	1100	1.33	1.1	2.19	38	0	0.16	0.77
	BCJ 3	L bar	2000	1100	1.33	1.1	2.92	33	0	0	0.64
	BCJ 4	L bar	2000	1100	1.33	1.1	3.65	34	0	0.33	0.78
	BCJ 5	L bar	2000	1100	1.33	1.1	3.65	38	300	0	0.72
	BCJ 6	L bar	2000	1100	1.33	1.1	3.65	35	300	0	0.68
	BCJ 7	L bar	2000	1100	1.33	1.1	3.65	35	300	0.76	0.68
Kordina	RE 2	L bar	3000	1000	2.00	0.9	2.41	25	240	0	0.66
	RE 3	L bar	3000	1000	1.50	1.8	2.41	40	400	0.26	0.96
	RE 4	L bar	3000	1000	1.50	1.2	2.41	32	51	0.19	0.83
	RE6	L bar	3000	1000	1.50	1.2	2.41	32	213	0.38	0.91
	RE7	L bar	3000	975	1.40	1.3	1.61	26	650	0.43	0.87
	RE8	U bar	3000	975	1.40	1.3	1.61	28	525	0.42	0.90
	RE9	U bar	3000	975	1.40	1.3	1.61	28	770	0.41	0.86
	RE10	U bar	3000	975	1.56	1.2	1.61	24	551	0.45	0.94
Taylor	P1/41/24	L bar	1290	470	1.43	2.4	4.10	33	240	0.3	0.97
	P2/41/24	L bar	1290	470	1.43	2.4	4.10	29	240	0.3	0.94
	P2/41/24A	L bar	1290	470	1.43	2.4	4.10	47	240	0.26	0.92
	A3/41/24	L bar	1290	470	1.43	2.4	4.10	27	240	0.3	0.88
	D3/41/24	L bar	1290	470	1.43	2.4	4.10	53	60	0.24	0.89
	B3/41/24	L bar	1290	470	1.43	2.4	4.10	22	240	0.75	0.92
	C3/41/24BY	U bar	1290	470	1.43	2.4	4.10	32	240	0.31	1.04
	C3/41/13Y	U bar	1290	470	1.43	1.4	4.10	28	240	0.33	0.95
Scott	C1AL	L bar	1700	750	1.40	1.1	4.29	33	50	0.188	0.87
	C4	L bar	1700	750	1.40	2.1	4.29	41	275	0.203	0.89
	C4A	L bar	1700	750	1.40	2.1	4.29	44	275	0.196	0.86
	C4AL	L bar	1700	750	1.40	2.1	4.29	36	50	0.218	0.86
	C7	L bar	1700	750	2.00	1.4	4.29	35	275	0.22	0.90
	C3L	U bar	1700	750	1.40	2.1	4.29	35	50	0.22	1.03
	C6	U bar	1700	750	1.40	2.1	4.29	40	275	0.21	1.05
	C6L	U bar	1700	750	1.40	2.1	4.29	46	50	0.19	0.94
	C9	U bar	1700	750	2.00	1.4	4.29	36	275	0.22	0.93
Scott & Hamill	C4ALNO	L bar	1700	750	1.40	2.1	4.29	42	50	0	0.88
	C4ALN1	L bar	1700	750	1.40	2.1	4.29	46	50	0.229	0.85
	C4ALN3	L bar	1700	750	1.40	2.1	4.29	42	50	0.478	0.78
	C4ALN5	L bar	1700	750	1.40	2.1	4.29	50	50	0.718	0.85
	C4ALHO	L bar	1700	750	1.40	2.1	4.29	104	100	0	0.86
	C6LNO	U bar	1700	750	1.40	2.1	4.29	51	50	0	0.92
	C6LN1	U bar	1700	750	1.40	2.1	4.29	51	100	0.19	0.96
	C4ALH1	L bar	1700	750	1.40	2.1	4.29	95.2	100	0.159	0.93
	C4ALH3	L bar	1700	750	1.40	2.1	4.29	105.6	100	0.302	0.97
	C4ALH5	L bar	1700	750	1.40	2.1	4.29	98.4	100	0.469	1.00
	C6LN3	U bar	1700	750	1.40	2.1	4.29	49	50	0.44	0.92
	C6LN5	U bar	1700	750	1.40	2.1	4.29	37	50	0.765	0.74
	C6LHO	U bar	1700	750	1.40	2.1	4.29	101	100	0	0.72
	C6LH1	U bar	1700	750	1.40	2.1	4.29	102	100	0.153	0.98
	C6LH3	U bar	1700	750	1.40	2.1	4.29	97	100	0.472	0.93
parker	4a	L bar	2000	850	1.67	0.9	1.09	39	0	0	c
	4b	L bar	2000	850	1.67	0.9	1.09	39	300	0	1.05
	4c	L bar	2000	850	1.67	0.9	1.09	37	600	0	0.83
	4d	L bar	2000	850	1.67	0.9	4.38	39	0	0	0.97
	4e	L bar	2000	850	1.67	0.9	4.38	40	300	0	0.92
	4f	L bar	2000	850	1.67	0.9	4.38	38	600	0	0.78
	5a	L bar	2000	850	1.67	0.9	2.67	42	0	0.404	c
	5b	L bar	2000	850	1.67	0.9	2.67	43	300	0.4	1.08
	5d	L bar	2000	850	1.67	1.4	2.67	43	0	0.6	c
	5e	L bar	2000	850	1.67	1.4	2.67	45	300	0.589	c
	5f	L bar	2000	850	1.67	1.4	2.67	43	600	0.6	0.86
										average	0.88
										standard deviation	0.10

5. THE STRUT AND TIE MODELING OF THE JOINTS

5.1. Introduction

The author investigated the previous models by Ortiz and Vollum in Chapter 4. In this chapter, a new strut and tie model is developed for monotonically loaded exterior joints eliminating the weaknesses of the previous models. The author's model is composed of two models. The first model is for joints without stirrups, while the second one is for joints with stirrups. The model is shown in Figure 5.1 in detail. The author's model also consists of a direct strut and two indirect struts in the joint. The difference between the author's model and Vollum's model are as follows:

Vollum is of the opinion that the indirect struts as well as the direct strut are equilibrated by the upper compressive rectangular stress block in the upper column in the vertical direction and by the beam compressive chord in the horizontal direction. This in other words mean that as the stirrup's contribution to joint shear increases, the width of the direct strut decreases in Vollum's model. The author's model on the other hand is based on the assumption that the truss mechanism is equilibrated by another strut coming from the upper column. Thus, the width of the direct strut is constant no matter what the stirrup force is. This is logical because as the stirrup ratio increases, the transverse tensile strain decreases resulting in an increase in the concrete strength of the joint. This in other words mean that the stirrups help the strut mechanism by confining the joint.

Tests by Aoyama have indicated that the proportion of joint shear force that is resisted by shear reinforcement reduces as the column axial load is increased. This is not reflected in Vollum's model . However, the author's model clearly accounts for it because as the column axial load is increased, the width of the direct strut increases decreasing the factor of redistribution.

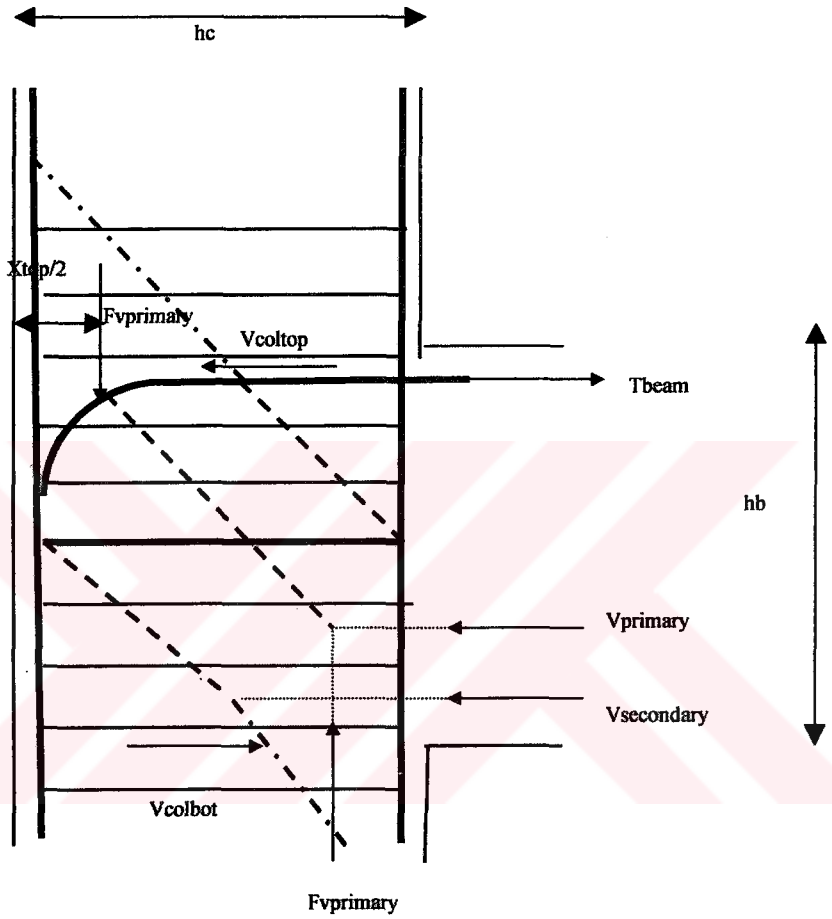

Figure 5.1. The strut and tie model suggested by author

The author's model is more simple than the model of Vollum and it realistically models the inadequacy of the beam tensile reinforcement to resist the horizontal component of the truss mechanism and the need for another mechanism to equilibrate the horizontal component of the truss mechanism.

Failure occurs due to the stress reaching the cracked concrete strength in the upper node while Vollum's model puts some upper limits on joint shear. The failure in author's model is related to the failure of the mechanisms adapted for the model while it is not for Vollum's. The author's models details are given below:

5.1.1. Vertical Joint Shear

$$F_v = C_{ctop} + C_{stop} + T_{sbot} \tag{5.1}$$

where; C_{ctop} is the force in the compressive rectangular stress block of the top column.

C_{stop} is the compressive force in the compressive bars of the top column.

T_{sbot} is the tensile force in the tensile bars of the bottom column.

5.1.2. Horizontal Joint Shear

$$V_j = T - V_{colupper} \tag{5.2}$$

where; T is the tensile force in the beam top bars

$V_{colupper}$ is the shear force in the upper column, the equation of which is given by:

$$V_{colupper} = P\,(L + 0.5\,h_c) / H \tag{5.3}$$

where; P is the applied loading in the beam.

h_c is the height of the column

H is the vertical distance between the horizontal restraints.

5.1.3. The Upper and lower column moments

The upper and lower column moments are given by the following equations:

$$M_{colupper} = V_{colupper} (0.5 (H- h_b) + d_b') \quad (5.4)$$

$$M_{colbottom} = 0.5 V_{colupper} (H- h_b + y_R) \quad (5.5)$$

where:

$$y_R = V_{colupper} / b_b \sigma_b \quad (5.6)$$

where; $V_{colupper}$ is the shear force in the upper column

b_b is the breadth of the beam

σ_b is the stress in the beam.

Vollum gives identical equations for the calculation of the upper and bottom column moments.

5.1.3. Beam Moments

The moment induced in the beam is calculated by the following equation:

$$M_{beam} = P (L + d') \quad (5.7)$$

where; P is the applied load in the beam.

L is the distance from the point of applied loading to the face of the column.

d' is the cover

5.1.4. Section analysis

The moments in the beam and the columns surrounding the joint are determined. The forces in the reinforcement and concrete are calculated by using the rectangular parabolic stress block of the Turkish Building Code TS500. A bi-linear stress strain diagram with an elastic modulus of 200 GPa is used. The procedure adapted for calculating the forces in the reinforcement is given below:

1. A failure load is assumed.
2. No factors of safety are adapted for the mean concrete strength.
3. The moments developing at the boundary of the joint due to the applied loading are calculated.

4. A value for the strain in the most compressed fiber is assumed. This assumed value can be between zero and ε_{cu} which is the maximum strain that the most compressed fiber can have. For a systematic approach a value as low as 0.0003 can be adapted.

5. The neutral axis depth is estimated from the force equilibrium and moment equilibrium conditions at the cross sections of beam and the columns. The strains in the reinforcement are calculated in terms of the neutral axis depth. From each determined ε_{ci} value, the stresses are calculated and checked against yielding.

$$\sigma_{si} = \varepsilon_{si} E_s \leq fy \tag{5.8}$$

6. Consequently, the forces at the boundary of the joint were determined. The forces were estimated by multiplying the area of the steel with the corresponding stress in that reinforcement.

$$F_{si} = A_{si}\ \sigma_{si} \tag{5.9}$$

Similarly, the force in the concrete compressive stress block is calculated.

7. The joint shear force is determined from the Equation 5.2.

A computer program is written for the above procedure. The program increases the strain assumed for the each column and the beam in small increments up until the moment equilibrium is satisfied. For each column and beam $1x10^6$ iteration is carried out. Finally the forces in the reinforcement and the concrete are calculated for each assumed applied load. Vollum, Fuji and Morita all suggested that there was a considerable amount of tensile shift from the assumption of plane sections remain plane. This is also taken into account as stated in the following sections. The parabolic stress block is replaced by the rectangular stress block of the Turkish Code. The depth of the equivalent rectangular stress block is calculated using the moment equilibrium.

5.1.5. Assumptions made when modeling the joint

The author assumed that no compressive reinforcement is provided for the joints. This can be justified because the joints are monotonically loaded joints. Therefore there is less need for high amount of compressive reinforcement to resist the reversed

cyclic loading. Therefore generally, the monotonically loaded joints are provided by negligible amount of compressive reinforcement. It is also assumed that the width of the direct strut is constant at failure for joints with and without stirrups. This is justified as well because, stirrups confine the joint core and consequently increase the efficiency of the direct strut mechanism. The authors are of the opinion that suggestion of the Vollum model which says that the width of the direct strut will decrease when the joint is provided with stirrups is not correct.

5.1.6. The depth of the beam and columns compressive rectangular stress blocks

The depth of the equivalent rectangular stress block in the beam is given by the following equation:

$$y = 2 (d_b - M_b / T_b) \quad (5.10)$$

where; y is the width of the compressive chord of the beam.
M_b is the moment in the beam induced due to the applied loading
T_b is the tensile force in the beam tensile reinforcement.

The depth of the rectangular stress blocks in the upper and lower columns are given by the equation:

$$x_{res} = h_c - 2 (M_{col} - (C_s + T_s) (0.5 h_c - d')) / C_c \quad (5.11)$$

where; h_c is the height of the cross section of the column
M_{col} is the moment induced in the column due to the applied loading
C_s is the compressive force in steel
T_s is the tensile force in the steel
d' is the cover
C_c is the compressive force in the rectangular stress block.

The compressive stress in the beam is given by:

$$\sigma = C_c / b_e x_{res} \quad (5.12)$$

where; be is the effective joint width which is given by:

$$b_e = (b_c + b_b) / 2 \quad (5.13)$$

5.1.7. The Angle of inclination of the direct and indirect struts

The cracks observed in the monotonically loaded exterior beam column joint tests of Ortiz (BCJ4 and BCJ7) reveal that the cracks run parallel to the direct and indirect struts. There is no change in the angle of inclination for the direct and indirect strut mechanisms. This means that the angle of inclination of the direct (primary) and indirect (secondary) struts can be accepted as the same. The author assumed that the angle of inclination of the direct and indirect struts are same and can be estimated as the ratio of the height of the beam to the height of the column.

$$\tan \theta = (h_b / h_c) \qquad (5.14)$$

where; h_b is the cross-sectional height of the beam
hc is the cross-sectional height of the column.

5.1.8. The Cracked Concrete Strength

The author adapted the recommendations of the CEB Model Code 90 due to the simplicity they provide. No factors of safety are adapted for the concrete cylinder strength. But the average cylinder strengths measured from control tests are directly used for the cracked and uncracked concrete strengths. The CEB Model Code recommends the following equations for the cracked and uncracked sections:

$$f_{cd} = 0.6 f_{cd} (1- f_{ck} / 250) \quad \text{(MPa)} \qquad (5.15\ A)$$

$$f_{cd} = 0.85 f_{cd} (1 - f_{ck} / 250) \quad \text{(MPa)} \qquad (5.16\ A)$$

The CEB Model Code 90 is modified as follows:

$$f_{cd} = 0.60 f_c (1- f_c/250) \qquad (5.15\ B)$$

$$f_{cd} = 0.85 f_c (1 - f_c/250) \qquad (5.16\ B)$$

where; f_c is the mean cylinder strength reported from experiments without any factors of safety and f_{ck} is the characteristic cylinder strength.

5.2. Model without stirrups

First, the model is developed for joints without stirrups. The most difficult part of the modeling was adjusting the width of the direct strut. A parametric study was carried

out to determine the width of the primary strut. It appeared that the width of the direct strut should be adjusted empirically as Vollum suggests.

5.2.1. Width of the direct strut in the top node

The width of the direct strut in the top node is different than the width of the bottom node. As stated in the preceding sections, the width of the top and bottom nodes are related to the widths of the compressive rectangular stress blocks of the beam and the upper and lower columns.

Paulay (1975) has stated that the most stressed region in the joint is top node. This is logical because the top node is a node where the tensile and compressive forces meet. The bottom node is biaxially compressed and therefore it is unlikely that failure will ever occur in the bottom node. Thus, the adjustment of the width of the top node is very important because it is very likely that failure will occur in the top node. The author made a parametric study to determine the width of the direct (primary) strut. The most logical results were obtained when the primary strut width is taken as :

$0.38\ h_c / \sin\theta$ at failure. (5.17)

where; h_c is the height of the cross section of the column.

θ is the angle of inclination of the direct strut which is calculated simply from:

$\tan\theta = h_b / h_c$

Ortiz tests have showed that at failure, the width of the top node is different from the assumption of plane sections remain plane. Thus, it is decided that the width of the top node should in some other ways be related to the width of the compressive stress block of the upper column at failure. This can only be achieved by a good strategy on the redistribution. The author adapted the strategy of Vollum for the redistribution of the column bar forces whose details are given below.

1. Column axial force is assumed as zero.
2. The force in the column bar forces is kept constant.
3. The force in the tensile column longitudinal reinforcement is increased in small increments until the width of the direct strut mechanism is equal to $0.4\ h_c / \sin\theta$

5.2.2. The Axial Force in the Direct Strut

As known, there is only the primary strut in the joints without stirrups and the indirect struts disappear. The force in the direct strut is given then by Eq. (5.18)

$$D = \sqrt{(F_v^2 + V_j^2)} \qquad (5.18)$$

where; F_v is the vertical shear in the joint

V_j is the horizontal shear in the joint

D is the axial force in the diagonal strut.

5.2.3. Failure

Failure occurs when the shear force resisted by the primary strut mechanism equals to the input shear. The resistance of the direct strut to joint shear is given by the following equation:

$$V_u = 0.6\, f_c (1 - f_c / 250) (b_b + b_c) / 2 (0.38\, h_c / \sin\theta) \cos\theta \qquad (5.19)$$

f_c is in MPa. The applied load is increased up until the shear in the joint is equal to the shear resisted by the primary strut mechanism.

5.2.4. Final procedure adapted for the joints without stirrups

The author's model for joints without stirrups is similar to Vollum's except the angle of inclination and the equations for the cracked concrete strengths. The procedure is summarized in the following paragraphs:

1. A failure load is estimated.
2. The vertical and horizontal shear forces are determined.
3. The boundary forces in the beam and columns are determined.
4. The redistribution of the forces in the upper column longitudinal reinforcement is taken into account.
5. The resistance of the direct strut is determined by Eq. (5.21)

   $$V_u = 0.6\, f_c (1 - f_c / 250) (b_b + b_c) / 2 (0.38\, h_c / \sin\theta) \cos\theta \qquad (5.21)$$
6. If the shear resisted by the direct strut equals to the shear in the joint, the procedure is stopped. If not the failure load should be increased/decreased until the above criterion is met.

5.3. Model with stirrups

Paulay had suggested that the vertical component of the secondary struts should be equilibrated by the intermediate column bars in the joint. Today, it is impossible to agree with the above conclusions because recent Japanese research by Fuji and Morita showed that intermediate column bars are ineffective in resisting the vertical shear in the joint and there should be other mechanisms equilibrating the secondary struts. Vollum suggested that the secondary struts are equilibrated by the upper compressive rectangular stress block. This is not acceptable as the inspection of BCJ4 and BCJ7 of Ortiz which both have joint stirrups show that the cracks are all parallel to the joint diagonal and some extend to the column longitudinal reinforcement of the upper column. This is an indication of the distress in these regions. In addition to this, the parametric study in Table 5.1 shows that the stirrup ratio can be classified as low, as in Ortiz specimen BCJ2 ; medium, as in Ortiz specimen BCJ4 and high, as in Scott specimen C4ALN3. These three type contribute in different amounts to joint shear. The bond conditions are increased for the beam longitudinal reinforcement when high amount of stirrups are provided in the joint.

Table 5.1. Results of the Parametric Study on the Relative Contributions of Truss and Strut Mechanisms to Shear

Specimen	Reported Stirrup Strains	Stirrup Force	Total Stirrup Force	Vj	The contribution of the strut mechanism to joint shear	The Expected Contribution of the Truss Mechanism to Joint Shear	The Horizontal Component of the Residual Force in the strut of the Truss Mechanism
Units	Microstrain	kN	kN	kN	kN	kN	kN
BCJ2	y7584	57	57	349.1	330.618	18.482	38.518
BCJ4	1887 y2990 y3003 1139	38 57 57 22	114	368.2	301.397	66.808	47.191
C4ALN3	2100 2880 2340	24 32.5 72	54	156.6	110.126	46.525	7.475

Table.5.2. Predicted Failure Loads of Ortiz specimens

Specimen	Detailing	Actual Failure Mode	Predicted Failure Mode	Cylinder Strength	Ppred/Pfail
Units	-	-	-	MPa	-
Ortiz					
BCJ1	L Bar	JS	JS	33.8	0.93
BCJ2	L Bar	JS	JS	37.8	0.88
BCJ3	L Bar	JS	JS	33	0.87
BCJ4	L Bar	JS	JS	34	0.98
BCJ5	L Bar	JS	JS	37.9	1.01
BCJ6	L Bar	JS	JS	35	0.94
BCJ7	L Bar	B	JS	35	0.89
				Average	0.93

Notes: No factors of safety are adapted for the concrete cylinder strength and the reported mean concrete cylinder strengths are used. y denotes yielding.

5.3.1.Modeling of the joint

The above mentioned parametric study will be explained in more detail here. The joint resists shear by two mechanisms. The first one is the strut mechanism. The second is the truss mechanism. Failure would occur certainly in the top node, as this region is the most stressed region in the joint. The widths of the top node and the bottom node will be different. In order to estimate the width of the top node, a parametric study was made on joints without stirrups and it was found out that the width of the primary strut was 0.38 h_c / (sinθ) at failure. The author applied the model without stirrups on the existing test data, the details of which can be seen in Tables 5.2 to 5.7. The shear strength of a joint without stirrups at the top node will be:

$V_{wos}=0.38\ h_c\ (b_c+b_b)f_{cr}/\ 2\tan\theta$

where

$\tan\theta = (h_b / h_c)$

The truss mechanism's contribution to shear should be superimposed on the contribution of the strut. The previous researchers such Sarsam and Phillips assumed that all the stirrups would yield at failure and all the stirrups would contribute to the shear strength. Some later researchers such as Ortiz assumed that the effective stirrups are those that are placed between the top of the compressive chord of the beam and the tensile bars at the top of the beam. Ortiz assumed that all the stirrups were at yield when failure occurred. Inspection of the test specimens of Ortiz showed that not all the stirrups were at yield at failure. A parametric study is made to investigate the contribution of the truss mechanism to joint shear. The beam flexural reinforcement is assumed to yield if flexural failure of the beam was anticipated. The joint shear in Table 5.1 is calculated on the basis that the applied loading is equal to that reported by Ortiz and Scott and Hamill from tests. It is clear from the Table 5.1 that BCJ4 which is reinforced with medium amount of stirrups, had a significant residual force in the strut of the truss mechanism which had to be equilibrated by a mechanism other than the bond force in the beam tensile reinforcement. As you increase the amount of the transverse stirrups as in C4ALN3, the percentage of the axial force in the strut of the truss mechanism which is equilibrated by bond force of

the beam tensile reinforcement increases. This is an indication that the truss mechanism is equilibrated by another strut coming from the upper column whose angle of inclination is dependent on bond conditions for the beam bars and the strains in the ties of the lower and upper columns. The shear force in the joint should be modified as follows if the struts coming from the upper column are considered.

$$V_j = T - V_{colupper} + C_{titop} \cos\phi \qquad (5.22)$$

where; C_{titop} is the axial force in the strut coming from the upper column which is equilibrated by the stirrups of the upper column in the horizontal direction.

ϕ is the angle of inclination of the strut coming from the upper column which is dependent on bond conditions for the beam longitudinal reinforcement and the strains in the ties of the lower and upper columns.

Table 5.3.The predicted failure loads and modes of the specimens of Parker and Bullmann (1997)

Specimen	Detailing	Actual Failure Mode	Predicted Failure Mode	Cylinder Strength	Ppred/Pfail
Units	-	-	-	MPa	-
Parker & Bullmann					
4a	L Bar	CF	C	39.2	1.576
4b	L Bar	J	C	39.2	1.355
4c	L Bar	J	C	36.8	1.076
4d	L Bar	J	JS	39.2	0.988
4e	L Bar	J	JS	40	1.318
4f	L Bar	J	JS	37.6	1.092
5a	L Bar	C	C	42.4	1.480
5b	L Bar	JS	C	43.2	1.344
5c	L Bar	B	C	43.2	1.310
5d	L Bar	C	JS	43.2	1.097
5e	L Bar	C	C	44.8	1.085
5f	L Bar	C	C	43.2	0.994
				Average	1.226

1.The specimens denoted with bold letters in the above table are the joints with stirrups.

Table 5.4. The predicted failure loads and modes of Kordina (1984)

Specimen	Detailing	Actual Failure Mode	Predicted Failure Mode	Cylinder Strength	Ppred/Pfail
Units	-	-	-	MPa	-
Kordina					
RE2	L Bar	JS	JS	25.3	1.209
RE3	L Bar	JS	JS	40.4	0.787
RE4	L Bar	JS	JS	32.2	1.092
RE5			B		1.290
RE6	No bend	JS	JS	32	0.772
RE7	L Bar	JS	JS	26	0.690
RE8	U Bar	JS	JS	28	0.838
RE9	U Bar	JS	C	28	0.808
RE10	U Bar	JS	JS	24	0.800
			Average	(excluding U bars) all together	1.013 0.920

As explained in Chapter 4, the relationship between the joint shear strength and the amount of stirrups was tri-linear.

When $\rho < 0.003$, the contribution of the stirrups to joint shear resistance can be neglected. This is logical because the graph shows very clearly that the line is almost horizontal when the amount of stirrups are increased up until 0.003.

$0.003<\rho < 0.0055$; the line shows that joint shear strength increases significantly within this region. This is the region of medium amount of stirrups. All the stirrups yield within this region.

$0.0055< \rho$; the graph shows that the increase is not as much as the previous region. Not all the stirrups yield within this range.

Table 5.5.Predicted failure loads and modes of specimens tested by Scott (1992)

Specimen	Detailing	Actual Failure Mode	Predicted Failure Mode	Cylinder Strength	Ppred/Pfail
Units	-	-	-	MPa	-
Scott					
C1	L Bar	B	JS	39.92	0.935
C1AL	L Bar	JS	JS	33.36	0.947
C2	L Bar vertical leg turned into upper column	JS	B	49.36	1.440
C4	L Bar	JS	JS	41.44	0.840
C3	U Bar	B	JS	36	0.868
C1A	L Bar	B	B	48	1.256
C4A	L Bar	JS	JS	44.32	0.817
C4AL	L Bar	JS	JS	35.76	0.756
C7	L Bar	JS	B	35.2	1.187
C3L	U Bar	JS	JS	35.52	1.018
C6	U Bar	JS	JS	39.84	1.077
C6L	U Bar	JS	JS	45.84	1.019
C9	U Bar	JS	JS	35.92	0.774
C8	L Bar vertical leg turned into upper column	JS	JS	44.48	0.956
C5	same as above	JS	JS	33.04	1.449
			Average	(excluding U bars)	0.960

Notes:

1.C denotes column failure, B denotes beam failure, JS denotes joint shear failure, P denotes beam bar pullout failure.

Unfortunately, we have very limited test data regarding the stirrup strains in the joint. Most researchers do not publish this important data. The only exception is that of Ortiz. Ortiz reported the stirrup strains of the specimens BCJ4 and BCJ7. The author based her modeling of the secondary struts on Table 5.5. BCJ4 is a typical joint with medium amount of joint stirrups. All the stirrups yield in BCJ4 at failure.

It is apparent from Table 5.1 that the contribution of the secondary strut mechanism to the joint shear defined by $V_j = T - V_{colupper}$ equation is much less than the actual stirrup force because some of the actual shear is resisted by the strut coming from the upper column. The percentage of the joint shear force defined by $V_j = T - V_{colupper}$ resisted by the truss mechanism is 18.14 % for BCJ4. The rest of the stirrup force will be assumed to be carried by the strut coming from the upper column. For C4ALN3, 29.7 % of the joint shear will be carried by the stirrups. As the amount of the stirrups are increased, the percentage of the joint shear force defined by $T-V_{colupper}$ resisted by the secondary strut mechanism increases. This indicates that as the amount of stirrups are increased in the joint, the bond conditions improve and more of the tensile force in the beam longitudinal reinforcement is resisted by the stirrups. If the joint is provided by medium amount of stirrups, 18.14 % of joint shear strength will be carried by stirrups. If the joint is has low amount of stirrups such as BCJ2 of Ortiz, the contribution of joint stirrups to joint strength will only be 5.29%.

5.4. Results

The results of the author's model can be summarized as below:

1. The contribution of the truss mechanism to joint shear strength is 29.7 % if sufficient transverse reinforcement is provided for the joint.
2. The model adapted gives very accurate predictions of the failure loads and modes.
3. Analysis of the above results shows that the model overestimates the failure loads of the test specimens that are reinforced by L bars turned up into column and U bars. This is because the model can not account for detailing.
4. The model is very simple.
5. The geometry of the top node is given in detail.
6. The stirrup's contribution to joint shear strength is taken satisfactorily into account.
7. The only solution to equilibrate the vertical joint shear should not be to use intermediate column bars. This model clearly explains that the ties in the

confinement regions of the upper and lower columns can equilibrate the truss mechanism as well.

5.5. The Parametric Studies on Author's model

The author carried out parametric studies on the response of model to the changes in the concrete cylinder strength, column axial load, joint aspect ratio and the column longitudinal reinforcement ratio. The influence of these parameters will be investigated both for joints with stirrups and joints without stirrups separately. If the joints are provided by only a single stirrup, the contribution to joint shear strength will be neglected.

Table 5.6. Predicted failure loads and modes of Specimens tested by Scott & Hamill

Specimen	Detailing	Actual Failure Mode	Predicted Failure Mode	Cylinder Strength	Ppred/Pfail
Units	-	-	-	MPa	-
Scott & Hamill					
C4ALN0	L Bar	P	JS	42.4	0.856
C4ALN1	L Bar	JS	JS	45.6	0.722
C4ALHO	L Bar		JS		0.925
C4ALH1	L Bar	B	JS	95.2	0.990
C6LH0	U Bar	JS	JS	100.8	1.000
C6LH1	U Bar	JS	JS	101.6	1.186
C6LN0	U Bar	JS	JS	51.2	1.238
C6NL3	U Bar	JS	JS	48.8	1.358
C6NL5	U Bar	JS	JS	36.8	0.914
C6LH3	U Bar	JS	B	96.8	1.220
C4ALN3	L Bar	JS	JS	41.6	0.966
C4ALH3	L Bar	B	B	105.6	1.106
C6LH5	U Bar	B	B	100	0.986
C4ALN5	L Bar	JS	JS	50.4	1.005
			Average	(excluding U)	

5.5.1. The Concrete Cylinder Strength

The predictions of the model regarding the influence of concrete cylinder strength on the normalized joint shear strength are given in Figure 5.2. The graph shows that there is a slight decrease in the normalized joint shear strength with the increase in the concrete cylinder strength. This is acceptable and is probably due to the normalization process because in reality the joint shear strength is not proportional to f_c but $\sqrt{f_c}$.

5.5.2. Column Longitudinal Reinforcement Ratio

The Figure 5.3. shows that the column longitudinal reinforcement ratio has no influence on the predicted normalized joint shear strength of joints without stirrups. This is in agreement with the parametric study of author in Figure 4.26b.

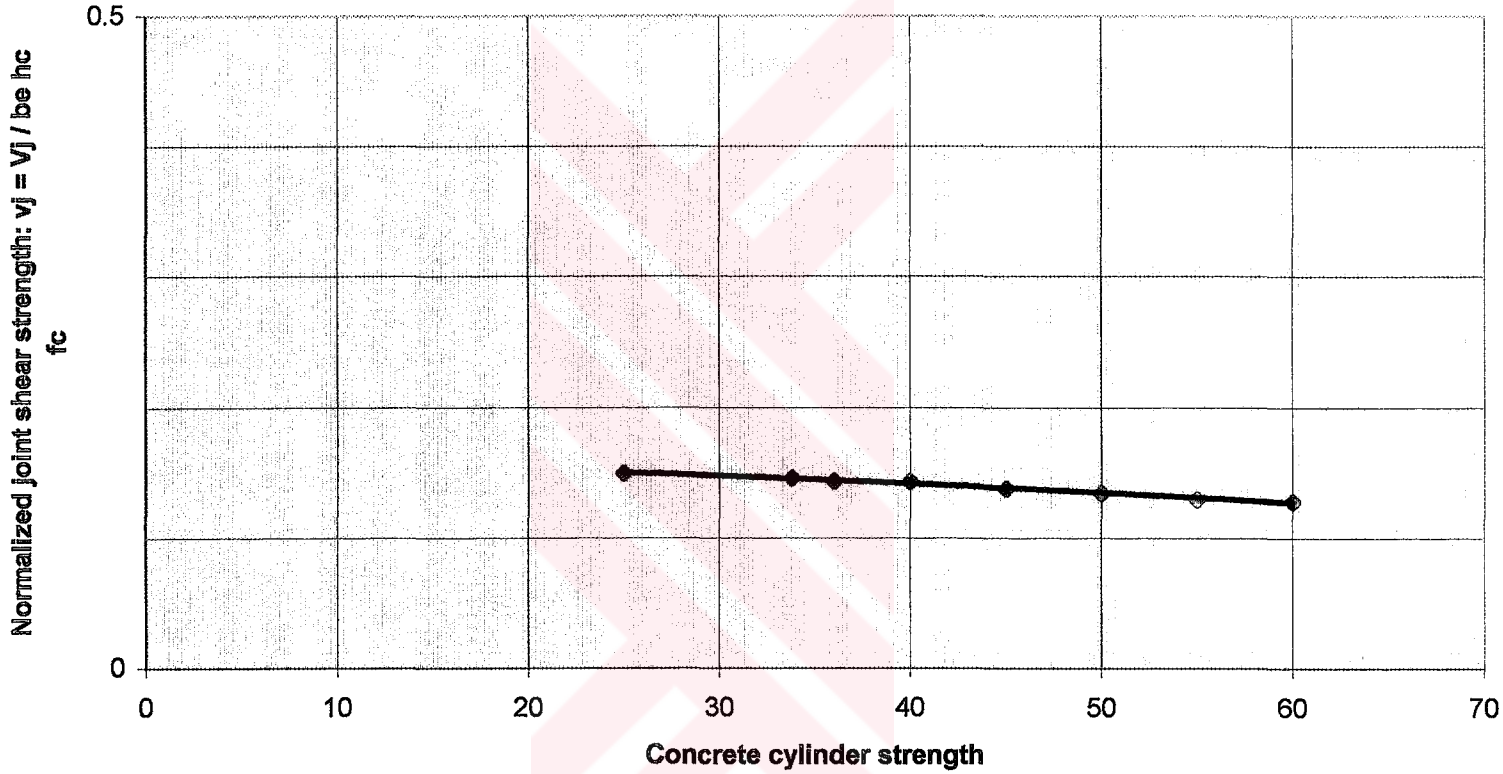

Figure 5.2. The influence of concrete cylinder strength on the predicted normalized joint shear strength of the author's model without stirrups

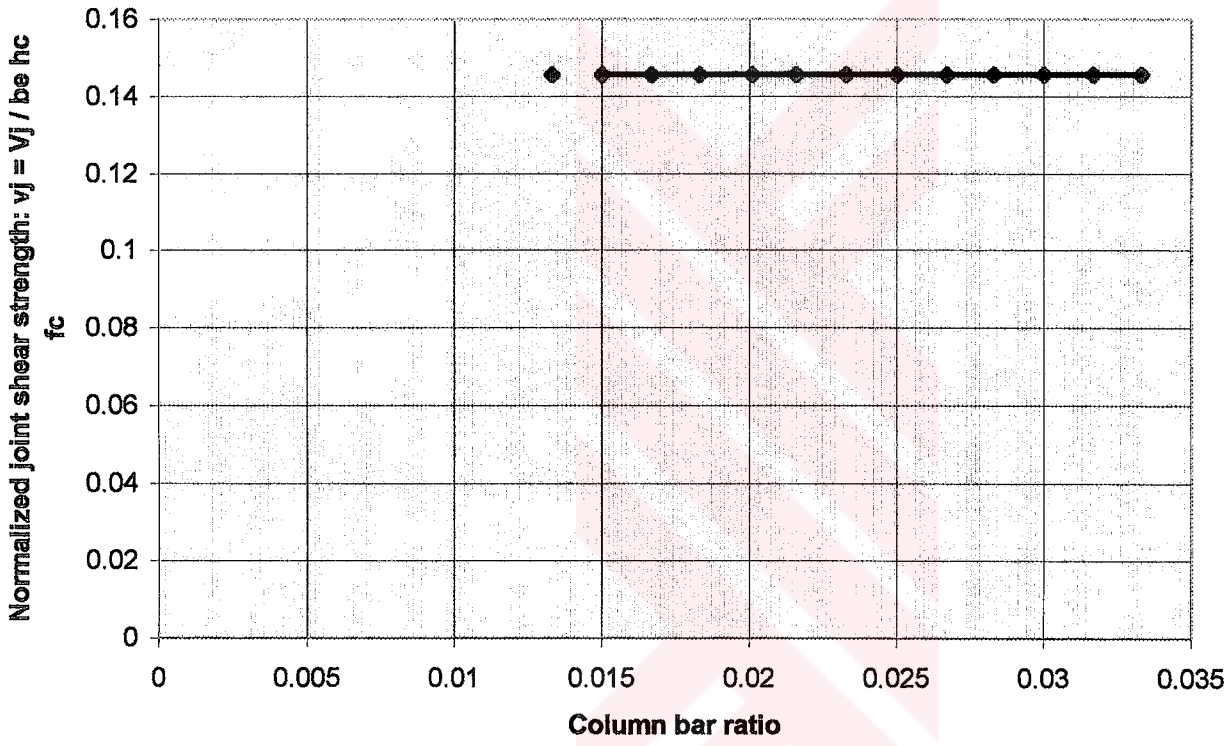

Figure 5.3. The effect of column bar ratio on the normalized joint shear strength of exterior beam column connections predicted by the author's model without stirrups

5.5.3. Joint Aspect Ratio

The influence of joint aspect ratio on the normalized joint shear strength predicted by the model of the author on joints without stirrups is investigated in Figure 5.4. The results reveal that as the joint aspect ratio is increased, the normalized joint shear strength decreases, which is in agreement with the parametric study of the author in Figure 4.26d.

5.5.4. Column Axial Load

In Figure 5.5, the author made a parametric study to investigate the influence of the column axial load on the predicted normalized joint shear strength of joints without stirrups which shows that the column axial load does not influence the joint shear strength. This is in agreement with the parametric study of authors in Figure 4.29.

5.5.5. Concrete Cylinder Strength (Joints with stirrups)

The predictions of the model regarding the influence of concrete cylinder strength on the normalized joint shear strength are given in Figure 5.6. The graph shows that there is a slight decrease in the normalized joint shear strength with the increase in the concrete cylinder strength. This is acceptable and is due to the normalization of the joint shear strength by f_c.

5.5.6. Joint aspect ratio (with stirrups)

The parametric study in Figure 5.7 shows that as the joint aspect ratio is increased, the normalized joint shear strength decreases. The predictions of the model are in agreement with the parametric study of the author in Figure 4.26d.

5.5.7. Column longitudinal reinforcement ratio (Joints with stirrups)

Another parametric study is carried out by the author whose details are given in Figure 5.8. The model predicts that the column longitudinal reinforcement ratio has no influence on the normalized joint shear strength of joints with stirrups. The prediction of the model is in agreement with tests as apparent from 4.26b.

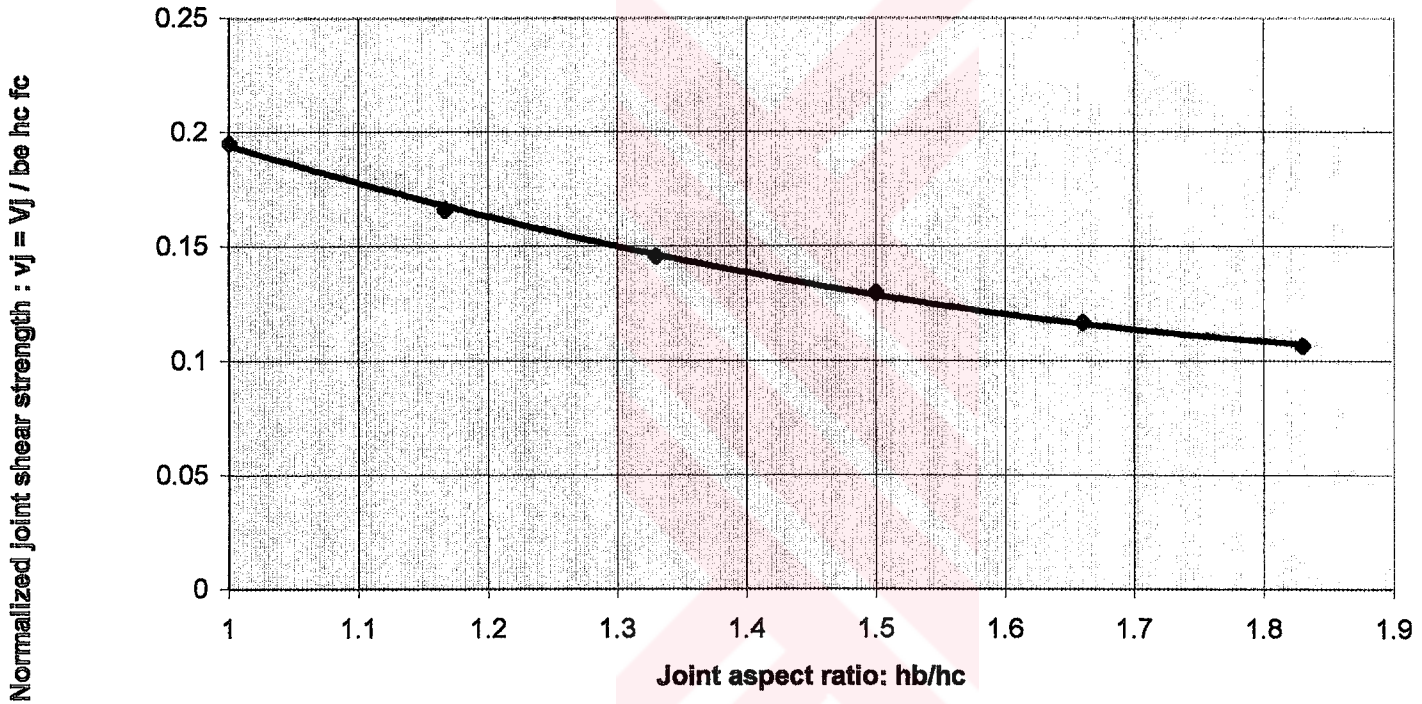

Figure 5.4. The effect of the joint aspect ratio on the normalized joint shear strength of joints without stirrups predicted by the author's model

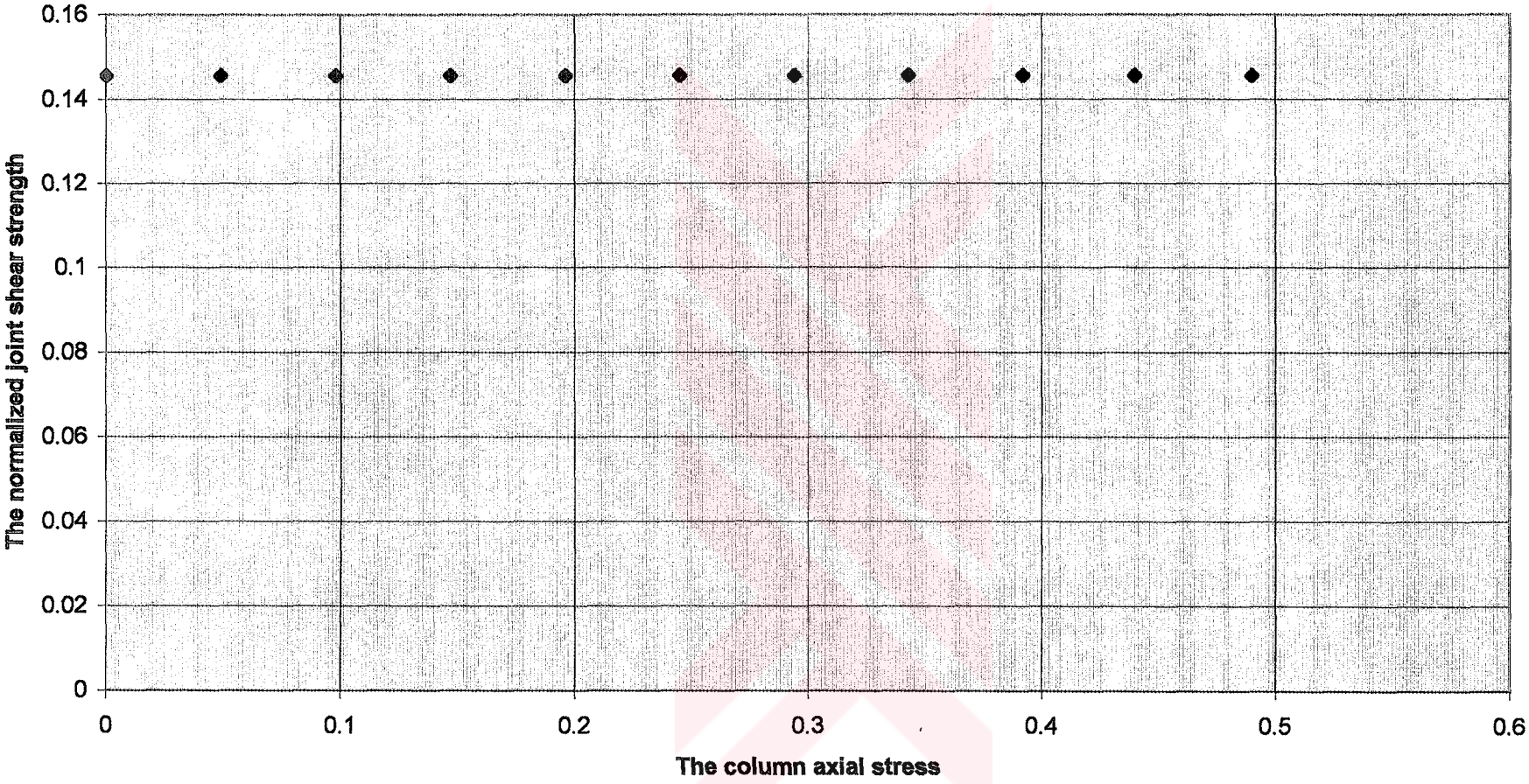

Figure 5.5. The influence of column axial stress on the predicted normalized joint shear strength of the author's model without stirrups

5.5.8. Column axial stress (with stirrups)

The parametric study in Figure 5.9 shows that the column axial load does not influence the joint shear strength. This is consistent with the test results analyzed in Chapter 4.

Table 5.7. Predicted Failure loads of Taylor

Specimen	Type of Detailing of the Beam Bars	Actual Failure Mode	Predicted Failure Mode	Cylinder Strength	Ppred/Pfail
Units	MPa	-	-	MPa	-
Taylor					
P1/41/24	4	J	J	33	0.746
P2/41/24	4	J	J	29	0.660
P2/41/24A	4	J	J	46.5	0.827
A3/41/24	4	J	J	27	0.606
A3/41/13	4	B	B	45	0.987
D3/41/24	4	B	J	53	0.780
D3/41/13	4	B	B	55.5	0.860
E3/41/24A	4	J	J	42.8	0.808
E3/41/24B	4	J	J	44.5	1.120
E3/41/24C	4	J	J	41.6	0.797
F3/41/24A	4	B	B	37.2	0.969
F3/41/24B	4	B	B	34.2	0.945
F3/41/24C	4	B	B	34.4	0.920
C3/41/24BY	2	J	J	31.7	0.870
C3/41/13Y	2	J	J	28.2	0.860
C3/41/24Y	2	J	J	59.5	0.959
Mean				40.193	0.857

5.6. A Simple Methodology for Predicting the Failure Modes

The author is of the opinion that one way of preventing the joint or column failures could be to put an upper limit on the beam longitudinal reinforcement ratio. Modeling of the joints without stirrups had shown that :

$$V_j = 0.38\, h_c / \sin\theta\, (b_c + b_b) / 2\; 0.6\, f_c (1 - f_c / 250) \cos\theta$$

$$V_j = 0.114\, h_c\, (b_c + b_b)\, f_c\, (1 - f_c / 250) / \tan\theta \qquad (5.23)$$

To stay on the conservative side, the shear force in the upper column will be neglected. The shear force in the joint should be equal to the resistance of the strut given by Equation 5.23.

$$0.87\, A_s\, f_y / b_b\, d_b = 0.114\, h_c (b_c + b_b)\, f_c (1 - f_c / 250) / \tan\theta\; b_b\, d_b$$

$$\rho_{b\,limit} = 0.13\, h_c\, (b_c + b_b)\, f_c\, (1 - f_c / 250) / \tan\theta\; b_b\, d_b$$

Conservatively, this limit will be adapted as follows:

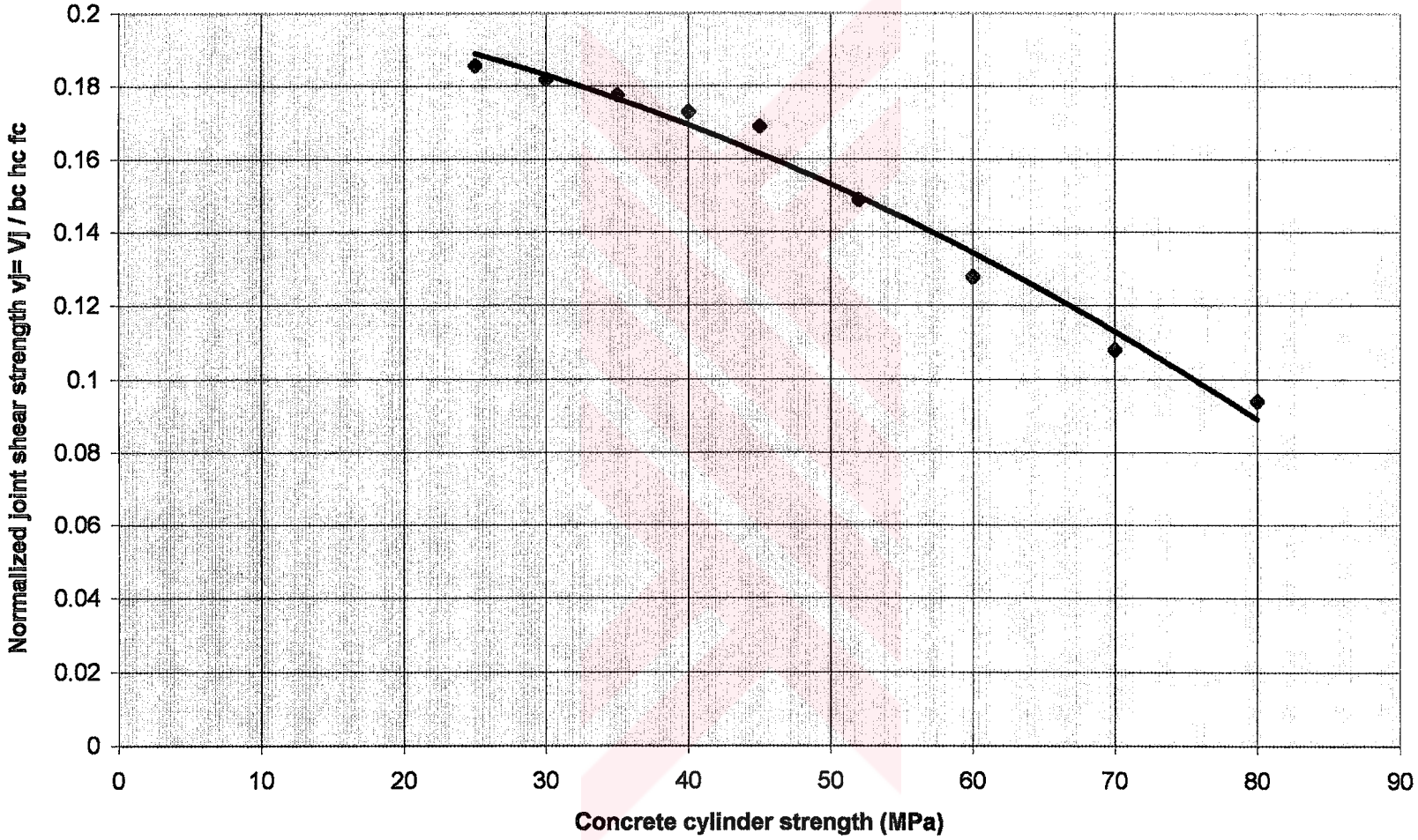

Figure 5.6. The effect of concrete cylinder strength on the normalized joint shear strength predicted by the author's model

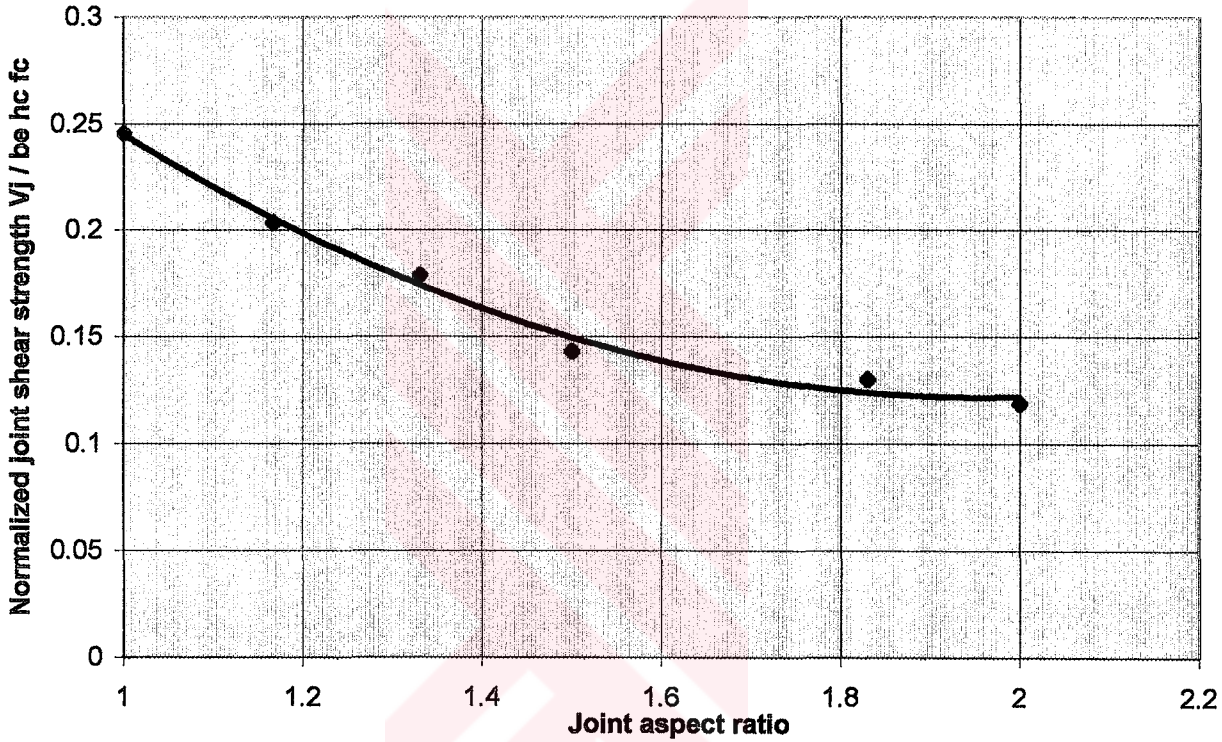

Figure 5.7 The effect of joint aspect ratio on the normalized joint shear strength of joints with stirrups predicted by the author's model

$$\rho_{b\,limit} = 0.15\, h_c (b_c + b_b)\, f_c (1 - f_c / 250) / \tan\theta\, b_b\, d_b \qquad (5.24)$$

The stirrups also influence the failure modes of monotonically loaded exterior beam column connections. This is natural due to the confining effect of stirrups. If the joints are fully confined by transverse reinforcement, then the cracked concrete strength of the joint will increase resulting in a strong connection. The author in chapter 4 had carried out a parametric study, the results of which showed the following:

If ρ = Asw / be hc ≤ 0.003 : The influence of the stirrups on the joint shear strength will be neglected.

If $0.003 \leq \rho \leq 0.0055$: The contribution of stirrups on the normalized joint shear strength will be 18.14 %. This range is the medium amount of stirrups. The stirrups all yield in this range at failure and failure usually initiated by the yielding of stirrups.

$\rho \geq 0.0055$: The contribution of stirrups on the normalized joint shear strength will be 29.7 % . This range is the high amount of stirrups. Not all the stirrups yield at this range.

The author developed a model which predicts the failure modes of monotonically loaded exterior beam column joints. The only model that predicts the failure modes is the model of Taylor in literature whose details are given in Chapter 4. The author had criticized the model of Taylor in that it does not take into account some important factors such as the column axial load, column longitudinal reinforcement ratio, stirrups and the detailing of the beam reinforcement. The author is of the opinion that Taylor's model should not be used to predict the failure modes of the exterior beam column joints.

The author's model predicts that the upper limits for the joints with medium and high amount of stirrups are as follows respectively.

$$\rho_{b\,limit} = 0.18\, h_c (b_c + b_b)\, f_c (1 - f_c / 250) / \tan\theta\, b_b\, d_b \qquad (5.25)$$

$$\rho_{b\,limit} = 0.22\, h_c (b_c + b_b)\, f_c (1 - f_c / 250) / \tan\theta\, b_b\, d_b\, f_y \qquad (5.26)$$

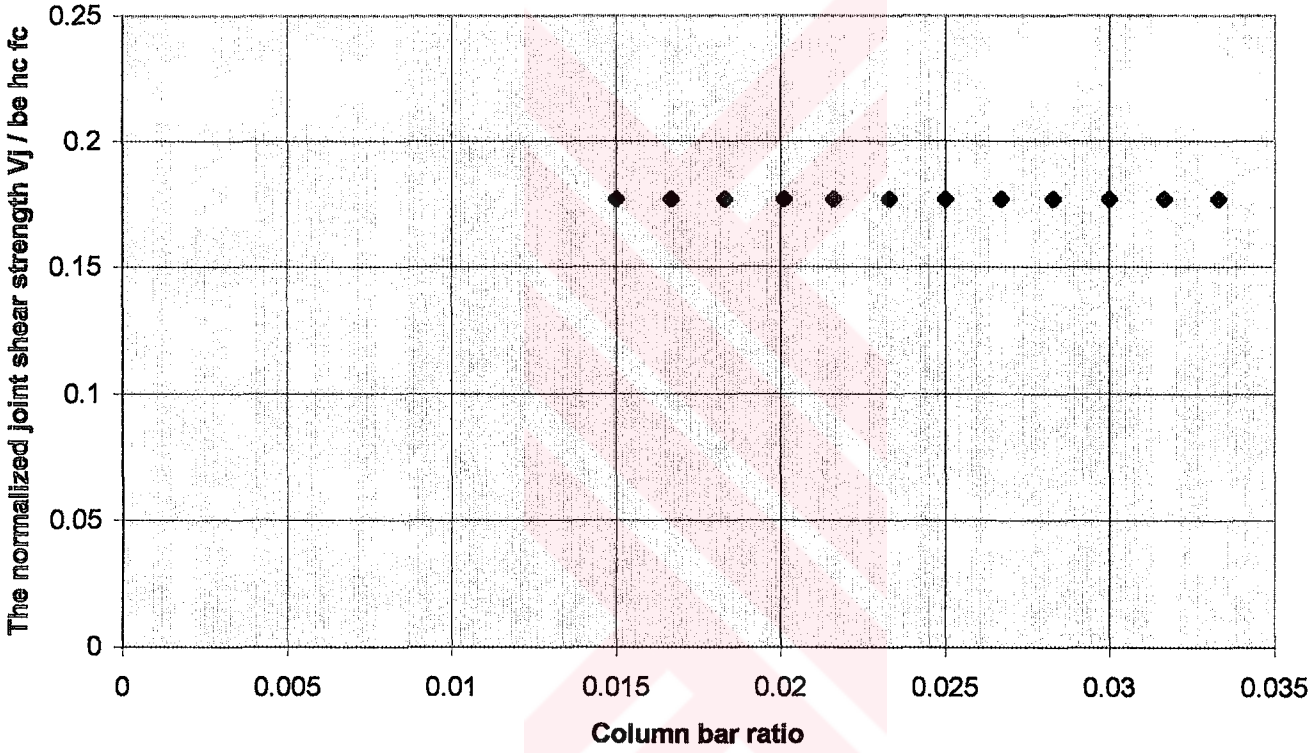

Figure 5.8 The effect of the column bar ratio on the normalized joint shear strength of joints with stirrups predicted by author's model

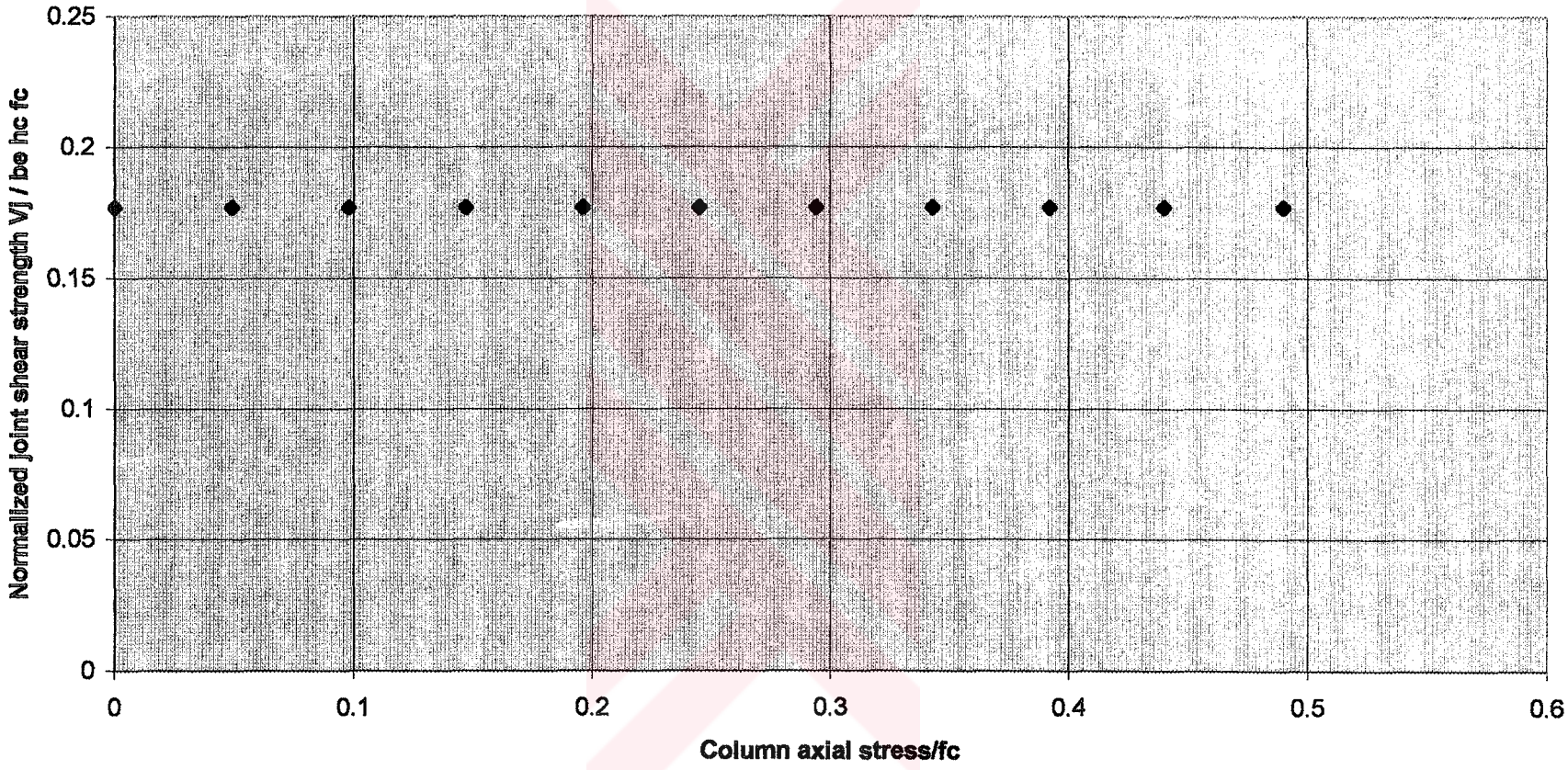

Figure 5.9. The effect of the column axial stress on the normalized joint shear strength of joints with stirrups predicted by the author's model

The author's models are given in Figures 5.10 and 5.11. Table 5.8 shows that the model estimates the failure modes of monotonically loaded exterior beam column joints accurately.

5.6.1. Results

The only model in literature that predicts the failure modes of monotonically loaded exterior beam column joints is the model of Taylor. The author is of the opinion that Taylor's model is incorrect due to the oversimplification of the factors influencing the failure modes of joints. Taylor said that by only limiting the beam longitudinal reinforcement ratio, the failure modes of joints can be predicted. The author of this thesis on the other hand showed that the factors influencing the failure modes of connections were column axial stress, stirrups, beam longitudinal reinforcement ratio, column longitudinal reinforcement ratio, h_c/d_b.

-The beam bar detailing:

The author had made a parametric study in chapter 4 showing that the joint shear strength of connections which have beam bars detailed in the form of U bars have 15 % less joint shear strengths than the connections which have beam bars bent down detail. This means the upper limit for the beam longitudinal reinforcement ratio proposed by the author should be decreased by 15 % when the beam longitudinal reinforcement are detailed in the form of U bars. The author applied her model on the tests of Scott which have all the three types of detailing. The model predicts that the failure mode of joints without stirrups and have a column axial stress higher than 0.053 and have column height to beam bar diameter higher than 10 are different for beam bars bent up detail and beam bars bent down detail or U bars. Figure 5.11 shows that the beam bars bent up detail exhibit shear failure, while the U bars or beam bars bent down detail exhibit beam failure. Although a joint has high column axial stress and high ratio of the column height to beam longitudinal reinforcement ratio and although the beam longitudinal reinforcement ratio of the joint is less than

the limit proposed by the author, the joints with beam bars bent up detail will still exhibit joint shear failure. The flexural failure of the beam is always preferred to shear failure of the joint. This shows that L bars bent up detail should not be used.

Table 5.8. The application of the simple methodology on the experimental database

Investigator	specimen	detail	N (kN)	$N/b_c d_c f_c$	P (kN)	Failure mode	Predicted Failure mode
Ortiz	BCJ 1	L bar	0	0	118	JS	JS
	BCJ 2	L bar	0	0	125	JS	JS
	BCJ 3	L bar	0	0	118	JS	JS
	BCJ 4	L bar	0	0	130	JS	JS
	BCJ 5	L bar	300	0.14	115	JS	JS
	BCJ 6	L bar	300	0.16	115	JS	JS
	BCJ 7	L bar	300	0.16	170	B	B
Kordina	RE 2	L bar	240	0.29	67	JS	JS
	RE 3	L bar	400	0.3	80	JS	JS
	RE 4	L bar	51	0.05	51	JS	JS
	RE6	L bar	213	0.2	66	JS	JS
	RE7	L bar	650	0.5	117	JS	JS
	RE8	U bar	525	0.37	105	JS	JS
	RE9	U bar	770	0.55	110	JS	JS
	RE10	U bar	551	0.46	100	JS	JS
Taylor	P1/41/24	L bar	240	0.47	35	JS	JS
	P2/41/24	L bar	240	0.54	35	JS	JS
	P2/41/24A	L bar	240	0.33	47	JS	JS
	A3/41/24	L bar	240	0.58	35	JS	JS
	D3/41/24	L bar	60	0.07	50	JS	JS
	B3/41/24	L bar	240	0.70	30	JS	JS
	C3/41/24BY	U bar	240	0.48	29	JS	JS
	C3/41/13Y	U bar	240	0.55	27	JS	JS
Scott	C1AL	L bar	50	0.086	22	JS	JS
	C1	L bar	275	0.39	26.2	B	B
	C4	L bar	275	0.38	30	JS	JS
	C4A	L bar	275	0.35	32	JS	JS
	C4AL	L bar	50	0.079	28	JS	JS
	C1A	L bar	275	0.33	26.8	B	B
	C3	U bar	275	0.43	25.9	B	B
	C7	L bar	275	0.45	32	JS	JS
	C3L	U bar	50	0.08	22	JS	JS
	C6	U bar	275	0.39	22	JS	JS
	C6L	U bar	50	0.06	26	JS	JS
	C9	U bar	275	0.43	28	JS	JS
S & Hamil	C4ALNO	L bar	50	0.067	27	P	P
	C4ALN1	L bar	50	0.062	34	JS	JS
	C4ALN3	L bar	50	0.068	35	JS	JS
	C4ALN5	L bar	50	0.057	40	JS	JS
	C4ALHO	L bar	100	0.055	43	P	P
	C4ALH1	L bar	100	0.059	43.4	B	B
	C4ALH3	L bar	100	0.054	46.1	B	B
	C4ALH5	L bar	100	0.058	48.7	B	B
	C6LNO	U bar	50	0.056	24	JS	JS
	C6LN1	U bar	100	0.112	25	JS	JS
	C6LN3	U bar	50	0.058	29	JS	JS
	C6LN5	U bar	50	0.077	34	JS	JS
	C6LHO	U bar	100	0.056	36	JS	JS
	C6LH1	U bar	100	0.056	37	JS	JS
	C6LH5	U bar	100	0.057	51.4	B	B
	C6LH3	U bar	100	0.059	41	JS	JS
parker	4a	L bar	0	0	118	C	C
	4b	L bar	300	0.104	138	JS	JS
	4c	L bar	600	0.22	170	JS	JS
	4d	L bar	0	0	150	JS	JS
	4e	L bar	300	0.102	160	JS	JS
	4f	L bar	600	0.215	183	JS	JS
	5a	L bar	0	0	213	C	C
	5b	L bar	300	0.094	236	JS	JS
	5d	L bar	0	0	226	C	C
	5e	L bar	300	0.090	295	C	C
	5f	L bar	600	0.19	322	JS	JS

The model also shows that a joint which has beam longitudinal reinforcement ratio less than the limit proposed by the author with a column axial stress higher than 0.053 and a ratio of the height of the column to beam bar diameter less than 10 and is supplied by a single stirrup in the joint has different failure modes for joints detailed by L bars bent down detail and U bar detail. The L bars bent down detail specimens exhibit beam failure while the U bars exhibit joint shear failure. The behavior of the joints will be improved if the beam bars bent down detail specimens are used instead of U bar or L bars bent up detail.

-The Joint Stirrups:

The joint stirrups also influence the failure modes of the monotonically loaded exterior beam column connections. The author had shown in chapter 4 that if the joint is provided by low amount of stirrups, the contribution of stirrups to joint shear resistance can be neglected. However, if the joint is provided by medium or high amount of stirrups, the joint shear resistance will be improved by 18.14 % and 29.7 % respectively. This is satisfactorily taken into account by increasing the limit imposed on the beam longitudinal reinforcement ratio for the joints with no or low amount of stirrups. Different upper limits for beam bar ratio for joints with high amount of stirrups and for joints with medium amount of stirrups are imposed in the model.

The model also shows a very important feature of monotonically loaded exterior beam column connections. As stated above, the author had done several parametric studies in Chapter 4 and had found out that the joints which have stirrup ratios less than 0.003 do not effect the joint shear strength of monotonically loaded exterior beam column connections. However, the author's model shows that the failure modes of joints is strongly effected by the provision of even a single stirrup. If a joint has low amount of stirrups with a beam bar ratio less than the limit proposed by the author and with a high column axial stress and a column height to beam bar diameter ratio less than 10, the provision of a single stirrup will change the failure mode from connection zone reinforcement pull out to beam flexural failure (if the joint has beam bars bent down detail) or to joint shear failure (if other detailing types are applied) for the beam bars. In the case of the failure mode of joints with a beam longitudinal

reinforcement ratio higher than the limit proposed by the author and with low amount of stirrups and with a column axial stress less than 0.005 and with a column bar ratio higher than 0.001 and with a height of the column to diameter of the beam bar less than 10 will change from connection zone reinforcement pull out to joint shear failure by the provision of a single stirrup in joints with beam bars bent down detail.

-Column Axial Load

It is apparent from the model that as the column axial load is increased, the failure modes change from column failure to joint to beam failure gradually. Therefore we can conclude that column axial load improves the failure mode of monotonically loaded exterior beam column connections.

-Column Bar Ratio

The column bar ratio is also influential in determining the failure mode. If the column bar ratio is less than a certain limit and if the same joint has low column axial stress, this certainly leads to column flexural failure in monotonically loaded exterior beam column connections. The model shows that failures in the upper column can be avoided if the column bar ratio is higher than a certain limit. This does not change whether the joint is provided with stirrups or not. The author's model is in agreement with the test results of Scott, Ortiz , Scott and Hamill , Parker Bullman and Kordina. However more experiments are needed to refine the model. One striking result of the model is that the model shows that the failure mode of monotonically loaded exterior beam column connections are insensitive to joint aspect ratio.

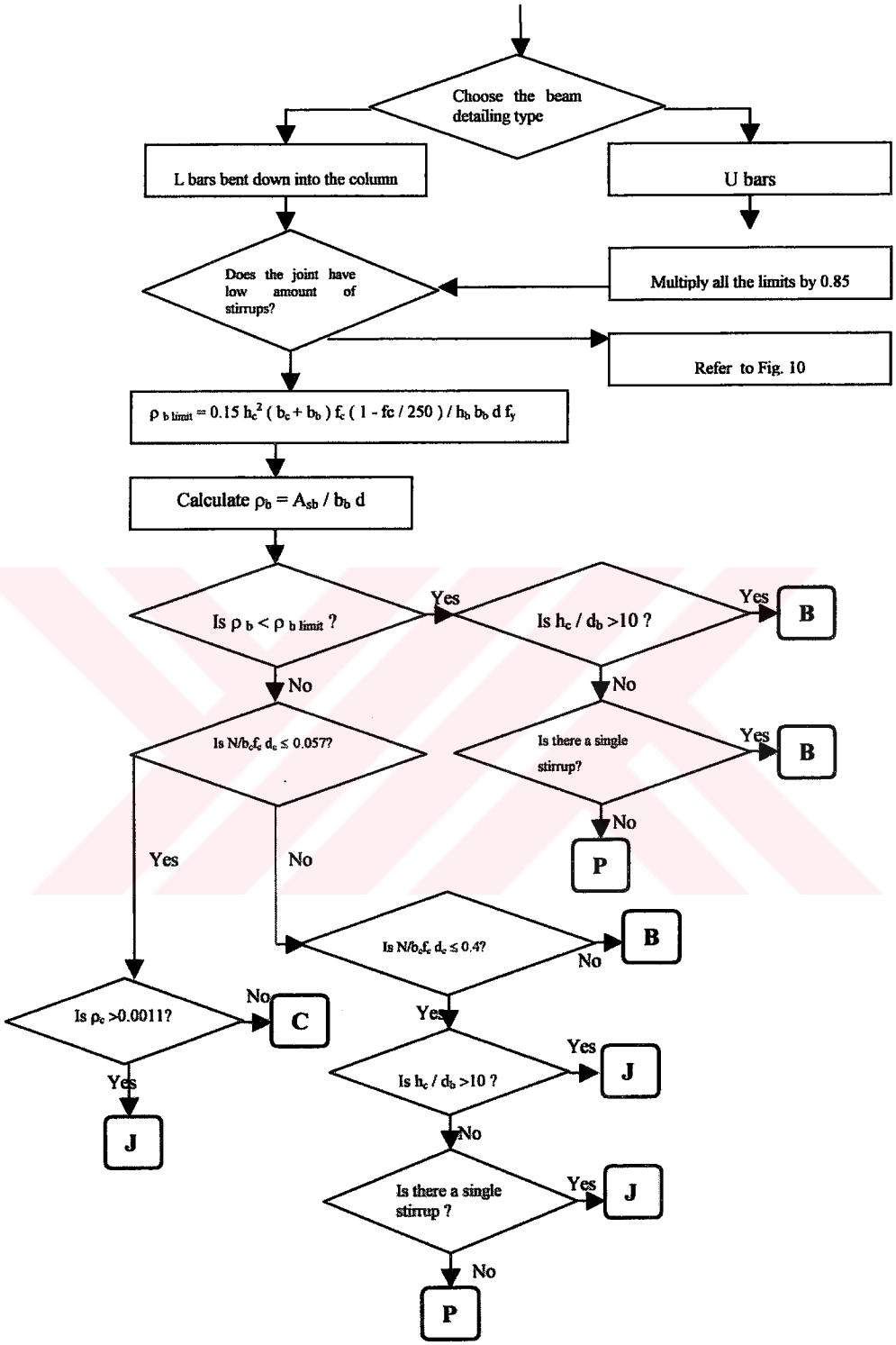

Figure 5.10. The methodology for predicting the failure modes of joints without stirrups

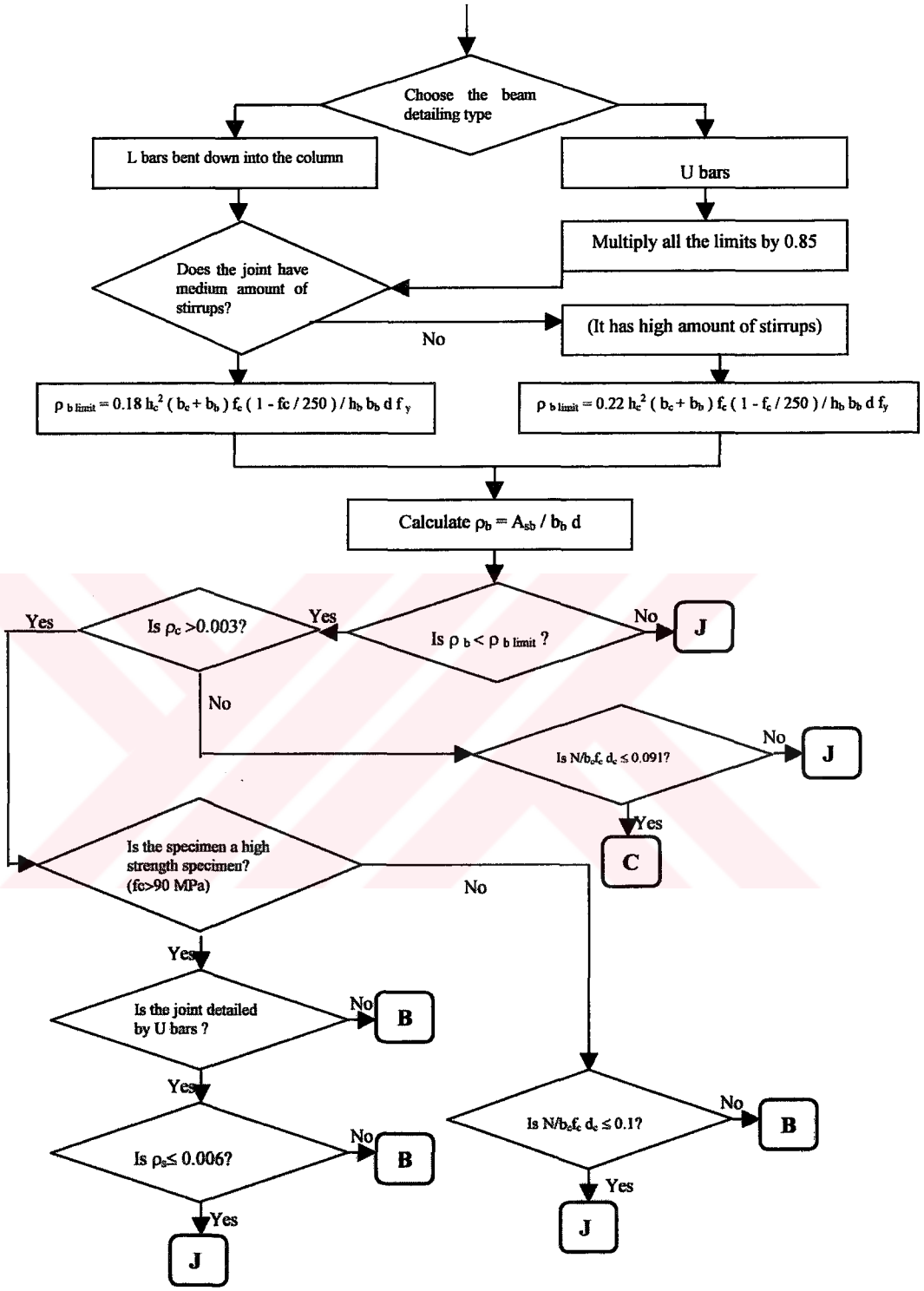

Figure 5.11. The methodology for predicting the failure modes of joints with stirrups

Note: P represents the connection zone reinforcement pullout, C represents the column failure, B represents the beam failure,JS represents the joint shear failure

6. CONCLUSIONS

6.1. Overview of the thesis

This thesis has three original contributions. The first is the proposal for a new design equation for predicting the joint shear strength. The second is the proposal for a new methodology for predicting the failure modes of joints and the third is the proposal for a new strut and tie model for joints.

6.2. The Proposed Design Equation

The following design equation is proposed by the author, for predicting the joint shear strength.

$$V_j = \frac{0.71\ \beta\ \gamma (100\ * \frac{A_{sb}}{b_b d})^{0.4289} (\frac{b_c + b_b}{2})\ h_c \sqrt{f_c}}{(\frac{h_b}{h_c})^{0.61}} + \alpha\ A_{sje} f_y \qquad (6.1)$$

where $\alpha = 0.664$ for joints with low amount of stirrups

$\alpha = 0.600$ for joints with medium amount of stirrups

$\alpha = 0.370$ for joints with high amount of stirrups

A_{sb} is the area of tensile reinforcement in the beam (mm^2)

b_c is the width of the column (mm)

b_b is the width of the beam (mm)

h_b is the cross-sectional height of the column (mm)

h_c is the cross-sectional height of the beam (mm)

d is the effective depth of the beam (mm)

A_{sje} is the area of the stirrups (mm^2)

f_y is the yield strength of the stirrups (MPa)

Results

The equation is an improvement to other equations because:

1. It realistically models the contribution of stirrups in the joint.
2. It takes the influences of beam longitudinal reinforcement ratio into account.
3. It realistically models the influence of the joint aspect ratio.
4. It realistically models the influence of concrete cylinder strength.
5. The equation is simple and accurately predicts the joint shear strength.

6.3. The proposed strut and tie model

A new strut and tie model is proposed by taking the weaknesses of the previously suggested models in literature. In this model, the angle of inclination of the direct strut can be accepted as shown below:

$\tan\theta = h_b/h_c$ (6.2)

The **CEB Code 90** equation (in MPa) given by the below equation is used for the cracked concrete strength due to the practicability it provides.

$$f_{cr} = 0.6 f_c (1 - \frac{f_c}{250}) \quad \text{in MPa} \quad (6.3)$$

The ultimate joint shear resistance of a joint without stirrups is given by the equation:

$$V_j = w f_{cr} b_e \cos\theta \quad (6.4)$$

w is the width of the direct strut mechanism (mm)

f_{cr} is the cracked concrete strength (MPa)

b_e is the effective joint width (mm)

θ is the angle of inclination of the direct strut mechanism

This formulation is applied to joints without stirrups and it has been found out that the failure loads are predicted most accurately when the equation has a constant of 0.114. The simplified equation is therefore;

$$V_j = 0.114\ h_c^2 (b_c + b_b) \frac{f_c (1 - \frac{f_c}{250})}{h_b} \qquad (6.5)$$

The inspection of tests has shown that not all the stirrups are at yield at failure. In this study, the influence of stirrups on the joint shear strength for low amount of stirrups is neglected, as the joint shear strength is not much influenced by low amount of stirrups. The joint shear strength is increased by 18.14 % average when the joint has a stirrup ratio of 0.003 to 0.0055. The joint shear strength increases by 29.7% when the joint is provided by high amount of stirrups. It is apparent that beam bars can not equilibrate the indirect strut mechanism and some other mechanism should be equilibrating the force in the indirect strut. In order to maintain equilibrium in the upper node, another strut coming from the upper column, which is equilibrated, by the upper column ties in the vertical direction and the stirrups of the confinement region of the column in the horizontal direction is necessary to equilibrate the force in the indirect strut. The proposed simple strut and tie model of authors is shown in Figure 5.1 and the below figure. The failure loads of joints in the experimental database are calculated by using the simple model shown in Figure 5.1. The average of the ratio of the predicted failure loads of the model to the actual failure loads of the specimens in the experimental database is 0.99. As apparent, the model gives accurate predictions of the failure loads.

Parametric studies are carried out to investigate the influence of the concrete cylinder strength, column longitudinal reinforcement ratio, column axial stress and the joint aspect ratio in joints with and without stirrups.

The model predicted that the joint shear strength normalized by the concrete cylinder strength, $V/b_e\ h_c\ f_c$, slightly decreased due to increasing concrete cylinder strength in joints without stirrups. This prediction is in agreement with the test data because the joint shear strength, in reality, is proportional to the square root of the concrete cylinder strength.

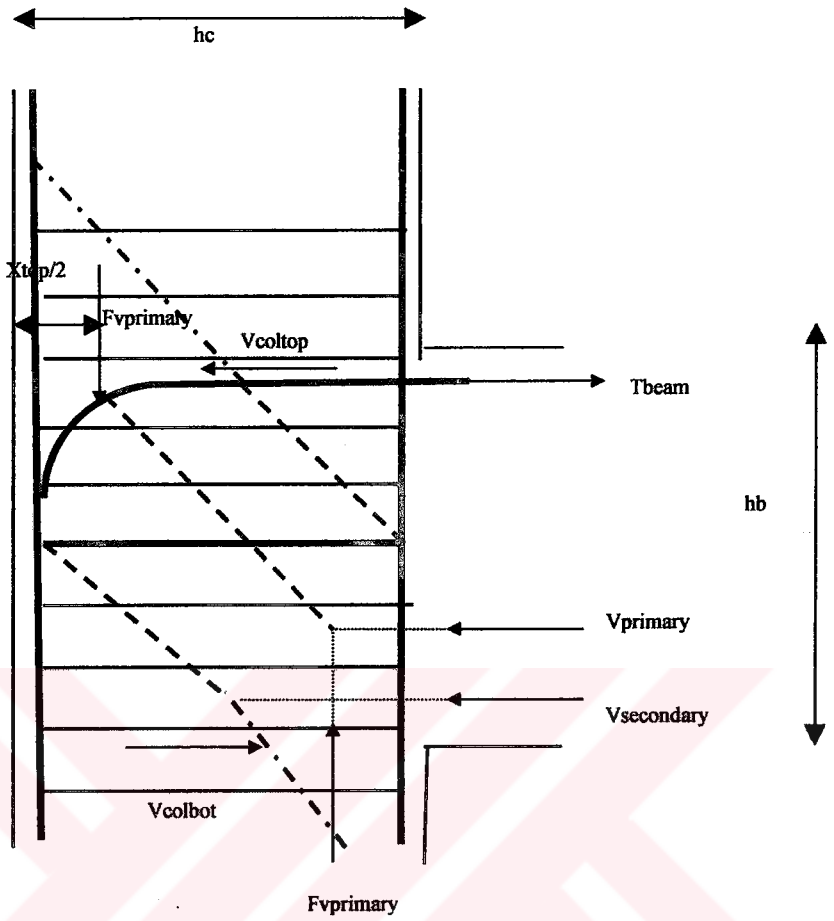

Figure 6.1: The proposed simple model of the author.

1. The model predicted that the joint shear strength, normalized by the concrete cylinder strength: $V/b_e\ h_c\ f_c$, slightly decreased due to increasing concrete cylinder strength in joints with stirrups. This prediction is in agreement with the test data because the joint shear strength, in reality, is proportional to the square root of the concrete cylinder strength, $\sqrt{f_c}$ not to f_c.
2. In joints without stirrups, the model predicted that the joint shear strength is independent of the column axial stress as the test data suggests.
3. In joints with stirrups, the model predicted that the joint shear strength is independent of the column axial stress as the test data suggests.
4. In joints without stirrups, the model predicted that the joint shear strength is independent of the column longitudinal reinforcement ratio as the test data suggests.

5. In joints with stirrups, the model predicted that the joint shear strength is independent of the column longitudinal reinforcement ratio as the test data suggests.
6. In joints without stirrups, the model predicted that the joint shear strength decreased with increasing joint aspect ratio. This is in agreement with the test data.
7. In joints with stirrups, the model predicted that the joint shear strength decreased with increasing joint aspect ratio. This is in agreement with the test data.

As apparent from the parametric studies, the model is in good agreement with the test data.

6.4. The Proposed Methodology for Failure Modes

In this part of the thesis, a new methodology for predicting the failure modes of joints is presented. The proposed methodology is different for joints without significant amount of stirrups and for joints with medium or high amount of stirrups. For joints without stirrups, the following limit equation is proposed for the beam longitudinal reinforcement ratio:

$$\rho_{b\,\lim} = 0.15\, h_c^{\,2}\,(b_c + b_b)\,\frac{f_c\,(1 - \frac{f_c}{250})}{h_b\; b_b d\; f_y} \tag{6.6}$$

For joints with medium stirrups, this limit is increased by 18 %.

$$\rho_{b\,\lim\,it} = 0.18 h_c^{\,2}(b_c + b_b)\frac{f_c(1 - \frac{f_c}{250})}{h_b b_b d\; f_y} \tag{6.7}$$

For joints with high amount of stirrups, this limit is increased by 30%.

$$\rho_{b\,\lim\,it} = 0.22 h_c^{\,2}(b_c + b_b)\frac{f_c(1 - \frac{f_c}{250})}{h_b b_b d\; f_y} \tag{6.8}$$

The model of author is shown in Figures 5.10 and 5.11.

Results:

1. In cyclically loaded joints, only 90^0 hooks are permitted and L bars bent up or U bar detail joints are not permitted. Monotonically loaded joints should also follow the same norm.
2. Column axial load significantly affects the failure mode. A specimen with a high column axial load and high column longitudinal reinforcement ratio and a beam longitudinal reinforcement ratio less than the proposed limits, with either medium (stirrup area ratio $A_{sje}/b_{eff}\ h_c$ between 0.003 and 0.0055) or high amount of stirrups (stirrup area ratio higher than 0.0055) is necessary for an exterior beam column connection for superior performance.
3. In monotonically loaded joints with medium or high amount of stirrups, the joints will never perform adequately unless their beam longitudinal reinforcement ratios are less than the proposed limits.
4. Stirrups affect the failure modes differently for cyclically loaded or monotonically loaded beam-column joints. Cyclically loaded joints with medium or high amounts of stirrups can exhibit anchorage failure. The monotonically loaded joints with medium and high amount of stirrups, however, are unlikely to exhibit anchorage failure.
5. The proposed value of 10 for h_c/d_b is too low for cyclically loaded joints to prevent anchorage failure. However, in monotonically loaded joints without stirrups, this lower limit is adequate to prevent anchorage failures.
6. In joints with medium and high amount of stirrups and with beam longitudinal reinforcement ratios less than that predicted by the proposed limits, the joints will exhibit column failure unless the column longitudinal reinforcement ratio and the column axial load are higher than the proposed limits in the proposed methodology.
7. The increase of the stirrup ratio above the limit of 0.006 has a more pronounced effect on the failure modes of the U bar detail specimens than the L bars bent

down detail specimens. The U bar detail specimens with stirrup ratios less than 0.006 are unlikely to exhibit beam failure although the beam longitudinal reinforcement ratio is less than the proposed limits.

6.5.Joint mechanics

In order to investigate the reliability of the proposed design equation, the established equations on the basic mechanics of reinforced concrete beam-column joints are investigated. This has been also previously discussed by **Paulay** and by **Bonacci & Pantazopoulou** for interior joints who have also taken into account the joint deformations. Both of the authors use the average stresses for equilibrium as shown in below which depicts the equilibrium of vertical and horizontal forces. Figures 4.48 and 4.49 show the joint geometry and the stress equilibrium respectively.

Figures show that equilibrium of forces in the horizontal direction require the average transverse compressive stress in the joint σ_x defined as:

$$\sigma_x = -\frac{A_{sb}}{b_{eff} h_b} f_s - \frac{A_{sje}}{b_{eff} h_b} f_w \tag{6.9}$$

where f_s is the average stress in the beam reinforcement,

f_w is the average stress in the transverse reinforcement

Consequently, the average normal concrete stress in the y direction σ_y can be expressed as :

$$\sigma_y = -\frac{A_{scol}}{b_{eff} h_c} f_{scol} - \frac{N}{b_{eff} h_c} \tag{6.10}$$

where f_{scol} is the average stress in the column reinforcement

N is the column axial load

Collins and Mitchell suggest the following equation for the maximum stress in concrete panels;

$$f_{2\max} = \frac{f_c}{0.8 + 170\varepsilon_1} \langle f_c \tag{6.11}$$

The principal compressive stress is given by;

$$\sigma_2 = \sigma_x + \sigma_y = -\tau_{av}(\tan\theta + \frac{1}{\tan\theta}) \tag{6.12}$$

σ_2 is also given from Mohr's circle as;

$$\sigma_2 = \left(2(\frac{\varepsilon_2}{-0.002}) - (\frac{\varepsilon_2}{-0.002})^2\right) f_{2\max} \tag{6.13}$$

Thus the average joint shear stress can be expresses as;

$$\tau_{av} = -\frac{\sigma_2}{(\tan\theta + \frac{1}{\tan\theta})} \tag{6.14}$$

The above equations show very clearly that as the principal tensile strain increases, the average joint shear stress decreases. Thus it is necessary to express the principal tensile strain in terms of the strains in the *x* and *y* directions in order to investigate the factors that influence the joint shear strength. From joint kinematics;

$$\varepsilon_1 = (\frac{\varepsilon_x - \varepsilon_y \tan^2\theta}{1 - \tan^2\theta}) \tag{6.15}$$

The next step will be to express the strains in the *x* and *y* directions in terms of the stresses.

$$\sigma_x = -\tau_{av}\tan\theta = -\frac{A_{sb}f_s}{b_{eff}h_b} \quad -\frac{A_{sje}f_w}{b_{eff}h_b} = -(\frac{A_{sb}}{b_{eff}h_b}\mu + \frac{A_{sje}}{b_{eff}h_b})f_w \tag{6.16}$$

where $\mu = f_s/f_w$

The strain in the *x* direction can therefore be expressed as;

$$\varepsilon_x = \frac{f_w}{E_s} = \frac{\tau_{av}\ \tan\ \theta}{E_s(\frac{A_{sb}\mu}{b_{eff}h_b} + \frac{A_{sje}}{b_{eff}h_b})} \tag{6.17}$$

The strain in the *y* direction can similarly be expressed as;

$$\varepsilon_y = \frac{f_{scol}}{E_s} = (\frac{\tau_{av}}{\tan\theta} - \frac{N}{b_{eff}h_c})\frac{b_{eff}h_c}{A_{scol}E_s} \tag{6.18}$$

If the strains in the x and y directions are substituted into the equation for determining the principal tensile strain and the angle of inclination is taken as the ratio of the height of the beam to the height of the column, the following equation is obtained.

$$\varepsilon_1 = \frac{1}{E_s(1-(\frac{h_b}{h_c})^2)}((\tau_{av}\frac{h_b}{h_c}(\frac{1}{\frac{A_{sb}\mu}{b_{eff}h_b}+\frac{A_{sx}}{b_{eff}h_b}}-\frac{1}{\frac{A_{scol}}{b_{eff}h_c}}))+\frac{N(\frac{h_b}{h_c})^2}{A_{scol}}) \quad (6.19)$$

The above equation shows that the principal tensile strain is increased by the joint aspect ratio and column longitudinal reinforcement ratio and the axial load on the column whereas it is decreased by increasing beam longitudinal reinforcement ratio and the stirrup ratio. The shear stress in the joint is dependent on the principal tensile strain as evident from Mitchell and Collins equation. It is therefore evident that the joint shear strength increases as the beam longitudinal reinforcement ratio and the transverse reinforcement ratio increases. The joint shear strength increases as the column load and the column longitudinal reinforcement increases but as the longitudinal column reinforcement and the column load increases, the principal tensile stresses increase which consequently decreases the normalised joint shear strength. Therefore the increase in the joint shear strength due to the equilibrium equations is offset by the increase in the principal tensile strain. The above conclusions are totally in accordance with the predictions of the author's equation.

6.6. Recommendations for future research

1. More tests are needed to investigate the behavior of joints with joint aspect ratios higher than 2.

2. The methodology suggested by the author for predicting the failure modes should be improved or supported by further tests. The applicability of the proposed limits should be further confirmed by tests.

3. Joint tests with slabs and transverse beams are needed.

6.7. Final words

At the back of the thesis, the algorithms of the various computer programs written by the author are provided. The computer programs written for the parametric studies are not provided but discussed in detail throughout the thesis. The author's conclusions are as follows:

1. The so called strut and tie models can and must be used only for monotonically loaded joints. This is mainly because, the stirrup strains are dependent on the loading history and the cracking and the extent of damage are influenced by the number of cycles. Furthermore in monotonically loaded joints, the model adapted will only reflect the behavior approximately. The model therefore can be used for predicting the failure loads, but for predicting the failure modes, the author suggests that her simple methodology should be used. As the strut and tie model adapted will always reflect the behavior of joints approximately, the author is of the opinion that the model should be as simple as possible.
2. The author suggests that her simple design equation is very useful in avoiding bad specimens such as the specimens of **Parker and Bullman** with low normalized joint shear strength.
3. The equation proposed is an improvement on the existing design equations. It is very accurate and is in agreement with the test data.

REFERENCES

Aoyama, H., 1993. Problems Associated with "Weak-Beam" Design of Reinforced Concrete Frames, in *A Volume Honoring Hiroyuki Aoyama,* pp.47-77, Ed. T.Okada, University of Tokyo, Tokyo.

ACI-ASCE Committee 352 1985. Recommendations for the design of beam-column joints in monolithic reinforced concrete structures, *ACI Journal, Proceedings* **82**, No:3, 266-283.

ACI 318-89, 1989. Building Code Requirements for Reinforced Concrete, *American Concrete Institute,* Detroit.

ATC 3-06, 1978. Tentative provisions for the development of the seismic regulations for buildings, *Applied Technology Council,* California.

Bonacci J. and Pantazopoulou S., 1992. Consideration of questions about beam-column joints, *ACI Journal,* **89**, 27-37.

CEB-FIP, 1990. Model Code for Concrete Structures, *CEB-FIP International Recommendations*, Paris.

Cheung, P.C., Paulay, T. and Park R., 1992. Some possible revisions to the seismic provisions of the New Zealand Design Code for moment resisting frames. *Bulletin of the New Zealand Society for Earthquake Engineering,* **25.**

Collins, M.P. and Mitchell, D., 1980. Shear and torsion design of prestressed and non-prestressed concrete beams, *PCI Journal*, **25**, 32-100.

Fujii, S. and Morita S., 1991. Comparison between interior and exterior reinforced concrete beam-column joint behavior, in *SP 123*, pp.145-166, Ed. J. Jirsa, American Concrete Institute, Detroit.

Halim, K.J., 1993. Behaviour of Three Dimensional Beam Column Slab Connections, in *A Volume Honoring Hiroyuki Aoyama,* pp.307-314, Ed. T.Okada, University of Tokyo, Tokyo.

Hsu, T. C., 1996. Toward a unified nomenclature for reinforced concrete theory, *Journal of Structural Engineering,* 122, **3**, 275-283.

Ichinose, T., 1991. Interaction between bond at beam bars and shear reinforcement in RC interior joints, in *SP 123*, pp.379-400, Ed. J. Jirsa, American Concrete Institute, Detroit.

Ishibashi, K., 1993. Bond Strength and Failure Mechanism within Beam-Column Joint, in *A Volume Honoring Hiroyuki Aoyama,* pp.287-296, Ed. T.Okada, University of Tokyo, Tokyo.

Kamimura, T., 1993. Shear Strength of Interior Beam Column Joints, in *A Volume Honoring Hiroyuki Aoyama*, pp.265-276, Ed. T. Okada, University of Tokyo, Tokyo.

Keong, Y.S., 1978. Prestressed beam-column joints, *Research Report,* **78/2** Department of Civil Engineering, University of Canterbury, 81 p.

Kitayama, K., 1993 Limitation of Beam Bar Bond Deterioration within Beam Column Joint, in *A Volume Honoring Hiroyuki Aoyama*, pp.297-306, Ed. T. Okada, University of Tokyo, Tokyo.

Kordina, K., 1984. Bewehrungsfuhrung in Ecken und Rahmenendknoten, *Deutcher Ausschuss für Stahlbeton*, **354**, pp93. (reference: Vollum (1998))

Kurose, Y., 1993. Design of Beam Column Joints for Shear, in *A Volume Honoring Hiroyuki Aoyama*, pp.277-286, Ed. T. Okada, University of Tokyo, Tokyo.

Leon, R., 1989. Interior Joints with Variable Anchorage Lengths, *ASCE Journal of Structural Engineering,* **115**.

MacGregor, J. G. 1988. Reinforced concrete mechanics and design, Prentice - Hall, Englewood Cliffs, N.J.

Marti, P., 1985. Basic tools of reinforced concrete beam design, *Journal of American Concrete Institute,* **82**, 46-56.

Megget, L.M. and Park R., 1971. Reinforced Concrete Exterior Beam Column Joints Under Seismic Loading, *New Zealand Engineering,* 341-353.

Nielsen, M.P., Braestrup, M.W., Jensen, B.C. and Bach, F., 1978. Concrete Plasticity-Beam Shear, Shear in Joints, Punching Shear, Danish Society for Structural Science and Engineering Structural Research Laboratory, Technical University of Denmark, Special Publication.

Nishimura Y. and Minami K., 1988. Anchorage behavior of bent bar in exterior beam column joints under seismic loading. *Proceedings of the 9th world conference on earthquake engineering,* Tokyo, Kyoto, JAPAN

Parker, D.E. and Bullman, P.J.M., 1995. Shear strength of reinforced concrete - the influence of shear span, *The Structural Engineer,* **73**, 413.

Parker, D.E. and Bullman, P.J.M., 1997. Shear strength within reinforced concrete beam - column joints, *The Structural Engineer,* **75**, 53-57.

Paulay, T., 1989. Equilibrium Criteria for Reinforced Concrete Beam-Column Joints, *ACI Structural Journal*, **86**, 635-643.

Paulay,T., Scarpas A., 1981. The behavior of exterior beam column joints". *Bulletin of The New Zealand National Society for Earthquake Engineering.* **14**, 131-144.

Park, R. and Keong Y. S., 1979. Tests on Structural Concrete Beam Column Joints with Intermediate Column Bars, *Bulletin of the New Zealand National Society for Earthquake Engineering*, **12**, 2361-2376.

Ramirez, J. A., and Breen, J. E., 1983. Proposed design procedure for shear and torsion in reinforced and prestressed concrete, Research report 248-4F, Center for Transport Res., University of Texas, Austin.

Reys de Ortiz, 1993. Strut and tie modelling of reinforced concrete short beams and beam column joints, *PhD thesis,* University of Westminster.

Schlaich, J., Schafer, K., 1991. Design and detailing of structural concrete using strut and tie models, *The Structural Engineer*, **69**, 113-125.

Schlaich, J., Schafer, K. and Jennewein, M., 1987. Toward a consistent design of structural concrete, *PCI Journal*, **32**, 74-150.

Suzuki, N., 1993. Strength and Deformation of Three Dimensional Beam-Column-Slab Assemblage, in *A Volume Honoring Hiroyuki Aoyama*, pp.315-322, Ed. T. Okada, University of Tokyo, Tokyo.

TS 500, 2000. Betonarme yapıların hesap ve yapım kuralları, *Türk Standartları Enstitüsü,* Ankara.

Taylor H.P.J. and Clarke J.L., 1976 Some detailing problems in concrete frame structures, *The Structural Engineer* January, **54**, 19-54.

Taylor H.P.J., 1974. The behavior of insitu concrete beam-column joints, *Cement and Concrete Association, Technical Report,* **42.492**.

Sarsam, K.F. and Phillips, M.E., 1985. The shear design of insitu reinforced beam-column joints subjected to monotonic loading. *Magazine of Concrete Research,* **37**, 16-28.

Scott, R.H., 1992. The effects of detailing on RC beam column connection behavior, *The Structural Engineer*, **70**, 318-324.

Scott, R.H., Feltham I. and Whittle, R.T., 1994. Reinforced concrete beam column connections and BS 8110, *The Structural Engineer*, **72**, 55-60.

Scott, R.H. and Hamill, S.J., 1998. Connection zone strain in reinforced concrete beam-column connections, 11th International Conference on Experimental Mechanics, Oxford, UK, 65-69.

Vecchio F.J. and Collins M.P., 1986. The Modified compression field theory for reinforced concrete elements subjected to shear, *ACI Journal,* **83**, 219-231

Vollum, R. L. , 1998. Design and analysis of exterior beam column connections, *PhD Thesis,* Imperial College, London.

A- APPENDIX

1. The model of Ortiz

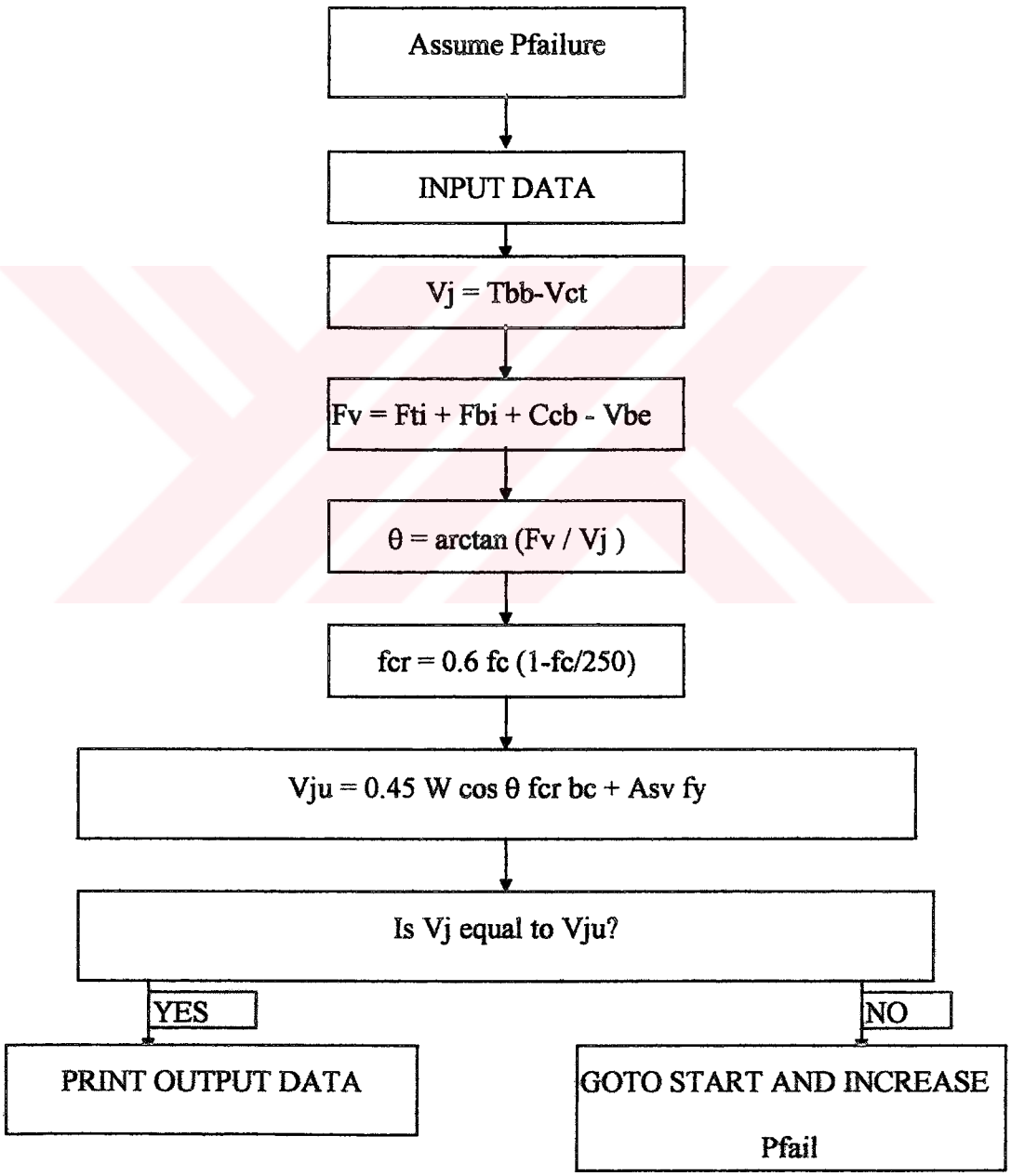

APPENDIX A

2. The Algorithm for the model of Vollum

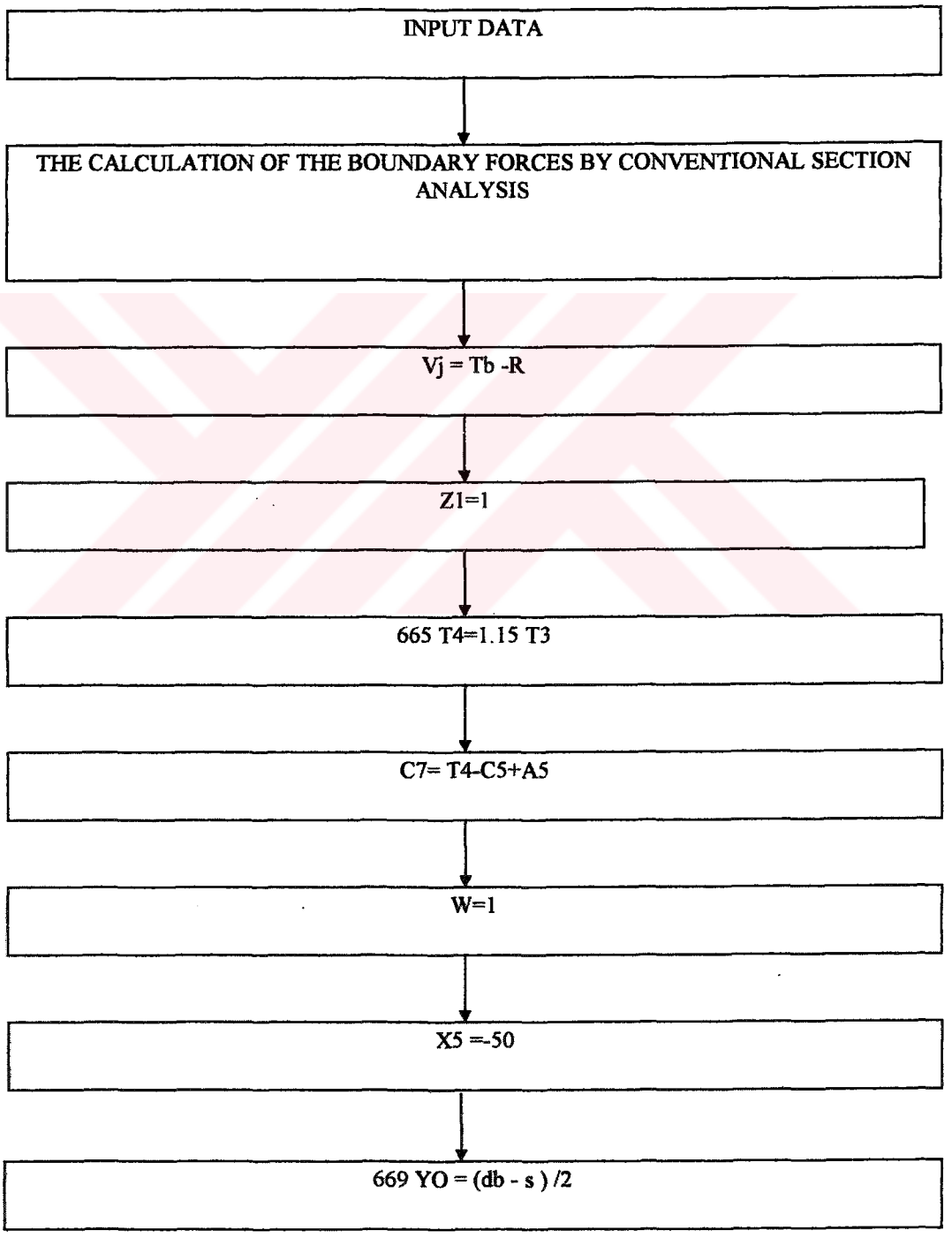

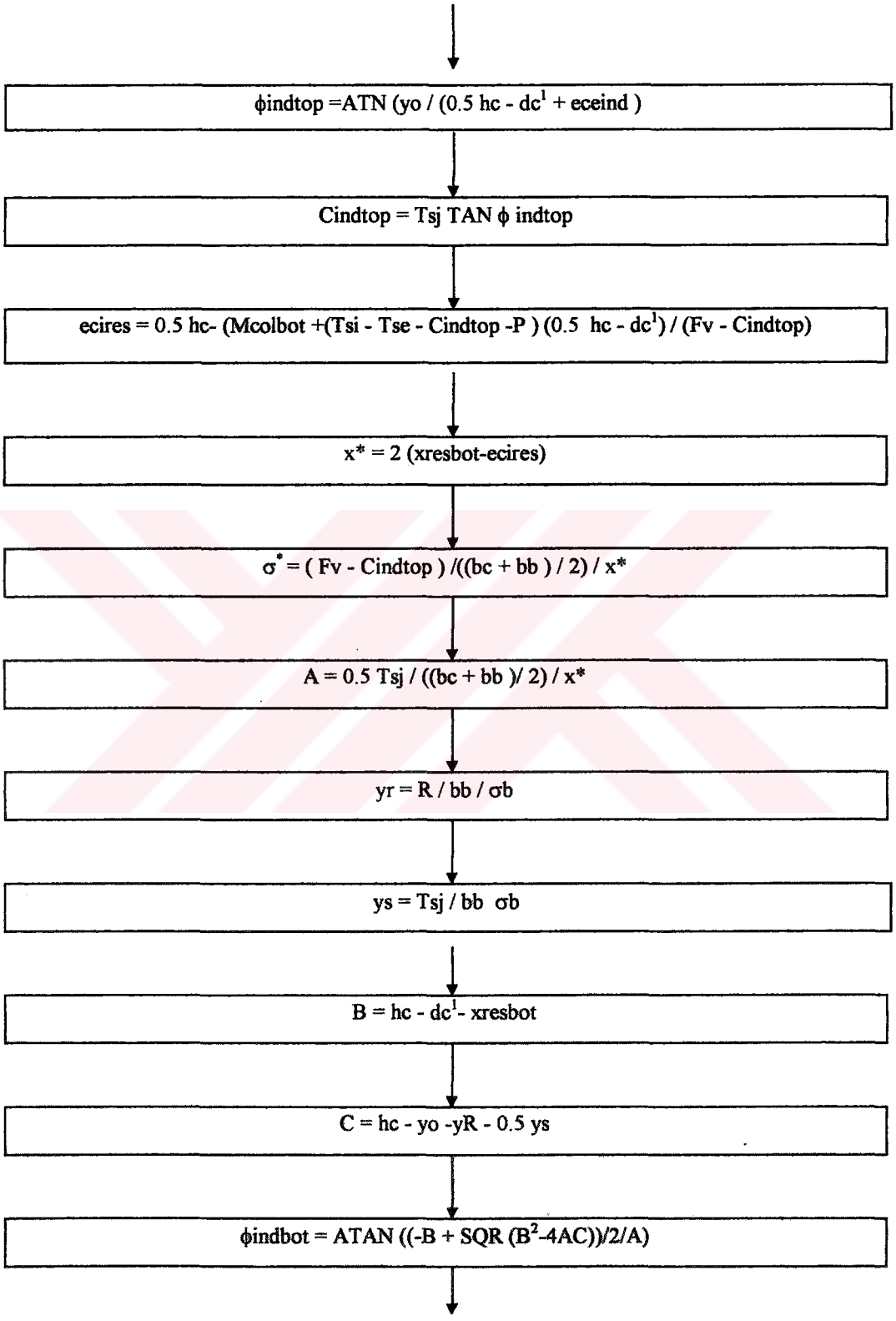
ϕindtop =ATN (yo / (0.5 hc - dc[1] + eceind)
Cindtop = Tsj TAN ϕ indtop
ecires = 0.5 hc- (Mcolbot +(Tsi - Tse - Cindtop -P) (0.5 hc - dc[1]) / (Fv - Cindtop)
x* = 2 (xresbot-ecires)
σ* = (Fv - Cindtop) /((bc + bb) / 2) / x*
A = 0.5 Tsj / ((bc + bb)/ 2) / x*
yr = R / bb / σb
ys = Tsj / bb σb
B = hc - dc[1]- xresbot
C = hc - yo -yR - 0.5 ys
ϕindbot = ATAN ((-B + SQR (B[2]-4AC))/2/A)

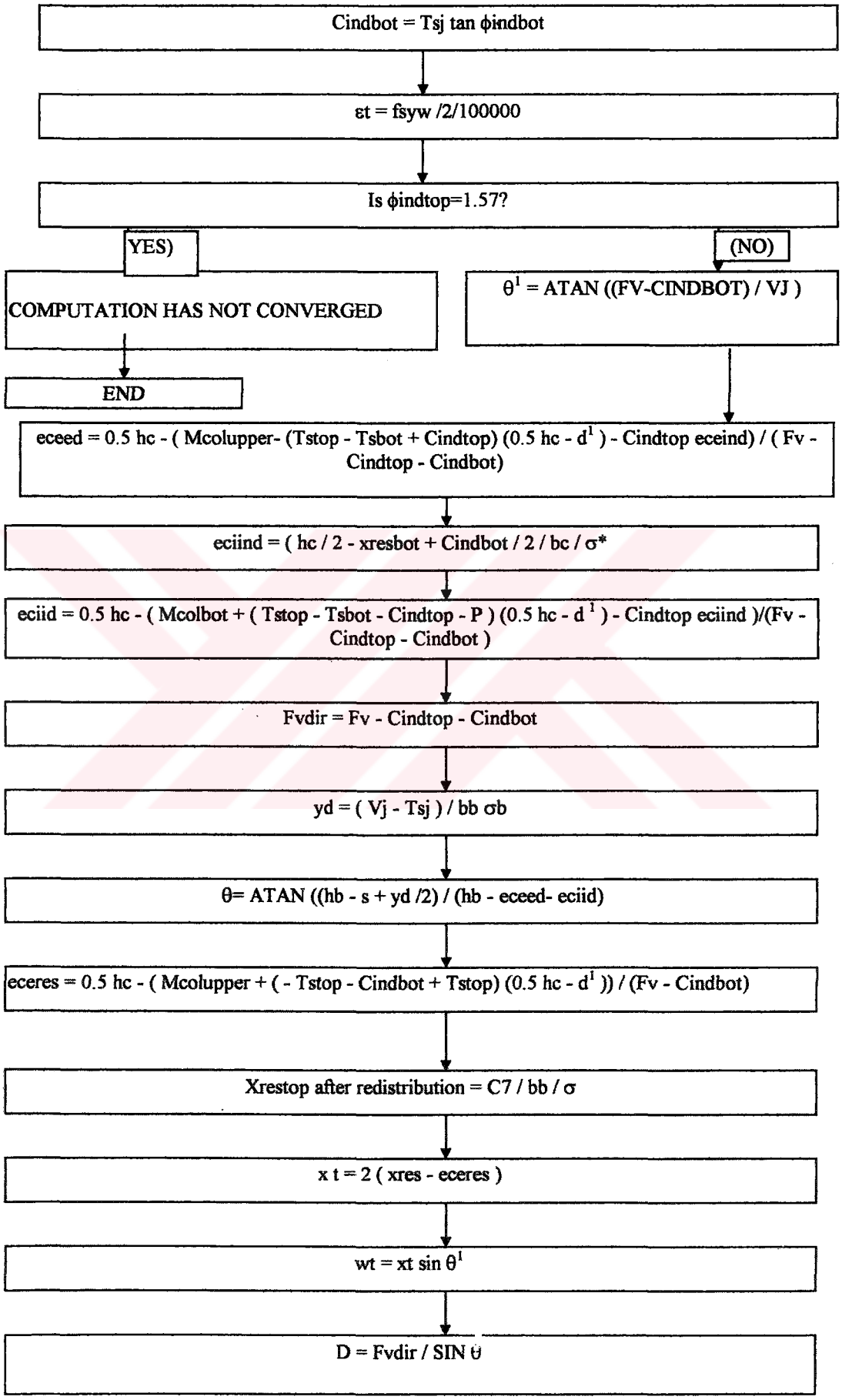
Cindbot = Tsj tan ϕindbot
εt = fsyw /2/100000
Is ϕindtop=1.57?
YES)
(NO)
COMPUTATION HAS NOT CONVERGED
θ1 = ATAN ((FV-CINDBOT) / VJ)
END
eceed = 0.5 hc - (Mcolupper- (Tstop - Tsbot + Cindtop) (0.5 hc - d1) - Cindtop eceind) / (Fv - Cindtop - Cindbot)
eciind = (hc / 2 - xresbot + Cindbot / 2 / bc / σ*
eciid = 0.5 hc - (Mcolbot + (Tstop - Tsbot - Cindtop - P) (0.5 hc - d 1) - Cindtop eciind)/(Fv - Cindtop - Cindbot)
Fvdir = Fv - Cindtop - Cindbot
yd = (Vj - Tsj) / bb σb
θ= ATAN ((hb - s + yd /2) / (hb - eceed- eciid)
eceres = 0.5 hc - (Mcolupper + (- Tstop - Cindbot + Tstop) (0.5 hc - d1)) / (Fv - Cindbot)
Xrestop after redistribution = C7 / bb / σ
x t = 2 (xres - eceres)
wt = xt sin θ1
D = Fvdir / SIN θ

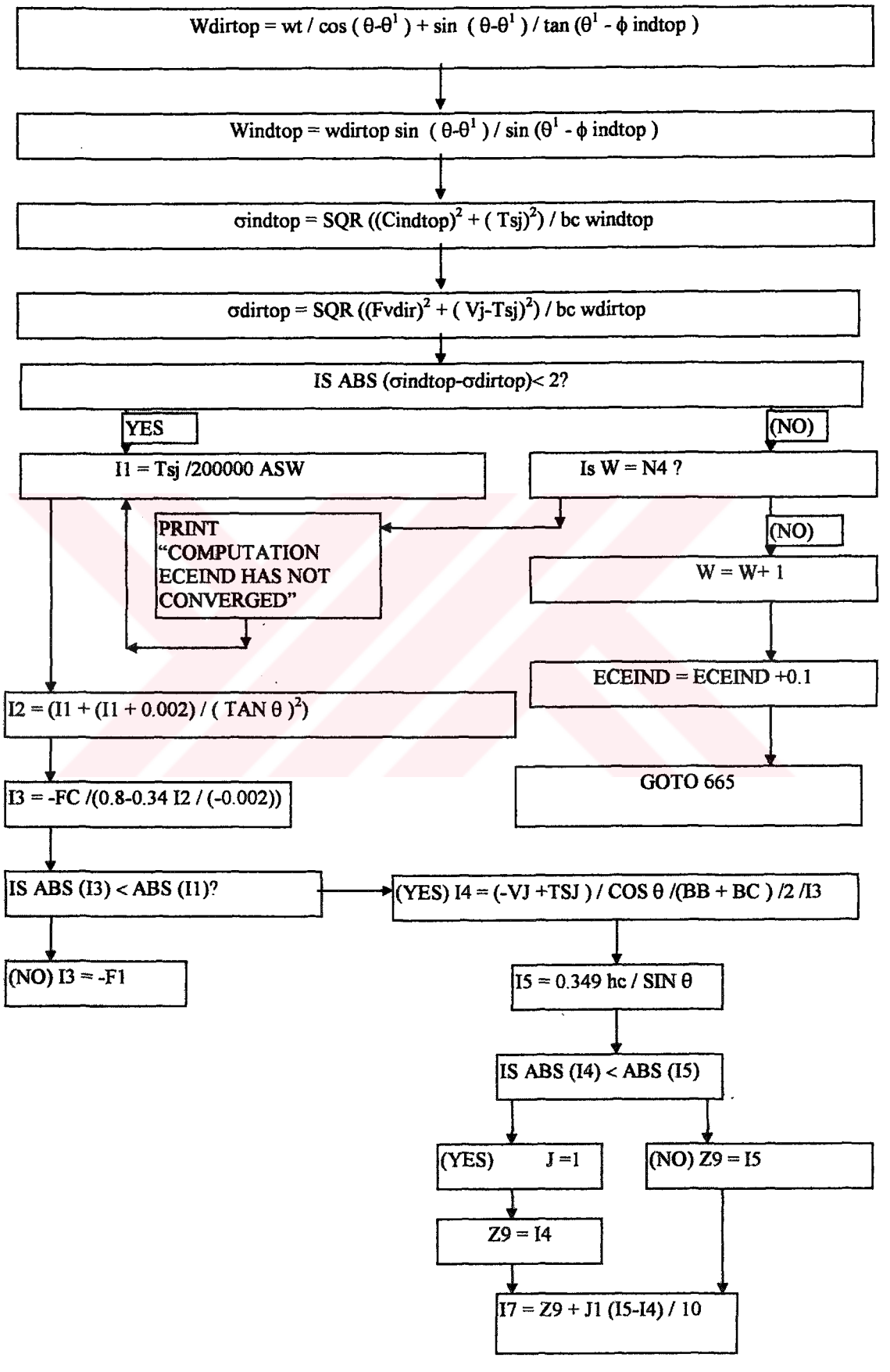
Wdirtop = wt / cos (θ-θ¹) + sin (θ-θ¹) / tan (θ¹ - ϕ indtop)
Windtop = wdirtop sin (θ-θ¹) / sin (θ¹ - ϕ indtop)
σindtop = SQR ((Cindtop)² + (Tsj)²) / bc windtop
σdirtop = SQR ((Fvdir)² + (Vj-Tsj)²) / bc wdirtop
IS ABS (σindtop-σdirtop)< 2?
YES
(NO)
I1 = Tsj /200000 ASW
Is W = N4 ?
PRINT "COMPUTATION ECEIND HAS NOT CONVERGED"
(NO)
W = W+ 1
ECEIND = ECEIND +0.1
I2 = (I1 + (I1 + 0.002) / (TAN θ)²)
GOTO 665
I3 = -FC /(0.8-0.34 I2 / (-0.002))
IS ABS (I3) < ABS (I1)?
(YES) I4 = (-VJ +TSJ) / COS θ /(BB + BC) /2 /I3
(NO) I3 = -F1
I5 = 0.349 hc / SIN θ
IS ABS (I4) < ABS (I5)
(YES) J =1
(NO) Z9 = I5
Z9 = I4
I7 = Z9 + J1 (I5-I4) / 10

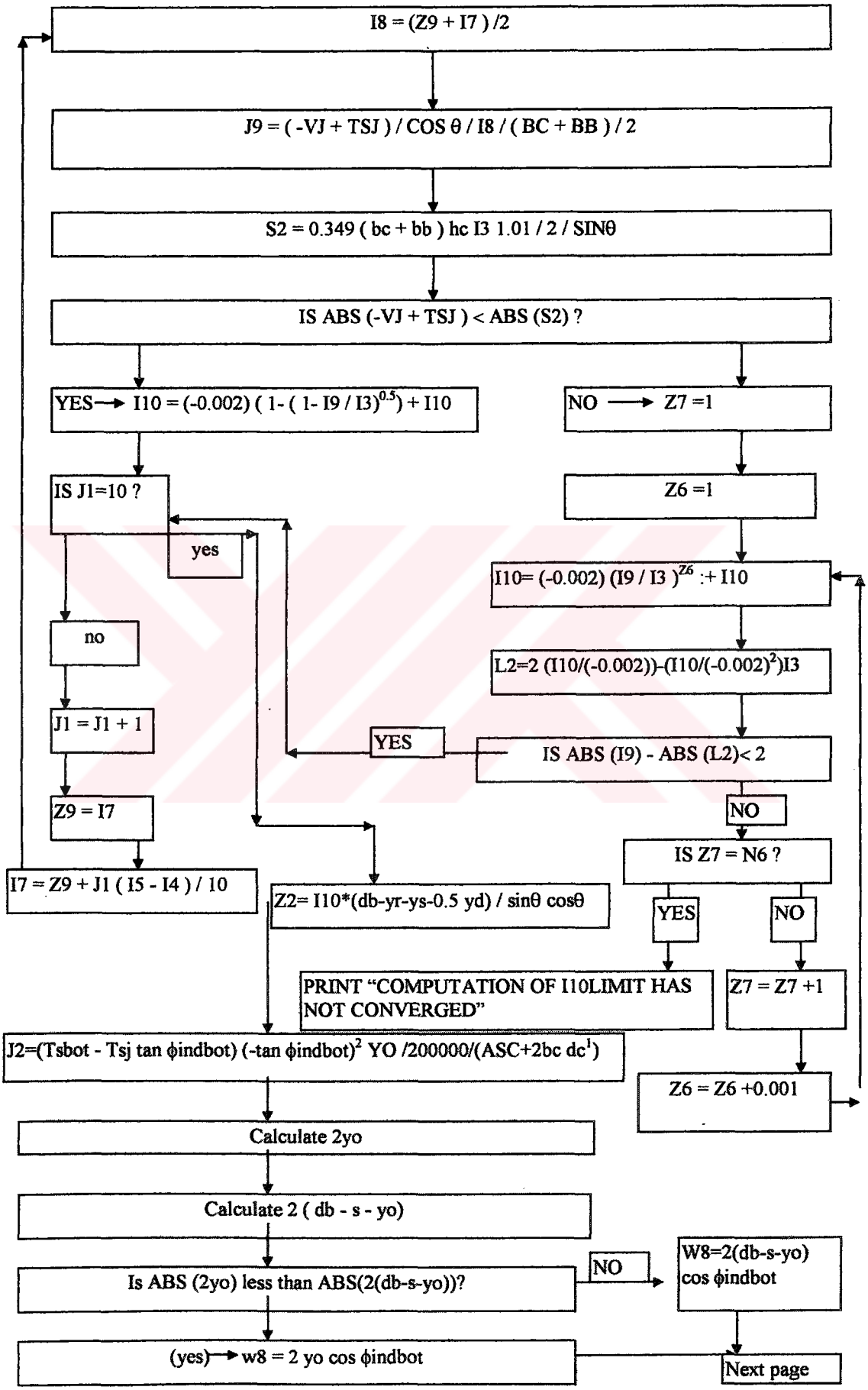
I8 = (Z9 + I7) /2
J9 = (-VJ + TSJ) / COS θ / I8 / (BC + BB) / 2
S2 = 0.349 (bc + bb) hc I3 1.01 / 2 / SINθ
IS ABS (-VJ + TSJ) < ABS (S2) ?
YES → I10 = (-0.002) (1- (1- I9 / I3)^0.5) + I10
NO → Z7 =1
IS J1=10 ?
yes
no
J1 = J1 + 1
Z9 = I7
I7 = Z9 + J1 (I5 - I4) / 10
Z6 =1
I10= (-0.002) (I9 / I3)^Z6 :+ I10
L2=2 (I10/(-0.002))-(I10/(-0.002)^2)I3
YES
IS ABS (I9) - ABS (L2)< 2
NO
IS Z7 = N6 ?
YES
NO
Z2= I10*(db-yr-ys-0.5 yd) / sinθ cosθ
PRINT "COMPUTATION OF I10LIMIT HAS NOT CONVERGED"
Z7 = Z7 +1
Z6 = Z6 +0.001
J2=(Tsbot - Tsj tan ϕindbot) (-tan ϕindbot)^2 YO /200000/(ASC+2bc dc^1)
Calculate 2yo
Calculate 2 (db - s - yo)
Is ABS (2yo) less than ABS(2(db-s-yo))?
NO
W8=2(db-s-yo) cos ϕindbot
(yes) → w8 = 2 yo cos ϕindbot
Next page

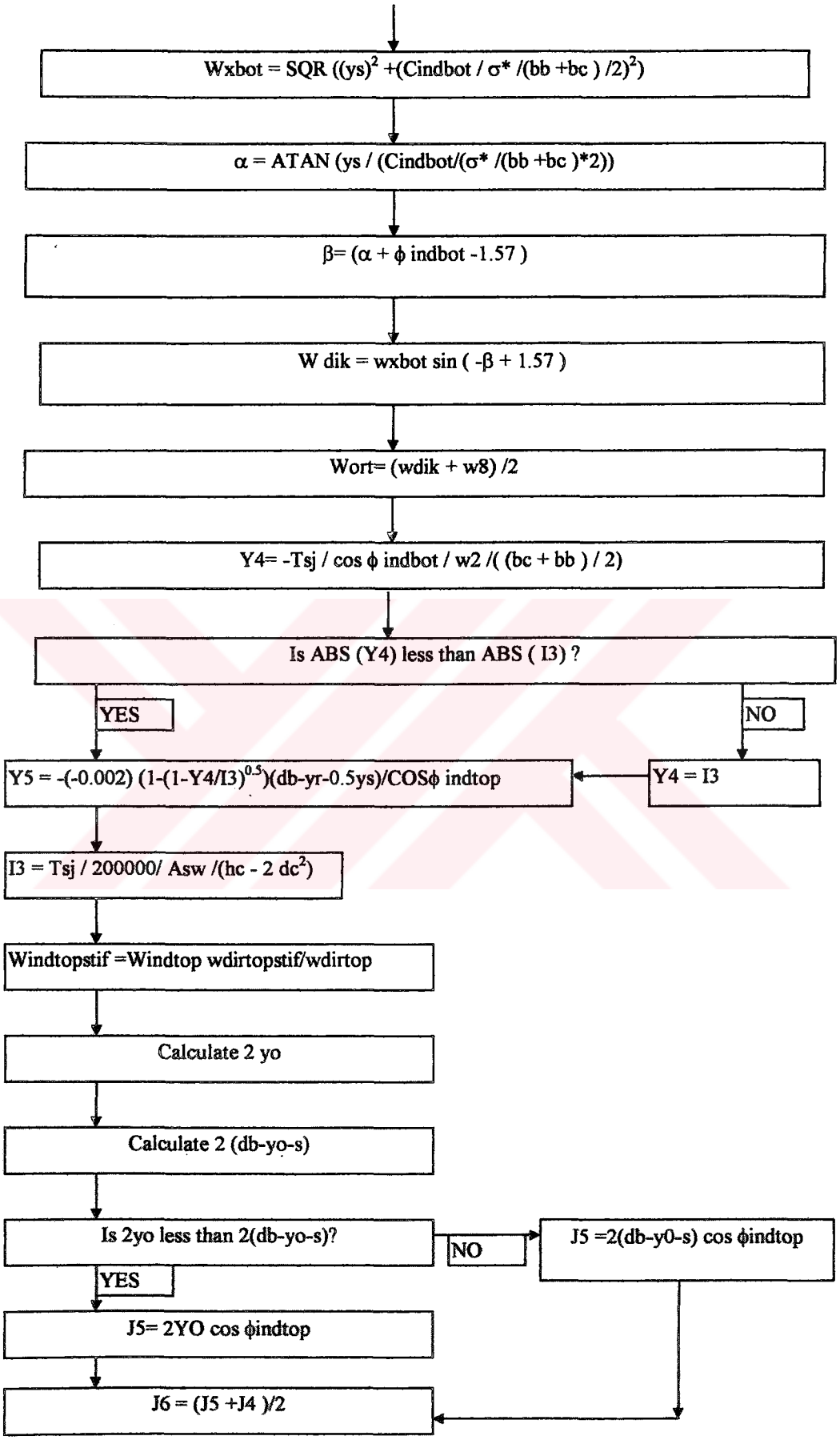
Wxbot = SQR ((ys)^2 +(Cindbot / σ* /(bb +bc) /2)^2)
α = ATAN (ys / (Cindbot/(σ* /(bb +bc)*2))
β= (α + ϕ indbot -1.57)
W dik = wxbot sin (-β + 1.57)
Wort= (wdik + w8) /2
Y4= -Tsj / cos ϕ indbot / w2 /((bc + bb) / 2)
Is ABS (Y4) less than ABS (I3) ?
YES
NO
Y5 = -(-0.002) (1-(1-Y4/I3)$^{0.5}$)(db-yr-0.5ys)/COSϕ indtop
Y4 = I3
I3 = Tsj / 200000/ Asw /(hc - 2 dc^2)
Windtopstif =Windtop wdirtopstif/wdirtop
Calculate 2 yo
Calculate 2 (db-yo-s)
Is 2yo less than 2(db-yo-s)?
NO
J5 =2(db-y0-s) cos ϕindtop
YES
J5= 2YO cos ϕindtop
J6 = (J5 +J4)/2

DOKUMANTASYON MERKEZ

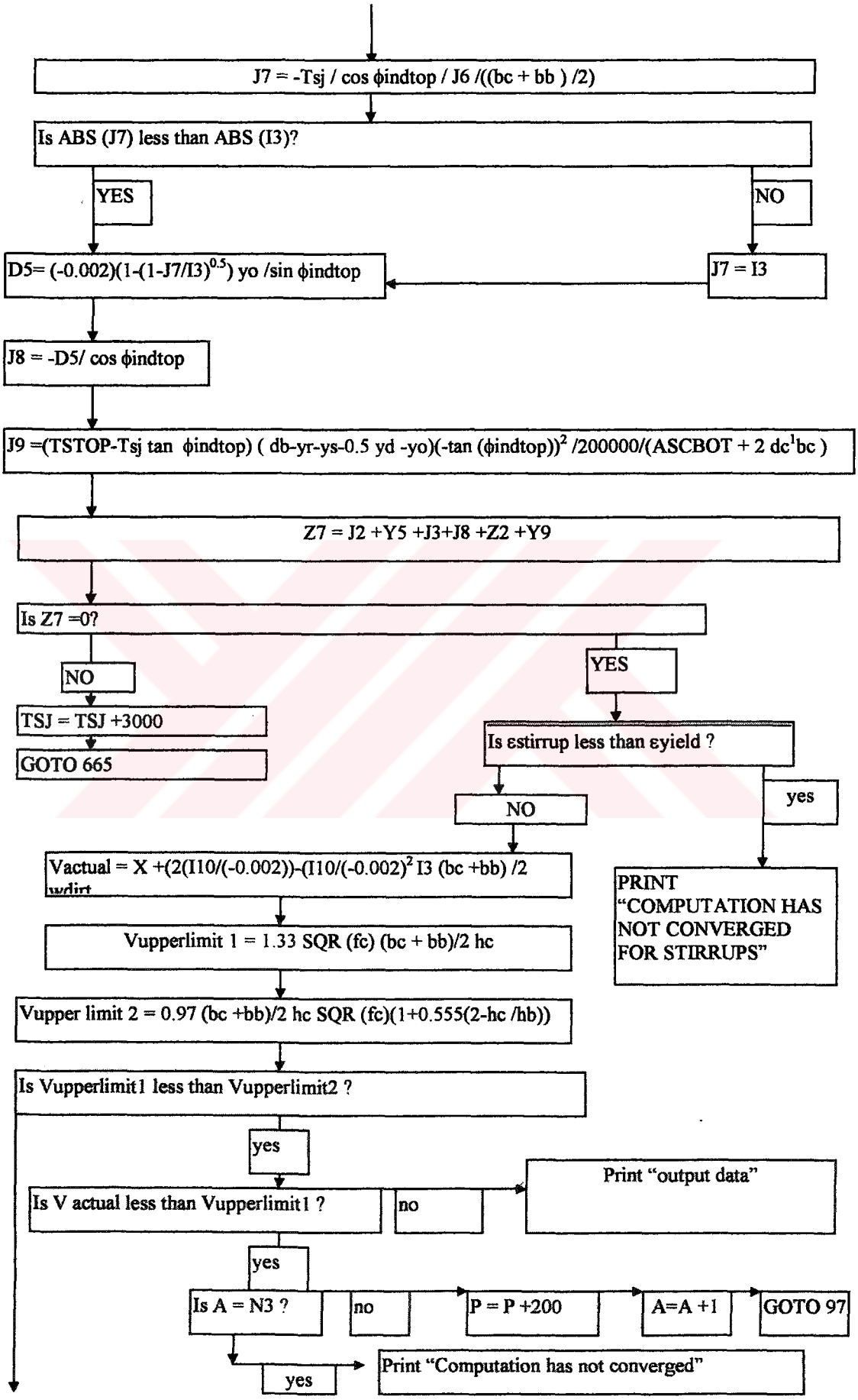

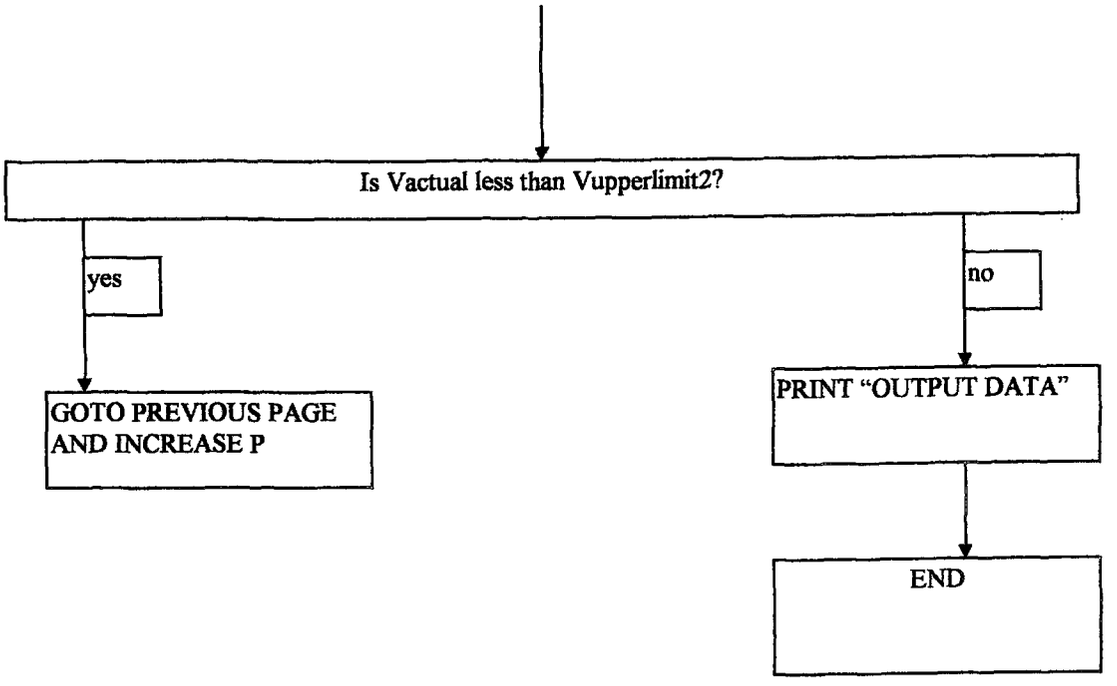
Is Vactual less than Vupperlimit2?
yes
no
GOTO PREVIOUS PAGE AND INCREASE P
PRINT "OUTPUT DATA"
END

3. The Algorithm for author's model

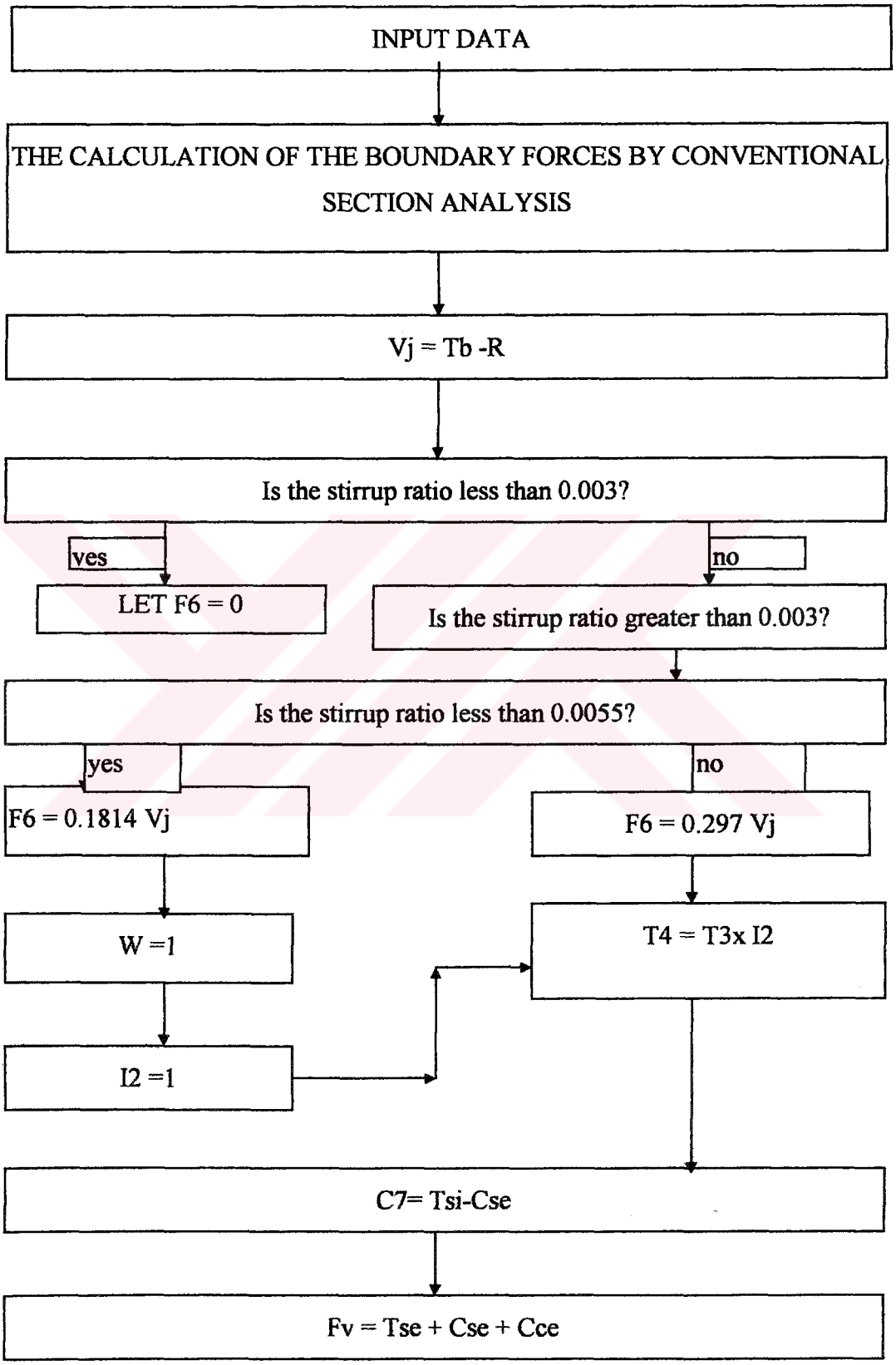

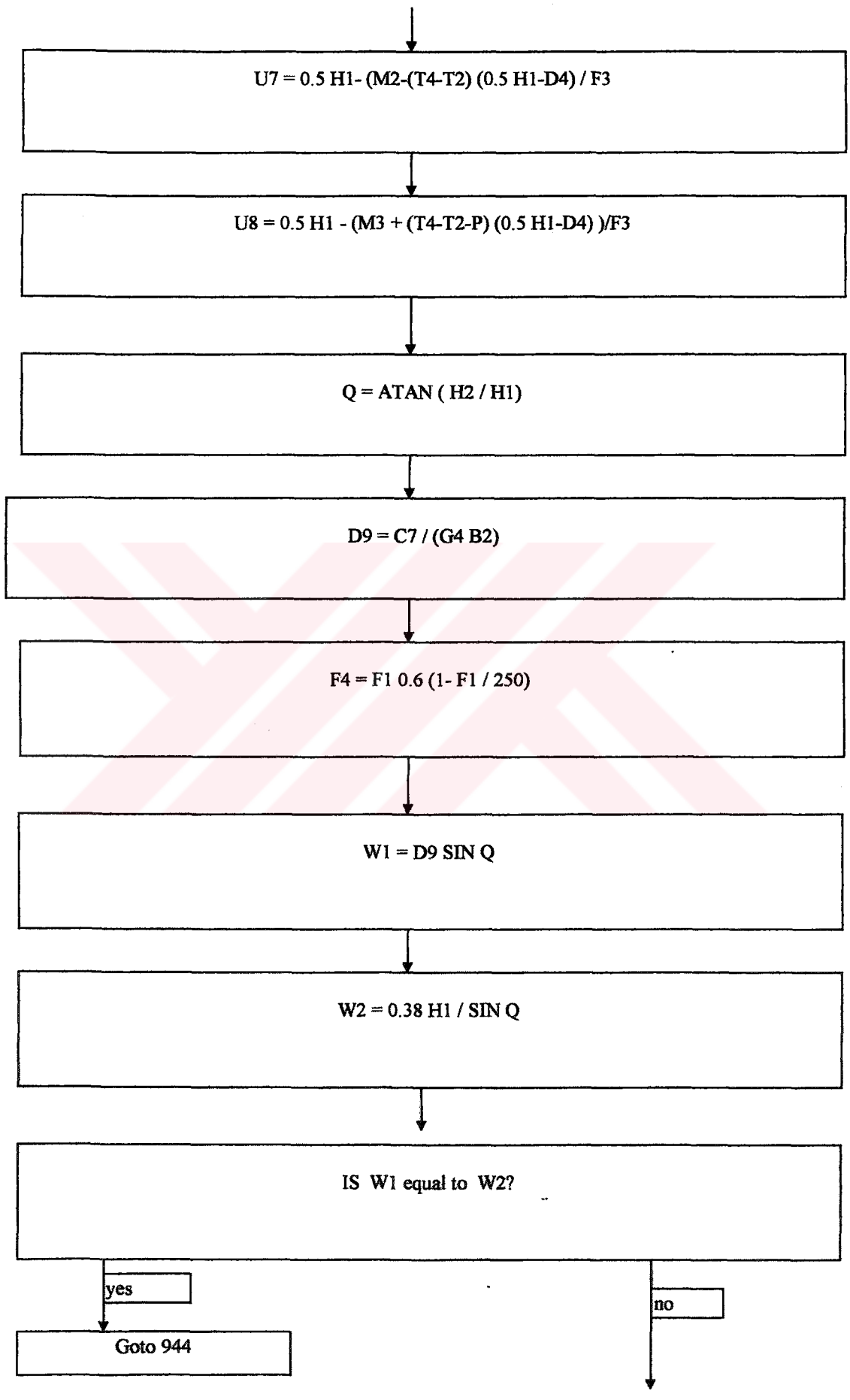
U7 = 0.5 H1- (M2-(T4-T2) (0.5 H1-D4) / F3
U8 = 0.5 H1 - (M3 + (T4-T2-P) (0.5 H1-D4))/F3
Q = ATAN (H2 / H1)
D9 = C7 / (G4 B2)
F4 = F1 0.6 (1- F1 / 250)
W1 = D9 SIN Q
W2 = 0.38 H1 / SIN Q
IS W1 equal to W2?
yes
Goto 944
no

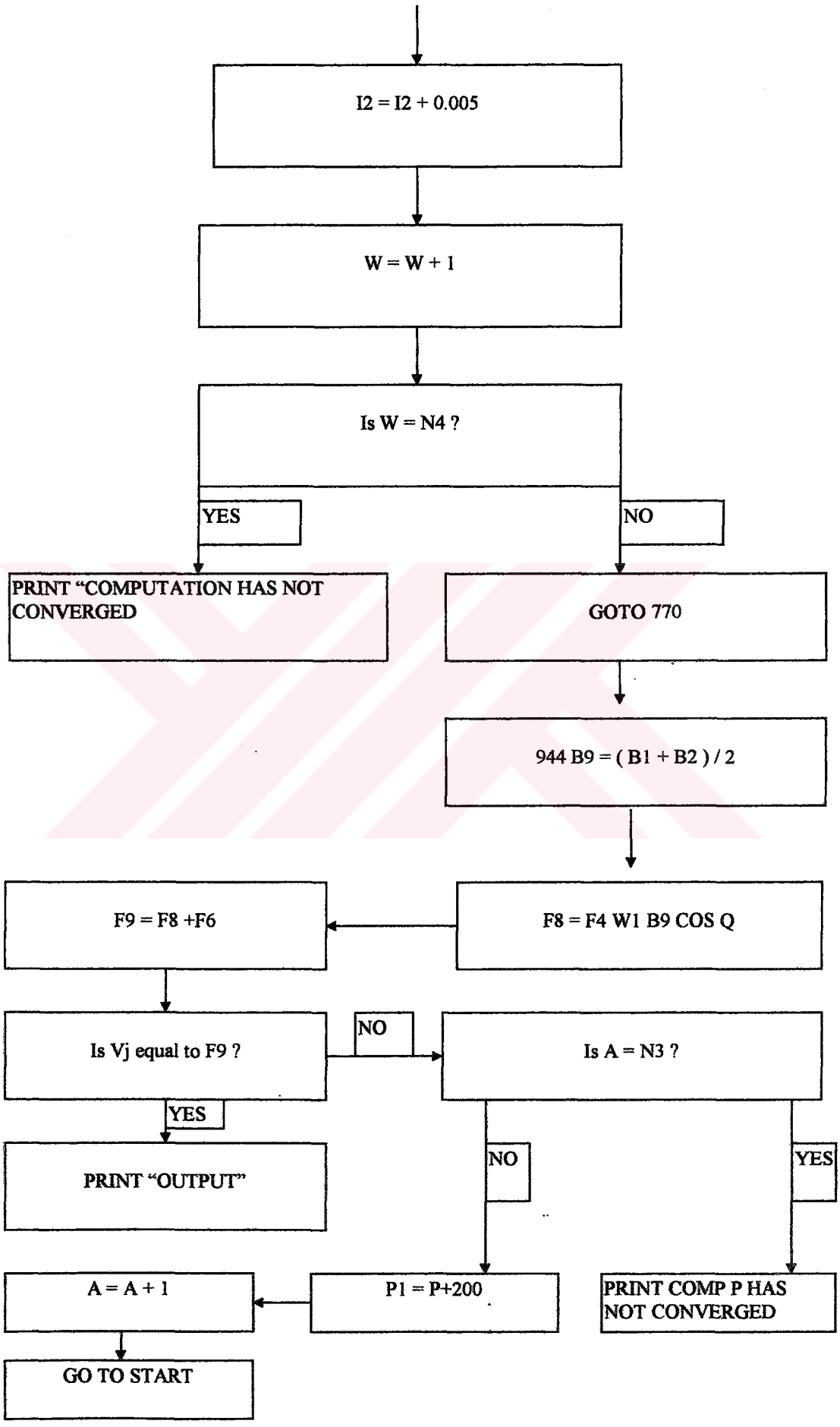
I2 = I2 + 0.005
W = W + 1
Is W = N4 ?
YES
NO
PRINT "COMPUTATION HAS NOT CONVERGED
GOTO 770
944 B9 = (B1 + B2) / 2
F9 = F8 +F6
F8 = F4 W1 B9 COS Q
Is Vj equal to F9 ?
NO
Is A = N3 ?
YES
PRINT "OUTPUT"
NO
YES
A = A + 1
P1 = P+200
PRINT COMP P HAS NOT CONVERGED
GO TO START

APPENDIX B

Table B.1. The Results of the Analysis of Scott and Hamill

Specimen	Cylinder Strength	Detailing	Failure Mode	Stirrups	N/fcbchc	$v_j = V_j / b_c h_c$	Ratio of Tensile Reinforcement
Units	MPa	-	-	-	-	MPa	-
Scott &Hamill							
C6NL3	48.8	U Bars	JS	2T6	0.045	6.36	1.74
C6ALN5	36.8	U Bars	JS	3T6	0.060	7.84	1.74
C6ALH3	96.8	U Bars	JS	2T6	0.045	8.94	1.74
C6ALH5	100	U Bars	JS	3T6	0.044	9.48	1.74
C6ALH0	100.8	U Bars	JS	0	0.044	9.38	1.74
C6ALH1	101.6	U Bars	JS	1T6	0.043	8.015	1.74
C6ALN0	51.2	U Bars	JS	0	0.043	5.252	1.74
C6ALN1	51.2	same	JS	1T6	0.100	5.988	1.74
Mean(UBars)	73.4				0.053	7.657	
C4ALN3	41.6	L Bars bent down	JS	2T6	0.053	8.03	1.74
C4ALH0	104	same	P	0	0.025	10.37	1.74
C4ALN5	50.4	same	JS	3T6	0.044	10.41	1.74
C4ALH3	105.6	same	B	2T6	0.042	9.617	1.74
C4ALH5	98.4	same	B	3T6	0.045	9.55	1.74
C4ALNO	42.4	same	P	0	0.062	6.58	1.74
C4ALN1	45.6	same	JS	1T6	0.058	8.339	1.74
C4ALH1	95.2	same	B	1T6	0.046	9.44	1.74
Mean(L Bars)	70.489				0.047	9.042	
Mean (Total)	73.15				0.050	8.349	

Table B-2. The results of the analysis carried out by the author on Taylor's tests.

Specimen	Cylinder *Strength*	Detailing	Failure Mode	Stirrups	N/fcbchc	$v_j = V_j / b_c h_c$	ρ_B
Units	Mpa	-	-	-	-	MPa	-
Taylor							
P1/41/24	33	Straight bar (not anchored)	JS	1T6	0.371	6	2.01
P2/41/24	29	same	same	1T6	0.422	5.815	2.01
P2/41/24A	46.5	same	same	1T6	0.263	7.34	2.01
A3/41/24	27	same	same	1T6	0.45	5.98	2.01
A3/41/13	45	same	B	1T6	0.272	5.42	2.01
D3/41/24	53	same	B	1T6	0.057	7.94	2.01
D3/41/13	55.5	same	B	1T6	0.055	5.499	1.178
E3/41/24A	42.8	same	JS	1T6	0.286	4.3	2.01
E3/41/24B	44.5	same	JS	1T6	0.275	0.588	2.01
E3/41/24C	41.6	same	JS	1T6	0.294	6.4	2.01
F3/41/24A	37.2	same	B	1T6	0.329	5.98	1.884
F3/41/24B	34.2	same	B	1T6	0.358	5.76	1.884
F3/41/24C	34.4	same	B	1T6	0.089	5.74	1.884
C3/41/24BY	31.7	U Bar	JS	1T6	0.386	4.817	2.01
C3/41/13Y	28.2	U Bar	same	1T6	0.434	4.255	1.178
C3/41/24Y	59.5	U Bar	same	1T6	0.206	0.512	2.01
Mean	40.19				0.284	5.146	

Table B-3.The results of the analysis of the normalized joint shear strengths of the tests of Scott , Hamill and Kordina

Specimen	Cylinder Strength	pstirrup	Failure Mode	Effective Joint Stirrups	Column Axial Stress/fc	Joint Shear Strength $v_j = V_j / b_e h_c \sqrt{fc}$	Ratio of Tensile Reinforcement	Joint Aspect Ratio	Asw fy /bc hc √fc	(Vj-Asw fy)/ be hc √fc
Units	MPa	-	-	-	-	MPa	-			
Scott										
C1	39.92	2.89	B	1T6	0.306	0.907	1.11	1.4	0.206	0.77
C1A	48	2.89	B	1T6	0.254	0.762	1.11	1.4	0.188	0.711
C1AL	33.36	2.89	J	1T6	0.066	0.839	1.11	1.4	0.188	0.613
C4	41.44	2.89	J	1T6	0.294	1.043	1.976	1.4	0.203	0.84
C4A	44.32	2.89	J	1T6	0.275	1.075	1.976	1.4	0.196	0.923
C4AL	35.76	2.89	J	1T6	0.062	1.086	1.976	1.4	0.218	0.867
C7	35.2	2.89	J	1T6	0.347	0.755	1.33	2	0.22	0.536
Mean	39.71				0.229	0.968		1.4		
C4ALN3	41.6	5.79	J	2T6	0.053	1.245	1.976	1.4	0.481	0.764
C4ALH0	104	0	P	0	0.021	0.919	1.976	1.4	0	0.919
C4ALN5	50.4	8.696	J	3T6	0.044	1.25	1.976	1.4	0.481	0.595
C4ALH3	105.6	5.8	B	2T6	0.042	0.935	1.976	1.4	0.302	0.63
C4ALH5	98.4	8.696	B	3T6	0.045	0.96	1.976	1.4	0.469	0.49
C4ALNO	42.4	0	P	0	0.062	0.91	1.976	1.4	0	0.913
C4ALN1	45.6	2.89	J	1T6	0.0587	1.116	1.976	1.4	0.229	0.886
C4ALH1	95.2	2.89	B	1T6	0.0466	0.967	1.976	1.4	0.159	0.833
MeanL Bars	70.489				0.0472	1.037		1.4		
Kordina										
RE2	25.28	0	J	0	0.237	0.918	0.785	2.125	0	0.918
RE3	40.4	3.93	J	1T10	0.247	1.182	0.982	1.625	0.26	0.92
RE4	32.24	0	J	1T8	0.039	0.876	1.047	1.625	0	0.876
RE7	25.7	5.238	J	3T8	0.439	1.32	1.17	1.5	0.434	0.886
Mean	30.905				0.240	1.074		1.6		

Table B-4. The results of the analysis of the tests of Scott and Scott and Hamill specimens regarding the joint aspect ratio

Specimen	Cylinder Strength	Type of Detailing of the Beam Bars	Failure Mode	Effective Joint Stirrups	Column Axial Stress/fc	Joint Shear Strength $v_j = V_j / b_e h_c \sqrt{fc}$	Ratio of Tensile Reinforcement	Joint Aspect Ratio
Units	MPa	-	-	-	-	MPa	-	
Scott								
C1	39.92	1	B	1T6	0.306	0.907	1.11	1.4
C1A	48	1	B	1T6	0.254	0.762	1.11	1.4
C1AL	33.36	1	J	1T6	0.066	0.839	1.11	1.4
C4	41.44	1	J	1T6	0.294	1.042	1.976	1.4
C4A	44.32	1	J	1T6	0.275	1.075	1.976	1.4
C4AL	35.76	1	J	1T6	0.062	1.086	1.976	1.4
C7	35.2	1	J	1T6	0.347	0.755	1.33	2
Mean	39.71				0.229	0.968		1.4
C4ALN3	41.6	1	J	2T6	0.053	1.245	1.976	1.4
C4ALH0	104	1	P	0	0.021	0.919	1.976	1.4
C4ALN5	50.4	1	J	3T6	0.044	1.25	1.976	1.4
C4ALH3	105.6	1	B	2T6	0.042	0.93587	1.976	1.4
C4ALH5	98.4	1	B	3T6	0.0452	0.96	1.976	1.4
C4ALNO	42.4	1	P	0	0.063	0.91	1.976	1.4
C4ALN1	45.6	1	J	1T6	0.058479	1.116	1.976	1.4
C4ALH1	95.2	1	B	1T6	0.04668	0.96786	1.976	1.4
Mean (L Bars)	70.489				0.047	1.0379		1.4

Table B5. The normalized joint shear strength of the test specimens of Ortiz and Parker and Bullman with column longitudinal reinforcement ratios

Specimen	Cylinder Strength	Type of Detailing	Failure Mode	Effective Joint Stirrups	Column Axial Stress/fc	Joint Shear Strength $v_j = V_j / b_c h_c$	Ratio of Tensile Reinforcement	Column bar ratio
Units	MPa	-	-	-	-	MPa	-	-
Ortiz								
BCJ1	34	L bar bent down	JS	0	0	5.287	1.072	2.19
BCJ2	38	same	JS	1T8	0	5.819	1.072	2.19
BCJ3	33	same	JS	0	0	5.561	1.072	2.92
BCJ4	34	same	JS	2T8	0	6.136	1.072	3.65
BCJ5	38	same	JS	0	0.131	5.335	1.072	3.65
BCJ6	35	same	J S	0	0.142	5.374	1.072	3.65
BCJ7	35	same	B	3T8	0.142	7.877	1.072	3.65
Mean	35.28					5.913		
Parker & Bullmann								
4a	39.2	L bar bent down	C	0	0	2.52	0.882	1.094
4b	39.2	same	JS	0	0.085	2.950	0.882	1.094
4c	36.8	same	JS	0	0.172	3.665	0.882	1.094
4d	39.2	same	JS	0	0	3.207	0.882	4.377
4e	40	same	JS	0	0.083	3.420	0.882	4.377
4f	37.6	same	JS	0	0.177	3.94	0.882	4.377
Mean	38.66					3.5		
5a	42.4	same	C	2T12	0	4.027	0.882	2.67
5b	43.2	same	JS	2T12	0.077	4.465	0.882	2.67
5c	43.2	same	B	2T12	0.146	4.45	0.882	2.67
5d	43.2	same	C	3T12	0	5.395	1.446	2.67
5e	44.8	same	same	3T12	0.074	5.755	1.446	2.67
5f	43.2	same	JS	3T12	0.154	6.32	1.446	2.67
Mean	43.3					5.069		
Total Mean	40.98					4.284		

T.C. YÜKSEKÖĞRETİM KURULU
DOKÜMANTASYON MERKEZİ

RESUME

Pelin GÜNDEŞ BAKIR was born in Istanbul in 13.03.1972. She graduated from Kadıköy Anadolu Lisesi in 1989 and obtained a BSc in Civil Engineering from Yıldız Technical University in 1993. In 1995, she obtained the DIC (Diploma of Imperial College). In the same year, she also obtained the MSc degree in Concrete Structures from Imperial College, University of London. In 1995, she started her PhD study in the Faculty of Civil Engineering of Istanbul Technical University under the supervision of Professor Hasan M. BODUROĞLU. Between years 1995-1999, she worked in industry and designed several business centres and residences. Since 1999, she has been working as a research assistant at the Mechanics Division of the Civil Engineering Department of Istanbul Technical University Pelin GÜNDEŞ BAKIR is the author of 26 international and 3 national papers and the co-author of a translation book. She is the member of American Society of Civil Engineers (ASCE), The Turkish Chamber of Civil Engineers and Architects and The Alumni Society of Imperial College of Science and Technology. Pelin GÜNDEŞ BAKIR has two certificates from Federal Emergency Management Agency of the United States of America, on Emergency Management and Earthquake Engineering respectively. She is married and has a son.